Oxygen sensing mechanisms in retinal vascular development and disease.

Clemens Lange

UCL Institute of Ophthalmology

Department of Genetics

11 - 43 Bath Street

London, EC1V 9EL

A thesis submitted for the degree of Doctor of Philosophy, University College London.

Date of submission: 04.08.2012

Declaration

I, Clemens Lange, confirm that the work presented in this thesis is my own. Where information has been derived from other sources, I confirm that this has been indicated in the thesis.

---------- (Clemens Lange)

“In the study of this membrane [retina] I for the first time felt my faith in Darwinism weakened, being amazed and confounded by the supreme constructive ingenuity revealed…”

Santiago Ramón y Cajal, *Recollections of My Life* (1898)

Abstract

Oxygen sensing is a fundamental biological process which is critical for appropriate development of the eye and implicated in neovascular eye disease including age-related macular degeneration, diabetic retinopathy and retinopathy of prematurity. This thesis describes a programme of work designed to investigate the role of hypoxia-inducible transcription factors (Hif's), its downstream effector proteins, and its upstream regulator, the von Hippel Lindau protein (Vhl), in the development of the eye and neovascular eye disease.

The first part of this work investigates the consequences of Hif activation in the developing retinal pigment epithelium (RPE) using a tissue specific *knockout* technology in mice. It demonstrates that appropriate regulation of Hif's by Vhl is essential for normal RPE and iris development, ocular growth and vascular development and indicates that ocular hypoxia may be a previously unrecognised mechanism in the development of microphthalmia.

The second part of this work studies the role of Hif1a in myeloid cells in the development of pathological neovascularisation using tissue-specific *knockout* technology and murine models for retinal and choroidal neovascularisation. It demonstrates that Hif1a signalling in myeloid cells contributes substantially to the development of retinal and choroidal neovascularisation and provides a rationale for developing antiangiogenic treatments that target Hif1a signalling in myeloid cells in neovascular eye disease.

The third part of this work investigates the oxygen distribution in the vitreous and its relation to HIF1a and its downstream molecules in proliferative diabetic retinopathy (PDR) in man. It identifies significant intraocular oxygen gradients in PDR with areas of hyperoxia and hypoxia and demonstrates increased levels of HIF1a in the vitreous in PDR which correlate with increased levels of inflammatory and angiogenic cytokines in PDR. These findings suggest that HIF1a activation by inflammation and/or hypoxia is a central feature in the progression of PDR and that its inhibition may potentially serve as a target for therapeutic intervention.

Table of contents

List of tables and figures

List of abbreviations

AMD	age-related macular degeneration
BBB	blood-brain barrier
BRB	blood-retinal barrier
BSA	bovine serum albumin
CNS	central nervous system
CNV	choroidal neovascularisation
CTGF	connective tissue growth factor
DNA	deoxyribonucleic acid
DR	diabetic retinopathy
ELISA	enzyme-linked immunosorbent assay
ENOS	endothelial nitric oxide synthase
EPO	erythropoietin
ERG	electroretinogram
ERM	epiretinal membrane
FA	fluorescence angiography
FACs	fluorescence activated cell sorting

FCS	foetal calf serum
FGF	basic fibroblast growth factor
FIH	factor inhibiting HIF
Flt1	fms-like tyrosine kinase-1 (or VEGFR-1)
Flox	flanked by loxP
GCL	ganglion cell layer
GFP	green fluorescent protein
HIF	hypoxia-inducible factor (human)
Hif	hypoxia-inducible factor (mouse)
HIF1a	hypoxia-inducible factor 1 alpha
HIF2a	hypoxia-inducible factor 2 alpha
HRE	hypoxia response element
ICG	indocyanin green
IHC	immunohistochemistry
IL	interleukin
ILM	internal limiting membrane
IDDM	insulin dependent diabetes mellitus

INL	inner nuclear layer
INOS	inducible nitric oxide synthase
IPL	inner plexiform layer
IS/OS	inner/outer photoreceptor segments
lysM	lysozyme murine
MCP-1	monocyte chemotactic protein-1
MH	macular hole
mRNA	messenger RNA
NFL	nerve fiber layer
NGS	normal goat serum
NNOS	neuronal nitric oxide synthetase
NO	nitric oxide
NOS	nitric oxide synthase
NV	neovascularisation
O_2	oxygen
OCT	optimal cutting temperature
OCT	optical coherence tomography

OIR	oxygen-induced retinopathy
ONL	outer nuclear layer
OPL	outer plexiform layer
PBS	phosphate buffered saline
PCR	polymerase chain reaction
PDGF	platelet derived growth factor
PDR	proliferative diabetic retinopathy
PFA	paraformaldehyde
PHD	prolyl hydroxylase
PR	photoreceptors
pVHL	von Hippel-Lindau tumour suppressor protein
RNA	ribonucleic acid
ROP	retinopathy of prematurity
RNV	retinal neovascularisation
ROS	reactive oxygen species
RPE	retinal pigment epithelium
SD	standard deviation

SEM	standard error of the mean
siRNA	small inhibiting ribonucleic acid
trp-1	tyrosinase related protein 1
VEGF	vascular endothelial growth factor
YFP	yellow fluorescent protein

Awards, publications and conference abstracts

Awards

1.) Moorfields Eye Hospital Research Medal (2012)

2.) Novartis Young Investigator Travel Award (2012)

3.) ARVO Travel Grant (2012)

4.) UCL Post-Graduate Student Conference Grant (2011)

5.) NIHR Summer School Research Award, Ashridge, UK (2010)

6.) PhD Poster-Prize, Institute of Ophthalmology, London, UK (2010)

Recent publications, relevant to this thesis

1.) **Lange CA**, Luhmann UFO, Mowat FM, West EL, Smith AJ, Fruttiger M, Sowden J, Maxwell P, Ali R, Bainbridge JW. Von Hippel-Lindau protein in the RPE is essential for normal ocular growth and vascular development. ***Development***, 2012 Jul;139(13):2340-50.

2.) Luhmann UFO, **Lange CA,** Robbie S, Munro P, Cowing J, Armer H, Luong V, Carvalho L, MacLaren R, Fitzke F, Bainbridge JW, Ali RR. Differential Modulation of Retinal Degeneration by *Ccl2* and *Cx3cr1* ChemokineSignaling*.* ***Plos One***, 2012 Jun;7(4):e35551.

3.) Mowat FM, Gonazalez F, Luhmann UFO, **Lange CA**, Smith AJ, Maxwell P, Ali RR, Bainbridge WB Endogenous erythropoietin protects neuroretinal function in ischaemic retinopathy**.** ***Am J Pathol.*** 2012 Apr;180(4):1726-39

4.) McKenzie JA, Fruttiger M, Abraham S, **Lange CA**, Stone J, Gandhi P, Wang X, Bainbridge J, Moss SE, Greenwood J. Apelin is required for non-

neovascular remodeling in the retina. ***Am J Pathol.*** 2012 Jan;180(1):399-409.

5.) **Lange CA**, Bainbridge JW. Oxygen sensing in retinal health and disease. ***Ophthalmologica.*** 2012;227(3):115-31.

6.) **Lange CA**, Stavrakas P, Luhmann UF, Ali RR, Gregor ZJ, Bainbridge JW. Intraocular Oxygen Distribution in Advanced Proliferative Diabetic Retinopathy. ***Am J Ophthalmol.*** 2011 Sep; 152(3):406-412.e3.

7.) Mowat FM, Luhmann UF, Smith AJ, **Lange CA**, Maxwell PH, Ali RR, Bainbridge JW. HIF1a and HIF2 are differentially activated in distinct cell populations in retinal ischaemia. ***PLoS One.*** 2010 Jun 14;5(6):e11103

Further publications

1.) Solebo AL, **Lange CA**, Bunce C, Bainbridge JW. Face-down positioning or posturing after macular hole surgery. **Cochrane Database Syst Rev,** 2011 Dec 7;(12):CD008228. Review.

2.) **Lange CA**, Membrey L, Ahmad N, et al., Gregor Z, Zambarakji H, Bainbridge JW. Pilot randomised controlled trial of face-down positioning following macular hole surgery. ***Eye (Lond)*** 2012 Feb, 26(2):272-7. doi: 10.1038/eye.2011.221

Conferences and meetings - oral contributions

1.) **Lange CA,** JW Bainbridge. The role of HIF1a in neovascular eye disease. **ISER**, Berlin, Germany, July 2012

2.) **Lange CA,** Mowat F, Sayed H, Leipner j, Ali RR, JW Bainbridge. The role of DDAH-2 in ischaemia induced retinal vascular disease. **RG** (meeting of the German Association for Retinal Disease), Aachen, Germany, June 2011

3.) **Lange CA**, Membrey L, Ahmad N, Wickham L, Maclaren R, Solebo L, Xing W, Bunce C, Ezra E, Charteris D, Aylward B, Gregor Z, Zambarakji H, Bainbridge J. “Pilot RCT of face-down positioning following macular hole surgery”, **BEAVRS** (British and Eire Academy for Vitreo-Retinal Surgery), Cardiff Nov 2010

4.) **Lange CA**, Membrey L, Ahmad N, Wickham L, Maclaren R, Solebo L, Xing W, Bunce C, Ezra E, Charteris D, Aylward B, Gregor Z, Zambarakji H, Bainbridge J. Pilot randomised controlled trial of face-down positioning following macular hole surgery, **RG 2010**, Freiburg, Germany

5.) **Lange CA,** Mowat F, Sayed H, Leipner J, Ali RR, JW Bainbridge.DDAH-2 deletion promotes vascular regeneration in retinal ischaemia“, **Cardiometabolic Science Meeting 2010**, London, UK

6.) **Lange CA**, Luhmann UFO, Gregor Z, Ali RR, Bainbridge JW. Intraocular oxygen in advanced diabetic retinopathy, **NIHR Summer School 2010**, Ashridge, UK

7.) **Lange CA**, Stavrakas P, da Silva J, Luhmann UFO, Gregor Z, Bainbridge JW.Spatial distribution of intraocular oxygen in advanced diabetic retinopathy, **WOC 2010**, Berlin

8.) **Lange CA**, Stavrakas P, da Silva J, Luhmann UFO, Gregor Z, Bainbridge JW. Oxygen and molecular mediators in advanced diabetic retinopathy, **MEH Alumni Meeting 2010**, London, UK

Conferences and meetings - poster contributions

1.) **Lange CA**, Fantin A, Denti L, Smith AJ, Ali RR, Ruhrberg C, Bainbridge JW. Inactivation of *Hif1a* in myeloid cells reduces retinal and choroidal neovascularisation. **ARVO 2012,** USA

2.) Wang X, McKenzie J, Jeffs N, Abraham S, Swire M, **Lange CA**, Bainbridge J, Moss S, Greenwood J. Leucine-rich Alpha-2 Glycoprotein 1 (Lrg1) Contributes To The Development Of Ocular Neovascularisation. **ARVO 2012,** USA

3.) **Lange CA**, F. Mowat, UFO Luhman, P. Kelly, A.J. Smith, J. Leiper, R.R. Ali, J. Bainbridge. DDAH-2 deletion promotes vascular regeneration in retinal ischaemia. **ARVO 2011,** USA

4.) Luhmann UFO, Mowat FM, **Lange CA**, Duran Y, Ali RR, Berger W, Bainbridge J. Norrin promotes Neovascularisation and Revascularisation in retinal ischaemia" **ARVO 2011,** USA

5.) Wang X, McKenzie J, **Lange CA**, Bainbridge J, Moss SE, Greenwood J. Leucine-rich repeat glycoprotein contributes to the development of ocular neovascularisation. **ARVO 2011,** USA

6.) **Lange CA,** Mowat F, Sayed H, Leipner j, Ali RR, JW Bainbridge. DDAH-2 deletion reduces pathological neovascularisation in a mouse model of retinal ischaemia", **Clinician Scientists in Training' meeting 2011**, Royal College of Physicians, London, UK

7.) John Greenwood, Jenny McKenzie, Marcus Fruttiger, **Lange CA**, Jay Stone, Xiaomeng Wang, James Bainbridge, Stephen Moss. Apelin is required for non-sprouting vascular remodelling in the developing and pathogenic retina. **ARVO 2011,** USA

8.) **Lange CA,** Mowat F, Sayed H, Leipner j, Ali RR, JW Bainbridge. DDAH-2 deletion promotes vascular regeneration in retinal ischaemia, **Cardiometabolic Science Meeting 2010**, London, UK

9.) **Lange CA**, Mowat FM, Luhmann UFO, Smith A, Maxwell P, Ali RR, Bainbridge JW. Von Hippel-Lindau expression in the retinal pigment epithelium is essential for normal eye development and vascular homeostasis", **ARVO 2010,** USA

Acknowledgements

I am profoundly grateful to my principal supervisor and mentor Prof James Bainbridge for his unfailing support, guidance and encouragement. I am thankful for his constant positive outlook and patience and for giving me invaluable perspective and insight in the clinical discipline. I would also like to thank Professor Robin Ali, my secondary supervisor, who has helped me with his great insight into “the bigger picture” throughout this work. I appreciate all that they have done for me, and look forward to working with them again in the future.

I am privileged and very grateful to have received generous funding from the National Institute for Health Research to carry out the work presented in this thesis. Many thanks to all of the members of staff and colleagues in the Department of Genetics and the Department of Cell Biology at the Institute of Ophthalmology who have helped me along the way. In particular, I would like to thank Allessandro Fantin, Christiana Ruhrberg, Yanai Duran, Alexander Smith, Emma West, Tassos Georgiadis, Michael Powner, Markus Fruttiger and Ulrich Luhmann for their technical advice and critical appraisal which was integral to this work. Furthermore I would like to thank Prof Thomas Reinhard and Prof Hans-Jürgen Agostini for their constant engouragment, support and guidance throughout the last years.

Last but not least, I am eternally thankful to my parents, my family and my friends for their love, patience and their belief in me. In particular, I dedicate this thesis to my wife Annabel, without whose immense selfless personal sacrifices, I would not have been able to finish this thesis and not be in such a privileged position in life. To each of the above I extend my deepest appreciation, I could not have done it without them.

1. Introduction

The retina has a uniquely high metabolic demand for oxygen that is normally met by an efficient vascular supply (Ames, III et al., 1992). Oxygen is used as an electron acceptor in many intracellular biochemical reactions and contributes to the synthesis of adenosine triphosphate (ATP) through aerobic metabolism that is required to support the metabolic demand of the developing and functioning retina, in particular that of the visual cycle. The functional reserve of oxygen in the retina is small and local oxygen deficiency (hypoxia) can cause neuroretinal dysfunction and degeneration that lead directly to vision loss. Maintenance of normal retinal function therefore depends on a continuous supply of oxygen and on the capability to detect and respond rapidly to hypoxia.

Local oxygen sensing mechanisms control adaptive responses that can help protect against hypoxic injury. In the retina, oxygen sensing mechanisms rapidly detect alterations in intracellular oxygen tension and respond with adaptive changes that redress the balance between oxygen supply and demand. These responses include changes in blood flow, protective metabolic adaptations and angiogenesis. The angiogenic response to retinal hypoxia is typically associated with oedema, haemorrhage and fibrosis that can exacerbate hypoxic neuroretinal injury, causing severe vision loss. This detrimental response is the target of novel therapies including inhibitors of vascular endothelial growth factor (VEGF). These therapies, however, fail to address the underlying hypoxia and do not consider appropriate beneficial adaptive responses to hypoxia.

With the aim to improve our understanding of oxygen sensing mechanisms and its adaptive responses in the retina, this thesis has investigated the role of hypoxia-inducible transcription factors (HIFs) in ocular development, in experimental models of retinal and choroidal neovascularisation and in the pathogenesis of diabetic retinopathy in man.

1.1 Anatomy of the human retina and its vasculature

The wall of the eyeball contains three main layers: an outer fibrous layer (the sclera), a middle vascular layer (the choroid) and an inner nervous tissue layer (the retina, figure 1.1A-B). The retina carries out the various functions required to achieve phototransduction – the process by which light is received and converted into neuronal impulses. The retinal layers of cells are generally viewed as two distinct tissue compartments: the inner, neurosensory retina, and the outer, retinal pigment epithelium (RPE).

1.1.1 Anatomy of the retina

1.1.1.1 Neurosensory retina

The neurosensory retina is a thin translucent tissue that varies in thickness from 0.5 mm at the disc to 0.1 mm at the ora serrata. It is firmly attached to the RPE at the ora serrata and the optic nerve head and held in place by intraocular pressure in the intermediate regions. The neurosensory retina is structured in a distinct layered pattern consisting of three nuclear layers and two sandwiched synaptic, plexifom layers (figure 1.1A-B):

The outer nuclear layer (ONL) contains the cell bodies of both cones and rod photoreceptors. The inner and outer segments (IS, OS) of photoreceptors are located in the photoreceptor layer (PR) between the ONL and the retinal pigment epithelium. Rod and cone photoreceptors differ in the visual pigment they contain and as a result respond to different light stimuli; rods contain the pigment rhodopsin and are sensitive to conditions of dim light whereas cones hold different cone opsins, depending on which subtype of cone cell they belong to, and respond to bright light of varying wavelengths allowing colour vision. In the human eye, a central portion of the retina, the macula, contributes most to visual acuity, as it contains the highest concentration of cone cells (150.000 cones cells/mm^2). Rods dominate the photoreceptor population in the periphery of the mammalian eye and are therefore responsible for peripheral vision.

The outer limiting membrane (OLM) is located between the plasma membranes of the inner segments and the apical processes of Müller glia. The OLM comprises a series of zonula adherens junctional complexes which seal off the light-sensitive photoreceptor inner and outer segments from the rest of the retina, limiting the diffusion of phototransduction cascade components (West et al., 2008).

The outer plexiform layer (OPL) consists of a dense network of synaptic connections between photoreceptor cells and neurons of the inner nuclear layer.

The inner nuclear layer (INL) contains bipolar, amacrine, horizontal and Müller glia cells which coordinate and modify the signals coming from photoreceptors.

The inner plexiform layer (IPL) contains the synaptic connections between cells of the inner nuclear layer and the ganglion cells of the innermost retinal layer.

The ganglion cell layer (GCL) contains displaced amacrine cells and ganglion cells which form the output from the retina to the brain via the optic nerve. The nerve fibers (axons) curve to the optic nerve forming the nerve fiber layer (NFL) which is separated from the vitreous by the inner limiting membrane (ILM) formed by astrocytes and the end feet of Müller cells.

1.1.1.2 Retinal pigment epithelium

The retinal pigment epithelium (RPE) is a monolayer of multifunctional, cuboidal epithelial cells located between the neurosensory retina and the choroidal vasculature (figure 1.1A-B). RPE cells are densely pigmented and form high columns at the posterior pole of the eye and become flatter, wider and less pigmented towards the periphery. Near the apex RPE cells are joined together by attachment girdles of tight junctions, which restrict aqueous diffusion across the layer contributing to the outer blood-retinal barrier. The basement membrane of RPE cells faces the choroid and contributes to Bruch's membrane. The RPE plays a critical role in the eye providing much of the trophic support which is required for development and maintenance of photosensitive retinal cells. In addition, RPE cells phagocytose photoreceptor outer segments, allowing them to be turned over and re-synthesised, and contribute to the visual cycle by uptake and recycling of by-products of the phototransduction cascade.

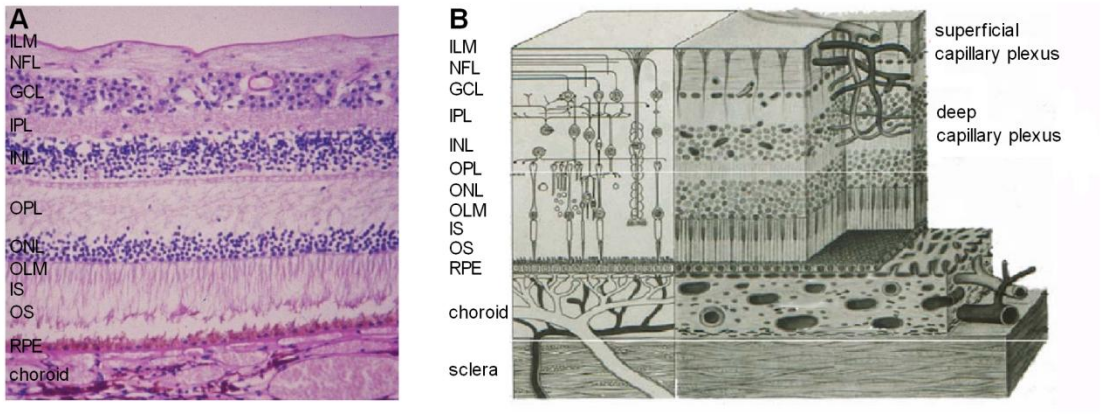

Figure 1.1 Anatomy of the human retina. Histology **(A)** and corresponding schematic **(B)** of the human retina. NB: The flat detachment above the RPE is a fixation artifact. ILM = inner limiting membrane; NFL = nerve fiber layer; GCL = ganglion cell layer; IPL = inner plexiform layer; INL = inner nuclear layer; OPL = outer plexiform layer; ONL = outer nuclear layer; OLM = outer limiting membrane; IS/OS = Inner and outer segments; RPE= retinal pigment epithelium. Images adapted from www.atlasofophthalmology.com (A) and from Mikroskopische Anatomie der Organe - Auge und Retina; H.-J. Wagner (B).

1.1.2 Anatomy of the retinal vasculature

The retinal layers are supplied by two discrete vascular networks – the retinal circulation composed of superficial and deep networks, and the choroidal circulation located under the retinal pigment epithelium (figure 1.1A, B).

1.1.2.1 The retinal vasculature

The central retinal artery is the first branch of the ophthalmic artery and enters the optic nerve approximately 1 cm posterior to the globe (figure 1.2A). Inside the eye, it emerges from the optic nerve head and divides into the superior and inferior papillary arteries, which in turn divide into nasal and temporal quadrantic branches (figure 1.2B). The retinal arteries are surrounded by a capillary free zone due to a sufficient oxygen supply through transarterial diffusion (figure 1.2C) (Pournaras et al., 2008). The branches of the superiortemporal and inferotemporal arteries give rise to a two-layered peri-macular vessel ring creating a foveal capillary-free zone which allows light to pass directly to the fovea without obstruction. From the inner surface of the retina arterioles extend into deeper layers forming distinct capillary networks. Depending on the thickness of the retina, this capillary meshwork can vary from three layers at the posterior pole to one layer in the periphery (Shimizu K and Kazuyoshi U, 1978). At the posterior pole the arterial branches supply the superficial radial peripapillary capillaries in the nerve fiber layer (RPCs), the inner capillary network located in the ganglion cell layer and the deep capillary network in the inner nuclear layer. The postcapillary venules drain through the corresponding venous system to the central retinal vein.

Retinal capillaries are 5–6µm in diameter and consist of non-fenestrated endothelial cells that are surrounded by pericytes in a 1:1 ratio. The retinal capillary endothelial cells possess numerous tight junctions and are the major component of the inner blood-retinal barrier. Retinal pericytes contain contractile proteins such as actin and myosin which can constrict or dilate depending on the vascular microenvironment and are directly involved in the local control of retinal blood flow (autoregulation).

1.1.2.2 Choroidal vasculature

The choroid is a highly vascularised tissue layer located between the retina and sclera. It is separated from the RPE by Bruch's membrane, from the sclera by the lamina fusca. The choroidal vasculature is nourished by 10 to 20 short posterior ciliary arteries (SPCA) that arise from the ophthalmic artery and pierce the posterior pole of the sclera to enter the choroid and supply the posterior portion of the choriocapillaris up to the equator. In addition, long posterior ciliary arteries (LPCA) nourished by the ophthalmic artery pierce the sclera and course anteriorly in the suprachoroidal space to their branch point near the ora serrata, sending branches posteriorly to supply the choriocapillaris up to the equator. The thickness of the choriocapillaris gradually decreases from 0.2 mm at the posterior pole to 0.1 mm at the ora serrata. Whereas the capillary network is dense and alveolar at the posterior pole (lobular pattern), the intercapillary spaces are widened and lobules become more polygonal and elongated at the equator (spindle pattern). In the far periphery choroid branching is less frequent and radial capillary orientation predominates (ladder pattern). Unlike most

vascular systems in the body the choroidal arteries and veins do not run parallel. Postcapillary venules form afferent veins that converge around the inner sclera of the four quadrants to vortex veins that pierce the sclera and drain into the superior and inferior ophthalmic veins (figure 1.2. A,D,E).

Choroidal vessels are surrounded by smooth muscle cells and controlled by a perivascular nervous plexus comprising both divisions of the autonomic nervous system (Bill and Sperber, 1990; Lutjen-Drecoll, 2006). The wall of the choriocapillaris facing Bruch's membrane is fenestrated with circular openings (fenestrae) measuring approximately 80 nm, Even though choroidal capillaries contain fenestrated endothelium and have no tight junctions, their adjacency to Bruch's membrane and the RPE with its intercellular junctions secure a tight blood-retinal barrier.

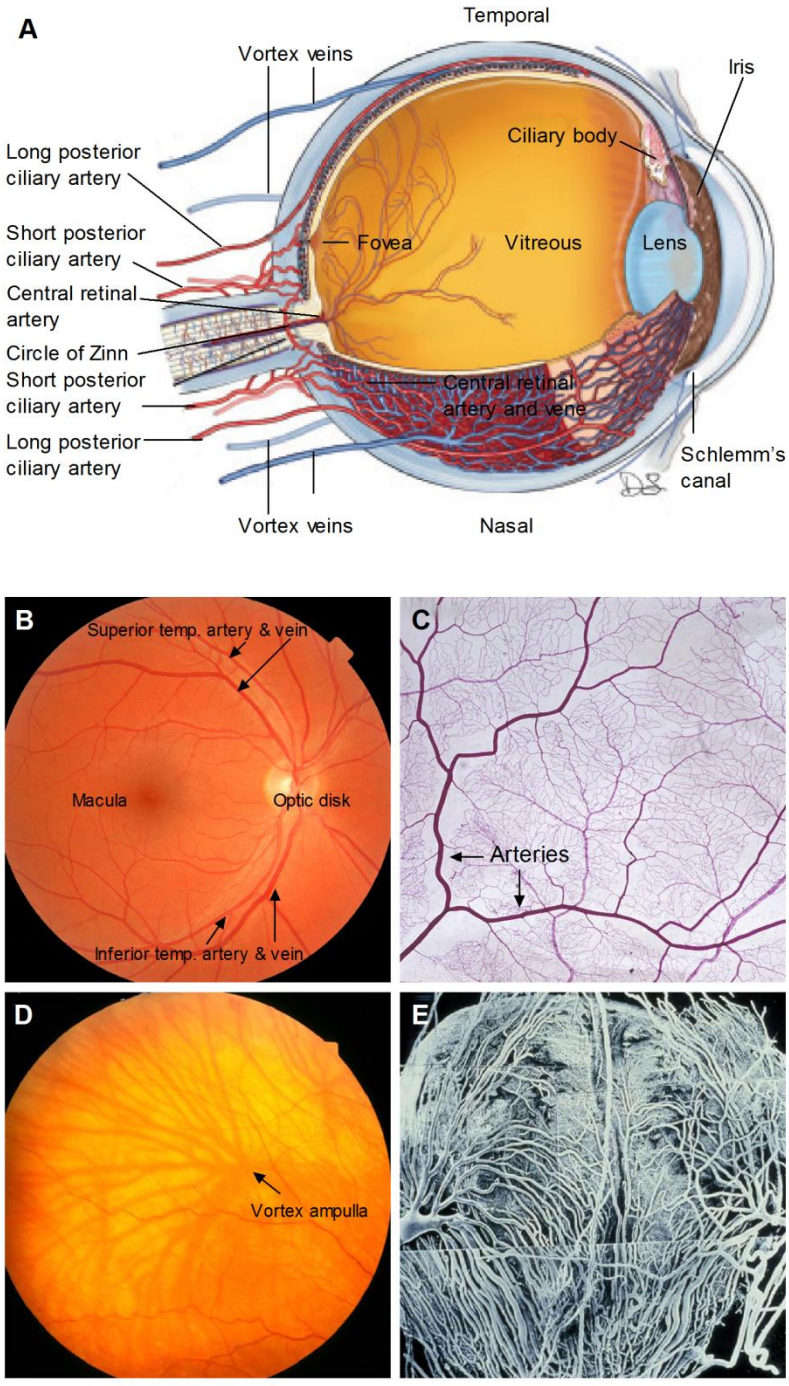

Figure 1.2 Retinal and choroidal vasculature. A) Cutaway drawing of the human eye. The view is from a superior position over the left eye and the horizontal section passes through both the optic disk and the fovea. **B,C)** Funduscopic view and histology of the retinal vasculature. **D,E)** Funduscopic view and vascular cast of the choroidal vasculature. Drawing by Dave Schumick. Images adapted from (Anand-Apte B and Hollyfield J K, 2010) and www.atlasofophthalmology.com.

1.1.3 Anatomy of the murine retina

As many of the experiments presented in this thesis deal with the retina of mice, some remarks on the development and anatomy of the murine retina are necessary. Even though the basic functional organisation of the murine retina is similar to the human retina, there are some differences:

The mouse has a relatively small eye and measures 3.4 mm from the centre of the cornea to the posterior pole. It is characterised by a relatively large cornea and lens, the latter accounting for 60% of the axial length (Remtulla and Hallett, 1985). As in other nocturnal mammals, rods greatly outnumber cones in the murine photoreceptor population at a ratio of 30:1. As in all mammals except the primates the mouse retina does not have a macula although the density of rods and cones peaks in the area centralis and decreases more peripherally.

In contrast to the human, mice are born with an avascular retina reflecting the fact that they are born at an earlier developmental stage. During the first week after birth the superficial layer of the retinal vasculature sprouts from the optic nerve head to the peripheral retina. Over the following two weeks three parallel vascular networks are established within different layers of the retina.

In adult mice multiple retinal arteries arise from the central retinal artery and radiate away from the optic nerve head across the vitreous surface of the retina feeding different regions of the mouse retina. Venous drainage follows the retinal arteries back to the optic nerve head and leaves the eye through the central retinal vene (Watson et al., 2012).

1.2 Development of the eye

1.2.1 Development of the optic cup and the retina

The vertebrate eye develops from three different germ layers: the neuroectoderm of the diencephalon, the surface ectoderm of the epithelium and the intervening neural crest/mesoderm (figure 1.3A). During the third week of human gestation the primitive forebrain sprouts on either side to form two optic stalks and vesicles which are surrounded by mesoderm, the primordium of the vascular (arachnoida and choroidea) and fibrous layer (dura mater and sclera). During the fourth week of gestation, the optical vesicle comes into contact with the surface ectoderm which thickens and invaginates together with the underlying neuroepithelium of the optic vesicle to form the lens placode (figure 1.1 B,E). The lens differentiates and invaginates until it pinches off from the epithelium. The optic vesicle is converted into a double-layered optic cup by invagination of its distal and inferior wall (figure 1.1C,F). The outer layer of this cup will form the sclera, choroid and pigment epithelium, the inner layer will become the neuroepithelium (figure 1.1 D,G). The periphery of the optic cup, including the presumptive RPE, contributes to the formation of the ciliary body and iris anteriorly. The invagination, which also involves the optic stalk, allows axons to exit from the ganglion of the invaginated layer (i.e. the later neuroepithelium) via the optic nerve and also enables the entry of choroidal vessels. The periocular mesenchyme and cranial neural crest cells migrate in during formation of the optic cup and contribute to the development of the cornea, iris, ciliary body, sclera and blood vessels of the eye.

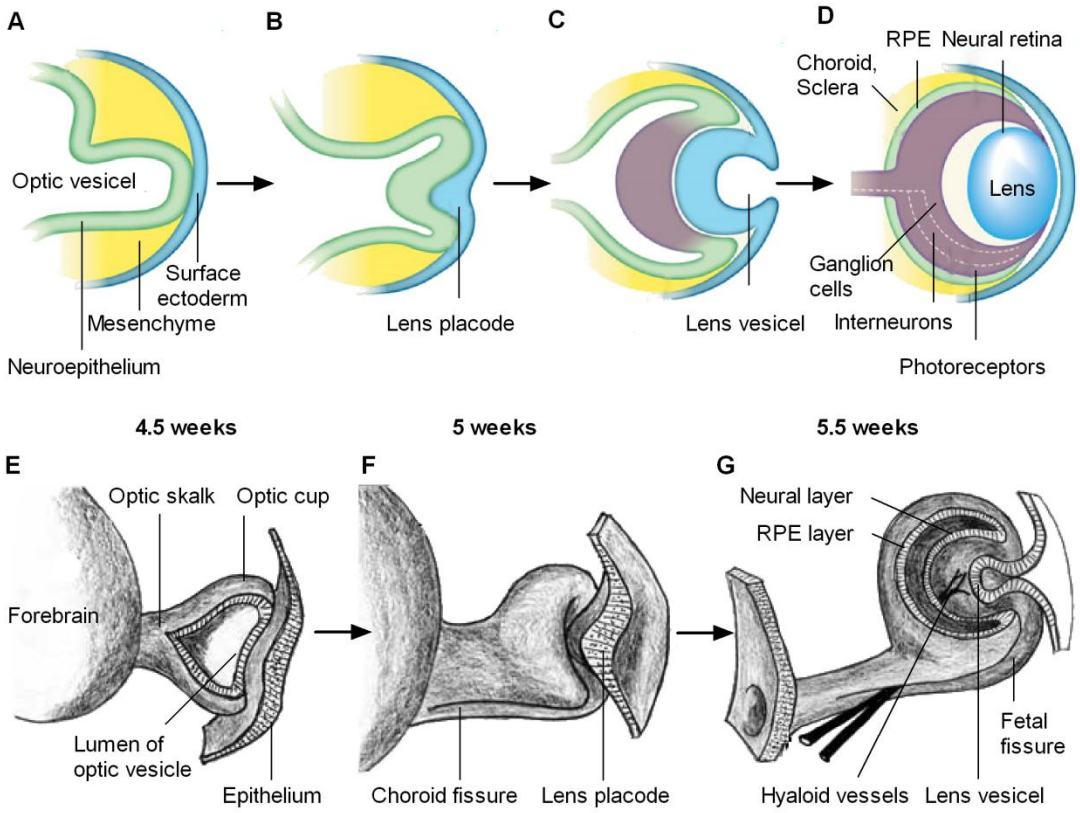

Figure 1.3 Development of the eye. At early stages of eye development, the optical vesicle induces thickening of the ectoderm and invagination of both epithelium (surface ectoderm) and underlying optic vesicle (neuroectoderm, **A-B,E-F**). The inner layer of the bilayered optic cup gives rise to the neural retina, the outer layer forms the sclera, choroid and retinal pigment epithelium (RPE, **C,G**). The mature neural retina comprises three cellular layers: photoreceptors, interneurons (horizontal, amacrine and bipolar cells), and retinal ganglion cells **(D)**. Adapted from (Ali and Sowden, 2011) and http://isc.temple.edu/neuroanatomy/lab/.

1.2.2 Development of the retinal vasculature

The development of the eye depends on the formation of a vascular system to provide nutrients and oxygen for the ocular tissues at the time of their active differentiation. During embryogenesis, this involves the *de novo* formation of blood vessels by differentiation of endothelial precursors to form the primary vascular network (vasculogenesis), and the formation of new blood vessels that branch off from existing vessels (angiogenesis) (Carmeliet, 2000). The brain and the eye are thought to be predominantly vascularised by angiogenesis (Fruttiger, 2007). However, there is accumulating evidence that the primary inner vascular plexus in the retina is formed by vasculogenesis (Chan-Ling et al., 2004). During the initial development of the eye, the oxygenation of the retina is ensured by the choroidal vessels and the hyaloid system. The vascularisation of the retina itself occurs only during the late gestation and is restricted to the inner part of the retina, with the outer retina completely avascular to avoid disturbance of light perception.

1.2.2.1 Development of the choroidal vasculature

The choroidal circulation develops at the same stage as the invagination of the optic vesicle and uveal development (Saint-Geniez and D'Amore, 2004). At the fourth week of gestation, the undifferentiated mesoderm surrounding the optic cup starts to differentiate into endothelial cells and a large plexus of primitive vessels adjacent to the RPE. The initial choriocapillaris develops by haemo-vasculogenesis, a process in which blood cells and blood vessels differentiate from a common precursor, the haemangioblast (Luty 2010). By the second

month of development the primitive vascular plexus envelops the entire exterior of the optic cup and the choriocapillary vessels begin to develop a basal lamina which, together with the basement membrane of the RPE, forms the initial Bruch's membrane, separating the neural retina from the choroid. In the third month of gestation the intermediate choroidal vasculature, the large choroidal vessels and anastomosis betwenn the vascular layers develop by angiogenesis (Luty 2010). The choroidal capillary network becomes almost completely organised by the twelfth week of gestation with connections to the posterior ciliary arteries and to rudimentary vortex veins that develop in all four quadrants of the eye. By the fourth month of gestation most of the choroidal vasculature matures (Anand-Apte B and Hollyfield J K, 2010).

Although the molecular mechanisms underlying the formation of the choroidal vasculature have not been fully defined, it is largely accepted that it depends on the presence of differentiated RPE cells and the production of inductive signal molecules such as VEGF, fibroblast growth factor (FGF)-9 and b-FGF (Saint-Geniez and D'Amore, 2004).

1.2.2.2 Development of the hyaloid vasculature

The process of intraocular vascularisation begins around the first gestational month with the entry of the hyaloid artery into the optic cup through the fetal fissure. The hyaloid artery extends through the primitive vitreous and reachs the posterior pole of the forming lens where it branches intensively to form a dense capillary network over the lens surface, the so called tunica vasculosa lentis (figure 1.4A). The hyaloid system is characterised by the absence of veins and

all hyaloid arterial vessels drain into the choroidal veins. As the lens develops, the tunica vasculosa lentis expands to reach the anterior part of the lens and forms the pupillary membrane. In later stages, in human during the second month of gestation, the hyaloid vasculature regresses and a vascular plexus emerges from the optic nerve head giving rise to the retinal vasculature (figure 1.4.B-C). The occlusion of the regressing capillaries has been suggested to depend on macrophages and on the levels of secreted growth factors such as Vegf and Angiopoietin 2 (Saint-Geniez and D'Amore, 2004).

.

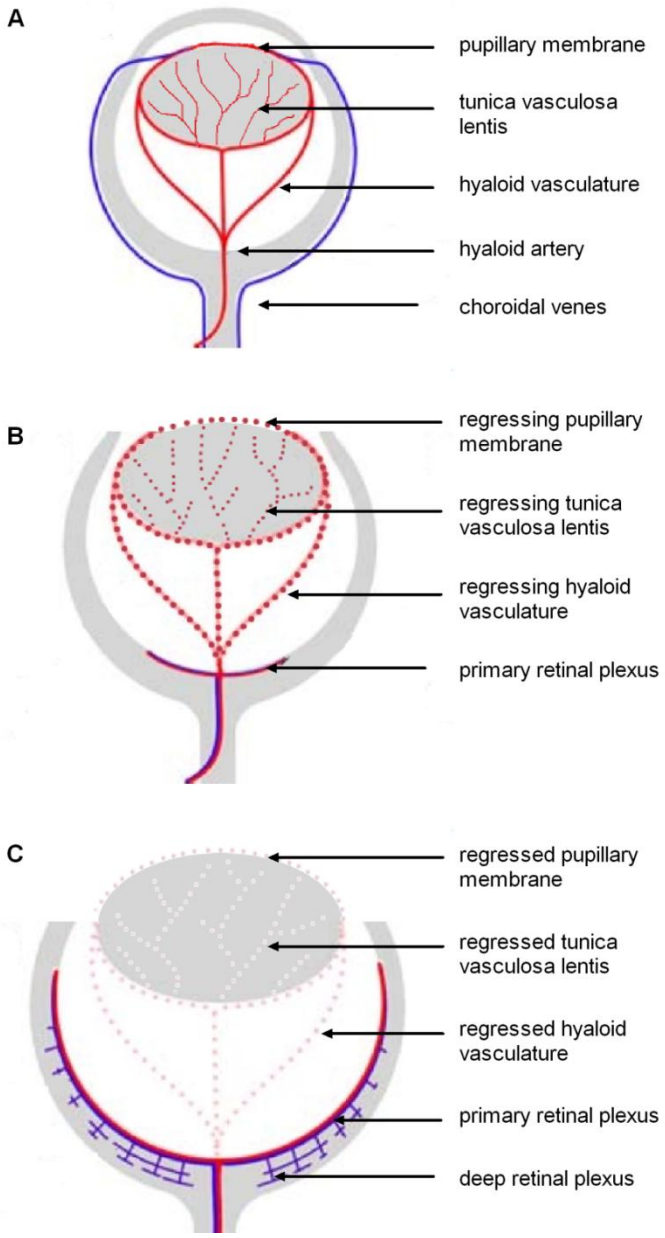

Figure 1.4 Development and remodeling of the hyaloid and retinal vasculature. Early in development, the hyaloid artery supplies the hyaloid vasculature, the tunica vasculosa lentis and the pupillary membrane; the venous drain is accomplished by the choroidal veins **(A)**. As the primary plexus grows into the retina, the hyaloid vasculature regresses **(B)** and the deeper plexus of the retinal vasculature develops from veins in the primary plexus (**C**). NB the choroidal vasculature is not shown in B and C. Adapted from (Fruttiger, 2007).

1.2.2.3 Development of the inner retinal vasculature

During early development the inner retina is metabolically supported by the hyaloid vasculature and remains avascular until the fourth month of gestation (figure 1.4A). As the retina matures and grows, the demand for oxygen and nutrition increases which necessitates the formation of a retinal vascular bed (Chan-Ling et al., 1995; Stone et al., 1995). Primitive retinal vessels emerge from the optic disc at the base of the hyaloid artery and spread to the periphery of the retina forming a primitive central retinal arterial system (figure 1.4B). The initial intense angiogenic process is followed by a process called pruning which describes the eradication of part of the vessels, in order to adapt the blood flow to the needs and physiologic characteristics of the differentiated tissues. Pruning occurs via selective endothelial cell death (Ishida et al., 2003) or via migration and relocalisation of endothelial cells (Hughes and Chang-Ling, 2000) and is particularly evident in the vicinity of arteries where capillary free zones emerge due to high oxygen tension present in arteries (Riva et al., 1986). Over time, as more vessels are added in the periphery, the primitive plexus is remodeled and starts to mature into a hierarchical vascular tree with clearly defined arteries, capillaries and veins. The primary vessel plexus at the inner retinal surface subsequently remodels into two parallel but inter-connected networks, located in the nerve fiber layer and the inner plexiform layers (figure 1.4C). These vascular beds are further remodelled by proliferation and apoptosis of endothelial cells which is closely controlled by hypoxia and Vegf gradients (Chan-Ling et al., 1995; Stone et al., 1995). The retinal vasculature in humans is fully mature at birth and remains quiescent unless the balance of angiogenic inhibitors is tipped

in favour of angiogenic activators (termed ‘angiogenic switch’) during hypoxia and ischaemia associated retinal disease (Carmeliet, 2000).

1.3 Perfusion and oxygenation of the retina

The retina is one of the most metabolically active tissues in the human body, consuming more oxygen per mg tissue than many other organs including the brain (Alm and Bill, 1972; Ames, III, 1992; ANDERSON, Jr. and SALTZMAN, 1964). Oxygen is transported to the retina by two independent physiologically different vascular circulations - the retinal circulation composed of superficial and deep capillary networks, and the choroidal circulation located under the retinal pigment epithelium (figure 1.5A).

1.3.1 Perfusion of the retina

The retinal circulation supplies oxygen mainly to the inner retina (Provis, 2001) and has a relatively low blood flow and high oxygen extraction (8 ml oxygen per 100 ml) compared to other tissues, resulting in a high arteriovenous oxygen saturation difference and low venous oxygen tension (Hickam et al., 1959; Hickam and Frayser, 1965). The retinal circulation has the capacity to autoregulate blood flow which helps to maintain oxygen homeostasis (Harris et al., 1998). Both endothelial and retinal cells release factors, such as nitric oxide (NO) and endothelin which modulate arterial tone, blood flow and oxygen delivery (Pournaras et al., 2008).

The choroidal circulation nourishes the outer retina including the retinal pigment epithelium and the photoreceptors. It has a 20-fold greater blood flow and a very

low rate of oxygen extraction compared with the retinal circulation resulting in a low arteriovenous difference and high reserve of oxygen transport capacity (Wangsa-Wirawan and Linsenmeier, 2003). The fenestrae of the choriocapillaris allow easy movement of large macromolecules into the extracapillary compartment. Oxygen, fluid and molecules escaping from these leaky vessels percolate through Bruch's membrane and have access to the basal side of the RPE. Whereas macromolecules are blocked from diffusing to the subretinal space by the outer blood-retinal barrier, oxygen can diffuse freely through the RPE and reach the photoreceptors (Anand-Apte B and Hollyfield J K, 2010).

1.3.2 Oxygenation of the retina

Inner retinal oxygenation has been measured directly using polarographic electrodes in several species including guinea pigs (Pournaras et al., 1989), cats (Linsenmeier, 1986), rats (Yu et al., 1994) and macaque (Ahmed et al., 1993) (figure 1.5B). In cats, rats and macaques, oxygen tension peaks in the inner and outer plexiform layers corresponding to the superficial and deep retinal vascular networks (figure 1.5C). The mean oxygen tension in the inner retina of the cat during dark adaptation is 18.5 mmHg (Linsenmeier and Braun, 1992) which is consistent with measurements of preretinal oxygen tension in cats of 18.9 mmHg (Alm, 1972). Although some studies reported no difference in oxygen consumption between darkness and steady illumination (Alder and Cringle, 1990; Medrano and Fox, 1995), the oxygen tension in the inner retina is slightly reduced in light adaptation compared with darkness (Linsenmeier and Braun, 1992). Retinal oxygen tensions are highest at the level of the choroid and drop

steeply between the choriocapillaris and the outer plexiform layer under light-adapted conditions. Mathematical modeling suggests that oxygen consumption is maximal in the inner segments of photoreceptor cells, amounting to 15 to 20 ml per 100 g of tissue per minute in the dark which reflects the metabolic demand of tightly packed mitochondria in this region (Haugh et al., 1990). In darkness, the partial pressure in the outer retina is considerably lower reaching 0 mmHg at the outer nuclear layer while the partial pressure in the choroid is unchanged (Ahmed et al., 1993; Linsenmeier, 1986). This finding reflects the increased oxygen consumption by photoreceptors in darkness which is needed for ATP production and maintenance of the dark current, in which Na+ ions are actively transported extracellularly by a Na+/K+ ATPase pump (Kimble et al., 1980). The low oxygen tension in the outer retina in darkness results in a reversed oxygen gradient and oxygen diffusion from the inner retinal circulation to the outer retina (Wangsa-Wirawan and Linsenmeier, 2003). The direct measurement of oxygen tension within the human retina has not been reported as it would present a significant risk of adverse effects.

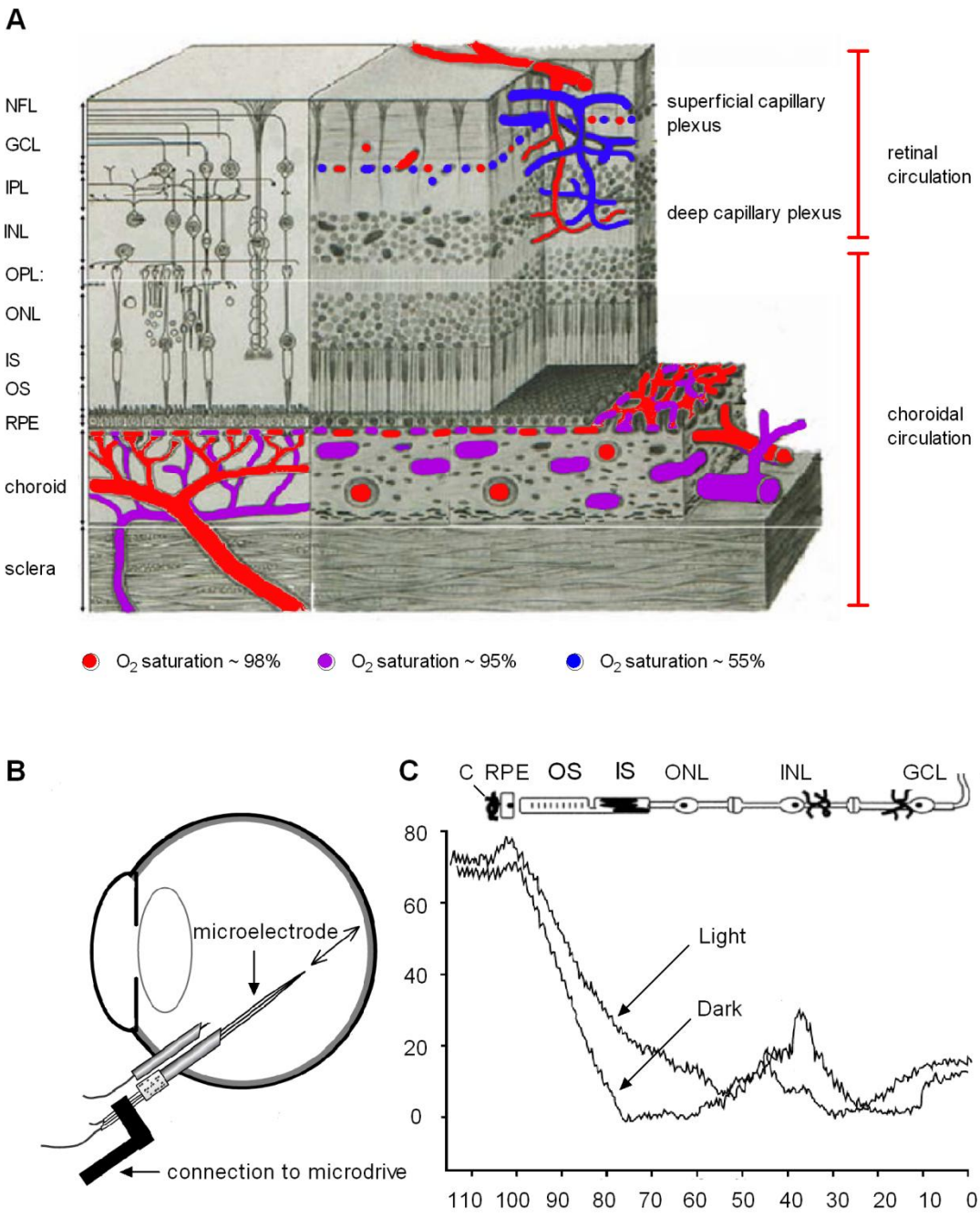

Figure 1.5 Perfusion and oxygenation of the retina. A) Schematic of the healthy retina and its vascular supply. NB: The vasculature is colour coded according to its oxygen saturation (Alm and Bill, 1970; Hardarson and Stefansson, 2010). RPE = retinal pigment epithelium; OS = outer segments; IS = inner segments; ONL= outer nuclear layer; OPL = outer plexiform layer; INL= inner nuclear layer; IPL= inner plexiform layer; GCL= ganglion cell layer; NFL= nerve fiber layer. Adapted from Mikroskopische Anatomie der Organe - Auge und Retina; H.-J. Wagner. B,C) Intraretinal oxygen tensions under light and dark adapted conditions in cats using an oxygen sensing microelectrode (Linsenmeier, 1986).

1.4 Oxygen sensing in the retina

Retinal hypoxia can be caused by systemic cardio-respiratory failure or local vascular insufficiency affecting the carotid, ophthalmic, retinal and/or choroidal circulations. The functional reserve of oxygen in the human retina lasts for only seconds and even transient localised oxygen deficits can produce irreversible cellular damage. Maintenance of normal retinal function therefore depends on a continuous supply of oxygen and the capability to detect and respond rapidly to local oxygen deficiency (Pournaras et al., 2008).

Systemic hypoxia is sensed by central chemoreceptors located near the respiratory centres in the brainstem medulla, and in the aortic and carotid bodies located on the aortic arch and at the bifurcation of the common carotid artery respectively (figure 1.6A-C). The mechanisms of hypoxia sensing in chemoreceptors involves hypoxia-induced depolarisation of mitochondrial membranes or suppression of K^+ channels, resulting in membrane depolarisation, calcium influx and secretion of neurotransmitters such as adenosine and dopamine (Lahiri et al., 2006). The release of these factors activates afferent nerve fibers in the glossopharyngeal (carotid body) or the vagus nerve (aortic bodies) projecting to the nucleus tractus solitarius in the medulla. In close coordination with other brainstem mechanisms including baroreceptor stimulation, activation of sympathetic efferent pathways induces adaptive cardio-respiratory responses to hypoxia that include increased

respiratory and cardiac rates, and modulation of regional blood flow by changes in vascular tone (Weir et al., 2005).

In addition to these systemic and regional responses, several mechanisms mediate adaptive responses to hypoxia within tissues at the cellular level. Mechanisms of oxygen sensing in the retina include acute changes in transmembrane ion permeability and stabilisation of key transcription factors which orchestrate multiple adaptive pathways to maintain oxygen homeostasis.

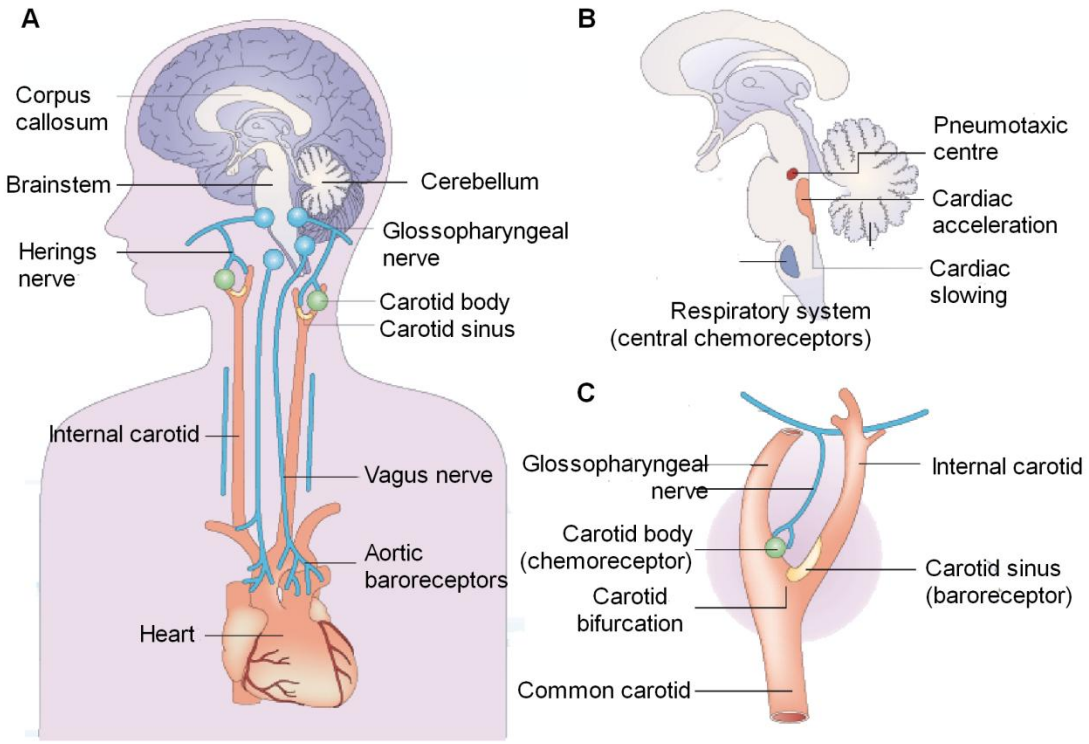

Figure.1.6 Systemic oxygen sensing. A) Structures and circuits involved in oxygen sensing at the systems level. B) Regulatory centres in the brainstem. C) Oxygen sensing at the carotid level.

1.4.1 Oxygen dependent ion channels

The literature on changes in ion permeability of the retinal vasculature cells upon hypoxia is sparse. Most of our understanding on these acute responses to hypoxia is based on the investigation of the microvasculature of the central nervous system. Since the microvasculature of the CNS and the retina share many similarities it is reasonable to deduce indirect evidence from these results for the retina. The resting membrane potential and the contractile status in smooth muscle cells and pericytes surrounding endothelial cells depend upon the balance of K^+, Ca^{2+} and Cl^- channel activity. In recent years, different oxygen sensitive ion channels have been suggested to function as oxygen sensors and to contribute to relaxation of vascular smooth muscle under hypoxic conditions. These channels are stimulated by low oxygen itself or by secondary changes to hypoxia, including reduced ATP levels, increased ADP levels and reduced intracellular pH (Lopez-Barneo et al., 1997). ATP-gated K^+ channels (K_{ATP}) in smooth muscle cells have been proposed to be a critical link between hypoxia and vasodilatation in coronary and cerebral arterioles during hypoxia. Under normoxic condition K_{ATP} channels are inhibited by intracellular ATP. During hypoxia, a lack of ATP results in increased transmembrane K^+ flux which is followed by cell hyperpolarisation, closure of voltage-dependent Ca^{2+} channels and a reduction in intracellular Ca^{2+} levels, resulting in vasorelaxation and dilatation (Daut et al., 1990; Standen et al., 1989). Furthermore, hypoxia has been shown to decrease Ca^{2+} flux in smooth muscle cells by a direct effect on Ca^{2+} channels or indirectly by changes in ATP, pH, Ca^{2+} and Mg^{2+} (Ohya and Sperelakis, 1989; Okashiro et al., 1992; Rekalov et al., 1997). The extent to

which such changes in ion permeability upon hypoxia also occur in retinal and choroidal arteriolar smooth muscle cells and pericytes is currently not well-defined.

1.4.2 Oxygen dependent transcription factors

A major advance in the field of oxygen sensing has been the discovery of the family of hypoxia-inducible transcription factors (HIFs). HIFs are heterodimeric transcription factors, each composed of one of the 3 oxygen-sensitive HIFalpha subunits (HIF1alpha, HIF2alpha and HIF3alpha) and the oxygen-insensitive and constitutively expressed HIFbeta subunit (ARNT, figure 1.7).

1.4.3.1 Oxygen-dependent regulation of HIF

In normoxic condition HIFs are continuously and rapidly hydroxylated by 3 different catalyzing prolyl-4-hydroxylase isoforms (PHD 1-3) in a reaction that has an absolute requirement for molecular oxygen as a co-substrate (figure 1.7)(Bruick and McKnight, 2001). Hydroxylation of proline residues changes the conformation of HIF1a and increases its affinity for the von Hippel Lindau protein (pVHL) and other factors including elongin B and elongin C (Kibel et al., 1995), Cullin 2 (Pause et al., 1997) and RBX1 (Iwai et al., 1999) which results in proteasomal proteolysis of HIF1a by the ubiquitin-proteasome pathway (Ivan et al., 2001; Maxwell et al., 1999). Normoxia also stimulates binding of ARD1 to HIF1a (Jeong et al., 2002) which acetylates lysine 532 in the oxygen-dependent degradation domain of HIF1a and thereby increases the interaction between HIF and VHL and promotes proteasomal degradation of HIF1a (Sharp and Bernaudin, 2004). In addition, HIF alpha subunits are hydroxylated at a specific

asparaginyl residue by another member of the 2-oxoglutarate-dependent-oxygenase superfamily, which was originally identified as a protein that binds HIF and was named factor inhibiting HIF (FIH) (Mahon et al., 2001). This asparaginyl hydroxylation abrogates the interaction between HIF1 and the transcriptional co-activator p300/CBP and provides a second oxygen-regulated mechanism by which HIFa molecules that escape the prolyl-hydroxylation/degradation pathway are prevented from activating gene transcription.

Under hypoxic conditions in contrast, prolyl hydroxylation is suppressed and HIFa subunits escape pVHL mediated degradation (Bruick and McKnight, 2001). Consequently, the alpha unit accumulates to high levels and is translocated to the nucleus where it dimerises with the beta unit (figure 1.7). The HIF1a/HIF1b dimer binds to p300/CBP and activates the hypoxia response element in various hypoxia-responsive target genes. This triggers the transcription of many genes that facilitate adaptation to low oxygen conditions including those encoding for vascular endothelial growth factor (VEGF) (Forsythe et al., 1996), inducible nitric-oxide synthase (iNOS) (Melillo et al., 1995), erythropoietin (EPO) (Wang and Semenza, 1996), endothelin-1 (ET-1) (Hu et al., 1998) and many others (table 1.1) (Sharp and Bernaudin, 2004). Although the increase of HIF1a in hypoxia is mainly controlled by the inhibition of the VHL degradation pathway, hypoxia was also shown to increase HIF1a translation by stabilisation of HIF mRNA in certain cell types (Bergeron et al., 1999).

1.4.3.2 Oxygen-independent regulation of HIF1a

Although originally named hypoxia-inducible factor, there is compelling evidence that HIFs can be activated by conditions other than hypoxia, such as ischaemic and inflammatory processes (Dalgard et al., 2004; Lu et al., 2002; Olson and van, V, 2011; Ren et al., 2011). HIF1a can be stabilised by lactate, pyruvate, and oxaloacetate independently of hypoxia (Dalgard et al., 2004; Lu et al., 2002; Ren et al., 2011). Moreover, nitric oxide was shown to stimulate HIF1a accumulation under normoxia by inhibition of prolyl-hydroxylases (Metzen et al., 2003). The relationship between HIF1a and NO, however, is controversially discussed as NO has also been reported to induce an increase in prolyl-hydroxylase-dependent degradation of HIF1a (Hagen et al., 2003). Furthermore various cytokines were reported to increase HIF1a levels, including insulin-like growth factor 1 (IGF1), interleukin-1ß (IL-1ß), transforming growth factor-ß (TGFß), tumour-necrosis factor-α (TNFα), insulin, and heregulin (Sharp and Bernaudin, 2004). The translation of HIF1a mRNA into protein is controlled by the phosphatidylinositol 3-kinase (PI3K)–AKT–FKBP12-rapamycin associated protein (FRAP) which is the mammalian target of rapamycin (mTOR) pathway and can be activated by various growth factors and cytokines (Treins et al., 2002).

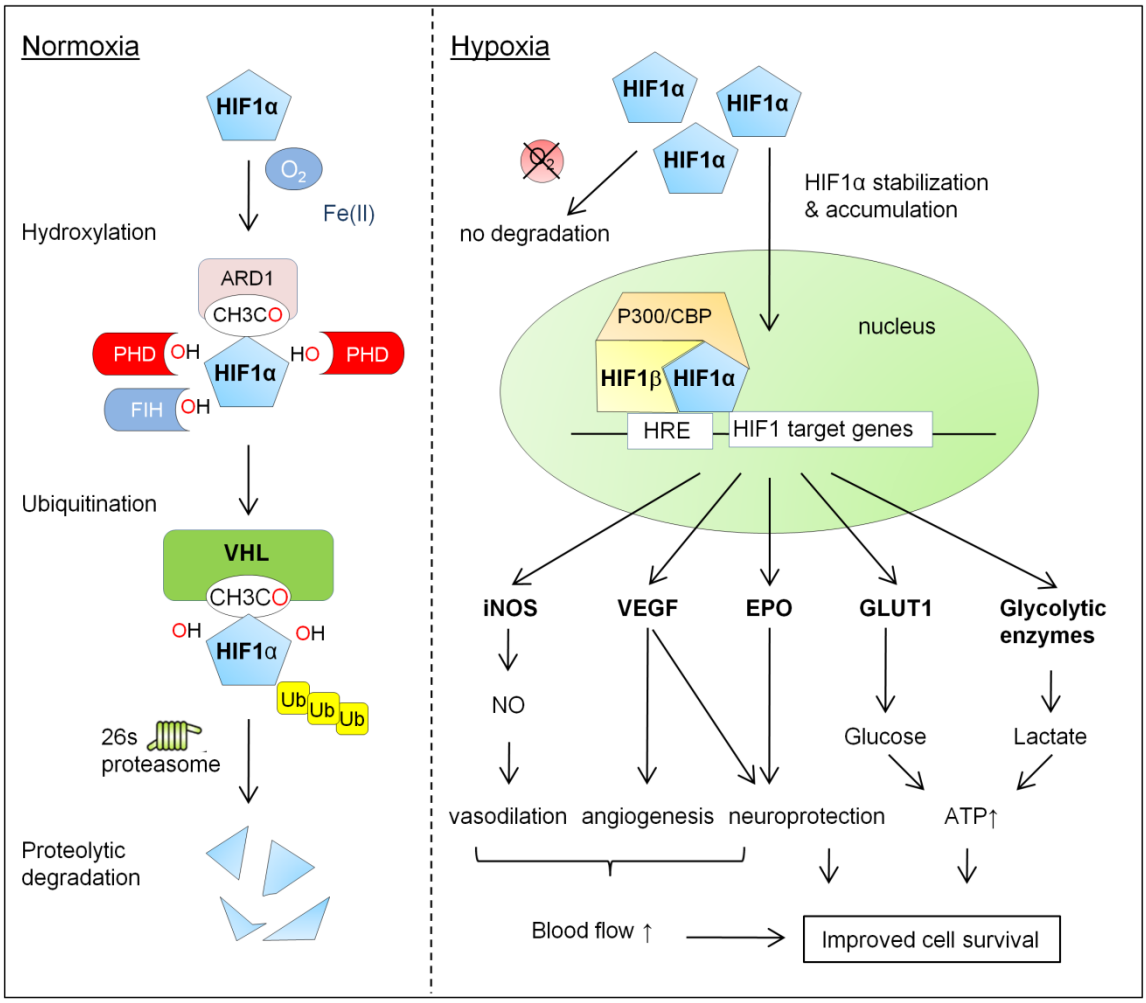

Figure 1.7 Oxygen dependent regulation and target genes of HIF1a. A) In normoxia, HIFa is hydroxylated by 'factor inhibiting HIF' (FIH-1) and prolyl-hydroxylase enzymes (PHD1-3). In addition, ARD1 acetylates lysine (L) 532 in HIFa to facilitate binding to the von Hippel Lindau protein (VHL) which promotes proteasomal degradation of HIF1a. B) Under hypoxic condition, hydroxylation of HIFa does not occur, which prevents VHL binding and HIFa degradation. HIFa accumulates in the cytosol and is translocated to the nucleus where it dimerises with HIF1b and activates hypoxia-response element in various target genes resulting in numerous adaptive responses to redress hypoxia.

1.4.3.3 Localisation and target genes of HIFa isoforms

HIF1a and HIF2a are expressed in different cells or tissues, resulting in activation of different target genes with non-overlapping functions. Whereas HIF1a is ubiquitously expressed and participates in most of the chronic cellular responses to low oxygen levels, HIF2a was originally thought to be restricted to endothelial cells and therefore initially named endothelial PAS domain protein 1 (EPAS, (Tian et al., 1997)). Recent work, however, has shown that HIF2a is more widely expressed than previously thought and is expressed in non-endothelial derived tissues such as lung, kidney, olfactory epithelium and adrenal gland (Lofstedt et al., 2007). Both HIF1a (Iyer et al., 1998) and HIF2a *knockout* mice (Tian et al., 1998) die in mid-gestation, with multiple cardiovascular malformations and mesenchymal cell death, showing that each gene has critical and non-redundant functions. Although HIF1a and HIF2a subunits are structurally similar in their dimerisation domains and DNA binding sites, they differ in their transactivation domains, which results in specific target gene regulation (Hu et al., 2007). Whereas HIF1a specifically regulates glycolytic genes (Hu et al., 2003; Wang et al., 2005) as well as carbonic hydrase-9 (Grabmaier et al., 2004) and BNIP3 (Raval et al., 2005), HIF2a exclusively regulates other factors such as the transcription factor Oct-4, cyclin D1, and TGF-α (Gunaratnam et al., 2003). Other hypoxia-inducible genes, such as vascular endothelial growth factor *(*VEGF*)*, facilitated glucose transporter-1 (GLUT1), adipose differentiation-related protein, adrenomedullin are regulated by both HIF1a and HIF2 (Hu et al., 2003). The role of HIF3a is poorly understood, but may regulate the activity of other HIFa isoforms as a dominant

negative regulation of HIFmediated control of gene expression (Makino et al., 2001).

1.4.3.4 HIF activation in the retina

Hypoxia-inducible transcription factors are activated in the retina both in development and disease. During retinal vascular development Hif1a is co-localised with Vegf in ganglion cells and cells along the inner border of the neuroblastic layer of mice which is consistent with a role in hypoxia, Vegf expression and physiological angiogenesis (Kurihara et al., 2010; Ozaki et al., 1999). Conditional inactivation of *Hif1a* in the peripheral retina results in arrested formation of the intermediate vascular plexus in the peripheral retina (Caprara et al., 2011), whereas an increase of Hifs in the neuroretina leads to dysmorphic retinal vascular development and persistence of embryonic vascular structures into adulthood (Kurihara et al., 2010; Lange et al., 2011). In healthy human and rat retina, HIF1a is detectable in the ganglion cell layer, inner nuclear layer, and outer nuclear layer suggesting that active HIF1a signalling occurs constitutively and has a physiological role in the human retina (Hughes et al., 2010). In addition to the physiological functions of Hifs in the retina there is accumulating evidence that HIFs also play a critical role in the pathogenesis of hypoxia associated retinal vascular disease (see chapter 1.6).

Role	HIF target genes	Reference
Vasomotor control		
	Adrenomedullin (ADM)	(Cormier-Regard et al., 1998)
	Nitric oxide synthase 2 (eNOS)	(Palmer et al., 1998)
	Nitric oxide synthase 3 (iNOS)	(Melillo et al., 1995)
	α1B adrenergic receptor	(Eckhart et al., 1997)
	Endothelin 1 (ET1)	(Hu et al., 1998)
	Tyrosin Hydroxylase	(Millhorn et al., 1997)
	Atrial natriuretic peptide	(Chun et al., 2003)
Angiogenesis		
	Vascular endothelial growth factor (VEGF)	(Forsythe et al., 1996)
	FLT1 (VEGF receptor 1, VEGFR1)	(Gerber et al., 1997)
	Platelet-derived growth factor B	(Kelly et al., 2003)
	Plasminogen-activator inhibitor-1	(Kietzmann et al., 1999)
	Apelin	(Ronkainen et al., 2007)
Hormonal regulation/ Erythropoiesis		
	Connective tissue growth factor (CTGF)	(Higgins et al., 2004)
	Erythropoietin (EPO)	(Wang and Semenza, 1993)
Iron metabolism		
	Transferrin	(Rolfs et al., 1997)
	Transferrin receptor	(Tacchini et al., 1999)
	Ceruloplasmin	(Mukhopadhyay et al., 2000)
Cell cycle control		
	DMT1	(Wang et al., 2010)
	p21 (WAF1/CIP1)	(Carmeliet et al., 1998)
	Insulin-like growth factor 2 (IGF2)	(Feldser et al., 1999)
	IGFBP1, IGFBP2, IGFBP3	(Tazuke et al., 1998)
	Endoglin	(Sanchez-Elsner et al., 2002)
	Wilms' tumour suppressor	(Wagner et al., 2003)
	α-Fetoprotein (negative regulation)	(Mazure et al., 2002)
Cell death		
	Calcitonin-receptor-like receptor	(Nikitenko et al., 2003)
	NIP3, NIX	(Bruick, 2000)
	P53	(An et al., 1998)
Cell migration		
	CXCR4	(Staller et al., 2003)
Energy metabolism		
	Glucose transporters 1 and 3 (GLUT1, GLUT3)	(Ebert et al., 1995)
	Prolyl-4-hydroxylase α1	(Takahashi et al., 2000)
	Phosphofructokinase	(Semenza et al., 1994)
	Lactate dehydrogenase A	(Semenza et al., 1994)
	Aldolases A and C	(Semenza et al., 1994)
	Pyruvate kinase M	(Semenza et al., 1994)
	Enolase 1	(Semenza et al., 1994)
	Hexokinases 1 and 2	(Iyer et al., 1998)
	Pyruvate dehydrogenase kinase	(Kim et al., 2006)
	Monocarboxylate transporter 4	(Ullah et al., 2006)
	Cytochrome oxidase isoform 2	(Fukuda et al., 2007)
	Glyceraldehyde phosphate dehydrogenase	(Graven et al., 1999)
	6-phospho-2-kinase/fructose 2,6 bisphosphatase	(Minchenko et al., 2003)
Miscellaneous		
	Plasminogen activator inhibitor (PAI1) 38	(Kietzmann et al., 1999)
	Transforming growth factor β3 (TGFβ3)	(Schaffer et al., 2003)
	Haem oxygenase 1	(Lee et al., 1997)
	Adenylate kinase 3	(O'Rourke et al., 1996)
	Phosphoglycerate kinase 1	(Semenza et al., 1994)
	Carbonic anhydrase 9	(Kaluz et al., 2002)
	Leptin	(Grosfeld et al., 2002)
	Rab20	(Hackenbeck et al., 2011)

Table 1.1 HIF target genes.

1.5 Adaptive responses to hypoxia in the retina

Retinal hypoxia can cause retinal degeneration and neuroretinal dysfunction that lead directly to vision loss. The oxygen sensing mechanisms described above control adaptive responses that can help protect against ischaemic injury and redress hypoxia. These responses comprise rapid compensatory changes in blood flow and expression of numerous genes (table 1.2) that activate adaptive molecular and cellular mechanisms.

1.5.1 Hypoxia-induced retinal vasodilatation

The inner retinal vasculature responds promptly to acute hypoxia by increasing vessel diameter and blood flow and thereby oxygen supply to the inner retina {Papst, 1982 527 /id;Linsenmeier, 1992 442 /id;Frayser, 1974 684 /id}. In humans, hypoxia leads to dilatation of retinal arterioles and venules by 8-9% within minutes (Brinchmann-Hansen et al., 1989). Prolonged hypoxia, in humans at high altitude, can increase retinal vessel diameter by 24% (Rennie and Morrissey, 1975); retinal blood flow can increase by 89% within 2 hours and by 174% after 7 weeks (Frayser et al., 1974). Choroidal blood flow is not significantly affected by moderate hypoxia suggesting that the choroidal circulation has excess capacity (Bosch et al., 2009; Kergoat et al., 2005). However, a substantial drop in venous oxygen saturation, such as can occur at prolonged high altitude, can induce increased choroidal blood flow that promotes oxygen delivery to the outer retina (Bosch et al., 2009).

The mechanisms that underlie hypoxia-induced vasodilatation involve changes in ion permeability in vascular smooth muscle cells and local generation of

vasoactive mediators (Pournaras et al., 2008). Various vasoactive compounds such as nitric oxide, hydrogen oxide, K^+, adenosine, GABA, adrenomedullin, excitatory amino acids and many others have been suggested as potential mediators of hypoxia-induced vasodilatation. Furthermore, it has been shown that hypoxia stimulates glial cells to release a 'retinal relaxing factor' that induces retinal vasodilatation independent of NO by activating a membrane bound Ca^{2+}/ATPase (Maenhaut et al., 2009). The direct link between hypoxia and the secretion of these factors has not been identified yet but may depend on changes in ATP levels and ion currents in hypoxic glial cells (Pournaras et al., 2008).

1.5.2 Hypoxia-induced retinal angiogenesis

A causative association between retinal hypoxia and angiogenesis was first suggested by Michaelson and further explored by Wise who speculated that a hypoxia-induced growth factor "factor X" was responsible for inducing retinal neovascularisation (Michaelson et al., 1954; Wise, 1956). Many candidate mediators have since been identified and VEGF has emerged as a particularly powerful proangiogenic growth factor (Aiello et al., 1994).

1.5.2.1 VEGF

VEGFs are a family of growth factors, expressed as a number of splice isoforms that vary in length and affinity to heparin (Holmes and Zachary, 2005). VEGFs bind to 2 high affinity receptors, VEGFR1 (de et al., 1992) and VEGFR2 (Millauer et al., 1993), promoting vascular permeability and proliferation of vascular endothelial cells in the eye (Miller et al., 1994), and facilitating the

migration of vessels by inducing the production of matrix metalloproteinases (Yancopoulos et al., 2000). VEGF signalling is essential for normal development of the retinal and choroidal vasculature (Marneros et al., 2005) and plays a central role in the pathogenesis and progression of common blinding disorders including diabetic retinopathy and age-related macular degeneration (AMD). Expression of VEGF and VEGFR1 is upregulated by activation of HIF1a in human retinal glial cells and RPE cells upon hypoxia (Liu et al., 2006; Zhang et al., 2007b). Hypoxia-induced upregulation of VEGF expression is inhibited by *siRNA* against HIF1a (Zhang et al., 2007b) and in retinal ischaemia by hyperoxia, presumably by promoting VHL-induced prolyl hydroxylation of HIFa (Pournaras et al., 1997). In the retina, increased levels of HIF1a precede VEGF upregulation and correlate both spatially and temporally with the development of retinal neovascularisation (Mowat et al., 2010).

1.5.2.2 Other HIF dependent angiogenic growth factors

In addition to mediating upregulated expression of VEGF and VEGFR1, HIFs promote the expression of several other proangiogenic factors in hypoxia, including adrenomedullin (ADM) (Cormier-Regard et al., 1998), plasminogen activator inhibitor (PAI) (Kietzmann et al., 1999), connective tissue growth factor (CTGF) and platelet-derived growth factor B (PDGFB)(Kelly et al., 2003). ADM is a ubiquitously expressed peptide initially isolated from phaechromyctoma (Kitamura et al., 1993) that protects endothelial cells against apoptosis (Ribatti et al., 2005). It is secreted from cultured human RPE in hypoxia (Udono et al., 2000) and associated with attenuation of ischaemia-induced injury (Zhu et al.,

2008). Platelet-derived growth factor B (PDGFB) is a potent mitogen for cells of mesenchymal origin. PDGFB elicits a variety of cellular responses including the migration, differentiation and function of a variety of specialised mesenchymal and migratory cell types, both during development and in the adult animal (Hoch and Soriano, 2003). Intraocular injection of adenovirus expressing a constitutively active form of HIF1a results in increased levels of PDGF-B in the eye which is associated with the formation of retinal neovascularisation (Kelly et al., 2003). CTGF controls growth, adhesion and survival of vascular endothelial cells (Perbal, 2004). Plasminogen activator inhibitor is the principal inhibitor of fibrinolysis and has been associated with promoting angiogenesis (Agirbasli, 2005). Both CTGF and PAI-1 levels are upregulated by hypoxia in cultured human RPE cells via HIF1a (Fuchshofer et al., 2009). The *in vivo* function of these molecules in the retina, however, is not well-defined and further studies will be necessary to elucidate their role in hypoxia driven physiological and pathological angiogenesis.

Increased retinal activity upon hypoxia		
Proteins	**species**	**reference**
HIF1a	rat	(Kaur et al., 2006)
HIF2a	mouse	(Thiersch et al., 2008)
NMDAR1	rat	(Kaur et al., 2006)
NMDAR2D	rat	(Crosson et al., 2009)
NMDAR2C	rat	(Crosson et al., 2009)
CCR2	rat	(Sivakumar et al., 2011)
GluR2	rat	(Kaur et al., 2006)
GluR3	rat	Kaur et al., 2006)
VEGF	rat	(Kaur et al., 2009)
IGF-I	rat	(Sivakumar et al., 2008)
IGF-II	rat	(Sivakumar et al., 2008)
Ang-2	rat	(Sivakumar et al., 2008)
nitric oxide	rat	(Kaur et al., 2006)
iNOS	rat	(Kaur et al., 2006)
eNOS	rat	(Kaur et al., 2006)
nNOS,	rat	(Kaur et al., 2006)
iNOS	rat	(Kaur et al., 2006)
Flk1	rat	Crosson 2009
Erythropoietin	rat	Crosson 2009
TNF-α	rat	(Sivakumar et al., 2011)
TNF-receptor 1	rat	(Sivakumar et al., 2011)
IL-1β,	rat	(Sivakumar et al., 2011)
IL-1 receptor 1	rat	(Sivakumar et al., 2011)
MCP-1	rat	(Sivakumar et al., 2011)
Decreased retinal activity upon hypoxia		
PEDF	rat	(Sivakumar et al., 2008)

Table 1.2 Hypoxia-induced molecular mediators in the retina.

1.5.3 Hypoxia-induced neuroprotection

1.5.3.1 Erythropoietin

Accumulating evidence indicates that HIFdependent expression of erythropoietin (EPO) can protect the retina against ischaemic injury. EPO is a glycoprotein produced in hepatocytes during development and by renal interstitial fibroblasts in the adult, in an oxygen-dependent manner controlled by HIF1a (Wang and Semenza, 1993). It acts as a hormone to regulate production of red blood cells in the bone marrow by preventing apoptosis of erythroid progenitor cells. In addition to its known function of stimulating haematopoiesis, EPO is expressed in many other adult tissues, including the spleen, the brain and the retina indicating a paracrine function (Fandrey, 2004). EPO and its receptor are expressed in the human retinal pigment epithelium and to some extend in the neuroretina (Garcia-Ramirez et al., 2008). Hypoxia-induced stabilisation of both HIF1a and HIF2a is associated with increased EPO expression in the eye (Grimm et al., 2002; Mowat et al., 2010). Activation of EPO receptors, which are expressed in photoreceptors (Grimm et al., 2002) and in the ganglion cell layer in rodents (Zhong et al., 2008), lead to autophosphorylation and activation of multiple signal transduction pathways including the Jak/STAT5 and AKT pathways that have multiple effects on gene transcription, caspase activation and inflammation (Li et al., 2004). EPO protects neuronal cells *in vitro* and *in vivo* by reducing nitric oxide-induced free radical damage (Sakanaka et al., 1998). Endogenous EPO is implicated in hypoxic preconditioning that protects photoreceptors against light-induced apoptosis (Grimm et al., 2002; Junk et al.,

2002) and can protect the retina against ischaemia-induced dysfunction (Mowat et al., 2010). Systemic EPO supplementation protects ganglion cells against ischaemia (Junk et al., 2002) and can protect the retinal vasculature against oxygen-induced vaso-obliteration (Chen et al., 2009). Reduction in local EPO by inhibition of HIF1a using the drug YC-1 (3-5'-hydroxymethyl-2'-furyl-1-benzylindazole) is associated with inhibition of retinal neovascularisation (DeNiro et al., 2010).

1.5.4 Hypoxia-induced adaption of retinal metabolism

1.5.4.1 Glucose metabolism

A critical adaptation to hypoxia is the ability of cells to utilise glucose by means other than mitochondrial oxidative phosphorylation, for which oxygen is an absolute requirement. Hypoxic activation of HIF1a shifts energy production from mitochondrial to glycolytic sources by inducing a wide range of genes involved in glucose metabolism (table 1.1) including GLUT1 that promotes glucose transport into the hypoxic cell (Badr et al., 1999; Ebert et al., 1995). In addition, HIF1a promotes expression of enzymes responsible for the glycolysis of intracellular glucose such as aldolase A (Iyer et al., 1998), hexokinases 1 and 2, phosphofructokinase 1 (Brahimi-Horn et al., 2007; Denko, 2008) and lactate dehydrogenase A. Under normoxic conditions pyruvate can be metabolised by oxygen-dependent mitochondrial oxidative phosphorylation to generate ATP efficiently. In hypoxia, however, pyruvate is converted by lactate dehydrogenase to lactate with less efficient generation of ATP. Hypoxic activation of HIF1a also downregulates mitochondrial function and oxidative phosphorylation by

promoting the expression of genes such as pyruvate dehydrogenase kinase 1 (Papandreou et al., 2006) and MAX interactor 1 (Zhang et al., 2007a) ultimately leading to reduced oxygen demand and consumption. The effect of these mechanisms is to compensate for hypoxia by reducing the oxygen demand while maintaining a supply of energy. In the retina, hypoxia induces an increase in extracellular concentration of lactate and increased utilisation of glucose (Doberstein et al., 1994). Lactate and glucose accumulates in the vitreous in proliferative diabetic retinopathy (Barba et al., 2010) and induction of hypoxia-responsive genes by cobalt chloride increases the expression of GLUT1 in the neuroretina.

1.6 Clinical significance of hypoxia in the retina

Retinal hypoxia has been associated with major causes of blindness including diabetic retinopathy, vascular occlusive disease, age-related macular degeneration and retinopathy of prematurity (Fulton et al., 2009; Stefansson, 2006; Stefansson et al., 2010). A common sequela to retinal hypoxia is the formation of aberrant new vessels which can lead to visual loss by increased vascular permeability causing retinal oedema, vascular fragility leading to haemorrhage, or fibrovascular scarring resulting in retinal detachment (Dorrell et al., 2007).

1.6.1 Age-related macular degeneration

Age-related macular degeneration (AMD) is the leading cause of blindness in people over the age of 60 in the western world (Congdon et al., 2003) and has been estimated to affect 18.5% among those 85 years or older (Mitchell et al., 1995). The etiology of AMD involves a complex interaction of genetic susceptibility, oxidative stress, environmental influences and inflammatory processes (Ding et al., 2009). Early signs of AMD include the presence of drusen and alterations of the RPE which can be followed by RPE atrophy (figure 1.10A), central retinal degeneration and a chronic, slow progressing loss of central vision. Approximately 10%–15% of all AMD patients convert to the exudative form of AMD which is defined by the development of choroidal neovascular membranes that result in the formation of subretinal fluid, haemorrhage and acute visual loss (figure 1.10B) (Tielsch et al., 1995). Current treatment options include laser photocoagulation, photodynamic therapy and anti-VEGF agents such as pegaptanib sodium and ranibizumab which have been approved for the treatment of neovascular AMD (Chiang and Regillo, 2011).

Accumulating evidence indicates that hypoxia is involved in the development and progression of age-related macular degeneration (Stefansson et al., 2010). Individuals with AMD are more likely to have reduced choroidal perfusion (Grunwald et al., 1998; Grunwald et al., 2005; Metelitsina et al., 2008) or watershed perfusion defects (figure 1.10C) (Chen et al., 2001) which is associated with a dropout of choroidal capillaries adjacent to active choroidal

neovascularisation (figure 1.10D) (McLeod et al., 2009). Thickening of Bruch's membrane and the formation of subretinal drusen increase the distance between the choroid and photoreceptors and may further limit oxygen availability (Bird, 1993; Stefansson et al., 2010). Hypoxia-induced expression of VEGF might paradoxically even exacerbate hypoxia by inducing accumulation of subretinal fluid which further increases the distance between the photoreceptors and the choroid (Stefansson et al., 2010). Hypoxia-induced activation of HIF signalling in the RPE and photoreceptors has been proposed to promote choroidal neovascularisation in AMD (figure 1.10E). HIF1a, HIF2a and VEGF expression was shown to be evident in RPE and CNV membranes (Inoue et al., 2007; Sheridan et al., 2009), with activation of HIF2a particularly prominent (Sheridan et al., 2009). However, little is known about the consequences of HIF activation in the RPE on the retina and its vasculature *in vivo*. This work therefore aims to study the function of Vhl and Hif1a in the RPE and to determine the consequence of Hif activation in the RPE using a tissue-specific conditional-*knockout* approach in mice.

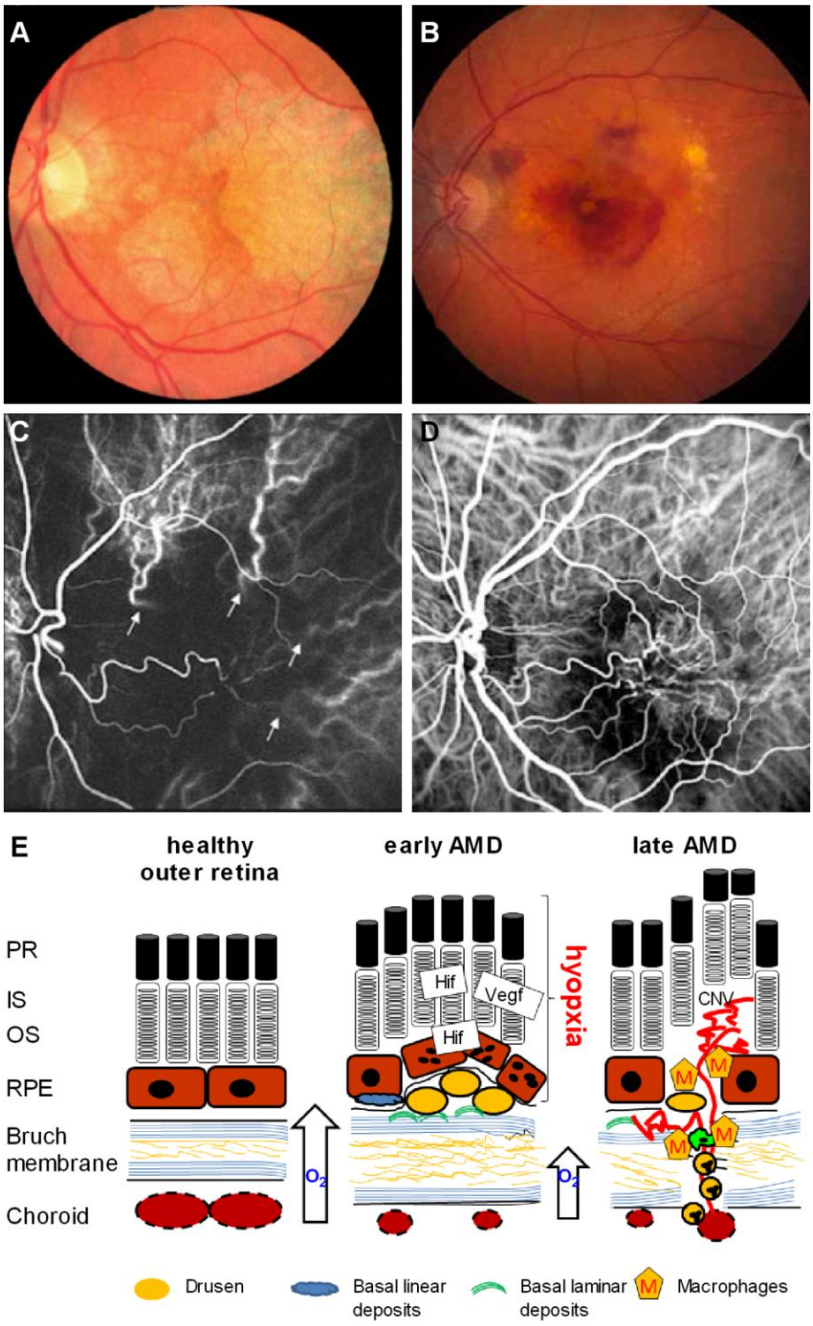

Figure 1.10 Clinical features of age-related macular degeneration. Color fundus images showing a large area of choroidal and pigment epithelial atrophy **(A)** and a subretinal haemorrhage from submacular neovascular fronds **(B)**. ICG angiography demonstrating a central watershed zone with decreased choroidal perfusion **(C)** which is associated with a choroidal neovascularisation in its center (**D**, late phase). **E)** Schematic demonstrating the postulated role of hypoxia and HIF signalling in the progression of AMD (Stefansson et al., 2010). Images adapted from www.atlasofophthalmology.com.

1.6.2 Diabetic retinopathy

Diabetic retinopathy (DR) is one of the most frequent and severe complications of diabetes mellitus with an estimated 30-45% prevalence of all diabetics worldwide (International Diabetes Federation). Diabetic retinopathy is the most common cause of blindness in middle-aged subjects accounting for at least 12.000 new cases in the US (Congdon et al., 2003) and for 1.500 new cases in the UK per year (Cormack et al., 2001). Diabetic retinopathy is caused by prolonged high blood glucose levels which can result in pericyte loss, oxidative stress and microvascular occlusion that commonly lead to hypoxia and ischaemia restricted to the inner retina. Early clinical signs of diabetic retinopathy include increased capillary permeability, haemorrhages and the formation of microaneurysms and capillary dilatation adjacent to areas of capillary nonperfusion (Pfister et al., 2008). As the disease progresses, the development of macular oedema, preretinal neovascularisation, haemorrhages, tractional retinal detachment can cause severe visual loss (figure 1.8). To this date the only approved therapy to prevent the development and progression of DR is a good glycemic control (UKPDS group, 1998). In more severe cases, such as advanced non-proliferative diabetic retinopathy and proliferative diabetic retinopathy, argon-laser retinal photocoagulation may be indicated which can result in a regression of the newly formed vessels (DRSR group 1981). Although effective, panretinal photocoagulation can cause severe adverse effects including decreased night vision, constricted visual field, persistent dilation of the pupil, or transient oedema of the retina. Refractory cases with PDR frequently require surgical intervention by pars plana vitrectomy which results in a

reduction of macular oedema and neovascularisation (Tachi and Ogino, 1996). Insight into the molecular mechanisms of neovascular eye disorders has provided new approaches for pharmacological treatment, i.e. the intravitreal application of antiangiogenic substances. Even though several antiangiogenic drugs such as the VEGF binding aptamer pegaptanib (Adamis et al., 2006; Cunningham, Jr. et al., 2005), the VEGF binding antibody bevacizumab (Avery et al., 2006; Jiang et al., 2008; Mason, III et al., 2008; Moradian et al., 2008; Simo and Hernandez, 2008; Thew, 2009) or its fragment ranibizumab (Chun et al., 2006) have promising effects and are already in clinical trials (e.g. NCT00407381, NCT00545870), an ideal pharmaceutical therapy to treat PDR has not yet been found.

Substantial evidence indicates important roles for HIF signalling and hypoxia in the pathogenesis and progression of diabetic retinopathy. Hif1a is upregulated by hyperglycemia in rodents (Li et al., 2006; Lin et al., 2011), and Hif2a is upregulated in the retina of mice with diabetes (Wright et al., 2010). In humans, the concentrations of both HIF1a and VEGF are increased in the vitreous of patients with proliferative diabetic retinopathy and correlate with disease activity (Wang et al., 2009). Other HIF1a-dependent downstream molecules such as EPO (Inomata et al., 2004), soluble VEGF receptor (Matsunaga et al., 2008) and CTGF (Kuiper et al., 2008) are increased in the vitreous of subjects with proliferative diabetic retinopathy. Furthermore, immunohistochemistry studies demonstrated a strong staining for HIF1a on surgically excised fibrovascular membranes from subjects with proliferative diabetic retinopathy (bu El-Asrar et

al., 2007; Lim et al., 2010). Taken together, these findings strongly suggest that HIFs are involved in the pathogenesis and progression of diabetic retinopathy by promoting adaptive responses to tissue hypoxia including the secretion of proangiogenic factors such as EPO, CTGF and VEGF.

The cellular origin of proangiogenic cytokines and their upstream regulators in DR, however, is still poorly understood. Increasing evidence suggests that activated myeloid cells, such as macrophages and microglial cells, accumulate in the inner retina of early DR and contribute to the development of retinal neovascularisation (Zeng et al., 2008a). Systemic depletion of macrophages by clodronate liposomes significantly reduces VEGFA levels as well as the development of retinal neovascularisation in mouse models of oxygen-induced retinopathy (OIR) (Kataoka et al., 2011). These data raised the possibility that myeloid cells are activated in DR and promote the development of retinal neovascularisation by releasing angiogenic factors such as VEGFA. Yet, the role of Hif1A and its contribution to *Vegfa* expression in myeloid cells recruited to sites of retinal neovascularisation has not been defined. This work therefore aims to explore the roles of myeloid cell derived *Hif1a and Vegf* in the development of retinal neovascularisation in the OIR mouse model by studying transgenic conditional *knockout* mice (see chapter 4).

Areas of capillary nonperfusion and decreased retinal blood flow detected by fluorescein angiography in early diabetic retinopathy (Kawagishi et al., 1995; Konno et al., 1996) have led to the current hypothesis that inner retinal hypoxia is a critical component in the pathogenesis and progression of diabetic

retinopathy (D'Amore, 1994; WISE, 1956). Direct evidence of tissue hypoxia in human diabetic retinopathy, however, is sparse and most of our knowledge is derived from experiments using diabetic animal models. Inner retinal oxygen tension is reduced by half in cats with long-term diabetes before capillary dropout is evident, suggesting that inner retinal hypoxia is preceding morphological changes (Linsenmeier et al., 1998). Furthermore hypoxia is evident in diabetic rats on magnetic resonance imaging (Trick and Berkowitz, 2005) and in diabetic mice on immunohistochemistry using the oxygen-dependent chemical probe pimonidazole (de Gooyer et al., 2006). Indirect evidence of the role of hypoxia in early diabetic retinopathy in man includes hyperoxia-induced reversal of electroretinographic changes (early oscillatory potential reduction) (Drasdo et al., 2002), ameliorated contrast sensitivity deficit (Harris et al., 1996) and reduced macular oedema (Nguyen et al., 2004). Oxygen tension measured using an optical oxygen probe in humans with diabetes is reduced in the mid-vitreous, a site which is believed to reflect global oxygenation of the retina (Holekamp et al., 2005). The distribution of oxygen across the human vitreous and retina and its relation to vitreous HIF1a and cytokine levels in PDR, however, is not well defined and will be further explored in this thesis.

.

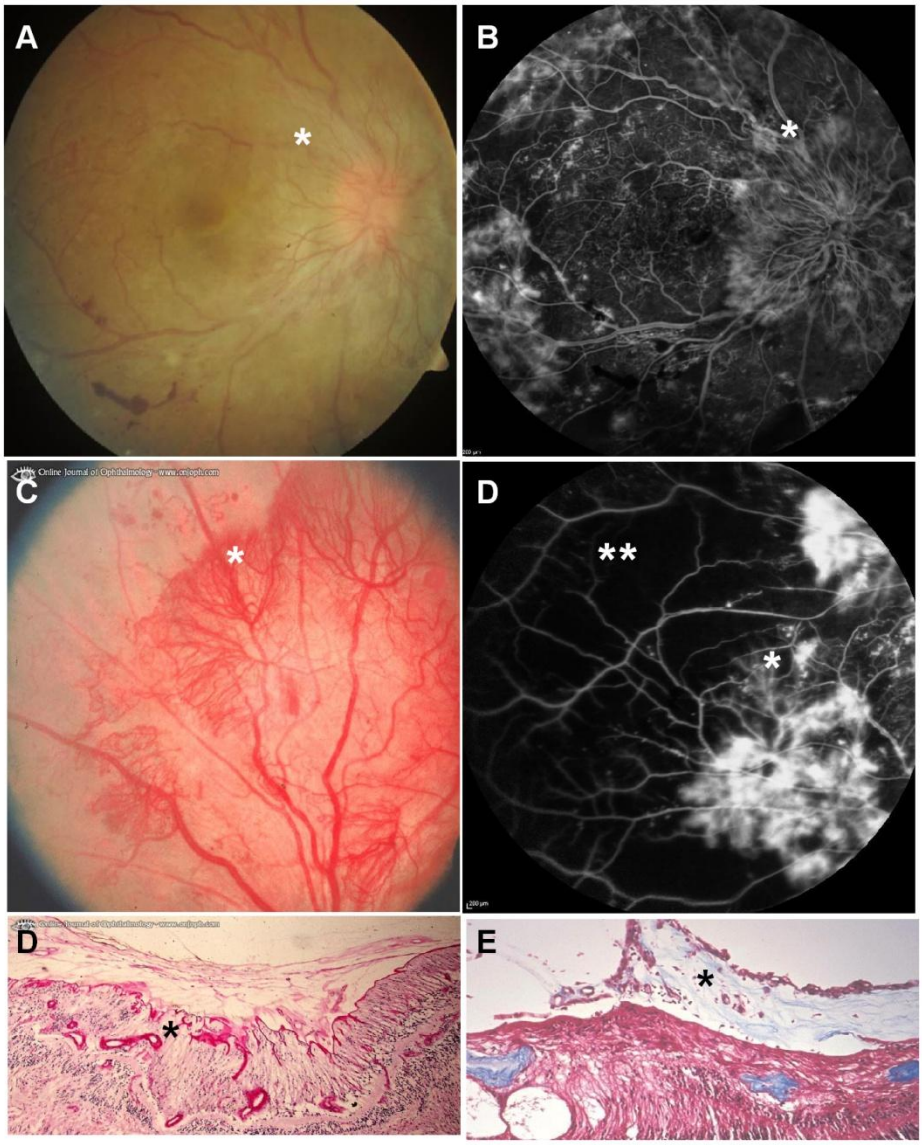

Figure 1.8 Clinical features of proliferative diabetic retinopathy. Color fundus images (A,C), fluorescein angiograms (B,D) and histological sections (D,E) showing preretinal neovascularisation (*) that typically occur at the disc and along the arcades close to ischaemic areas (**). Images adapted from www.atlasofophthalmology.com.

1.6.3 Vascular occlusive disease

Retinal vascular occlusive diseases develop when terminal veins or arteries are blocked resulting in hypoperfusion and hypoxia of the inner retina. Central retinal vein occlusion (CRVO) and branch retinal vein occlusion (BRVO) are found in individuals over 50 years old and are associated with common cardio-metabolic risk factors such as diabetes mellitus, systemic hypertension and atherosclerotic cardiovascular disease (Rodriguez et al., 2010). Central and branch retinal vein occlusion are caused by a thrombus which blocks retinal perfusion (Laatikainen, 1976). The ischaemic forms of central retinal vein occlusion, hemi-central retinal vein occlusion and branch retinal vein occlusion all frequently lead to the formation of retinal neovascularisation and a poor visual outcome (figure 1.9A-B) (Hayreh et al., 1983; Hayreh and Podhajsky, 1982). Arterial occlusions cause an abrupt reduction in retinal blood flow and occur mostly as a result of atherosclerosis or an embolic event. The most common site of obstruction is the central retinal artery behind the lamina cribrosa (figure 1.9C-D). Whereas central retinal artery occlusion causes a widespread loss of vision, branch retinal artery occlusion causes a segmental loss of vision. Nonperfusion of the inner retinal vasculature compromises the energy and oxygen supply to the retina, which, if prolonged, leads to permanent retinal degeneration. The prognosis for vision is poor, as even after restoration of perfusion, recovery of vision is minimal (Hayreh et al., 1983).

Both central and branch retinal vein occlusion have been associated with a variable degree of capillary nonperfusion on fluorescein angiography (Hayreh,

2005; Laatikainen, 1976) and tissue hypoxia in the inner retina (Hardarson and Stefansson, 2010; Yoneya et al., 2002). Experimental retinal vascular occlusion in animal models results in inner retinal ischaemia and hypoxia (Bardy and Tsacopoulos, 1978; Pournaras et al., 1985; Pournaras et al., 1990a; Stefansson et al., 1981) resulting in anoxic cell death (Donati et al., 2008) and a rapid failure of neuroretinal function (Zhang et al., 2008). In some animal models retinal hypoxia was followed by the formation of retinal neovascularisation and extracellular oedema similar to the one observed in human (Pournaras et al., 1990a). In humans, central retinal vein occlusion is associated with reduced mid-vitreous oxygen levels (Williamson et al., 2009); while venular oxygen saturation is reduced arteriolar saturation can be relatively spared (Hardarson and Stefansson, 2010). In central retinal vein occlusion, hypoxia and vitreous upregulation of VEGF (Noma et al., 2011) and EPO (Stahl et al., 2010), are consistent with retinal activation of the HIF pathway.

To date there is no known effective medical treatment available for either the prevention of or the treatment of vascular occlusive disease. Fibrinolytic therapy is of limited use in the treatment of these diseases as emboli are frequently not fibrin based (Hayreh, 2005). Current treatment options for retinal neovascularisation in vascular occlusive disorders include panretinal laser photocoagulation or in severe cases pars plana vitrectomy. New approaches for pharmacological treatment include the intravitreal application of antiangiogenic substances, such as anti-VEGF or corticosteroids to reduce retinal oedema (Rehak and Wiedemann, 2010). Even though several antiangiogenic drugs

seem to have promising effects and are already in clinical trials (e.g. NCT01028248) an ideal pharmaceutical therapy to treat vascular occlusive disease has not yet been found.

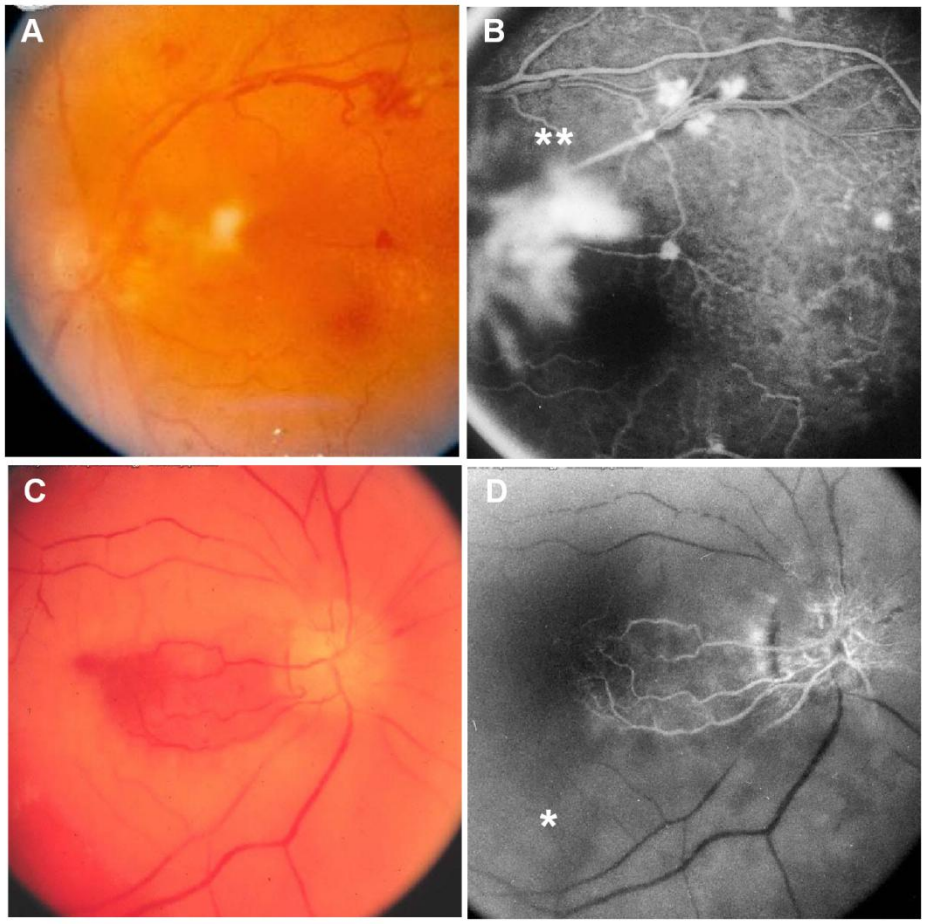

Figure 1.9 Clinical features of retinal vascular occlusive disease. Color fundus images (A,C) and correspondent fluorescein angiograms (B,D) of a branch retinal vein occlusion (A,B) and a central artery occlusion (C,D) showing areas of retinal neovascularisation (**) and nonperfusion (*). NB Perfused cilioretinal artery (D) which is present in 33% of eyes and nourished by the short posterior ciliary artery independent of the central artery. Images adapted from www.atlasofophthalmology.com.

1.6.4 Retinopathy of prematurity

Retinopathy of prematurity (ROP) is a major cause of blindness in children in the developed and developing world (Gilbert, 2008). It was first identified by Terry in 1942 and associated with premature birth and slightly later with oxygen supplementation in premature infants (Terry, 1944). Following the advent and progress of neonatology, infants with very low birth weight survive today and account for the substantial number of new cases of ROP in recent years (Palmer, 1996). Retinopathy of prematurity is a biphasic disease consisting of an initial phase of vessel growth cessation followed by a second phase of vessel proliferation. The first phase of ROP occurs from birth to postmenstrual age of 30-32 weeks. As the human retina is vascularised in the final trimester of gestation, the retina of prematurely born infants is incompletely vascularised with an avascular periphery. In this phase prematurely born babies are exposed to hyperoxia for pulmonary reasons which can cause growth retardation of retinal vessels. As the infant matures, the retina becomes increasingly metabolically active resulting in tissue ischaemia and hypoxia in the avascular periphery. The second phase of ROP begins around 32-34 weeks postmenstrual age and is associated with hypoxia-induced formation of retinal neovascularisation which can extend into the vitreous causing tractional retinal detachment and severe visual complications (Patz, 1968). For prognostic and therapeutic reasons staging of the disease was proposed based on the presence of a demarcation line (stage 1), the formation of an elevated ridge at

the demarcation (stage 2), preretinal fibrovascular proliferation (stage 3) and retinal detachment (stage 4, figure 1.11 A-H (ICROP, 2005))

Substantial evidence indicates an important role for HIF and its downstream factors VEGF and EPO in ROP. In the murine ROP model, both Hif1a and Hif2a signalling is increased in the avascular area (Mowat et al., 2010) and inhibition of Hif1a results in reduced Vegf and Epo levels which are associated with reduced retinal neovascularisation (DeNiro et al., 2010).

To date, the only approved treatment for ROP is laser photocoagulation of the non-vascularised peripheral retina (Ng et al., 2002). Although this treatment can reduce the incidence of blindness by approximately 25% in infants with ROP, it is associated with poor visual acuity after treatment and significant risks including corneal oedema, intraocular haemorrhage and cataract formation (Chen et al., 2011). Because of the significant role of VEGF in inducing retinal neovascularisation in ROP (Sato et al., 2009), anti-VEGF treatment has been suggested as a promising treatment option for ROP (Mintz-Hittner et al., 2011). Recent advances in angiogenesis research have also suggested a number of new ways to potentially treat ROP, such as targeting IGF1 signalling (Hellstrom et al., 2001) and dietary supplementation with omega-3 polyunsaturated fatty acids (Stahl et al., 2011).

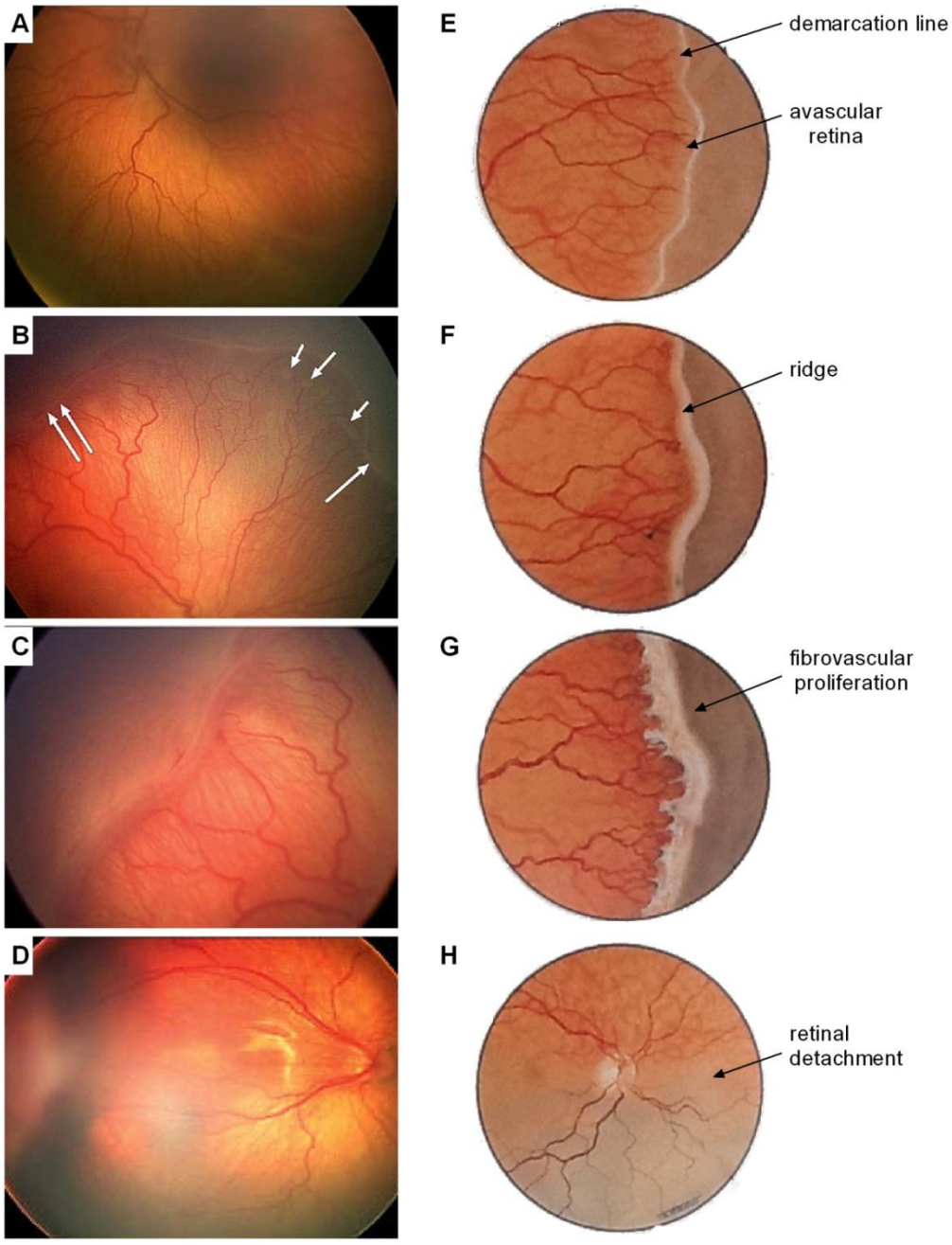

Figure 1.11 Clinical features of retinopathy of prematurity. Fundus photography demonstrating a demarcation line in ROP stage 1 **(A)**, the ridge between vascularised and avascular retina (single long arrow) and small isolated vascular tufts ("popcorn", short arrows) typical for ROP stage 2 **(B**), beginning fibrovascular infiltration of the vitreous (stage 3, **C**) and retinal detachment (stage 4, **D**). **E-H)** Corresponding drawings illustrating the key features of ROP stage 1-4. Adapted from (ICROP, 2005; J J Kanski, 1999).

1.7 Animal models of retinal hypoxia and neovascularisation

Animal models of retinal ischaemia and hypoxia are used to learn more about disease mechanisms, its diagnostics and potential treatments. They include models of diabetic retinopathy, vaso-occlusive disease, retinopathy of prematurity and choroidal neovascularisation.

1.7.1 Models of diabetic retinopathy

Diabetes in animals can occur spontaneously in the context of obesity, hyperinsulinaemia and insulin resistance or can be induced by a variety of experimental procedures, e.g. by means of surgery, viral infection or the administration of hormones and chemical agents (Mordes and Rossini, 1981). A number of rodent models exhibit clinicopathological features of human diabetic retinopathy, such as streptozotocin induced rats (Hammes et al., 1998), galactose fed rodents (Kern and Engerman, 1996; Roy et al., 2003) and genetically modified mice (Cohen et al., 2008; Shinohara et al., 2000). Many of these rodent models develop pre-proliferative retinal disease such as increased vascular permeability, capillary basement membrane thickening, microaneurysm formation, functional abnormalities and neuronal loss (Aizu et al., 2002), and are used to study the biology and treatment of early diabetic retinopathy. Despite many attempts to develop suitable models that accurately reflect human diabetic eye disease, very few animal models develop the severe vasoproliferative forms of diabetic retinopathy (Kador et al., 1995; Yamada et al., 2005). This is likely to relate to the short duration of diabetes in rodent models in comparison with diabetes in humans.

1.7.2 Models of retinal vascular occlusions

Retinal vascular occlusion can be induced in various rodent models by intravenous injection of a photoactive dye that is activated by laser exposure. Several models of retinal arterial (Braun and Linsenmeier, 1995; Yu et al., 2005) and venous (Miller et al., 1994; Yu and Cringle, 2001a) occlusions have been reported and were associated with increased inner retinal hypoxia, rapid neuronal degeneration and necrosis (Osborne et al., 2004). The induction of reproducible ischaemia and downstream abnormalities in these models, however, is difficult to attain and neovascularisation occurs only in a few models as a very late consequence of ischaemia (Tamura, 2001). Experimental models of vascular occlusion are therefore limited to examine retinal hypoxia and its downstream effects.

1.7.3 Models of oxygen.-induced retinopathy

Oxygen-induced retinopathy in the mouse and rat is a short term and reproducible model of hypoxic and ischaemic retinopathy (Penn et al., 1994; Smith et al., 1994). Exposure of neonatal animals to high concentrations of oxygen in the early postnatal period results in the development of central capillary vaso-obliteration which is associated with increased inner retinal hypoxia (Mowat et al., 2010) and the formation of retinal neovascularisation (Lange et al., 2007). The most commonly used mouse OIR model, the “75 model” (Smith et al., 1994), involves exposure to 75% oxygen from p7-p12. This mouse model demonstrates central retinal vaso-obliteration in contrast to a peripheral location in human ROP and rat OIR (Smith et al., 1994). This may be

because sufficient oxygen is supplied from the choroid at the thinner peripheral retina alongside the contribution of the hyaloid to peripheral retinal perfusion. In rodent OIR, neovascularisation can be quantified either by quantifying the area of neovascularisation and vaso-obliteration on vessel stained retinal flatmounts (Gardiner et al., 2005) or by serial section analysis of intravitreal vessels (Smith et al., 1994).

1.7.4 Models of choroidal neovascularisation

Models of choroidal neovascularisation include the laser-induced CNV model, models of injections of proangiogenic molecules and *knockout* or *knockin* transgenic mice. Based on the observation that choroidal neovascularisation can occur after argon laser photocoagulation in humans (Francois et al., 1975) Francois and Ryan (Ryan, 1979) developed a primate model to study the nature of choroidal neovascularisation. Since then the laser model has been adapted to monkeys, rabbits, (Kimura et al., 1995) rats, (Dobi et al., 1989) and mice (Balaggan et al., 2006; Dobi et al., 1989). In the laser-induced CNV model, argon laser photocoagulation of the posterior pole results in rupture of Bruch's membrane and in CNV formation which is associated with an increased number of macrophages and the expression of proangiogenic factors (Sakurai et al., 2003). Studies in monkeys have shown that the new vessels arise at the site of the laser and can infiltrate the subretinal space, or in a few instances enter the vitreous cavity (Archer and Gardiner, 1981b). Electron microscopy on laser-induced CNV lesion has demonstrated that the new capillary sprouts are comprised of primitive endothelial tubes, pericytes, and a loose basement-

membrane like material (Archer and Gardiner, 1981a). The laser-induced CNV model is by definition, more acute than age-related macular degeneration and does not reflect the pathogenesis of CNV formation in human AMD, although inflammation may play a role in each (Ryan, 1979). Despite many attempts to develop suitable models that develop spontaneous CNV formation, very few publications demonstrate convincing data. Okamoto et al. have reported the formation of retinal and subretinal neovascularisation in the rhodopsin-VEGF transgenic mice. The neovascularisation arose from the retinal vasculature rather than from the choroidal vasculature and this model may relate more closely to the human Retinal Angiomatous Proliferation (RAP), a variant of “wet” AMD (Okamoto et al., 1997). Lai et al. developed four human VEGF165 over-expressing transgenic mouse lines driven by the rhodopsin promoter. The animals developed phenotypes ranging from mild to severe retinal neovascularisation but did not show any choroidal neovascularisation (Lai et al., 2005).

1.8 Therapeutic intervention for retinal hypoxia

1.8.1 Improving retinal perfusion and oxygen delivery

Hypoxia resulting from disorders of retinal perfusion is addressed clinically by appropriately managing specific underlying causes. For example, endarterectomy is conventional management for carotid stenosis, and optimal management of blood glucose and blood pressure can slow progression of retinal vascular disease (Boscia, 2010; Rehak and Wiedemann, 2010). Experimental interventions for retinal vascular occlusions include radial optic neurotomy for CRVO, adventitial sheathotomy for BRVO, and embolectomy for BRAO. In addition to redressing perfusion deficits, the availability of oxygen to the retina may be enhanced by increasing supply or by reducing demand for oxygen itself. Increased oxygen delivery may be achieved by inhalation of hyperbaric or supplemental oxygen. Hyperbaric oxygen treatment is reported to ameliorate the blood-retinal barrier breakdown in diabetic retinopathy in rats (Chang et al., 2006). Supplemental inhaled oxygen for 3 months was associated with improved diabetic macular oedema (Nguyen et al., 2004). While these interventions are unlikely to provide practical treatment options, the findings provide further evidence of the importance of hypoxia in diabetic retinopathy.

1.8.2 Improving inner retinal oxygenation by panretinal photocoagulation

Panretinal photocoagulation (PRP) promotes regression of pathological retinal neovascularisation and is the conventional treatment for proliferative

retinopathies associated with chronic hypoxia. PRP causes thermal destruction of retinal pigment epithelial cells and adjacent photoreceptors, which are replaced by glial cells with relatively low oxygen consumption (Roider et al., 1992; Thompson et al., 1996). Reduced local consumption of oxygen at sites of photocoagulation has been proposed to promote oxygen diffusion from the choroidal circulation to the inner retina and to relieve inner retinal hypoxia locally (Stefansson, 2006). Evidence supporting this hypothesis has been provided by studies in the cat (Stefansson et al., 1986), the pig (Pournaras et al., 1990b), the rabbit (Funatsu et al., 1997) and in the human (Stefansson et al., 1992). Application of PRP is followed by vascular constriction consistent with autoregulatory adaption to locally increased oxygenation (Gottfredsdottir et al., 1993) and with reduction in VEGF and VEGF receptors levels in the vitreous (Aiello et al., 1994; Augustin et al., 2001). Although PRP offers a powerful technique to protect central vision against the consequences of retinal neovascularisation, conventional photocoagulation strategies cause predictable adverse impact on peripheral vision, contrast sensitivity and night vision, and safer alternative approaches are highly desirable.

1.8.3 Improving inner retinal oxygenation by vitrectomy

Vitrectomy can reduce retinal neovascularisation and macular oedema (Blankenship and Machemer, 1985; Hoerle et al., 2002) while increasing the rate of cataract formation and iris neovascularisation (Schachat et al., 1983; van Meurs et al., 1996). These clinical observations can be explained by changes in ocular oxygenation associated with the promotion of fluid currents in the vitreous

cavity (Stefansson, 2006). The vitreous gel has a relatively low oxygen tension, possibly maintained by a high ascorbate content that acts as an oxygen sink to protect the lens from oxidative damage (Shui et al., 2009). The removal of vitreous gel and its replacement with aqueous facilitates diffusion of both oxygen and growth factors. Vitrectomy results in increased oxygen tension in the mid-vitreous and is associated with accelerated development of nuclear sclerotic lens opacity (Holekamp et al., 2006). Vitrectomy may promote diffusion of oxygen to the retina from the anterior segment and possibly from better-perfused areas of the retina to areas of retinal hypoxia (Stefansson et al., 1981). Conversely, increased clearance of hypoxia-induced vasoactive growth factors such as VEGF from the eye following vitrectomy may account for iris neovascularisation and neovascular glaucoma (Stefansson, 2009).

1.8.4 Improving inner retinal oxygenation by maintaining light-adaptation

Arden and colleagues have suggested that inner retinal hypoxia in diabetes may be aggravated by dark adaptation because the metabolically-demanding dark current of photoreceptor cells in the outer retina reduces availability of oxygen to the inner retina (figure 1.5C). He further postulated that progression of diabetic retinopathy may be controlled by minimising dark adaptation to promote retinal oxygen availability (Arden et al., 1998). Preliminary reports suggest that application of trans-lid retinal illumination during sleep to one eye of subjects

with non-proliferative diabetic retinopathy is associated with improved outcome (Arden et al., 2010).

1.8.5 Targeting adaptive responses to hypoxia

VEGF is an attractive target in hypoxic and ischaemic eye disease as VEGF-induced neovascularisation is disorganised and leaky and contributes significantly to visual loss. In recent years, three major anti-VEGF treatments have been developed and applied to ocular neovascularisation in a number of clinical trials.

Pegaptanib sodium (Macugen™) is an RNA oligonucleotide aptamer that selectively inhibits the $VEGF_{165}$ isoform (Fine et al., 2005; Ng and Adamis, 2006). Treatment with pegaptanib was reported to improve visual outcome in neovascular AMD (Gonzales, 2005; Singerman et al., 2008) and diabetic macular oedema (Cunningham, Jr. et al., 2005). These studies suggest that pegaptanib is likely to be a safe and effective therapy. Pegaptanib has been approved by the FDA for the treatment of neovascular AMD and large scale prospective clinical trials into its use in other ischaemic eye diseases are ongoing.

Ranibizumab (Lucentis™) is a humanised anti-VEGF antibody fragment targeting all isoforms of VEGF (Lowe et al., 2007). It has been shown to be an effective antiangiogenic treatment for the treatment of neovascular AMD (Brown et al., 2006; Brown et al., 2009; Chang et al., 2007; Regillo et al., 2008). Side effects after intravitreal injection of Ranibizumab include increase in intraocular

pressure, inflammation and progression development of cataract (Rosenfeld et al., 2005) (Brown et al., 2009). Ranibizumab was licensed for the treatment of neovascular AMD by the FDA in 2006 and large scale prospective clinical trials into its use in diabetic retinopathy are ongoing.

Bevacizumab (Avastin™) is a monoclonal antibody targeting all isoforms of VEGF and was originally developed as a cancer therapeutic. The use of Bevacizumab in the treatment of neovascular eye disease is currently unlicensed but provides a cost effective alternative to ranibizumab (Michels et al., 2005). Systemic use of Bevacizumab has been associated with hypertension (Cobleigh et al., 2003; Hurwitz et al., 2004; Yang et al., 2003) and increased risk of thromboembolism possibly related to the drug's effect on enhancing inflammation (Ratner, 2004).

The clinical trials published to date suggest that VEGF inhibition is a powerful and effective treatment option for hypoxia associated neovascular eye disease. However, treatment does not fully reverse blindness and repeated treatments are frequently required. The application of VEGF inhibitors which target all isoforms of VEGF should be carefully evaluated for intraocular and systemic safety before being approved for the treatment of other forms of hypoxic retinopathy. Furthermore, consideration should be made to the important role of VEGF isoforms in retinal vascular development (Chan-Ling et al., 1995; Feeney et al., 2003; Ng et al., 2001) and in neuroprotection (Nishijima, 2007; Saint-Geniez et al., 2008) when applying VEGF inhibitors to the immature eye to treat neovascularisation associated with retinopathy of prematurity.

1.9 Aims of the project

The purpose of the work presented in this thesis was to further elucidate the roles of hypoxia, hypoxia sensing mechanisms and downstream effector pathways in eye development and neovascular eye disease. Specifically, I focused on the following three interrelated topics:

1) Activation of HIF in the RPE has been proposed to contribute to disease progression and promote choroidal neovascularisation in age-related macular degeneration. I therefore aimed to explore the consequences of Hif activation in the RPE on the retina and its vasculature using transgenic mice. As activation of Hif in the RPE surprisingly resulted in a dramatic and interesting early ocular phenotype, I focused on the role of Hif in the RPE during development.

2) Activated myeloid cells, such as macrophages and microglial cells, have been shown to accumulate at sites of retinal hypoxia/ischaemia in neovascular eye disease and proposed to contribute to the development of neovascularisation. I therefore aimed to study the role of Hif1a and its downstream effector protein Vegf in myeloid cells in the development of retinal and choroidal neovascularisation in transgenic *knockout* mice.

3) Hypoxia-induced activation of HIF and the expression of downstream cytokines have been suggested to contribute to disease progression and the development of neovascularisation in diabetic retinopathy. I therefore aimed to explore the distribution of oxygen across the human vitreous and retina and study its association to vitreous HIF1a and cytokine levels in PDR in man.

2. Material and Methods

2.1 Buffers and reagents

All reagents were obtained from Sigma Aldrich (Sigma-Aldrich Ltd. Gillingham, UK) unless otherwise stated.

ELISA wash buffer: 0.05% Tween 20 in PBS, pH 7.2-7.4 (R&D Systems, UK, Cat No WA126)

ELISA reagent diluent: 1% BSA in PBS, pH 7.2-7.4, 0.2 µm filtered

ELISA stop solution: 2 N H_2SO_4

ELISA substrate solution: 1:1 mixture of Colour Reagent A (H2O2) and Colour Reagent B (Tetramethylbenzidine, R&D Systems Cat no DY999)

Immunohistochemistry block: 1% bovine serum albumin, 5% goat serum, 0.01% Tween-20 in PBS

PBS: PBS tablets (Oxoid Ltd. Basingstoke UK): 1 tablet per 100ml distilled water, to make a 1l solution containing 8 g NaCl, 0.2g KCl, 1.15g Na2HPO4; 0.2g KH2PO4.

PBST: PBS 1x with 0.05% (v/v) Tween-20.

Proteinase K buffer: 30mM Tris-HCl pH 8.0 0.5% (w/v) SDS.

Protein medium for ELISA: 1% Proteinase inhibitor in RIPA buffer

Serras fixative: 60% (v/v) ethanol, 30% (v/v) saturated formaldehyde, 10% (v/v) concentrated acetic acid.

2.2 Molecular biology

2.2.1 Purification of genomic DNA and polymerase chain reaction for genotyping

Genomic DNA was extracted from murine ear-clip samples by proteinase K (0.1mg/ml) digestion at 55˚C for 12 hours. The digest was spun at 14000 RPM for 10 minutes to eliminate any contaminations and the supernatant was added to 1ml of 100% of isopropanol to precipitate the DNA. After another spin at 14000 RPE for 10min the DNA pellet was resuspended and washed in 70% ethanol and spun down again. The washed pellet was finally resuspended in sterile water on a heated shaker (55°C) for 30 minutes. Genomic DNA was stored short-term at 4˚C or long term at -20˚C. PCR reactions were performed using a commercially available master mix containing Taq polymerase (Thermo scientific 1.1 x ReadyMix PCR Master Mix 1.5 mM $MgCl_2$, ABgene, Epsom UK). Routinely, a 25µl volume was used with 0.5µl of DNA, 0.075µl 100µM primers, with distilled water used to make up the volume to 25µl. PCR sequences and conditions, and expected product sizes are shown in Appendix 1.

2.2.2 DNA electrophoresis

After PCR amplification, DNA fragments were separated on a 2% (w/v) agarose gel. Ethidium bromide (1µl of 10mg/ml concentration per 50ml of gel) was added to visualise nucleic acid bands. Samples were loaded onto the gel using gel-loading buffer (6x; 0.25 % (w/v) bromophenol blue in water). A 1 kb DNA ladder (Bioline Ltd., UK) was added and run at the same time to provide a standard

size marker. The voltage was set between 180V for 60 minutes. Finally, the gels were photographed on an ultraviolet transilluminator (G-Box, Syngene, Cambridge, UK).

2.2.3 Purification of RNA, manufacture of cDNA and quantitative real-time PCR

Real-time polymerase chain reaction (RT-PCR) was performed with the kind help of Anastasios Georgiadis (Department of Genetics, Institute of Ophthalmology, London, UK) who assisted with RNA isolation, cDNA manufacture and mRNA quantification. Eyes were homogenised and RNA was extracted using a commercial kit (RNeasy Mini Kit, Qiagen, UK). Purified RNA was stored in DEPC treated water (Invitrogen Ltd., Paisley, UK) at -80˚C until use. The amount of template RNA was measured using a small-volume spectrophotometer (Nanodrop ND-1000, ThermoScientific, Wilmington, DE USA). For each experiment, equal amounts of RNA were used for all samples as a template for cDNA manufacture. cDNA was made from template RNA using a commercial kit (Quantitect Reverse Transcriptase kit, Quiagen Ltd., UK) according to manufacturer's instructions and stored at -20˚C until use.

Real-time quantitative RT-PCR was performed using a commercial thermal-cycler (Applied Biosciences 7900HT) with its associated software (Applied Biosciences SDS version 2.2.2). Real-time PCR reagents were obtained commercially (Roche Diagnostics Ltd., Burgess Hill, UK). The 5' nuclease technique based on Taq-polymerase and FAM labelled hydrolysis probes was used for all real-time reactions using commercially designed primer/probe

combinations (Roche Universal Probe Library, sequences for all primers and probes are shown in Appendix 1). All reactions were performed in triplicate. For all test samples, the endogenous control β-actin was used to verify equal loading and to facilitate relative quantitation calculation. A water-only control sample was included for each primer/probe combination on each test plate to verify the lack of contaminants in the mixture. For each experiment, a suitable control sample was used to compare the test samples. The ΔΔ-Ct method of relative quantitation was used to compare data, and only data from samples in a single plate run at the same time were compared statistically.

2.2.4 Protein isolation and quantification

For quantification of protein in murine tissues, retinal or choroidal/RPE samples or whole eyes were collected and immediately snap frozen in liquid nitrogen. After homogenisation in sterile PBS with protease inhibitors (Sigma Aldrich, Gillingham, UK) using a glass homogeniser, the homogenate was spun at 7000rpm for 10 minutes. The concentration of protein in each sample was measured using a Lowry-based colorimetric protein assay done in triplicate (DC protein assay kit, Bio-Rad, Hemel Hempstead UK) and compared to a bovine serum albumin standard curve. Samples were diluted in assay buffer to bring the concentration to within the linear portion of the standard curve (0.2 - 0.9mg/ml).

For quantification of protein in human tissues, undiluted vitreous samples (0.3 - 1ml) were obtained from the mid-vitreous of diabetic and non-diabetic individuals using a vitreous cutter at the start of vitrectomy, prior to intraocular infusion of

fluid. The vitreous was collected in EDTA coated Eppendorf tubes (Eppendorf UK Limited, Cambridge, UK) and stored on ice. Blood samples were obtained by venous puncture following surgery (5ml) and stored on ice. The vitreous and blood samples were transferred to the Institute of Ophthalmology for further processing within maximal 45 minutes. The vitreous was subsequently centrifuged at 500g for 10min, and the blood sample at 1500g for 15min, at 4°C to remove the cellular components. The supernatants were aliquoted and stored at -80°C. The protein concentration of each sample was determined using a Lowry-based colorimetric protein assay performed in triplicate (DC protein assay kit, Bio-Rad, Hemel Hempstead UK) as described above.

2.2.4.1 ELISA for murine Vegf, Hif1a and Hif2a

Murine Vegf, Hif1a and Hif2a protein levels were quantified using commercial available ELISA kits (Mouse Hif1a DuoSet, IC R and D Systems Europe Abingdon UK; Hif2a ELISA kit, antibodies-online, Germany; Mouse Vegf DuoSet ELISA development kit, R and D Systems Europe Abingdon UK) according to the protocol of the manufacture. Briefly, a 96-well plate was coated with 100µl of diluted capture antibody overnight and blocked with reagent diluent (1% BSA in PBS) for one hour. After a washing step with 200µl of wash buffer (00.05% Tween 20 in PBS), 50µl of murine protein samples were added in duplicates to the plate for two hours at room temperature. The wells were washed with 200µl of wash buffer (00.05% Tween 20 in PBS) and 100µl of detection antibody was added to each well for two hours at room temperature. The wells were washed again and covered with 100µl of Streptavidin-HRP for 20 minutes followed by

another wash step and incubation with substrate solution (1:1 mixture of Colour Reagent A (H_2O_2) and Colour Reagent B (Tetramethylbezidine), OptEIA^{TM}, BD Bioscience, CA, USA) for 20 minutes. Finally, 50µl of stop solution (2N H_2SO_4) was added to each well and the optical density of each well was immediately determined using a microplate reader set at 450nm with a reference at 650nm (Emax, Molecular Devices Ltd. Berkshire UK). The results of each sample were compared to a standard curve of known concentration. To correct for total protein levels, Vegf, Hif1a and Hif2a protein levels are presented per milligram of whole eye protein.

2.2.4.2 ELISA for human HIF1a

Human HIF1a protein was quantified in vitreous and plasma samples using a commercial available ELISA kit (Human HIF1a DuoSet IC R and D Systems Europe Abingdon UK) according to the protocol of the manufacture. Briefly, a 96-well plate was coated with 100µl of diluted HIF1a capture antibody overnight and blocked with reagent diluent (1% BSA in PBS) for one hour. Vitreous and plasma samples were brought to room temperature and added in duplicate to the plate. After a washing step with 200µl of wash buffer (00.05% Tween 20 in PBS) 100µl of detection antibody was added to each well for two hours at room temperature. The wells were washed and covered with 100µl of Streptavidin-HRP for 20 minutes followed by another wash step and incubation with substrate solution (1:1 mixture of Color Reagent A (H_2O_2) and Color Reagent B (Tetramethylbezidine) for 20 minutes. Finally, 50µl of stop solution (2N H_2SO_4) was added to each well and the optical density of each well was immediately

determined using a microplate reader set at 450nm with a reference at 650nm (Emax, Molecular Devices Ltd. Berkshire UK). The results of each sample were compared to a standard curve of known concentration.

2.2.4.3 Cytometric bead array for human cytokines (CBA)

Multiplex bead analysis was kindly performed by Chris Cox (Director of Clinical Services, BioAnaLab Limited, Oxford, UK) as previously described (Groer and Shelton, 2009). Both vitreous and plasma samples were analyzed using the Milliplex Human Cytokine Panel 1 (Catalog number MPXHCYTO-60K; Millipore UK Ltd) for the following 42 cytokines: EGF, Eotaxin, FGF-2, Fit-3L, Fractalkine, G-CSF, GM-CSF, GRO, IFNα2, IFN-γ, IL-1α, IL-1β, IL-1Rα, IL-2, IL-3, IL-4, IL-5, IL-6, IL-7, IL-8, IL-9, IL-10, IL-12 (p40), IL-12 (p70), IL-13, IL-15, IL-17, IP-10, MCP-1, MCP-3, MDC, MPI-1α, MIP-1β, PDGF-AA, PDGF-AB, sCD40K, sIL-2Rα, RANTES, TGFα, TNFα, TNFβ and VEGF in a single sample. Samples were brought to room temperature and added in duplicate to 96-well filter-bottom plates. Antibody-coated capture beads were added to the wells and incubated on a plate shaker at 4° C overnight. After a washing step, beads were further incubated with biotin-labelled secondary antibody for 1 hour and then incubated with streptavidin-phycoerythrin for 30 minutes. 100 µl of sheath fluid was added to each well and samples were analysed using a bioassay analyzer (model 200; Luminex, Austin, TX). Cytokine concentrations were determined from standard curves prepared on each plate and expressed as picogram per milliliter (pg/ml). Concentrations below the detection limit of 3.2pg/ml are treated as having a value of 1.6pg/ml for the purposes of the analysis.

2.3 *In vivo* techniques in mice

2.3.1 Animals and breeding

2.3.1.1 Animals

All animals were used with University College London ethics committee approval and under a UK Home Office project licence and personal licence (PIL 70/22032). All procedures were performed in accordance with the Association for Research in Vision and Ophthalmology Statement for the Use of Animals in Ophthalmic and Vision Research. All mice in this study were maintained on a C57BL/6J background.

Mouse lines used in the study include:

- **C57Bl/6J** mice were obtained from Harlan UK Ltd. Bicester UK
- ***Vhl*$^{flox/flox}$** mice (Haase et al., 2001) were obtained from Patrick Maxwell (UCL Department of Medicine, London, UK)
- ***Hif1a*$^{flox/flox}$** mice (Ryan et al., 2000) were obtained from Patrick Maxwell (UCL Department of Medicine, London, UK)
- ***Vhl*$^{flox/flox}$*;HIF1a*$^{flox/flox}$** mice were bred by myself in the Biological Resource Unit of the Institute of Ophthalmology, London, UK
- ***trp-1 cre*** mice (Mori et al., 2002) were obtained from Pierre Chambon (Institute of Genetics, University of Strasbourg, France)
- ***lysM cre*** mice (Clausen et al., 1999) were obtained from Christiana Ruhrberg (Department of Cell Biology, Institute of Ophthalmology, UCL, London)

2.3.1.2 Breeding

Transgenic mice expressing cre recombinase under the control of the RPE cell-specific *tyrosinase-related protein 1* promotor, referred to as *trp-1* (Mori et al., 2002), were mated with *Vhl*$^{floxed/floxed}$ mice (Haase et al., 2001), *Hif1a*$^{floxed/floxed}$ mice (Ryan et al., 2000), or double floxed *Vhl*$^{floxed/floxed}$*;Hif1a*$^{floxed/floxed}$ mice. Transgenic mice expressing cre recombinase under the control of the myeloid cell-specific lysozymeM promotor, referred to as *lysM* (Clausen et al., 1999), were mated with *Vhl*$^{floxed/floxed}$ mice (Haase et al., 2001) and *Hif1a*$^{floxed/floxed}$ mice (Ryan et al., 2000). All experiments were controlled with age-matched littermates without the *cre* transgene (referred to as *control*). Genotyping was performed at weaning age or before using earclip genomic DNA. All procedured animals were genotyped at euthanasia for a second time to confirm their genotype.

2.3.2 Anaesthesia

If required, mice were anaesthetised using an intraperitoneal injection of a mixture containing medetomidine hydrochloride (1mg/ml, Domitor™ Pfizer animal health, Kent, UK), ketamine (100mg/ml, Fort Dodge Animal Health, Southampton UK) and sterile water in the ratio 5:3:42. Mice were recovered using an intraperitoneal injection of the reversal agent atipamezole hydrochloride (5mg/ml, Antisedan™ Pfizer animal health, Kent, UK) in sterile water (ratio 1:50). Mice were monitored in the recovery period and body temperature was maintained using a heat pad. Local anaesthesia using topical

0.5% amethocaine drops (Minims, Bausch and Lomb Ltd, Kingston-upon-Thames, UK) was provided when necessary.

2.3.3 Intraperitoneal injection

Intraperitoneal injection (i.p.) was performed for fluorescein and indocyanin green (ICG) angiography and terminal procedures. A maximum volume of 0.15ml was injected for pre-weaning mice, 0.25ml for adult mice. Injections were made at either side of midline (alternating for repeated injections) using a 30g hypodermic needle and a 1ml syringe.

2.3.4 Macroscopical examination of mouse eyes

In order to characterise the ocular development and eye growth, the eye diameter was assessed at different time points during development by measuring the distance from the optic nerve head to the center of the cornea using an electronic digital caliper. To further document the ocular development macroscopically, enucleated eyes were imaged at different time points during development using a digital camera (Lumix 12x, DMC-TZ7, Panasonic).

2.3.5 Indocyanin green and fluorescein angiography

To analyse the ocular vascular phenotype in mice *in vivo*, fluorescein (FA) and indocyanin green (ICG) angiography was performed. Mice were anaesthetised and injected with 0.2 ml of 1% fluorescein sodium (Akorn, Decatur, IL) or 0.2 ml of 5mg/ml ICG in dH_2O in the peritoneum and fundus images were captured three minutes later using the autofluorescent channel of Spectralis^{TM} HRA2 digital angiography system (Heidelberg engineering, Heidelberg, Germany). *In*

vivo fluorescein angiography after laser CNV induction (see below) was performed without anaesthesia using a small animal fundus camera with appropriate filters (Kowa Genesis, Tokyo, Japan).

2.3.6 The mouse model of oxygen-induced retinopathy (OIR)

Pups and their nursing mothers were placed in a 75% oxygen supply chamber from postnatal day 7 to postnatal day 12 as previously described (Mowat et al., 2010). A constant low flow of 80% oxygen and 20% nitrogen was provided to a closed perspex chamber. The oxygen level was monitored three times a day, and maintained at 75% ±2% O_2. If necessary the oxygen levels in the chamber were increased by adding 100% of oxygen or decreased by opening the chamber. Mice were checked three times daily and the nursing mother was removed from the chamber to breathe room air (21% oxygen) for a minimum of 2 hours a day to minimise lung toxicity associated with hyperoxia in adults. The mice were exposed to a standard 12 hour light-dark cycle and returned to constant room air (21% O_2) at p12. Pups were weighed and culled at p12 or p17 to assess the neovascular and vaso-obliterative fraction of the total retinal area. To ensure the validity of each experiment one animal per litter was culled at p12 and the hyperoxia induced vaso-obliterative area was determined on a vessel stained flatmount. A vaso-obliterative area of 20-50% was considered as a result of a valid experiment.

2.3.6.1 Imaging and analysis

Retinal flatmounts were dissected and stained with TRITC-conjugated isolectin B4, collagen 4 or CD31 as described below. Retinal flatmounts were imaged

using a confocal laser scanning microscope (Leica DM5500Q, Wetzlar, Germany) at 5x magnification. Single x/y plane was taken from each quadrant of the retina and the central retina at 1024 x 1024 resolution. Composite images were produced and exported as a *.tiff file using the Leica imaging software (LAS AF, Leica, Wetzlar, Germany). Images were loaded into an image analysis program (Image J) and converted to 16bit grayscale images. The area of the total retina and the vaso-obliterative area were delineated using the freehand selection tool as previously described (Banin et al., 2006). Areas of neovascularisation were outlined, and the manual selection tool was used to highlight the bright neovascular areas only. The neovascular area and ischaemic area were quantified and represented as percentages of total retinal area.

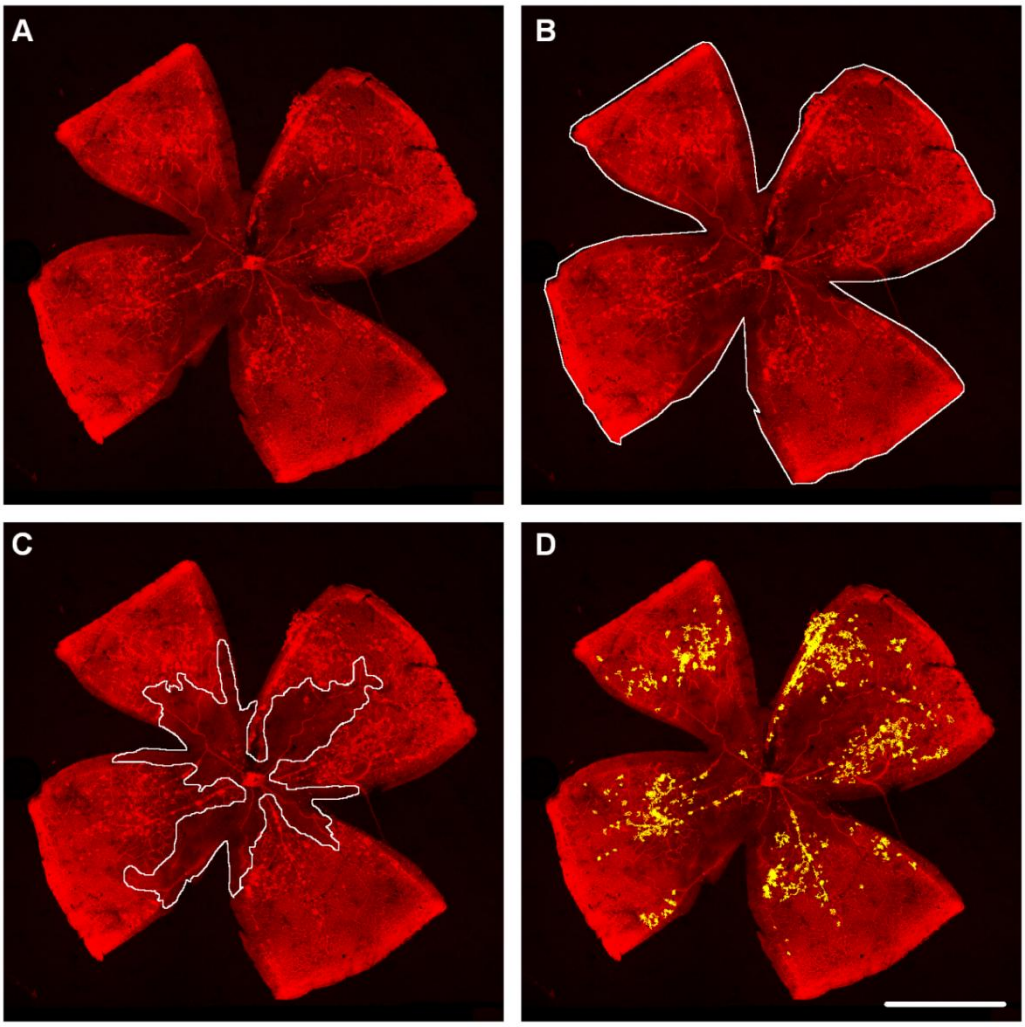

Figure 2.1 Analysis of retinal ischaemia and neovascularisation

Retinal vessels were labelled with fluorescent TRITC-conjugated BS lectin. Retinas were flatmounted and imaged (A, x5 magnification). Image analysis software (ImageJ) was used to delineate and measure the total retinal area (B), the area of central ischaemia (C) and neovascularisation (D). Ischaemia and neovascularisation were presented as a percentage of the total retinal area. Scale bar = 1mm

2.3.7 The mouse model of laser-induced choroidal neovascularisation

Choroidal neovascularisation was induced by rupturing Bruch's membrane using a slit-lamp-mounted diode laser system (wavelength 680nm; Keeler, UK) at 210mW power, 100ms duration and 100μm spot diameter. These settings consistently generate a subretinal gas bubble which indicates an adequate laser-induced rupture of Bruch's membrane and successful induction of CNV. Only eyes in which laser-induced subretinal bubble formation occurred were included in the analysis. Eyes were also excluded if there was significant cataract or keratopathy formation which prevented good fundus view and could affect laser energy delivery or angiography. For subsequent assessment of CNV lesion size energy was targeted at 3 areas approximately 3-4 disc diameters from the optic nerve head at the 10 o'clock, 2 o'clock and 6 o'clock positions and avoiding any vessels.

2.3.7.1 Imaging and analysis

In vivo fluorescein angiography (FFA) was performed at 3 days, 1 and 2 weeks after laser injury. Images from the early (90 seconds after fluorescein injection) and late (7 minutes) phases were obtained using a small animal fundus camera with appropriate filters (Kowa Genesis, Tokyo, Japan). The pixel area of CNV-associated hyperfluorescence was quantified for each lesion using image-analysis software (Image J; National Institute for Health, US; free download from http://rsbweb.nih.gov/ij/) (Collins, 2007). The border of each lesion was delineated using the free-hand area selection tool and the pixels of each lesion was highlighted and automatically counted after adjusting for an appropriate

threshold level. Confluent lesions and lesions surrounded by retinal bleeding were excluded in all experiments.

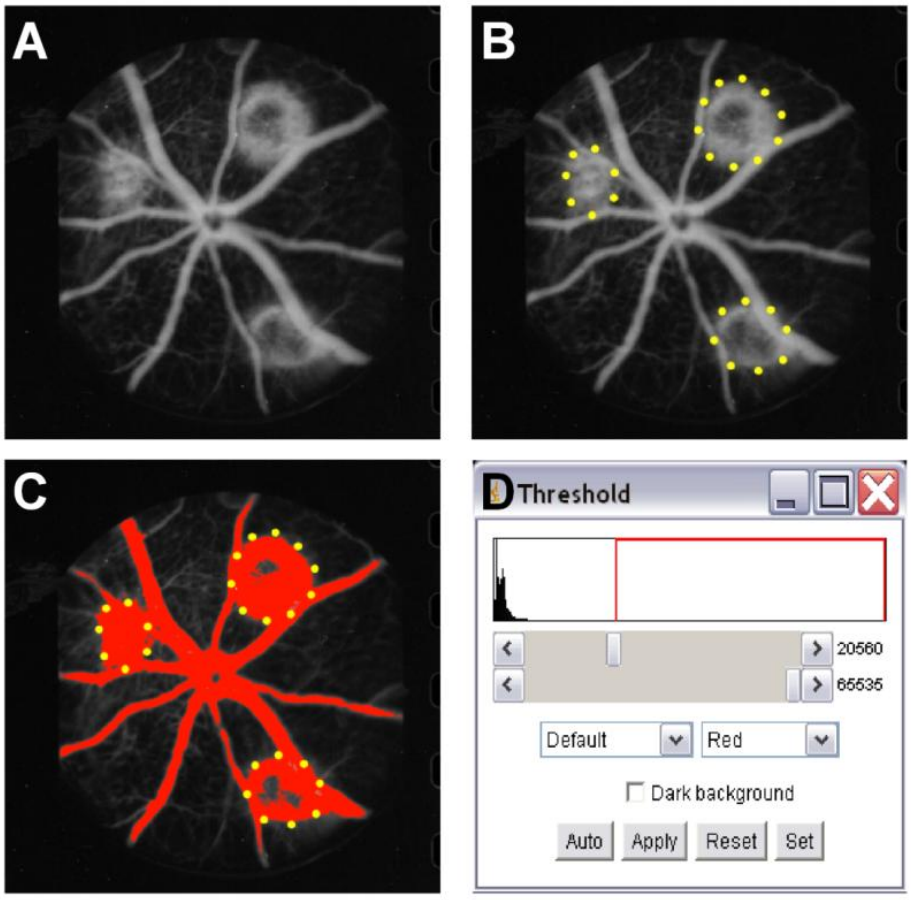

Figure 2.2 Analysis of laser-induced choroidal neovascularisation on fluorescein angiograms. A,B) Image analysis software (ImageJ) was used to delineate the borders of a choroidal neovascularisation on a fluorescein angiogram. C,D) The “threshold function” of ImageJ was used to highlight and automatically count the pixels of the choroidal neovascularisation.

2.3.8 Electroretinography

Standard photopic and scotopic flash Ganzfeld electroretinography (ERG) were recorded from 2-3 month old mice in a standardised fashion. Following dark adaption overnight (>14 hours) mice were anesthetised with a single intraperitoneal injection as described above. The pupils were dilated using one drop each of 0.5% tropicamid (Minims, Bausch and Lomb, Kingston-upon-Thames, UK) to each eye. Contact corneal platinum electrodes were placed on each eye and one reference electrode sublingually. The ground electrode was placed subdermally in the midline at the base of the tail. Water based ocular lubricant (Viscotears, Novartis Pharmaceuticals UK Ltd, Camberley, UK) was placed on each cornea to improve electrical contact with the electrode and to keep the eye moisturised during procedure. The head was placed in a standardised position in the Ganzfeld bowl and great care was taken to keep the electrodes impedance symmetrical and low (between 5-10kOhm). ERGs were recorded from both eyes simultaneously using the Espion ERG Diagnosys system (Diagnosys LLC, Cambridge, UK).

For scotopic examination, single-flash recordings were obtained at increasing light intensities from 0.001 to 3 cd/m^2 with an interstimulus interval of 30 (0.001–1 cd/m^2) and 60 (3 cd/m^2) seconds. Following light-adaption for 10 minutes at 10cd/m^2 intensity, photopic single-flash recordings were obtained at increasing light intensities from 0.1 -10 cd/m^2 with an interstimulus interval of 30 (0.001–1 cd/m^2) and 60 (3 cd/m^2) seconds. Ten responses per intensity level were

averaged and the a- and b-wave amplitudes were analysed using an Espion software (Diagnosys LLC).

2.3.8.1 Analysis of ERG data

Measurements for amplitude were obtained from the trough of the a wave and the peak of the b-wave. The photopic a-wave was defined as the maximal negative amplitude after the onset of light exposure. The photopic b-wave was defined as the maximal positive amplitude after the onset of light exposure compensating visually for the waveforms of the oscillatory potentials. Statistical comparison was performed at the 1cd.s/m^2 intensity which represents a mixed cone-rod response (Lei et al., 2006).

2.4 *In vivo* techniques in humans

2.4.1 Oxygen measurements in the human vitreous

2.4.1.1 Study population

The study on vitreous oxygenation in PDR was performed in accordance with the Declaration of Helsinki and approved by the Moorfields and Whittington Research Ethics Committee (REC reference number 07/Q0504/17). 14 individuals having vitrectomy surgery for advanced proliferative diabetic retinopathy (PDR), and 14 control subjects having surgery for idiopathic epiretinal membranes or full-thickness macular hole were recruited in this study. Prior to entering the study, informed consent was obtained from all subjects. As previous intraocular surgery can change the intra-ocular distribution of oxygen

(Holekamp et al., 2005), individuals with any history of intra-ocular surgery including cataract surgery were excluded. In order to allow the surgeons the best possible view during the intraoperative oxygen measurements individuals with the presence of intraocular haemorrhage or inflammation were excluded. Because systemic hyperoxia can influence intraocular oxygen tensions (Yu and Cringle, 2001b), only patients having surgery under local anesthesia who maintained peripheral oxygen saturations of 95% minimum during surgery without supplementary inhaled oxygen were included in this study (table 2.1).

Inclusion criteria	**Exclusion criteria**
• Patients listed for vitrectomy under local anaesthesia	• Patients unable to give informed consent
• Patients with PDR (study group), MH or ERM (control)	• Hx of pulmonal disease (e.g. asthma or COPD)
• Age > 16 years of age	• Previous intraocular inflammation
	• Peripheral O_2 saturation <95% during surgery
	• Previous intraocular surgery

Table 2.1 Inclusion and exclusion criteria for the study on intraocular oxygen in PDR

2.6.1.2 Measurement of oxygen tension

Intraocular oxygen measurements were kindly performed by Zdenek Gregor, Panagiotis Stavrakas and James Bainbridge (Vitreo-retinal service, Moorfields Eye Hospital, London, UK) using an Oxylab pO_2 optical sensor (Oxford Optronix, Oxford, United Kingdom) set in fast mode (one measurement per second). Prior to measuring oxygen tensions in the eyes of human subjects, the effect of gas sterilisation and endoscopic illumination on the reliability of the sensor was determined in gas mixtures of known oxygen tensions (0-147.4mmHg). Oxygen probes were gas-sterilised (Sterrad 100Nx, Johnson&Johnson, USA) prior to use in human subjects. Using a 20-gauge 3-port pars plana technique the surgeons sited the infusion cannula in the inferotemporal port without turning on the intraocular infusion. The oxygen probe was introduced via a heavy liquid cannula through a second port into the vitreous cavity and an endoscopic light pipe was introduced through the third port. Oxygen tensions were measured by holding the sensor at specific sites in the eye for at least 35 seconds until the monitor recorded constant values. Oxygen tensions were measured in the anterior vitreous 3mm posterior to the posterior pole of the lens (1), the mid vitreous (2), at the retinal surface one disc-macula diameter temporal to the macula (3a), at the retinal surface superior to the superotemporal arcade (3b) and at the retinal surface in the mid-periphery (superior equator, 4). Furthermore, oxygen tensions were recorded at the retinal surface of tractional retinal detachments and above and between photocoagulated areas in subjects with proliferative diabetic retinopathy (figure 2.3). All preretinal measurements were taken with the probe in light contact with the retinal surface. To determine

the test-retest variability of the sensors *in vivo,* and to identify any artefactual disturbance of intraocular oxygen tension caused by the measurement technique itself the mid vitreous oxygen tension was measured at both the start and the completion of the measurements. Once the measurements were completed and the vitreous sample collected (see below), the intraocular infusion was turned on and the vitreous surgery was performed as planned.

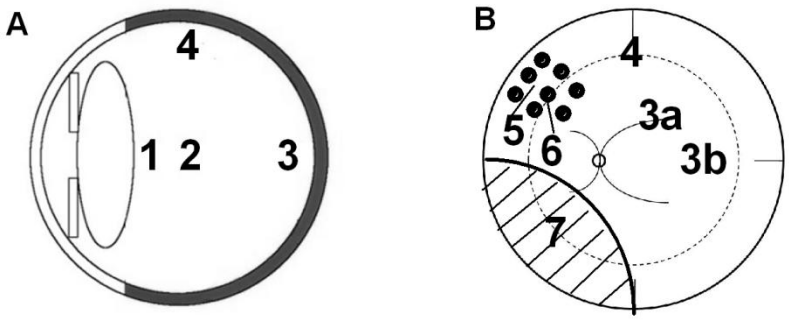

Figure 2.3 Sites of intraocular oxygen measurements. A) Intraocular oxygen tension was measured in the anterior vitreous (1) and in the mid vitreous (2). **B)** Preretinal oxygen tension were measured at the retinal surface superior to the superotemporal arcade (3a), one disc-macula diameter temporal to the macula (3b), in the mid-periphery (superior equator, 4), above and between photocoagulated areas (5,6) and above areas of tractional retinal detachments in subjects with proliferative diabetic retinopathy

2.5 Histology and immunohistochemistry

2.5.1 Tissue processing on paraffin embedded tissue

Animals were terminally anaesthetised with intraperitoneal injection of pentobarbital (Euthatal™ Merial Animal Health Ltd. Harlow, UK) and perfused via intracardiac puncture with ice-cold fixative (4% PFA). As standard, tissue was fixed for 12 hours in 4% PFA at 4˚C then embedded in paraffin. Tissues were processed in an automated machine (Leica TP1020) and embedded in paraffin blocks for sectioning. Sections were cut on a microtome (Shandon sledge, Runcorn, UK) routinely at 6µm, and mounted on polylysine coated slides (Thermofisher Loughborough, UK). Sections were stored at room temperature until staining.

2.5.2 Immunohistochemistry on paraffin embedded tissue

Sections were dewaxed in xylene and rehydrated though grades of alcohol (100%, 90% and 80% of ethanol) to distilled water. Sections were stained with haematoxylin (nuclei) and eosin (cytoplasm) and washed thoroughly. Next, sections were dehydrated for 5 minutes in 95% ethanol, 5 minutes in 100% ethanol and at the end for 15 minutes in xylene. The slides were coversliped using xylene based Permount (Fisher scientific, UK). A drop of Permount was placed on the slide using a glass rod, taking care to leave no bubbles. The coverslip was angled and let fall gently onto the slide. Slides were dried overnight in the hood.

2.5.3 Tissue processing on frozen tissue

Fixation was dependent on the individual immunohistochemistry protocol used. Routinely, animals were terminally anaesthetised with pentobarbital (Euthatal™ Merial Animal Health Ltd. Harlow, UK) and perfused via intracardiac puncture with ice-cold paraformaldehyde (4% (w/v)) in PBS pH 7.4. Eyes were then post fixed in paraformaldehyde (4% (w/v)) for 5-10 minutes. Eyes were embedded in optimal cutting temperature medium (Tissue Tek OCT medium, Raymond Lamb, Eastbourne, UK) before freezing. Retinal cryosections were cut using a cryostat (Bright OTF 5000, Huntingdon, UK) in a sagittal direction at between 12-20μm thickness. Details of section thickness are given in specific chapter methods. Sections were collected onto polylysine coated slides (Thermofisher Loughborough, UK), air dried and stored at -20˚C until staining.

2.5.4 Immunohistochemistry on frozen tissue

Sections were defrosted for 10 minutes at room temperature, and rehydrated in PBS for 10 minutes at room temperature. Blocking solutions comprised PBST with 5% normal goat serum and 1% bovine serum albumin. All antibodies were incubated in blocking solution, antibody conditions varied depending on the primary antibody used. After intensive washing, sections were incubated with fluorescent secondary antibodies (Invitrogen Ltd., Paisley, UK) for 4 hours at room temperature and counterstained with blue fluorescent DAPI (1:1000, Invitrogen Ltd., Paisley, UK) for 10 minutes at room temperature. Where double immunohistochemistry was performed, it was ensured that primary antibodies from different host species were used to avoid potential cross reactivity. In all

immunohistochemical experiment, incubations omitting the primary antibody were performed as controls for non-specific secondary antibody binding.

2.5.5 *In situ* hybridisation on frozen sections

The *in situ* hybridisation experiments for *Vegf* were performed with the kind help of Michael Powner and Marcus Fruttiger (Department of Cell Biology, Institute of Ophthalmology, UCL London, UK).

Eyes were fixed in 4% PFA in PBS for 24 hours at 4°C and cryoprotected in 20% (w/v) sucrose in PBS overnight at 4°C. Eyes were embedded in OCT compound (Raymond and Lamb, Sussex, UK), frozen in liquid nitrogen and stored at -20°C until further use. Cryosections (15µm) were collected on Vectabond (Vector Laboratories, Burlingham, USA)-coated slides and air-dried for four hours. Digoxigenin-labelled probes against full length mouse *Vegf* mRNA (coding region and 3' UTR) were diluted in hybridisation buffer and applied directly to sections and hybridised overnight at 65°C. Subsequent visualisation of RNA hybrids was carried with alkaline phosphatase-conjugated anti-digoxigenin antibodies according to the manufacturer's instructions using NBT/BCIP as a colour reagent (Roche Diagnostics GmbH, Mannheim, Germany). Pigment in the RPE was subsequently bleached by incubating the sections first in $KMnO_4$ (0.25% in H_2O) for 10 min at RT and then in oxalic acid (1% in H_2O) for 20 min at room temperature.

2.5.6 Tissue processing for retinal flatmounts

For flatmount preparation, animals were routinely perfused with 4% (w/v) PFA, and eyes were fixed for 1 hour after enucleation. The cornea, lens and iris were dissected and four radial cuts were made through the RPE, choroid and retina. The RPE/choroid complex was carefully dissected from the retina and both unfolded on a plastic dish. Samples were postfixed with 4% PFA for 1 hour at 4°C or in 100% methanol at -20°C until further use. Once staining was completed, retinas were mounted ganglion cell layer up in aqueous fluorescent mounting medium (Dako Ltd., Ely, UK) with a cover slip.

2.5.7 Immunohistochemistry on retinal flatmounts

Retinal and choroidal flatmounts were washed in PBS and incubated with primary antibodies (table 2.2) or 0.1mg/ml TRITC conjugated *Bandeiraea simplicifolia* (*BS*) lectin (Sigma Aldrich, Gillingham UK) diluted in blocking solution overnight at 4˚C. Flatmounts were thoroughly washed in PBS and incubated with fluorescent secondary antibodies (Invitrogen Ltd., Paisley, UK) for 4 hours at room temperature. Finally retinal and choroidal flatmounts were mounted with fluorescent aqueous mounting medium (Dako Ltd., Ely, UK) with the ganglion cell layer or RPE uppermost.

1° ab (host)	cell type labelled	company	1° ab	2° ab
Caspase 3 (rabbit)	Apoptotic cells	Abcam, US, ab 2302	1:20, overnight, 4˚C	1:200 4h RT
Collagen IV (rabbit)	Vascular endothelial cells	AbD Serotec, Oxford, UK, 2150-1470	1:300, overnight, 4˚C	1: 500 4h RT
Cre (rabbit)	Cre recombinase	Novagen, 69050, M00000463	1:200, overnight, 4˚C	1: 500 4h RT
GFAP (rabbit)	Astrocytes, Mueller glia	DAKO, Ref Z0334, Lot 0006609	1:500, overnight 4˚C	1: 500 4h RT
Hif1a (rabbit)	Hif1a	Novus Biologicals, NB100-479, Lot P1	1:1-200, overnight, 4˚C	1: 500 4h RT
Otx2 (rabbit)	PR progenitors RPE (in adults)	Abcam (ab21990)	1:100, 4˚C overnight	1: 500 4h RT
Pax6 (rabbit)	PR progenitors	Covance (PRB-278P)	1:300, 4˚C overnight	1: 500 4h RT
P-histone H3 (rabbit)	Proliferating cells	Chemicon Milipore, MA, US E173	1:500, overnight, 4˚C	1:200 4h RT
Ribeye/ CtBP2 (mouse)	Synapses	BS Transduction Laboratories, 612044	1:500, overnight, 4˚C	1: 500 4h RT
Recoverin (rabbit)	Photoreceptors	Chemicon, Ref AB5585, Lot LV1480447	1:1-2000, overnight, 4˚C	1: 500 4h RT
Rhodopsin	Rods	Sigma Aldrich Ltd.,UK, cat#O4886, Clone RET-P1	1:1000, overnight, 4˚C	1:500, 4h RT
YFP (rabbit)	YFP positive cells	MBL, MA, US, code 598	1:500, overnight, 4˚C	1: 200 4h RT

Table 2.2 Primary antibodies used on cryo sections.

1° ab (host)	cell type labelled	source	1° ab	2° ab
Collagen IV (rabbit)	Vascular endothelial cells	AbD Serotec, Oxford, UK, 2150-1470	1: 200, overnight 4 ˚C	1:200, 4h RT
F4/80 (rat)	Macrophages. Microglia	AbD Serotec, Oxford, UK, Cl:A3-1	1:500	1:200, 4h RT
Iba1 (rabbit)	Macrophages, microglia	WAKO, Japan, Code No. 019-19741	1:500, overnight, 4˚C	1: 200, 4h RT
Pecam (rabbit)	Endothelial cells	BD Pharmingen, CA, US, Code MEC 13.3	1:200, overnight, 4˚C	1: 200, 4h RT
TRITC conjugated *BS* lectin	Vascular endothelial cells, monocytes	Sigma Aldrich, L2140	0.1mg/ml	N/A

Table 2.3 Primary antibodies used on retinal and choroidal flatmounts.

2.5.8 Imaging and analysis

Fluorescence images were obtained using a confocal laser scanning microscope (Zeiss LSM 710, Hertfordshire, UK). Confocal sections were obtained using a 20x or 40x water immersion plan apochromat lens. Z-stacks were 3D reconstructed and surface rendered using Imaris software (Bitplane, Zurich, Switzerland). For quantification of proliferating and apoptotic cells, the number of cell nuclei stained with caspase 3 or phospho-histone H3 were counted in the iris, retina and RPE in 5 central cryosections 60µm apart. An average value per animal was calculated and used in subsequent analysis. Paraffin and semithin sections were imaged using a light microscope (Zeiss Axio

Observer Z1, NY, US). The number of RPE cells on semithins was quantified as described above. For ultrastructural imaging, a transmission electron microscope (TEM model 1010; JEOL, Tokyo, Japan) was used operating at 80kV. All images were captured with a digital camera (QImaging micropublisher 5.0 digital camera, QImaging, BC Canada) and exported as tiff files into Image J for quantification (developed by Wayne Rasband, National Institutes of Health, Bethesda, MD; available at http://rsb.info.nih.gov/ij/index.html).

2.6 Graphical representation of data and statistical analysis

All statistical analysis and graph composition was performed in a commercial program (GraphPad Prism version 5.00 for Windows, San Diego, USA). In all graphs, error bars indicate standard error of the mean (SEM) if not differently indicated. When comparing animals (for example when comparing the effect of genotype), all values were calculated or averaged on a per-animal basis, to ensure all data were independent. P values of $p<0.05$ were considered statistically significant. When comparing two normally distributed groups, a student's t-test was used. Details of t-tests used are given in specific chapter methods. When comparing 3 or more groups, a repeated-measures analysis of variance (ANOVA) was performed. Suitable post-tests were performed to compare groups of interest, as detailed in specific chapter methods. Correlation of the *in vitro* oxygen measurements and the *in vivo* test-retest measurements were calculated using the Pearson correlation coefficient. Differences in intraocular O_2 tensions between subjects with diabetes and controls, and in the concentrations of cytokines detected in more than 5 vitreous samples were

analyzed using a two tailed Mann-Whitney test and expressed as mean ± SEM. To correct for multiple univariate analyses, the Bonferroni correction algorithm of error I level was applied for the cytokine microarray analysis to retain the global error level at 5%. P values less than 0.0039 (=0.05/13) were considered statistically significant. Correlations between cytokine concentrations and intraocular oxygen tensions were determined using the non-parametric Spearman correlation coefficient.

3. The roles of Vhl and Hif1a in ocular and vascular development

3.1 Introduction

Molecular oxygen is essential for the development, growth and survival of multicellular organisms. Hypoxic microenvironments and oxygen gradients are generated physiologically during embryogenesis and organogenesis, including brain, heart and eye development (Caprara and Grimm, 2012; Patterson and Zhang, 2010; Trollmann and Gassmann, 2009). Tissue responses to local oxygen availability drive and coordinate the development of the blood, vasculature, the nervous system and other organs (Simon and Keith, 2008). In the eye, development of the retinal vasculature occurs in response to physiological hypoxia (Chan-Ling et al., 1995) generated by the increasing metabolic demand of differentiating neural cells (Stone et al., 1995). Hif signalling has been proposed to mediate this adaptive response to hypoxia during development and was shown to control normal retinal vascularisation and regression of the hyaloid vasculature in the developing neuroretina (Kurihara et al., 2010).

The retinal pigmented epithelium (RPE) is critical for the development of the eye and its vasculature. It is developmentally derived from the outer layer of the bilayered optic cup and contributes together with the peripheral neuroretina to the formation of the ciliary body and iris anteriorly. Normal development of the RPE is important for subsequent development of the choroidal vasculature

(Bharti et al., 2006) as well as closure of the optic fissure, retinal neurogenesis and neuronal cell projections (Bumsted and Barnstable, 2000; Martinez-Morales et al., 2001; Raymond and Jackson, 1995; Scholtz and Chan, 1987). Genetic ablation of the RPE or disruption of RPE specification genes during development in the mouse eye results in RPE transdifferentiation to neuroretina, coloboma and microphthalmia (Bharti et al., 2006; Marneros et al., 2005; Sakaguchi et al., 1997). In the adult, the mature RPE provides photoreceptor cells with metabolic support, recycles visual pigment, phagocytoses photoreceptor outer segment membranes, and maintains the blood-retina barrier and the health of the choroidal vasculature (Arjamaa et al., 2009; Sheridan et al., 2009). Hypoxia and Hif signalling at the level of the RPE has been proposed to play a critical role in the regulation of proangiogenic cytokines in the development of sight-threatening pathological choroidal neovascularisation in age-related macular degeneration (Stefansson et al., 2010).

Whereas the role of Vhl and Hif signalling in the developing neuroretina has been studied in detail (Caprara et al., 2011; Kurihara et al., 2010; Lange et al., 2011), little is known about the function of these factors in the RPE on the developing eye and its vasculature. Conditional inactivation of *Hif1a* in the developing RPE has been shown to have no effect on the development of the eye and its vasculature (Marneros et al., 2005). The consequences of *Hif1a* activation in the developing RPE, however, remain unclarified.

3.2 Aims

The aim of this chapter was to explore the function of Vhl and Hif1a signalling in the RPE on the developing eye and its vasculature. This was addressed by characterizing the ocular and vascular development of mice with a tissue-specific conditional *knockout* of *Vhl* in the RPE. Furthermore, I aimed to delineate distinct roles of Hif1a in the RPE for ocular and vascular development by characterizing mice with conditional inactivation of both *Vhl* and *Hif1a* in the RPE.

3.3 Methods and results

3.3.1 Conditional inactivation of *Vhl* in the RPE leads to Hif1a mediated aniridia and microphthalmia

To characterise the effect of *Vhl* inactivation in the RPE on eye development, *knockin* mice expressing cre recombinase under the control of the pigmented epithelium specific promoter *trp1* (*tyrosinase related protein 1*, referred to as *C57Bl6$^{trp1\text{-}cre}$ mice*) were mated with *Vhl$^{floxed/floxed}$* mice (Haase et al., 2001). The macroscopic phenotype of *Vhl$^{trp1\text{-}creKO}$* mice and control littermates was assessed at different time points during development (n=6-8 animals per genotype and timepoint). Abnormal ocular and iris development in *Vhl$^{trp1\text{-}creKO}$* mice were observed with 100% penetrance (figure 3.1A, B). The eye growth of *Vhl$^{trp1\text{-}creKO}$* mice was similar to littermate controls during fetal development. Postnatally, however, *Vhl$^{trp1\text{-}creKO}$* mice developed significant microphthalmia with a mean diameter of 2.1 ±0.13 mm compared with 3.0 ±0.21 mm in control mice at one month old ($p<0.0001$, figure 3.1C). To evaluate whether the observed phenotype in *Vhl$^{trp1\text{-}creKO}$* mice is mediated by Hif1a, mice with conditional inactivation of both *Vhl* and *Hif1a* in the pigmented epithelium were generated. This was achieved by crossing *Vhl;Hif1a$^{flox/flox}$* mice with mice expressing cre recombinase under the *trp1* promoter. *Vhl;Hif1a$^{trp1\text{-}creKO}$* mice demonstrated normal iris and ocular development resulting in a normal postnatal ocular diameter of 2.8 mm at one month of age (s.d. ±0.22, figure 3.1A-C). These data suggest that Vhl dependent Hif1a degradation is essential for normal iris and ocular development.

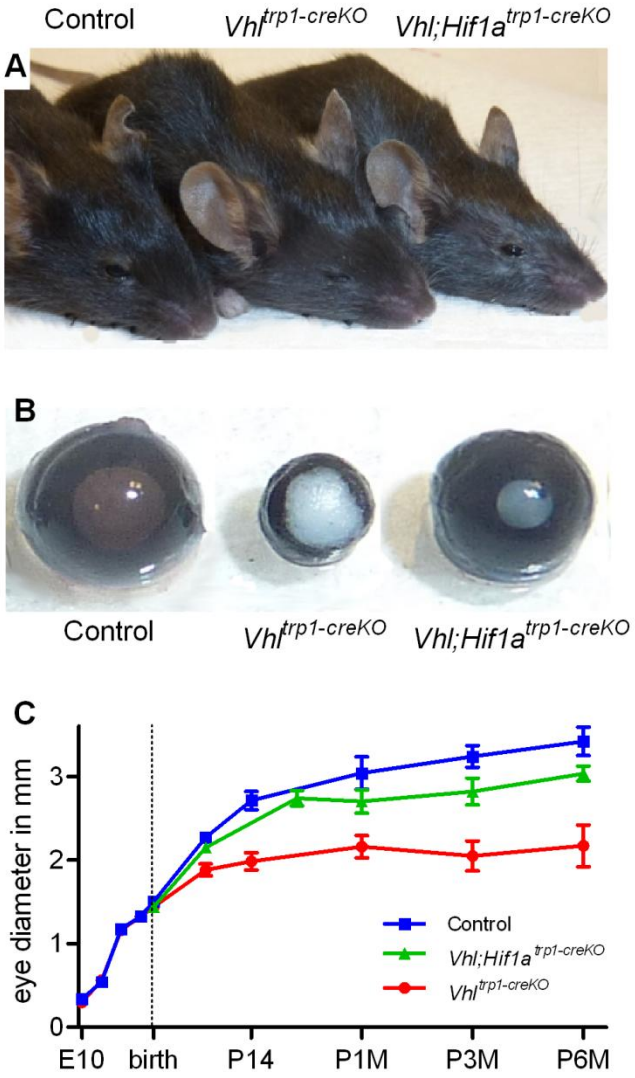

Figure 3.1 Conditional inactivation of *Vhl* in the RPE leads to Hif1a mediated aniridia and microphthalmia. Representative images of *Vhl*$^{trp1\text{-}creKO}$, *Vhl;Hif1a*$^{trp1\text{-}creKO}$ and control mice **(A)** and corresponding enucleated eyes **(B)** at one month of age. Timecourse of eye growth in *Vhl*$^{trp1\text{-}creKO}$ (red line), *Vhl;Hif1a*$^{trp1\text{-}creKO}$ (green line) and control mice (blue line, **C**). Error bars indicate ±SD. M=month, E=embryonic, P=postnatal.

3.3.2 Conditional inactivation of *Vhl* in the RPE increases levels of Hif1a, Hif2a and downstream angiogenic factors

To assess the specificity of *cre* expression in pigmented epithelial cells, ocular sections of *C57BL/6*$^{trp1\text{-}cre}$ mice were stained for cre recombinase at E14.5. *C57BL/6*$^{trp1\text{-}cre}$ mice demonstrated a strong expression of *cre* in the RPE and in a few neuroretinal cells of the distal optic cup, the primordium of the iris and ciliary body (figure 3.2A). This data is in line with the original publication describing the *C57BL/6*$^{trp1\text{-}cre}$ mouse line and indicates a strong and specific expression of *cre recombinase* in the RPE and iris (Mori et al., 2002).

To determine the effect of targeted deletion of *Vhl* in the developing RPE on ocular distribution of Hif1a and Vegf, Hif1a immunohistochemistry and Vegf *in-situ* immunohistochemistry was performed on ocular sections of *Vhl*$^{trp1\text{-}creKO}$, *Vhl;Hif1a*$^{trp1\text{-}creKO}$ and littermate controls at E14.5. *Vhl*$^{trp1\text{-}creKO}$ mice demonstrated a strong activation of Hif1a in the RPE which was absent in both *Vhl;Hif1a*$^{trp1\text{-}creKO}$ and control mice (figure 3.2 B-G). *In situ* hybridisation demonstrated increased *Vegf* expression in the RPE of both *Vhl*$^{trp1\text{-}creKO}$ and *Vhl;Hif1a*$^{trp1\text{-}creKO}$ mice (figure 3.2 H-J) indicating that RPE-specific inactivation of *Vhl* leads to a Hif1a-independent upregulation of Vegf in the RPE. Increased *Vegf* expression apparent in the neuroretina of these animals indicates secondary non-cell autonomous effects that are independent of Hif1a.

To determine the concentration of the Vhl target proteins Hif1a, Hif2a as well as Vegf at the onset of microphthalmia, protein concentration was measured in whole eyes of *Vhl*$^{trp1\text{-}creKO}$, *Vhl;Hif1a*$^{trp1\text{-}creKO}$ and control mice at P0 by ELISA

(range 5-7 mice per group). Hif1a, Hif2a and Vegf protein levels were significantly increased in *Vhl*$^{trp1\text{-}creKO}$ mice compared with littermate controls (p=0.002 for Hif1a, 0.01 for Hif2a and 0.01 for Vegf). In contrast, *Vhl;Hif1a*$^{trp1\text{-}creKO}$ mice revealed similar Hif1a levels and significantly increased Hif2a and Vegf protein levels compared with littermate controls (p=0.01 for Hif2a and Vegf, figure 3.2K).

To determine further the effect of Hif stabilisation in the RPE on ocular levels of downstream target genes, the expression of *Epo*, *Flt1*, *Pdgf-b* and *Vegf* mRNA was measured in whole eyes of *Vhl*$^{trp1\text{-}creKO}$, *Vhl;Hif1a*$^{trp1\text{-}creKO}$ and control mice at P0 by real-time PCR (n=7 per group). *Epo* mRNA levels were increased in both *Vhl*$^{trp1\text{-}creKO}$ and *Vhl;Hif1a*$^{trp1\text{-}creKO}$ mice compared with littermate controls (p=0.03). *Flt1* levels were increased in *Vhl*$^{trp1\text{-}creKO}$ mice compared with littermate controls (p=0.08). *Vhl;Hif1a*$^{trp1\text{-}creKO}$ mice, however, revealed normal Flt1 levels compared with littermate control. *Pdgf-b* and *Vegf* RNA levels appear to be increased in both *Vhl*$^{trp1\text{-}creKO}$ and *Vhl;Hif1a*$^{trp1\text{-}creKO}$ mice compared with littermate controls although this did not reach statistical *significance* (p=0.2 for *Pdgf-b*, p=0.27 for *Vegf*, figure 3.2L).

Taken together, these data suggest that RPE-specific inactivation of *Vhl* leads to early stabilisation of Hif1a in the pigmented epithelium and a Hif1a-independent increase of Vegf in the RPE. Subsequently, a Hif1a-dependent increase in *Flt1* and Hif1a-independent increases in *Vegf* and *Epo* levels suggest primary RPE-specific and secondary neuroretinal perturbation of angiogenic factors.

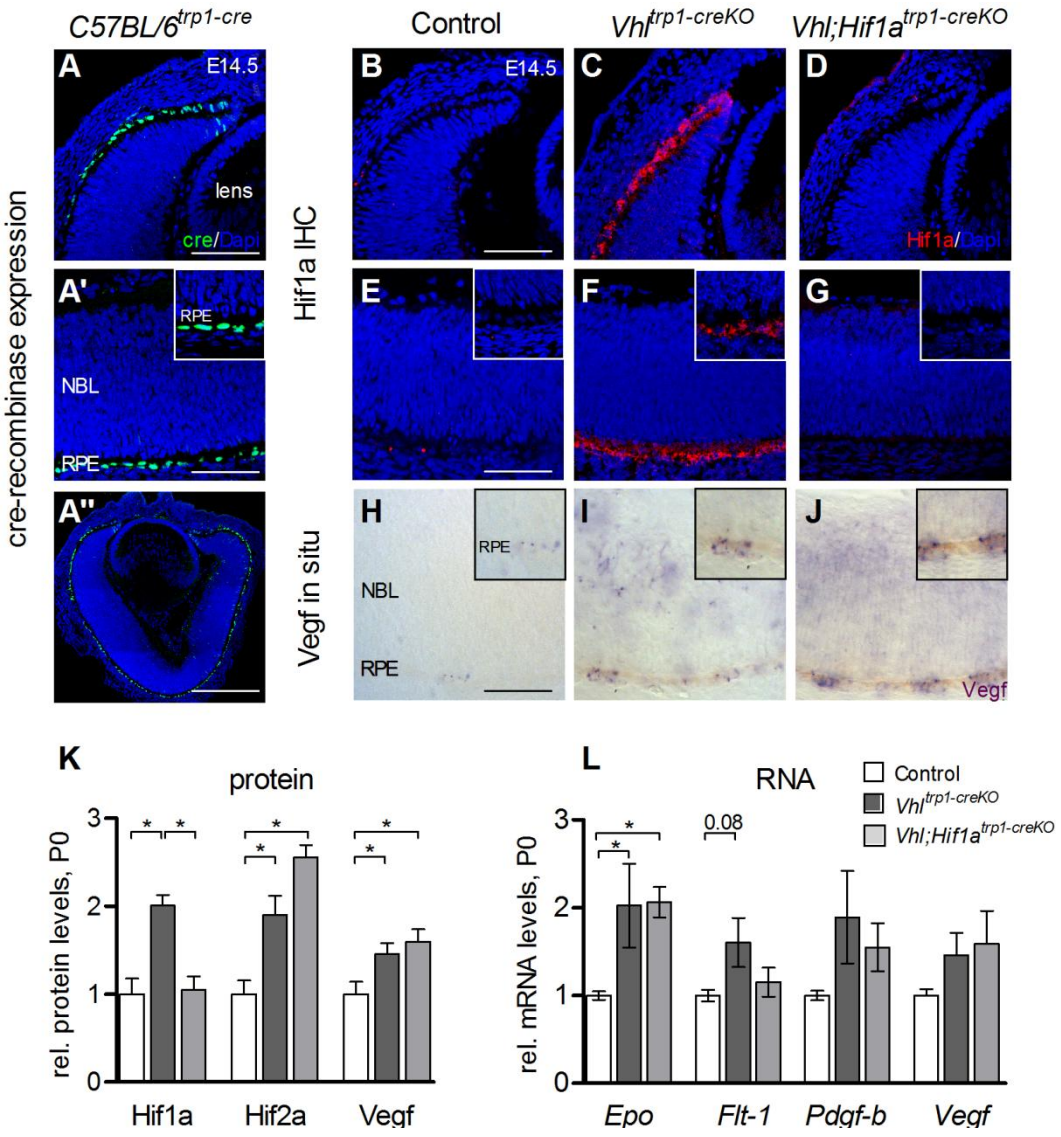

Figure 3.2 Conditional inactivation of *Vhl* in the RPE increases levels of Hif1a, Hif2a and downstream angiogenic factors. (A) Representative cre immunohistochemistry in *C57BL/6*$^{trp1\text{-}cre}$ mice at E14.5 demonstrates a specific cre expression in the RPE. **(B-G)** Representative Hif1a immunohistochemistry in *Vhl*$^{trp1\text{-}creKO}$, *Vhl;Hif1a*$^{trp1\text{-}creKO}$ and control mice at E14.5 shows an RPE-specific activation of Hif1a in *Vhl*$^{trp1\text{-}creKO}$ mice which is absent in *Vhl;Hif1a*$^{trp1\text{-}creKO}$ and control mice. **(H-J)** Representative *Vegf in situ* hybridization (performed by M.Powner, IoO UCL) demonstrating increased expression of *Vegf* in the RPE and neuroretina in *Vhl*$^{trp1\text{-}creKO}$ and *Vhl;Hif1a*$^{trp1\text{-}creKO}$ mice. **(K)** ELISA data: Quantification of Hif1a, Hif2a and Vegf protein levels in *Vhl*$^{trp1\text{-}creKO}$, *Vhl;Hif1a*$^{trp1\text{-}creKO}$ and control mice at birth (range 5-7 animals per group). **(L)** RT-PCR data: Quantification of *Epo*, *Flt-1*, *Pdgf-b* and *Vegf* mRNA levels in *Vhl*$^{trp1\text{-}creKO}$, *Vhl;Hif1a*$^{trp1\text{-}creKO}$ and control mice at birth (n=7 eyes per group, performed by A.Georgiadis, IoO, UCL). *= $p<0.05$. Error bars indicate mean ±s.e.m. Scale bars: 75µm in row D, 50µm in row A' and K-M,150µm A'.

3.3.3 Conditional inactivation of *Vhl* in the pigmented epithelium results in early abnormal ocular development and retinal degeneration in the adult

To further elucidate the developmental defect in *Vhl*$^{trp1\text{-}creKO}$ eyes, histology on H&E stained paraffin sections was assessed at different pre- and postnatal time points (range 3-5 mice per genotype per timepoint, figure 3.3A-U). In line with the macroscopical examination, *Vhl*$^{trp1\text{-}creKO}$ eyes revealed a rudimentary development of the iris and ciliary body and reduced RPE pigmentation from E17 onwards (figure 3.3H,I). At E17 rather than the typical forward extension and thinning of the periphery of the optic cup demarcating the beginnings of the development of the ciliary body and iris, *Vhl*$^{trp1\text{-}creKO}$ mice show a lack of growth and forward extension of the pigmented layer and an abnormal backward folding extension of the neuroepithelium (figure 3.3I). By P7, the retina of *Vhl*$^{trp1\text{-}creKO}$ mice began to fold and form rosettes which increased over time in both number and size becoming most prominent at P31 (figure 3.3L,M). Although the eye growth of *Vhl*$^{trp1\text{-}creKO}$ mice was significantly reduced in postnatal development, the lens developed normally and occupied the vitreous cavity and the anterior chamber in the young adult (figure 3.3N). *Vhl;Hif1a*$^{trp1\text{-}creKO}$ mice in contrast showed a normal iris and ciliary body development and normal ocular growth with both anterior chamber and vitreous cavity and retina remaining preserved (figure 3.3O-U). Nonetheless, *Vhl;Hif1a*$^{trp1\text{-}creKO}$ showed a few irregularities in retinal layering in the periphery and a persistent hyaloid vasculature at P31 (figure 3.3T,U). Taken together, these data support the initial finding that Vhl

dependent Hif1a degradation is essential for normal iris, RPE and ocular development and indicates that it is associated with retinal degeneration in the adult.

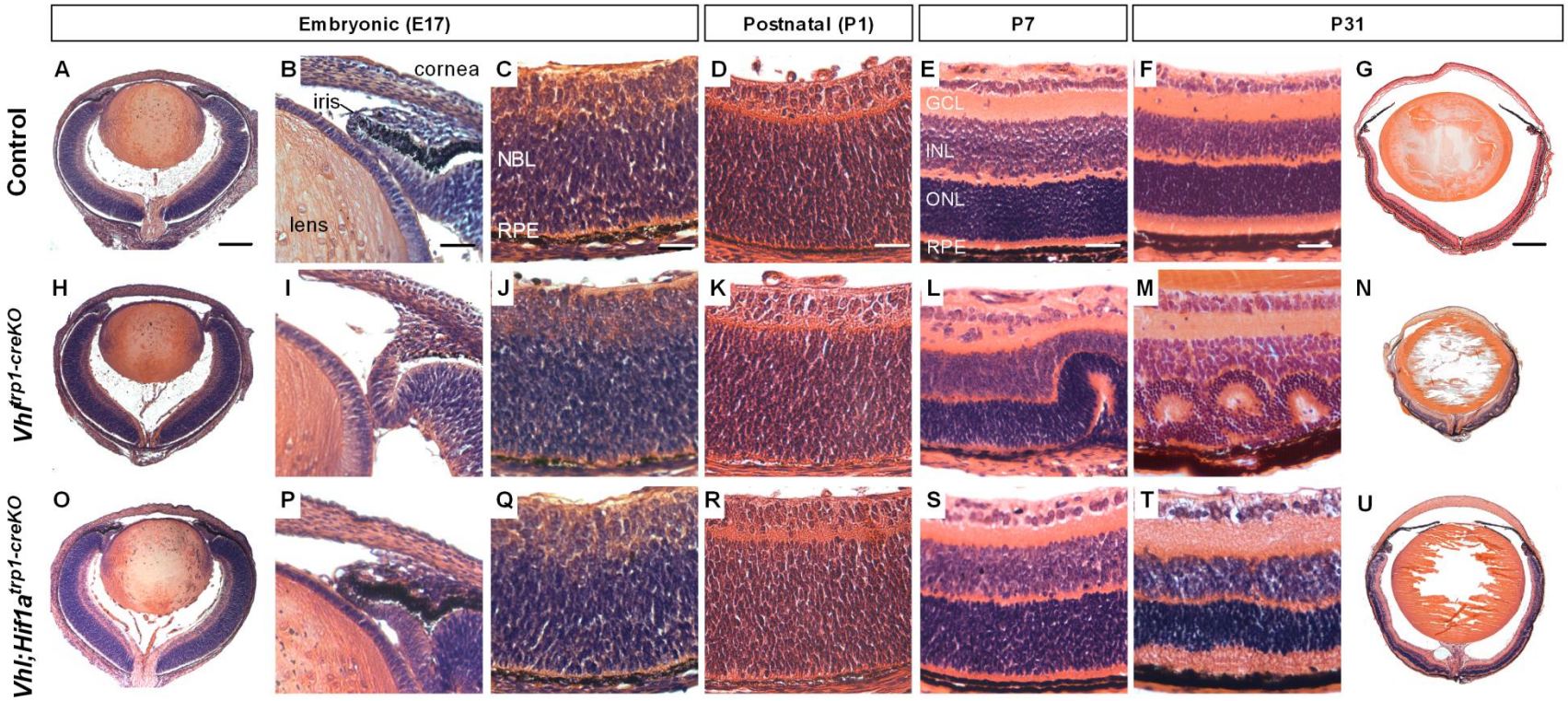

Figure 3.3 *Vhl*$^{trp1\text{-}creKO}$ *mice* show early defects in iris and RPE development associated with retinal degeneration and microphthalmia in the adult that are mediated by Hif1a. Representative H&E histology in *Vhl*$^{trp1\text{-}creKO}$, *Vhl;Hif1a*$^{trp1\text{-}creKO}$ and control animals at E17 **(**columns **A,B,C)**, P1 (column **D**), P7 (column **E**) and P31 (columns **F,G**). Scale bars: 250 µm in column A, 25 µm in column B, 20 µm in column C-F, 500 µm in column G.

3.3.4 Conditional inactivation of *Vhl* leads to a Hif1a mediated abnormal morphology and reduction of RPE cells

To determine the effect of *Vhl* inactivation on RPE morphology and survival, we characterised the RPE in further detail by semithin and ultrastructural analysis, and quantified apoptosis by caspase 3 immunohistochemistry at P0 (n= 4-5 animals per group).

Vhl$^{trp1\text{-}creKO}$ mice demonstrated a 60 % (s.d. ±4%) reduction in the number of RPE cells compared with littermate controls t P0 (figure 3.4A,D,J; $p<0.0001$). Ultrastructural analysis revealed a dysmorphic RPE with dystrophic changes and a reduction in the content of melanin granules. The remaining granules appeared to be irregularly shaped, and melanin granules with the typical fusiform shape were scarce in number. Although the remaining RPE cells were sparse and the thickness of the RPE reduced, Bruch's membrane was preserved (figure 3.4B,E). Furthermore, *Vhl*$^{trp1\text{-}creKO}$ mice demonstrated a significant increase of apoptotic cells in the RPE and in the pigmented iris ($p<0.0001$, figure 3.4C,F,K,M). The rate of apoptosis in the developing neural retina, however, was similar to that of littermate controls at birth ($p=0.22$, figure 3.4L). *Vhl;Hif1a*$^{trp1\text{-}creKO}$ mice, in contrast, demonstrated a normal RPE cell number and morphology and a normal rate of apoptosis in the RPE, iris and neuroretina compared with wildtype controls (figure 3.4G-M). These findings indicate that Hif1a-mediated cell death is responsible for reduction in RPE and pigmented iris cell number in *Vhl*$^{trp1\text{-}creKO}$ mice and suggest a critical role for Vhl in regulating Hif1a levels for normal RPE, iris and eye development.

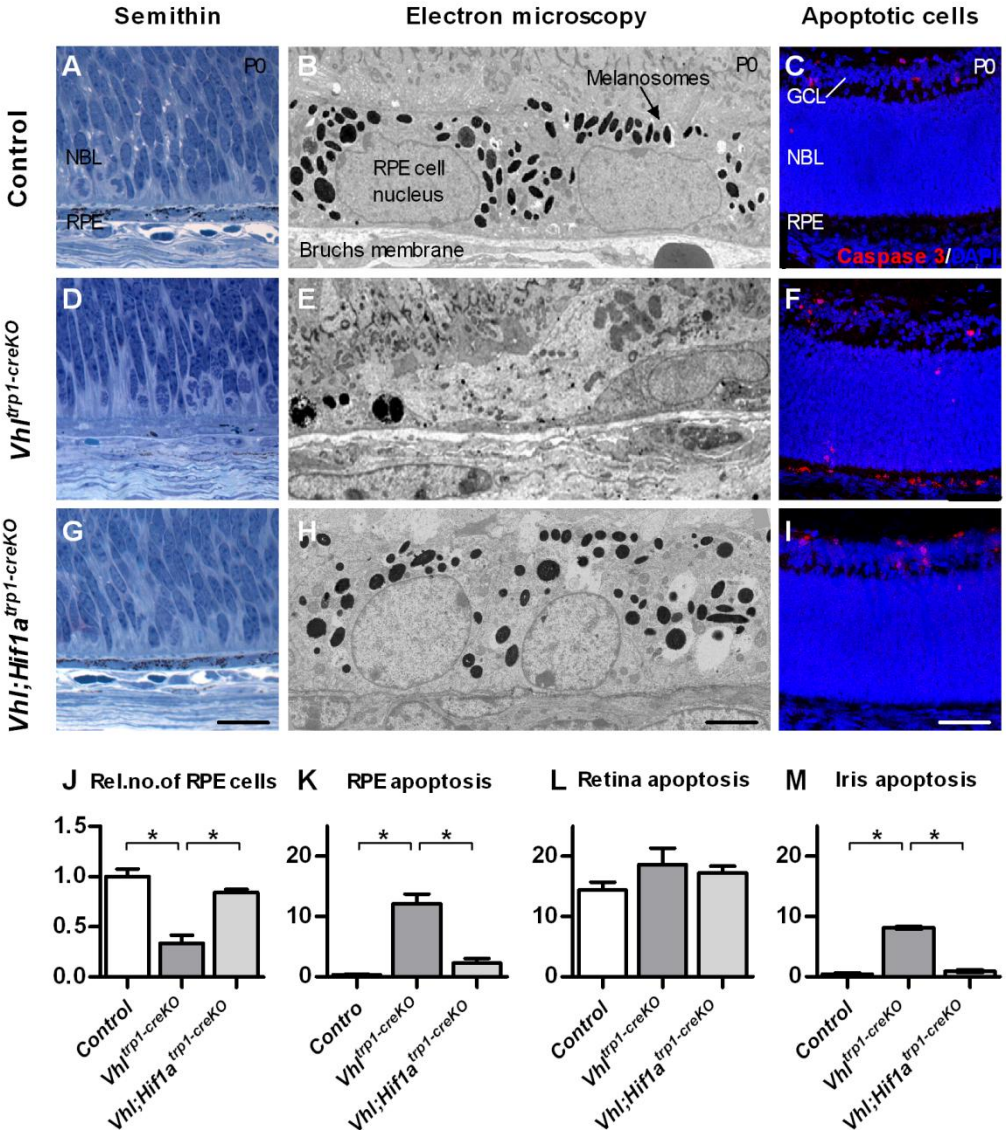

Figure 3.4 Conditional inactivation of *Vhl* in the RPE results in Hif1a mediated apoptosis and dystrophy of RPE cells. Semithin **(A,D,G)** and electron microscopy histology **(B,E,H)** show a reduced and dystrophic RPE in *Vhl*$^{trp1\text{-}creKO}$ compared with *Vhl;Hif1a*$^{trp1\text{-}creKO}$ and control littermates at P0. Representative caspase-3 immunohistochemistry (**C,F,I**) demonstrate increased apoptosis in the RPE and iris in *Vhl*$^{trp1\text{-}creKO}$ compared with *Vhl;Hif1a*$^{trp1\text{-}creKO}$ and control littermates at P0. Quantification of RPE cells **(J)** and apoptotic cells in the RPE, retina and iris in *Vhl*$^{trp1\text{-}creKO}$, *Vhl;Hif1a*$^{trp1\text{-}creKO}$ and control littermates at P0 **(K-M).** * = p<0.05, ANOVA Test. Error bars = ±SEM. Scale bars: 20 µm in A,D,G, 5 µm in B,E,H and 50 µm in C,F and I.

3.3.5 Conditional inactivation of *Vhl* results in Hif1a mediated reduced proliferation of retinal precursor cells

To determine the effect of RPE cell death in *Vhl*$^{trp1\text{-}creKO}$ mice on neuroretinal development, the rate of neuroretinal cell proliferation was assessed by phospho-histone H3 immunohistochemistry at birth (range 4-5 mice per group).

Conditional inactivation of *Vhl* in the RPE was associated with a significant reduction of mitotic cells in the proliferation zone of the developing retina compared with littermate controls (p=0.009, figure 3.5A-F, J). Additional inactivation of *Hif1a* in the RPE in *Vhl;Hif1a*$^{trp1\text{-}creKO}$ mice resulted in a normal rate of neuroretinal cell proliferation compared with control animals (figure 3.5G-J). The level of proliferation in RPE and in the pigmented iris cells, however, was similar in *Vhl*$^{trp1\text{-}creKO}$, *Vhl;Hif1a*$^{trp1\text{-}creKO}$ and control mice at birth (p=0.35 for RPE, p=0.27 for iris cell proliferation, figure 3.5K-L).

These data demonstrate that Hif1a stabilisation in the pigmented epithelium in *Vhl*$^{trp1\text{-}creKO}$ mice is associated with secondary effects on neuroretinal cell proliferation and retinal development that may contribute to the development of microphthalmia.

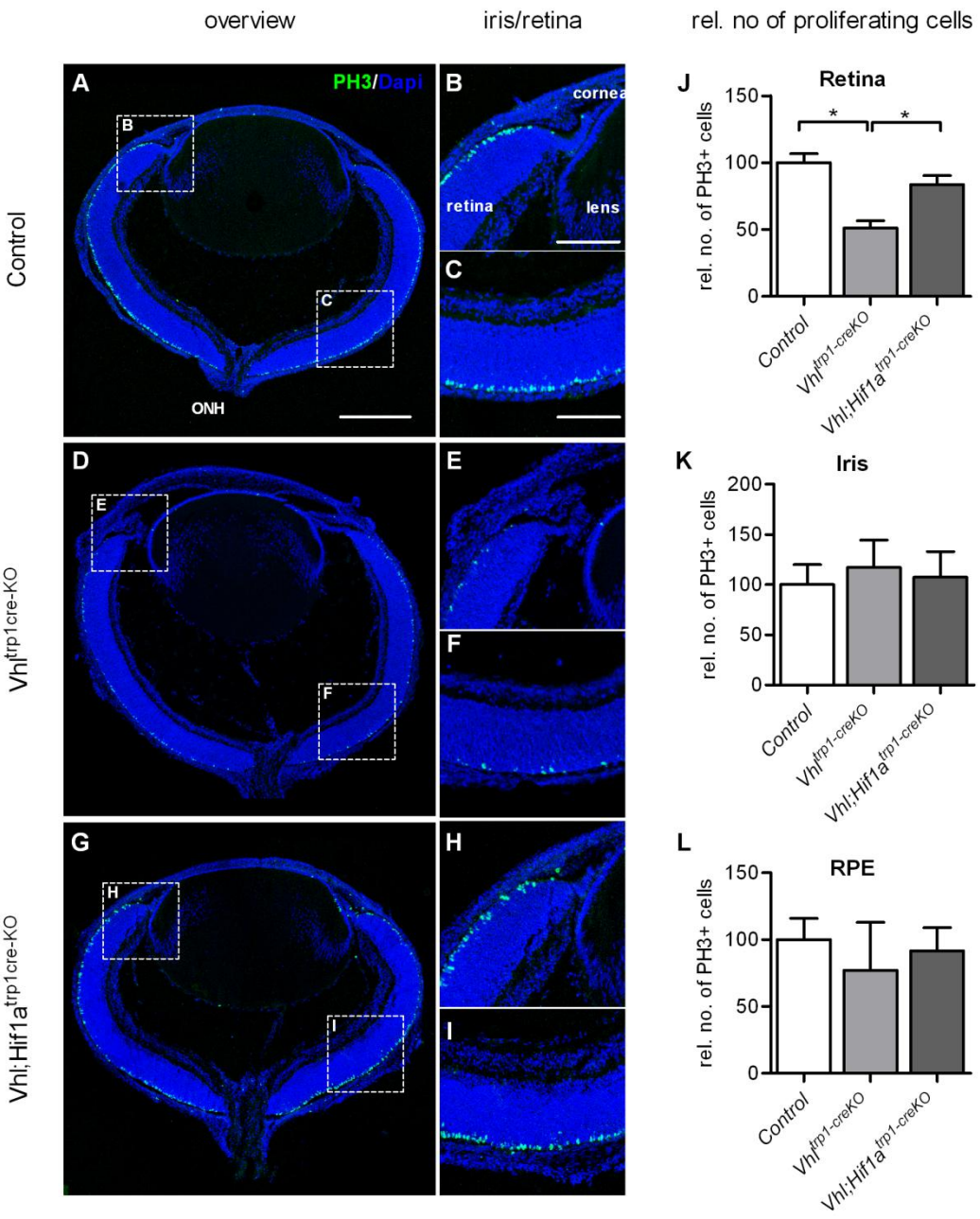

Figure 3.5 Conditional inactivation of *Vhl* in the RPE results in Hif1a mediated reduction of proliferating retinal precursor cells. Representative phospho-histone H3 (PH3) immunohistochemistry staining in the eye, anterior chamber and retina in *Vhl*$^{trp1\text{-}creKO}$, *Vhl;Hif1a*$^{trp1\text{-}creKO}$ and controls at P0 **(A-I)**. Relative quantification of the number of proliferating cells in the retina, iris and RPE in *Vhl*$^{trp1\text{-}creKO}$ compared with *Vhl;Hif1a*$^{trp1\text{-}creKO}$ and control littermates at P0 **(J-L)**. Error bars indicate mean ±SEM. * = p<0.05, ANOVA Test. Scale bars: 300 µm in A,D,G, 100 µm in B,E,H and 80 µm in C,F,I.

3.3.6 Conditional inactivation of *Vhl* in the RPE alters expression levels and distribution of Pax6 and Otx2

Since microphthalmia and aniridia have been associated with mutations in *Pax6* (Hill et al., 1991; Jordan et al., 1992), *Otx2* (Matsuo et al., 1995) and *Mitf* (Cheli et al., 2010), the cellular distribution of Pax6 and Otx2 and the global expression levels of *Otx2*, *Pax6* and *Mitf* was assessed in the eyes of $Vhl^{trp1\text{-}creKO}$, $Vhl;Hif1a^{trp1\text{-}creKO}$ and control mice at birth by immunohistochemistry and RT-PCR respectively. Immunohistochemistry demonstrated a similar distribution of Pax6 in the central neuroretina of $Vhl^{trp1\text{-}creKO}$, $Vhl;Hif1a^{trp1\text{-}creKO}$ and control mice (figure 3.6A-F). Within the distal retina, i.e. the primordium of the iris, however, Pax6 expressing cells were reduced in $Vhl^{trp1\text{-}creKO}$ mice compared with $Vhl;Hif1a^{trp1\text{-}creKO}$ and control mice (figure 3.6B). *Pax6* RNA expression was significantly decreased in $Vhl^{trp1\text{-}creKO}$ compared with control mice at birth ($p=0.02$, figure 3.6G). $Vhl;Hif1a^{trp1\text{-}creKO}$ mice in contrast showed normal global *Pax6* expression levels compared with wildtype controls. These data suggest that conditional inactivation of *Vhl* in the RPE and pigmented iris progenitor cells leads to reduced levels of Pax6 expressing cells in the distal part of the optic cup by birth which may contribute to the abnormal iris development.

Immunohistochemistry staining for Otx2 revealed similar Otx2 levels in the neuroretina of $Vhl^{trp1\text{-}creKO}$ and control mice, increased staining in the neuroretina of $Vhl;Hif1a^{trp1\text{-}creKO}$ mice and normal staining in the RPE in both $Vhl^{trp1\text{-}creKO}$, $Vhl;Hif1a^{trp1\text{-}creKO}$ compared with control mice (figure 3.6 H-M). Global *Otx2* RNA expression levels were also similar in $Vhl^{trp1\text{-}creKO}$ mice compared with control

animals suggesting that conditional inactivation of *Vhl* results in microphthalmia that is independent of Otx2. Global *Otx2* mRNA levels were twofold increased in *Vhl;Hif1a*$^{trp1\text{-}creKO}$ mice compared with *Vhl*$^{trp1\text{-}creKO}$ and control mice (p=0.0001, figure 3.6N) suggesting that other Vhl dependent molecules affect neuroretinal Otx2 expression and localisation in a Hif1a-dependent manner.

Furthermore RT-PCR analyses demonstrated similar global expression levels of *Mitf* in *Vhl*$^{trp1\text{-}creKO}$ and *Vhl;Hif1a*$^{trp1\text{-}creKO}$ eyes compared with littermate controls (p=0.5, figure 3.6O). Although subtle and regional differences in Mitf expression cannot be excluded, these findings suggest that the development of microphthalmia in *Vhl*$^{trp1\text{-}creKO}$ mice may be independent of Mitf.

Taken together these data highlight the critical role of Vhl and Hif1a signalling in the RPE for normal distribution and expression of important transcription factors involved in ocular development. The findings indicate that conditional inactivation of *Vhl* in the pigmented epithelium leads to microphthalmia and aniridia, in a mechanism that involves Hif1a-dependent increased RPE and iris apoptosis, reduced proliferation of retinal progenitor cells, and reduced Pax6 expression in the distal optic cup.

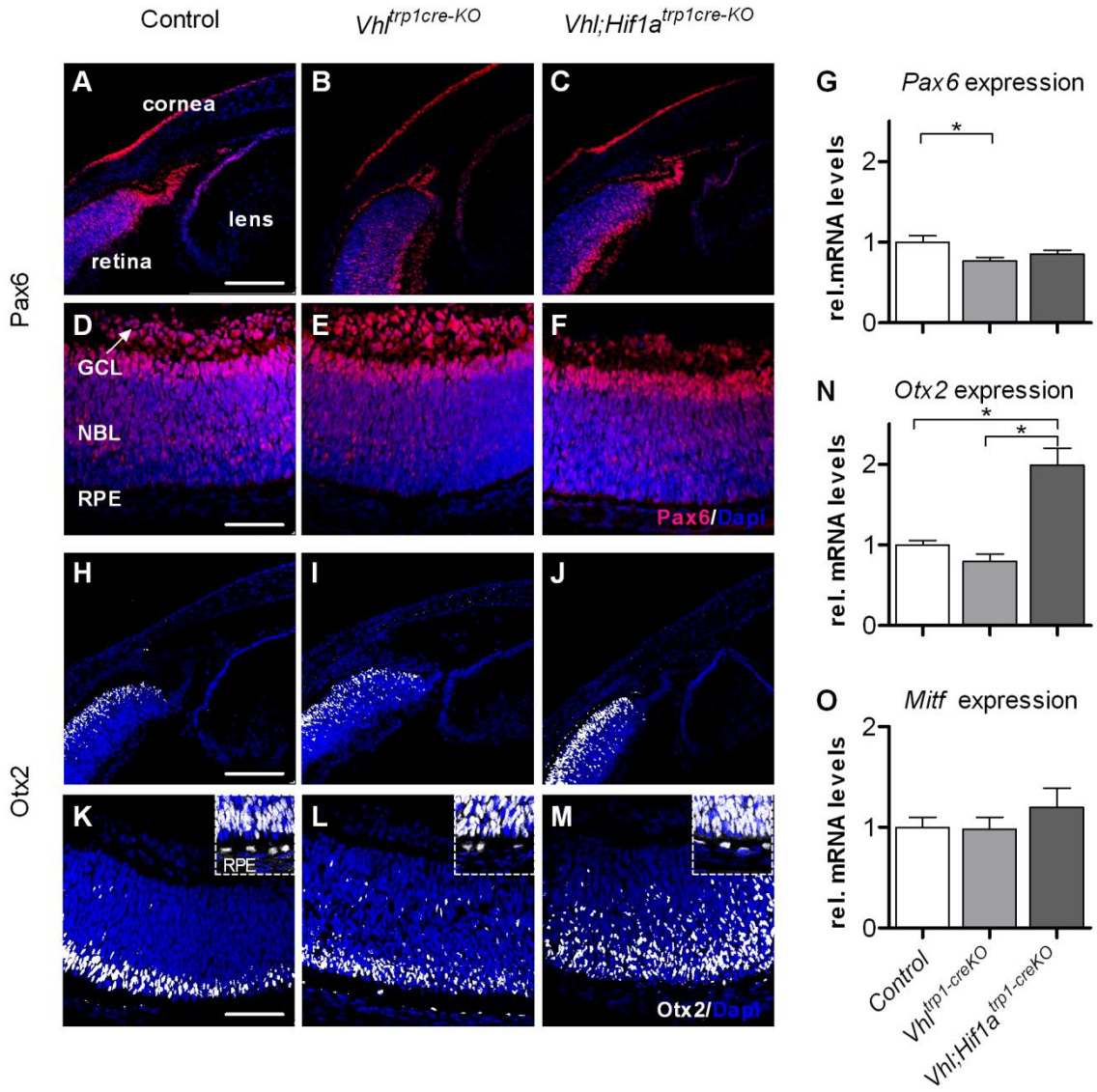

Figure 3.6 Conditional inactivation of *Vhl* in the RPE affects expression levels and localisation of Pax6 and Otx2 in the neuroretina. Representative immunohistochemistry and global relative mRNA levels for *Pax6* (**A-G**), *Otx2* (**H-M**) and *Mitf* (**O**, RNA levels only) in *Vhl*$^{trp1\text{-}creKO}$, *Vhl;Hif1a*$^{trp1\text{-}creKO}$ and littermate control mice at birth. *Vhl*$^{trp1\text{-}creKO}$ mice demonstrate reduced Pax6 staining in the anterior retina (B) and decreased global *Pax6* expression (**G**) compared with *Vhl;Hif1a*$^{trp1\text{-}creKO}$ and littermate control mice. Otx2 expression is mislocalised and increased in *Vhl;Hif1a*$^{trp1\text{-}creKO}$ mice compared with *Vhl*$^{trp1\text{-}creKO}$ and control mice (**H,M**). Scale bars: 150µm in rows B,I; 75µm in rows E,L. GCL, ganglion cell layer; NBL, neuroblast layer; RPE, retinal pigment epithelium. Error bars indicate mean ±SEM. * = $p<0.05$.

3.3.7 Conditional inactivation of *Vhl* in the RPE causes persistence of embryonic vascular structures and the formation of chorioretinal anastomosis in the adult

As Hifa stabilisation in the RPE was found to be associated with an early increase in angiogenic factors, the vascular phenotype of the anterior (figure 3.7A-F) and posterior chamber (figure 3.8A-O) was investigated in $Vhl^{trp1\text{-}creKO}$ and littermate controls by *in vivo* ICG angiography and immunohistochemistry (n=4-6 animals per group). *In vivo* ICG angiography demonstrated a perfused vascular network in the anterior chamber of $Vhl^{trp1\text{-}creKO}$ mice at P21 (figure 3.7E) consistent with a persistent pupillary membrane. However, collagen IV stained cryosections demonstrated vascular staining in the corneal stroma, indicating that this vasculature may be situated within the cornea (figure 3.7F). $Vhl;Hif1a^{trp1\text{-}creKO}$ mice, in contrast, exhibited a normal vasculature of the iris and ciliary body and an avascular cornea (figure 3.7H,I). Furthermore, $Vhl^{trp1\text{-}creKO}$ mice demonstrated a persistent hyaloid vasculature (figure 3.8F,G) and a disorganised retinal vasculature with abrogated vascular layering and chorioretinal anastomosis at P21 (figure 3.8H-J). Similarly, $Vhl;Hif1a^{trp1\text{-}creKO}$ mice exhibited persistent hyaloid vessels, a dense intra retinal vascular network with abrogated vascular layering and chorioretinal anastomosis (figure 3.8K-O). These vascular changes were associated with macroscopic intraretinal and vitreous bleedings (figure 3.8L inlay). These data suggest that Vhl mediated Hif1a regulation is essential for normal vascularisation of the anterior chamber whereas other Vhl regulated pathways control vascularisation of the retina.

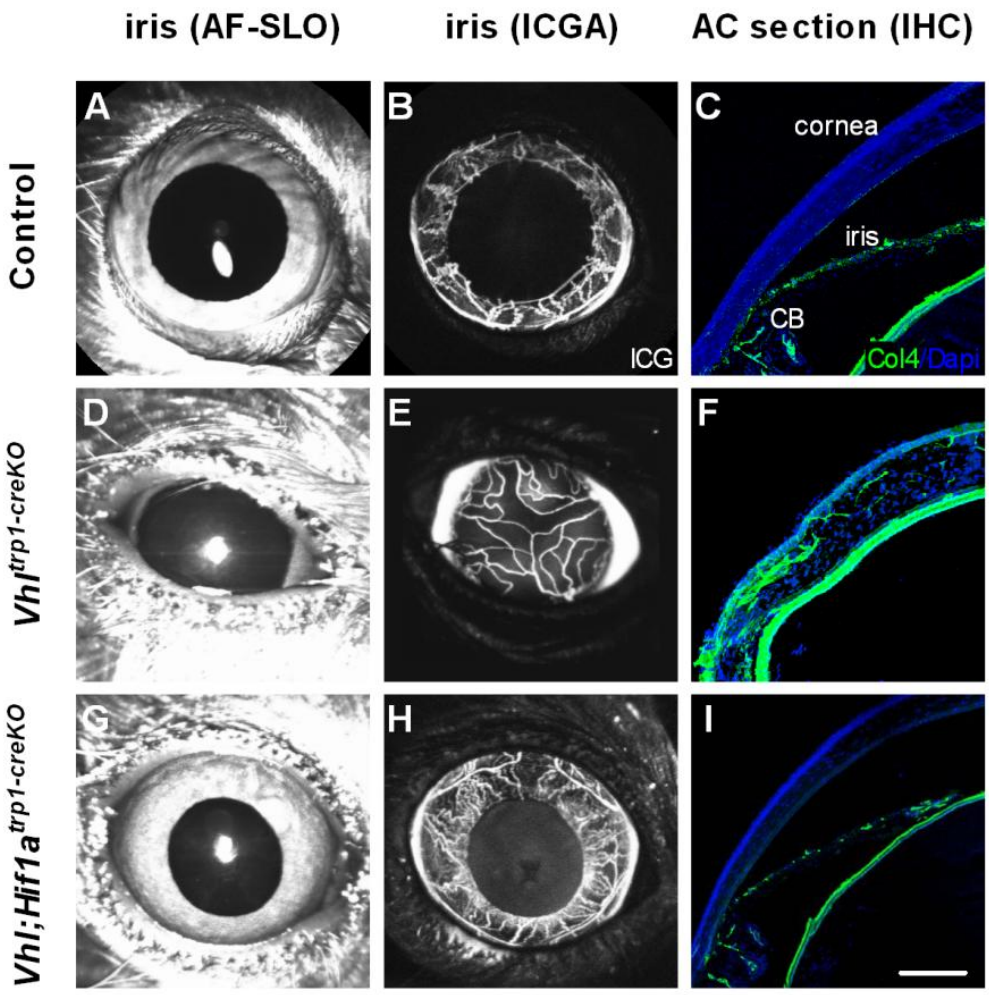

Figure 3.7 *Vhl*$^{trp1\text{-}creKO}$ mice exhibit a Hif1a dependent abnormal vascular phenotype in the anterior chamber. Infrared imaging **(A,D,G),** indocyanin-green angiography **(B,E,H)** and collagen IV stained cryosections **(C,F,I)** of *Vhl*$^{trp1\text{-}creKO}$, *Vhl;Hif1a*$^{trp1\text{-}creKO}$ and control littermates at P21 show a perfused vascular network in the anterior chamber of *Vhl*$^{trp1\text{-}creKO}$ mice which is absent in *Vhl;Hif1a*$^{trp1\text{-}creKO}$ and control mice. AF-SLO = autofluorescence scanning laser ophthalmoscope ICGA= indocyanin-green angiography. AC = anterior chamber. CB = ciliary body. Scale bar: 75 µm.

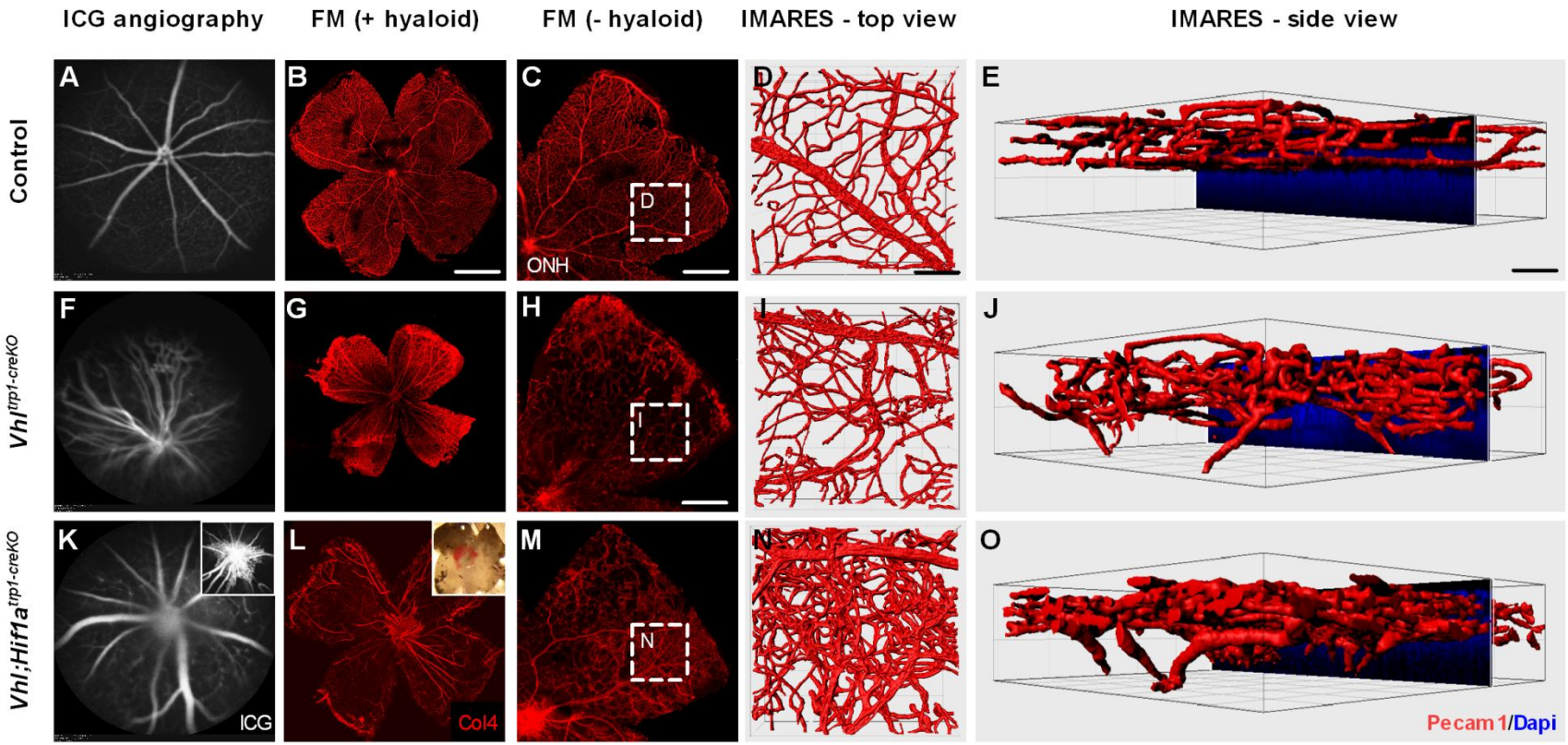

Figure 3.8 *Vhl*$^{trp1\text{-}creKO}$ mice show a Hif1a independent persistence of the hyaloid vasculature and a disorganised retinal vasculature. Indocyanin-green angiography **(A,E,I)** and corresponding collagen4 stained retinal flatmounts **(B-D, F-H, J-L)** show a persistent hyaloid vasculature in *Vhl*$^{trp1\text{-}creKO}$ and *Vhl;Hif1a*$^{trp1\text{-}creKO}$ mice at P21**.** *Vhl*$^{trp1\text{-}creKO}$ and *Vhl;Hif1a*$^{trp1\text{-}creKO}$ mice demonstrate a disorganised retinal vasculature with retinal vessels growing in the outer retina **(F-O).** *Vhl;Hif1a*$^{trp1\text{-}creKO}$ exhibit a dense and disorganised retinal vasculature **(L,M,N)** which can be associated with intraretinal haemorrhage **(inlay L)**. FM = flatmount; SLO = scanning laser ophthalmoscope. Scale bar: 1 mm for B,F,J and 50 µm C-D, G-H and K-L.

To characterise the vascular phenotype in more detail, the ocular vasculature was examined on cryosections at different timepoints during retinal vascular development (n=4-5 animals per group per timepoint, figure 3.9A-P). Compared with littermate controls, *Vhl*$^{trp1\text{-}creKO}$ mice revealed a normal retinal vasculature until postnatal day 7, demonstrating a superficial vascular network and vessels diving into the outer plexiform layer in the central retina (figure 3.9H). In temporal association with the observed rosette formation, *Vhl*$^{trp1\text{-}creKO}$ mice exhibit disorganised retinal vasculature and chorioretinal anastomosis from P14 onwards (figure 3.9I,J). *Vhl;Hif1a*$^{trp1\text{-}creKO}$ mice present with a similar disorganised retinal vasculature and chorioretinal anastomosis as seen in *Vhl*$^{trp1\text{-}creKO}$ mice from P14 onwards (figure 3.9O,P).

These data indicate that *Vhl* expression in the RPE is critical for normal layering of the retinal vasculature and maintenance of the blood-retina barrier that is independent of Hif1a.

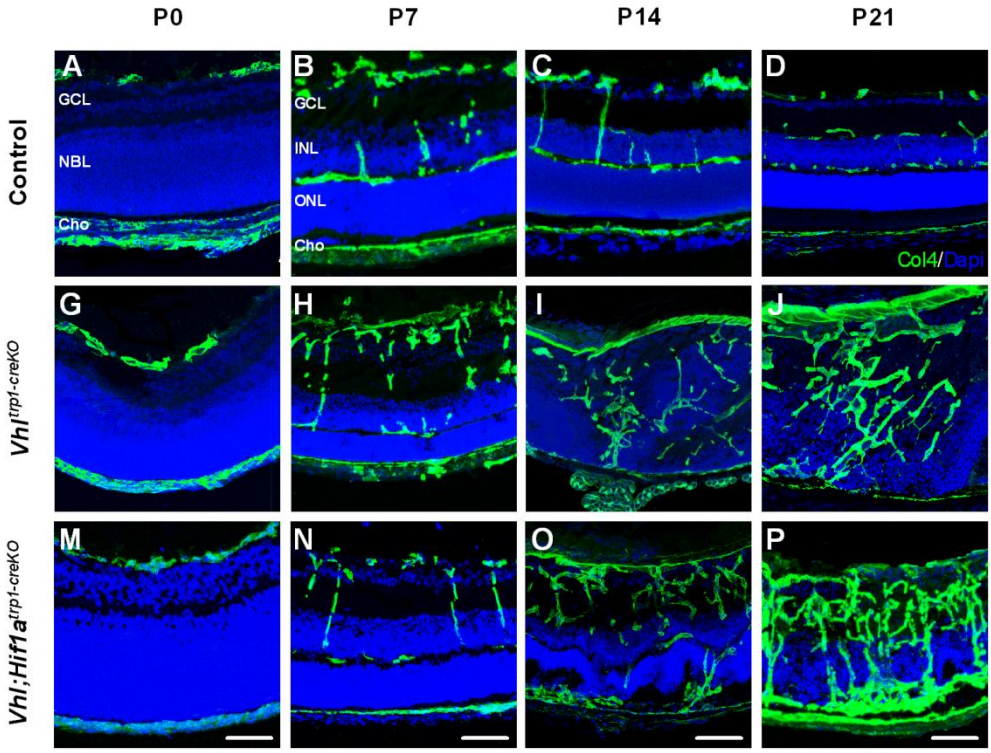

Figure 3.9 Conditional inactivation of *Vhl* in the RPE results in disruption of the retinal vascular architecture and in the formation of chorioretinal anastomosis. Representative collagen-4 stained cryosections of control **(A-D)**, *Vhl;Hif1a*$^{trp1\text{-}creKO}$ **(G-J)** and *Vhl*$^{trp1\text{-}creKO}$ mice **(M-P)** at different time points during development demonstrate a disorganised retinal vasculature and chorioretinal anastomosis **(I,O)** in *Vhl;Hif1a*$^{trp1\text{-}creKO}$ and *Vhl*$^{trp1\text{-}creKO}$ mice. GCL, ganglion cell layer; NBL, neuroblast layer; Cho, choroid; INL, inner nuclear layer, ONL, outer nuclear layer; Scale bar: 25 µm.

3.3.8 Conditional inactivation of *Vhl* in the RPE causes retinal degeneration in the adult

To determine the long-term consequences of *Vhl* deletion in the RPE, retinal changes were examined in adult $Vhl^{trp1\text{-}creKO}$ mice in detail by immunohistochemistry and electroretinography (range 5-7 animals per group). Adult $Vhl^{trp1\text{-}creKO}$ mice (8 weeks) develop a severe retinal degeneration with absent retinal lamination, a reduction of rhodopsin and recoverin expression, and reduced synapse formation as shown by GFAP, rhodopsin, recoverin and CtBP immunohistochemistry (figure 3.10F-H). These morphological changes were associated with absent photopic and scotopic ERG function at all light intensities tested (figure 3.10I,J,P,Q). Additional inactivation of *Hif1a* in the RPE restores retinal lamination but does not abrogate GFAP activation or rescue rhodopsin and recoverin expression, or synapse formation (figure 3.10K-M). This is associated with detectable scotopic a-waves at light intensities higher than 0.1 cd.s/m^2 indicating the presence of functioning photoreceptor cells, but highly-attenuated b-waves consistent with reduced formation of synapses that is essential for bipolar cell activation (figure 3.10N-Q).

These data suggest that Vhl expression in the RPE during development is critical for the maturation of a normal functioning retina. Vhl-dependent Hif1a degradation in the RPE promotes normal retinal layering but does not appear to control maturation of the outer retina, which may depend on other Vhl-dependent factors such as Hif2a.

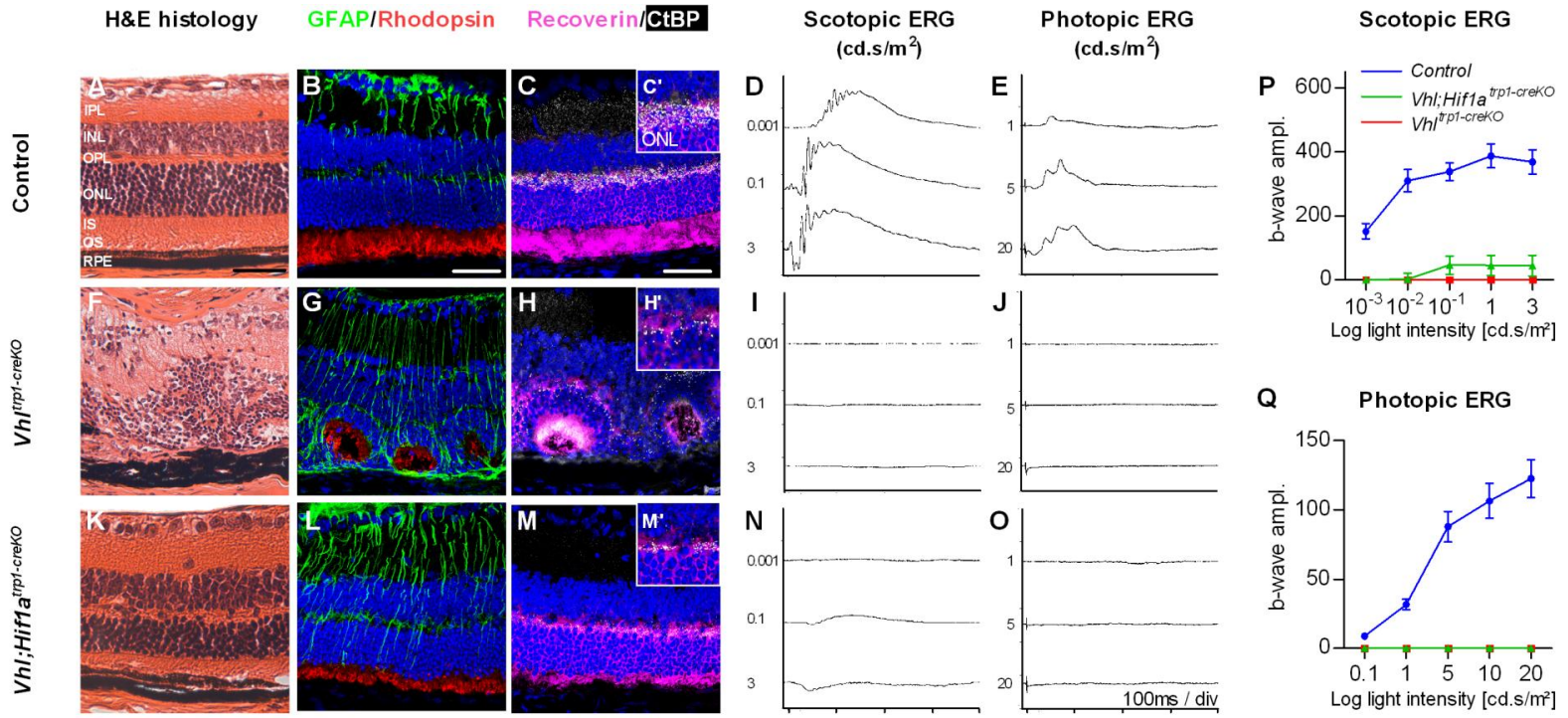

Figure 3.10 Conditional inactivation of *Vhl* in the RPE results in retinal degeneration in the adult which is partly dependent on Hif1a. Compared with littermate control **(A-E)** *Vhl*$^{trp1\text{-}creKO}$ demonstrate an extensive retinal degeneration with absent retinal layering **(F)**, increased GFAP associated scarring **(G)**, decreased rhodopsin and recoverin expression and reduced synapses formation **(G,H)** which is associated with absent photopic and scotopic ERG function **(I,J)**. Additional inactivation of *Hif1a* in the RPE **(K-O)** restores retinal layering **(K)** but still results in increased GFAP activation **(L)**, reduced rhodopsin and recoverin expression and decreased synapsis formation **(L,M).** This is associated with traces of a-waves at high light intensities in the scotopic ERG **(N,P)** and absent photopic ERG responses **(O,Q)**. Mean b-wave amplitude (±s.e.m.) under photopic and scotopic condition at different light intensities **(P,Q)**. Scale bar (column A-C): 50 µm. Scale, column D: 0.2 mV/div; column E 0.1 mV/Div.

3.4 Discussion

In the eye, oxygen plays a critical role in both physiological vascular development and common blinding diseases. The RPE is essential for normal ocular development and is implicated in the pathogenesis of hypoxia-induced retinal vascular disease (Stefansson et al., 2010). However, the role of the oxygen sensing VHL/HIF1a pathway in the RPE and its contribution to the development of the eye and its vasculature has not previously been examined. In this chapter I investigated the function of Vhl and Hif1a in the developing RPE using a tissue-specific conditional *knockout* approach. Deletion of *Vhl* in the RPE results in a significant increase of Hif1a and Hif2a protein which is associated with a severe developmental phenotype, including the development of aniridia, microphthalmia and a strong pathological vascular phenotype in the anterior and posterior segments. Interestingly, aniridia, microphthalmia and the anterior vascular phenotype, but not the vascular phenotype in the retina, could be rescued by additional deletion of Hif1a in the RPE. These findings indicate that Vhl-dependent regulation of Hif1a in the RPE and pigmented iris cells is critical for normal ocular and iris development whereas other Vhl-dependent pathways in the RPE determine normal retinal vascularisation. The results also suggest that ocular hypoxia may be a previously unrecognised mechanism in the development of microphthalmia and that reduced systemic oxygenation, for example in placental insufficiency, could have major effects on ocular development through activation of HIFs in the RPE.

The results in this chapter demonstrate that conditional inactivation of *Vhl* in the RPE is associated with Hif1a-dependent increased apoptosis of RPE and pigmented iris cells. This finding is consistent with the results of recent studies which show that conditional inactivation of *Vhl* in the neuroretina is associated with increased apoptosis of photoreceptor cells (Kurihara et al., 2010; Lange et al., 2011). It is important to point out that Hif1a regulates not only survival genes via its control of cellular proliferation, metabolism and vasomotor control (Sharp and Bernaudin, 2004), but can also induce expression of pro-apoptotic factors. Hif1a can promote p53-mediated hypoxia-induced apoptosis in neurons of the CNS (Halterman et al., 1999), in part by upregulation of pro-apoptotic genes such as Bnip3, Nix, Igfbp3 and also by downregulation of anti-apoptotic genes like Bcl2 (An et al., 1998; Bacon and Harris, 2004; Carmeliet et al., 1998). These Hif1a-mediated pro-apoptotic mechanisms may be responsible for the RPE and iris cell loss in $Vhl^{trp1\text{-}creKO}$ mice and contribute to the observed microphthalmia and aniridia. These findings are consistent with the finding that toxic ablation of the RPE *in vivo* results in disorganisation of the retinal layer and an immediate arrest of eye growth (Raymond and Jackson, 1995). Furthermore, RPE cell loss in $Vhl^{trp1\text{-}creKO}$ mice is associated with a secondary reduction in proliferating iris and retinal progenitor cells that may further contribute to the development of aniridia and microphthalmia.

Mutations in various transcription factors, including the microphthalmia-associated transcription factor (*Mitf*), the paired box gene 6 (*Pax6*) and the orthodenticle protein homolog 2 (*Otx2*) are associated with the development of

aniridia and microphthalmia (Fuhrmann, 2010). *Mitf* plays a key role in melanocyte differentiation, proliferation and survival. *Mitf knockout* mice develop severe microphthalmia which is similar to that in *Vhl*$^{trp1\text{-}creKO}$ mice (Cheli et al., 2010). Inactivation of *Mitf* results in apoptosis of melanocytes (McGill et al., 2002) by downregulation of the critical anti-apoptotic mediator Bcl2, which protects RPE cells *in vitro* (Liang et al., 2000). The findings in this chapter indicate that conditional inactivation of *Vhl* in the RPE is associated with normal global expression levels of *Mitf*. Although regional differences in Mitf expression in the eyes of *Vhl*$^{trp1\text{-}creKO}$ mice cannot be excluded, these data suggest that conditional inactivation of *Vhl* in the RPE results in microphthalmia that is independent of Mitf.

Pax6 is one of the key transcription factors involved in the complex process of eye development and plays multiple distinct roles in lens, iris and retinal development, involving interactions with other transcription factors (Hever et al., 2006). Haploinsufficiency of Pax6/PAX6 has been implicated in a number of congenital eye disorders in both humans and mice, including aniridia, microphthalmia and anterior segment malformations. The results of this chapter demonstrate that conditional inactivation of *Vhl* in the RPE is associated with a reduction of Pax6 in the distal optic cup and pigmented iris primordium which appears to be Hif1a-dependent. Normal Pax6 expression in the distal optic cup is essential for iris development and reduced expression at this site results in iris hypoplasia (vis-Silberman et al., 2005). The data suggest that a Hif1a-mediated loss of the RPE and the pigmented iris primordium can reduce Pax6 expression

in the distal optic cup and may therefore contribute to the absent iris development in *Vhl*$^{trp1\text{-}creKO}$ mice. Future studies will have to address the interaction of Vhl-Hif with the Pax6 pathway to elucidate further the developmental mechanisms responsible for aniridia.

Otx2 is a transcription factor involved in the regional specification of the eye, particularly the RPE in early development (Martinez-Morales et al., 2001). After eye regions are specified, Otx2 expression is up-regulated in post-mitotic neuroblasts that will eventually differentiate into the various cell types of the neural retina (Bovolenta et al., 1997). While Otx2 homozygous embryos display a severe head phenotype lacking the anterior neuroectoderm, heterozygous deletion of Otx2 can be associated with eye anomalies including anterior segment malformations and microphthalmia (Acampora et al., 1995; Matsuo et al., 1995). The results presented in this chapter demonstrate that conditional inactivation of *Vhl* in the RPE does not affect Otx2 expression in the retina and RPE suggesting that microphthalmia in *Vhl*$^{trp1\text{-}creKO}$ mice may be independent of Otx2. However, inactivation of both *Vhl* and *Hif1a* results in mislocalised and increased *Otx2* expression in the neuroretina suggesting that other Vhl-dependent mechanisms may affect neuroretinal Otx2 expression and localisation in a Hif1a-dependent manner.

Furthermore, conditional inactivation of *Vhl* in the RPE results in severe retinal degeneration with undetectable photopic and scotopic ERG responses in the adult. Additional inactivation of *Hif1a* in the RPE restores retinal lamination and detectable scotopic ERG a-wave responses that indicate the presence of

functioning photoreceptor cells. The reduced formation of synapses that are essential for bipolar cell activation, in these animals may account for the persistent attenuation of ERG b-waves. These data suggest that Vhl expression in the RPE during development is critical for the maturation of a normal functioning retina. Vhl-dependent Hif1a degradation in the RPE promotes normal retinal layering but does not appear to control maturation of the outer retina, which may depend on other Vhl-dependent factors such as Hif2a.

Whereas conditional inactivation of *Hif1a* in the RPE results in a normal ocular and vascular phenotype (Marneros et al., 2005), the conditional inactivation of *Vhl* in the RPE leads to striking anterior and posterior vascular changes. Adult $Vhl^{trp1\text{-}creKO}$ mice demonstrate persistence of the pupillary membrane and the hyaloid vasculature that usually regress early in development (Ito and Yoshioka, 1999). These embryonic vascular structures may persist in response to an early proangiogenic environment and high Vegf levels derived from RPE and pigmented iris cells and subsequently in response to secondary changes in the neuroretina. Interestingly, the anterior vascular phenotype, but not the retinal vascular phenotype is rescued by additional conditional inactivation of *Hif1a*. This indicates an important primary role of Vhl-dependent Hif1a regulation for iris cell survival and the vascular development of the anterior chamber. The increased expression of Vegf and other angiogenic factors in the RPE and secondarily in the neuroretina in $Vhl^{trp1\text{-}creKO}$ mice may also be responsible for the dysmorphic and disorganised retinal vascular phenotype. Additional inactivation

of *Hif1a* in the RPE did not abrogate Vegf overexpression in the RPE or neuroretina nor rescue the vascular phenotype. This indicates that other Vhl regulated downstream molecules, such as Hif2a, may be responsible for Vegf expression in the RPE, the secondary increase of angiogenic factors in the neuroretina and the associated vascular phenotype. Retina-specific inactivation of *Vhl* leads to a similar but milder vascular phenotype compared with $Vhl^{trp1\text{-}creKO}$ mice, including the persistence of hyaloid vasculature and the pupillary membrane (Kurihara et al., 2010; Lange et al., 2011). In contrast to our results, Kurihara et al reported that a combined inactivation of *Vhl* and *Hif1a* in the neuroretina rescues the vascular phenotype suggesting that the observed phenotype was Hif1a-mediated. This difference may be explained by the different localisation of *Vhl* inactivation (RPE vs. neuroretina) suggesting that the consequences of HIF1a stabilisation in the neuroretina differ from those of HIF1a in the RPE. Furthermore, our findings demonstrate that conditional inactivation of *Vhl* or *Vhl;Hif1* results in the secondary formation of chorioretinal anastomoses. These vascular malformations were evident from P10 onwards although Hif1a and Vegf protein levels are already significantly upregulated at birth. Oshima et al have shown that mice with overexpression of Vegf in RPE develop normal retinal and choroidal vasculature without spontaneous CNV formation. However, perturbation of the RPE and the Bruch's membrane by subretinal injection leads to the development of choroidal neovascularisation in transgenic mice overexpressing Vegf in the RPE (Oshima et al., 2004). Therefore it is possible that spontaneous perturbation of the blood-retina barrier

by Hif1a-mediated RPE cell death in *Vhl*$^{trp1\text{-}creKO}$ mice might promote the observed formation of chorioretinal anastomoses.

3.5 Conclusion

Work in this chapter has shown the importance of Vhl and Hif1a signalling in the RPE for normal eye growth, iris development and vascular integrity. Appropriate regulation of Hif1a by Vhl is essential for normal RPE and iris development, ocular growth and vascular development in the anterior chamber, whereas Vhl dependent regulation of other downstream molecules is critical for maintaining normal retinal vasculature. Ocular hypoxia may be a previously unrecognised mechanism in the development of microphthalmia, and reduced systemic oxygenation, for example in placental insufficiency, could have major effects on ocular development through activation of HIF in the RPE.

4. The role of oxygen sensing mechanisms in myeloid cells in the development of retinal and choroidal neovascularisation

4.1. Introduction

Oxygen gradients and hypoxic microenvironments are common features in development and in ischaemic and inflammatory disease. Bone marrow-derived myeloid cells such as neutrophils, dendritic cells and macrophages are a diverse group of mononuclear cells that are attracted to these hypoxic and ischaemic microenvironments and mediate the local immune response in development, health and disease (Ransohoff and Cardona, 2010).

During development, myeloid progenitors from the yolk sac colonise the developing central nervous system and contribute to the direction of the invading vasculature (Streit, 2001), the removal of apoptotic cells (Parnaik et al., 2000) and synaptic pruning (Stevens et al., 2007). In health, circulating and resident myeloid cells are quiescent and functionally dormant. In disease, however, myeloid cells are activated and recruited to areas of ischaemia and inflammation contributing to angiogenesis and inflammation (Noonan et al., 2008). Myeloid cells that migrate into non-perfused and ischaemic tissue encounter a very challenging microenvironment which is characterised by low levels of oxygen and glucose and high concentrations of lactate and reductive metabolites (Nizet and Johnson, 2009; Saadi et al., 2002). In order to survive and maintain their function in oxygen deprived condition, myeloid cells must adapt to the

demanding environment. It is widely accepted that this adaptive response to hypoxia in myeloid cells is mediated by activation of hypoxia-inducible transcription factors. Hif1a activation in myeloid cells orchestrates the metabolic shift to anaerobic glycolysis (Cramer et al., 2003), extends the lifespan of functional neutrophils by inhibiting apoptotic pathways (Walmsley et al., 2005) and increases the production and secretion of inflammatory and angiogenic molecules such as tumour necrosis factor (TNF), vascular endothelial growth factor (Vegf) and nitric oxide (figure 4.1, (Burke et al., 2002; Peyssonnaux et al., 2005). Conditional inactivation of *Hif1a* in myeloid cells results in a reduced inflammatory response in experimental models of acute inflammation, including arthritis and inflammatory skin disease (Cramer et al., 2003) which highlights the critical role of Hif1a signalling in myeloid cells for inflammatory processes.

In the eye, myeloid cells control blood vessels branching and fine-tune vascular density and remodeling during retinal and hyaloid vascular development (Kurihara et al., 2011; Stefater, III et al., 2011). In the adult, the retina contains three distinct populations of myeloid-derived cells including perivascular macrophages, parenchymal microglia and a recently described population of dendritic cells (Xu et al., 2007b). Replenishment of myeloid populations in the healthy retina has been suggested to be accomplished both by *in situ* proliferation of resident cells (Kloss et al., 1997; Lee et al., 1994) and via recruitment of bone marrow (BM)-derived macrophages (Xu et al., 2007a). Under pathological condition, e.g. in response to tissue insults, circulating monocyte precursor cells are quickly recruited to injured retinal tissue and

differentiate into tissue macrophages and microglia (Caicedo et al., 2005) which carry out phagocytosis of tissue debris and release a diverse array of vascular and proinflammatory mediators. The conventional understanding is that macrophages can be subdivided into a M1 (classically activated) or M2 (alternatively activated) population. M1 macrophages are characterised by a pro-inflammatory phenotype and activated by lipopolysaccharide and interferon gamma to promote T-helper-1 (T_H1) responses and secrete bactericidal factors. M2 macrophages, in contrast, exhibit an immunosuppressive phenotype and release cytokines that promote a T_H2 response (Mantovani et al., 2002). Compelling evidence indicates that activated microglia and macrophages play a critical role in the development of retinal and choroidal neovascularisation. Activated microglia/macrophages have been found to be markedly increased in the retina in human diabetic retinopathy and in subretinal membranes in age-related macular degeneration (Skeie and Mullins, 2009; Zeng et al., 2008b). Macrophages were also found to be increased in mouse models of retinal and choroidal neovascularisation and suggested to promote pathological angiogenesis (Sakurai et al., 2003). Systemic depletion of macrophages by clodronate liposomes has been shown to significantly reduce Vegf levels and hamper the development of retinal and choroidal neovascularisation in the OIR and laser CNV mouse model (Kataoka et al., 2011; Sakurai et al., 2003). Although there is no direct proof yet, these results raised the possibility that activated blood-recruited macrophages and microglia are promoting the development of retinal and choroidal neovascularisation by expressing

angiogenic factors including VEGF. The role of Hif1a signalling in myeloid cells and its contribution to Vegf expression and the development of retinal and choroidal neovascularisation, however, is largely unknown.

4.2. Aims

The aim of this chapter is to investigate the role of oxygen sensing mechanisms in myeloid cells in the development of pathological ocular neovascularisation. In particular I aim to determine the roles of Hif1a, its downstream effector protein Vegf, and its upstream regulator Vhl, in myeloid cells during the development of retinal and choroidal neovascularisation.

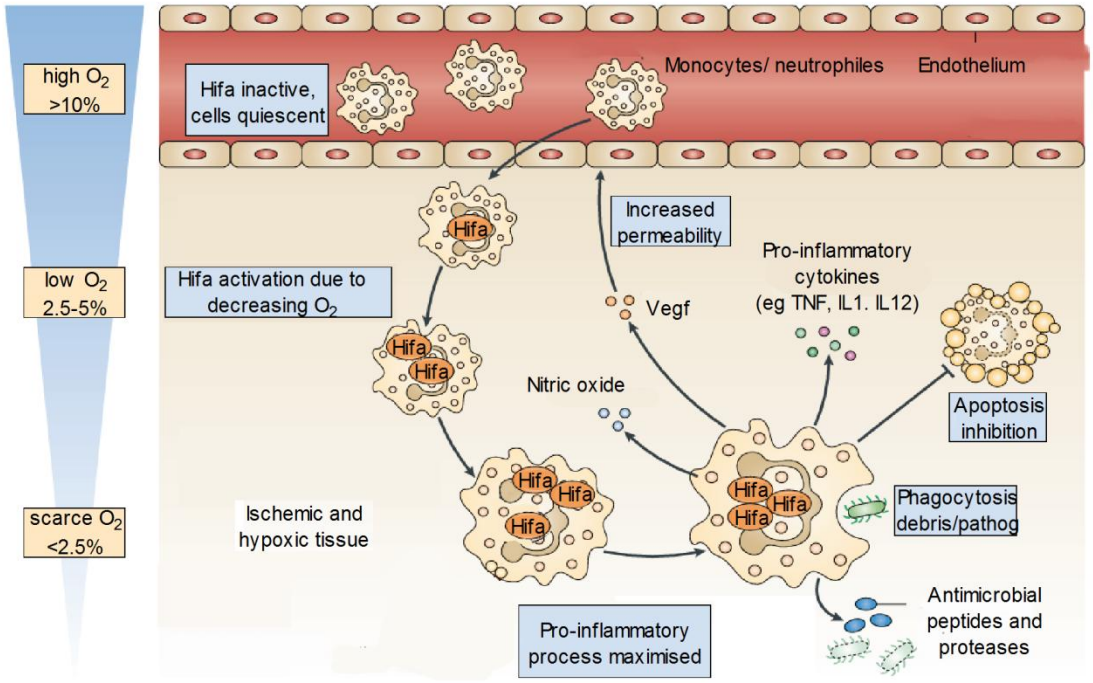

Figure 4.1 Hif activation in myeloid cells in microenvironments of hypoxia. Myeloid-derived phagocytes such as monocytes and neutrophils have low levels of Hif as they circulate in the oxygen-rich blood. When recruited to tissue sites of ischaemia, they transmigrate across the endothelium and encounter decreasing oxygen tensions which results in Hif activation. HIF activity promotes phagocytosis of cell debris and pathogens; inhibits apoptosis to increase phagocyte lifespan; stimulates the release of granule proteases, vascular endothelial growth factor (VEGF, which increases vascular permeability) and pro-inflammatory cytokines (such as tumour necrosis factor (TNF), interleukin 1 (IL-1) and IL-12); and activates the production of nitric oxide by inducible nitric oxide synthase. Adapted from (Nizet and Johnson, 2009).

4.3. Methods and results

The work presented in this chapter was kindly supported by Christiana Ruhrberg (Department of Cell Biology, Institute of Ophthalmology, UCL, London) who provided the *C57BL/6*^{lysMcre} mice and Alessandro Fantin (Department of Cell Biology, Institute of Ophthalmology, UCL, London) who assisted with experimental procedures, in particular with the staining and imaging of the ocular samples.

4.3.1 Spatial and temporal distribution of myeloid cells in the OIR model

To investigate the spatial and temporal distribution of myeloid cells in the development of retinal neovascularisation in the OIR model, *knockin* mice expressing cre recombinase under the control of the myeloid specific promoter *lysM* (*lysozyme M*, referred to as *lysMcre mice*) were crossed to *Rosa26YFP* mice. 50% of the resulting offspring (referred to as *Rosa26-YFP*^{lysMcre} *mice*) expressed cre recombinase under the myeloid cell specific *lysM* promotor which resulted in conditional deletion of a floxed stop codon and consequent YFP expression under the transcriptional control of the *Rosa26* locus.

Rosa26-YFP^{lysMcre} mice and littermate controls were exposed to 75% hyperoxia from postnatal day 7 to 12 and then returned to room air. Retinal flatmounts and ocular cryosections were dissected 2 and 5 days after oxygen incubation (i.e. p14 and p17) and stained with anti-collagen4 and anti-YFP. *Rosa26-YFP*^{lysMcre}

mice demonstrated equally distributed and ramnified YFP positive myeloid cells in the vascular and avascular area at P14 (figure 4.2B, B'). At P17, YFP and IB4 expressing myeloid cells accumulated in the area of neovascularisation and were closely associated with neovascular tufts (figure 4.2D, D'). Depending on the size of the neovascular tufts, 4-10 myeloid cells surrounded each area of vascular proliferation that extended towards the vitreous (figure 4.2D',E).

As cre recombinase can have cell toxic effects that may compromise normal cell survival and function (Loonstra et al., 2001), the effect of *cre* expression in myeloid cells on vascular changes in the OIR model was investigated. Compared with littermate controls, *Rosa26-YFP*^{lysMcre} exhibited a similar area of vasoobliteration (41.8±1.2% vs. 42.9±3.4%, p=0.7) at P14 indicating that *cre* expression in myeloid cells has no effect on vessel regression during the hyperoxic phase in the OIR model. At P17, *Rosa26-YFP*^{lysMcre} demonstrated a similar area of vasoobliteration (26.5±1.8% vs. 29.5±1.8%, Mann-Whitney-Test p=0.6) and retinal neovascularisation (21.1±0.7% vs. 20.8±1.1%, p=0.7) compared with littermate controls indicating that cre expression in myeloid cells has no effect on the vascular changes in the OIR model (figure 4.2 F,G).

Taken together, these data demonstrate that *lysMcre* positive myeloid cells accumulate at sites of retinal neovascularisation in the OIR model and that cre expression in myeloid cells has no effect on the vascular response in the OIR model. These data indicate that *B6C57*^{lysmCre} *mice* are a suitable tool to study the role of Hif1a activation and Vegf expression in myeloid cells in the development of retinal neovascularisation in the OIR mouse model.

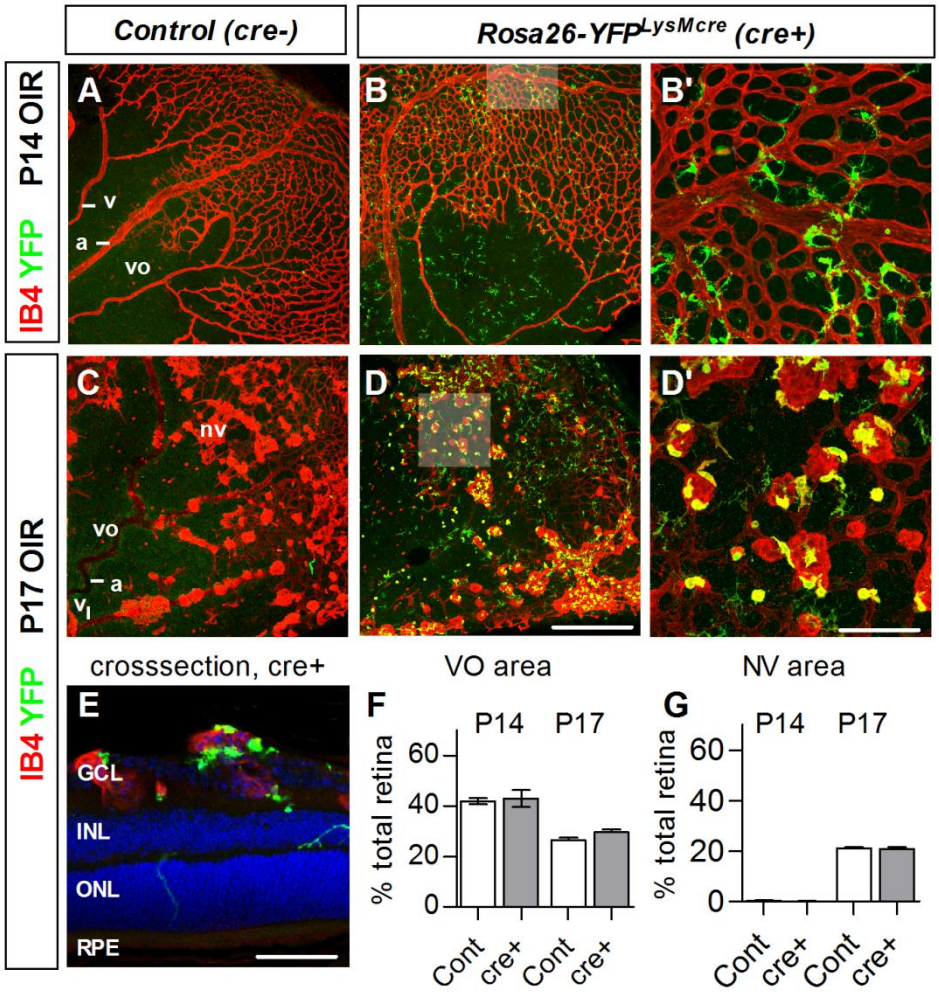

Figure 4.2 LysMcre expressing myeloid cells accumulate around retinal neovascularisation in the OIR model. Representative retinal flatmount of a *Rosa26-YFP*^{lysMcre} mouse and littermate control in the OIR model stained with the vascular marker isolectin B4 and an antibody for YFP on postnatal day (P) 14 **(A,B)** or P17 **(C,D)**. **B'** and **D'** show higher magnification images of the areas shaded in B,D. Examples of arteries (a), veins (v), the area of vasoobliteration (vo) and nevoascularisation (nv) are indicated in **A** and **C.** Note ramified YFP-positive myeloid cells at P14 (**B'**) and strongly IB4-and YFP-positive myeloid cells associated with a neovascular tuft at P17 **(D')**. Retinal crosssection of a *Rosa26-YFP*^{lysMcre} mouse stained with Ib4, anti-YFP and Dapi demonstrates the pretretinal localisation of the neovascularisation and surrounding lysMcre positive myeloid cells **(E)**. Quantification of the area of vasoobliteration and neovascularisation in control and *Rosa26-YFP*^{lysMcre} mice at P14 and P17 shows no effect of *cre* expression in myeloid cells on the vascular changes in the OIR model **(F,G)**. Scale bar: 150µm in A-D, and 50µm in B', D' and E.

4.3.2 Conditional inactivation of *Hif1a* or *Vegf* in myeloid cells reduces the development of retinal neovascularisation in the OIR model

To determine the role of Hif1a signalling and Vegf expression in myeloid cells in the development of retinal neovascularisation, *C57Bl6*^{lysMcre} mice were mated with *Hif1a*$^{floxed/floxed}$ (Ryan et al., 2000) or *Vegfa*-floxed mice (Gerber et al., 1999). The resulting offspring (referred to as *Hif1a*^{lysMcre} and *Vegf*^{lysMcre}) exhibit a cell-specific deletion of the *Hif1a* and the *Vegf* gene in approximately 75-95% of neutrophils and peritoneal macrophages (Cramer et al., 2003) and have a normal postnatal viability and no deviant phenotype.

Hif1a^{lysMcre} and *Vegf*^{lysMcre} mice were exposed to 75% hyperoxia from postnatal day 7 to 12 and then returned to room air. Retinal flatmounts were dissected 5 days after oxygen incubation (i.e. P17) and stained for the retinal vasculature with anti-IB4 antibodies. The area of vasoobliteration and neovascularisation in *Hif1a*^{lysMcre} and *Vegf*^{lysMcre} mice was assessed at P17 and normalised to littermate controls (n= range 8-18 independent eyes per group). Results were compared using an ANOVA test with a Tukey post test to correct for multiple testing.

Hif1a^{lysMcre} mice demonstrated a similar area of ischaemia at P17 compared with littermate controls (85.8±25.3% vs. 100±13.6%, p=0.14). The area of retinal

neovascularisation, however, was significantly reduced compared with littermate controls at P17 (48.7±19.7% vs. 100±25.7%, p=0.001). Similarly, conditional inactivation of *Vegf* in *Vegf*^{lysMcre} mice resulted in a normal area of vasoobliteration (123.1±56.3% vs. 100±13.6%, p=0.1) and a significant reduction of retinal neovascularisation (47.8±33.5% vs. 100±25.7%, p=0.003) compared with littermate controls (figure 4.3).

These data indicate that Hif1a activation and Vegf expression in myeloid cells has no effect on the revascularisation of the ischaemic area but contributes substantially to the development of retinal neovascularisation in the OIR model.

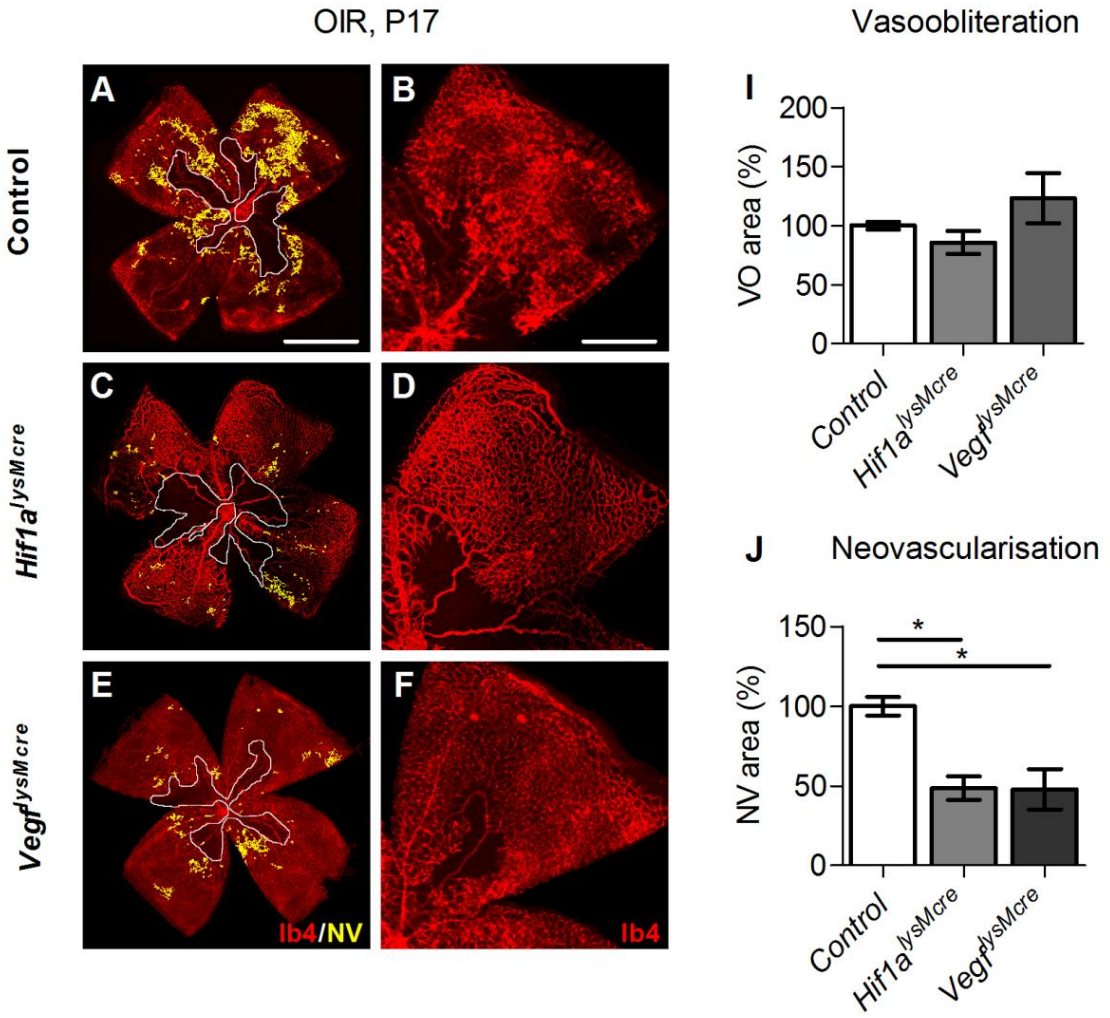

Figure 4.3 Conditional inactivation of *Hif1a* or *Vegf* in myeloid cells reduces retinal neovascularisation in the OIR mouse model. (A-F) Representative vessel stained retinal flatmounts (column **A**) and images with higher magnification (column **B**) at P17 after OIR induction demonstrate a similar area of vasoobliteration (outlined in white) and a reduced area of neovascularisation (highlighted in yellow) in *Hif1a*^{lysMcre} and *Vegf*^{lysMcre} mice compared with littermate controls. **(I, J)** Relative quantification of the area of vasoobliteration and neovascularisation in control, *Hif1a*^{lysMcre} and *Vegf*^{lysMcre} mice at P17. Error bars indicate ±SEM. Scale bar: 1mm in column A, 500µm in column B. * t-test $p<0.005$.

4.3.3 LysM cre expressing myeloid cells accumulate around laser-induced choroidal neovascularisation

As myeloid cells have been shown to be important mediators in the development of choroidal neovascularisation (Sakurai et al., 2003), the temporal and spatial distribution of lysMcre expressing myeloid cells was investigated in *Rosa26-YFP*^{lysMcre} mice in the laser-induced CNV model. Three focal laser burns were applied to the RPE of 6-8 weeks old *Rosa26-YFP*^{lysMcre} mice and littermate controls (range 3-4 animals per group) using an Argon laser. As macrophage infiltration was reported to peak 3 days after laser injury (Sakurai et al., 2003) and CNV size analysis is routinely performed at 14 days after laser injury (Balaggan et al., 2006), the choroid and RPE were harvested at these timepoints and stained for the macrophage marker F4/80, the myeloid and vessel marker isolectin B4 (IB4) and for YFP.

Immunohistochemical analysis demonstrated that lysMcre expressing myeloid cells accumulate within and around choroidal neovascularisation at 3 and 14 days after CNV induction (figure 4.4A, B). The majority of YFP positive cells were positive for F4/80 and IB4 and therefore likely to be macrophages (figure 4.4B$_{1-3}$, wavy arrows). Some YFP positive cells, however, were negative for IB4 and F4/80 (figure 4.4B$_{1-3}$, arrowheads) indicating that they may be myeloid cells other than macrophages which are recruited from the blood stream, such as monocytes or neutrophils. Only a few cells that were F4/80 and IB4 positive were negative for YFP (figure 4.4B$_{1-3}$, arrows) demonstrating a high efficiency of lysMcreYFP expression in myeloid cells.

To determine if cre expression in lysM positive myeloid cells influences the development of laser-induced choroidal neovascularisation, the area of CNV was assessed in *Rosa26-YFP*^{lysMcre} mice and littermate controls at 3, 7 and 14 days after laser application using fluorescein angiography. Compared with littermate controls, *Rosa26-YFP*^{lysMcre} mice demonstrated a similar area of choroidal neovascularisation in the early phase of the angiography at 3 (100±41.9% vs. 98.0±45.1%, p=0.97), 7 (100±85.1% vs. 120.3±46.7%, p=0.24) and 14 days after laser CNV induction (100±90.4% vs.74.1.0±42.6%, p=0.97). In the late phase of the angiography, *Rosa26-YFP*^{lysMcre} mice revealed a similar degree of leakage compared with control animals at 3 (100±41.7% vs. 93.9±33.0%, p=0.58), 7 (100±49.3% vs. 92.1±38.9%, p=0.87) and 14 days after laser (100±48.1% vs. 68.1±20.1%, p=0.74). This data suggests that cre expression in lysM activated myeloid cells does not influence the area and the leakage of laser-induced CNV at 3, 7 and 14 days after laser.

Taken together, these data demonstrate that *lysMcre* expressing myeloid cells accumulate at sites of choroidal neovascularisation in the laser CNV mouse model and that cre expression in these cells does not influence CNV formation. These data suggest that *lysMcre* mice are a suitable tool to study the role of Hif1a signalling and Vegf expression in myeloid cells in the development of laser-induced choroidal neovascularisation.

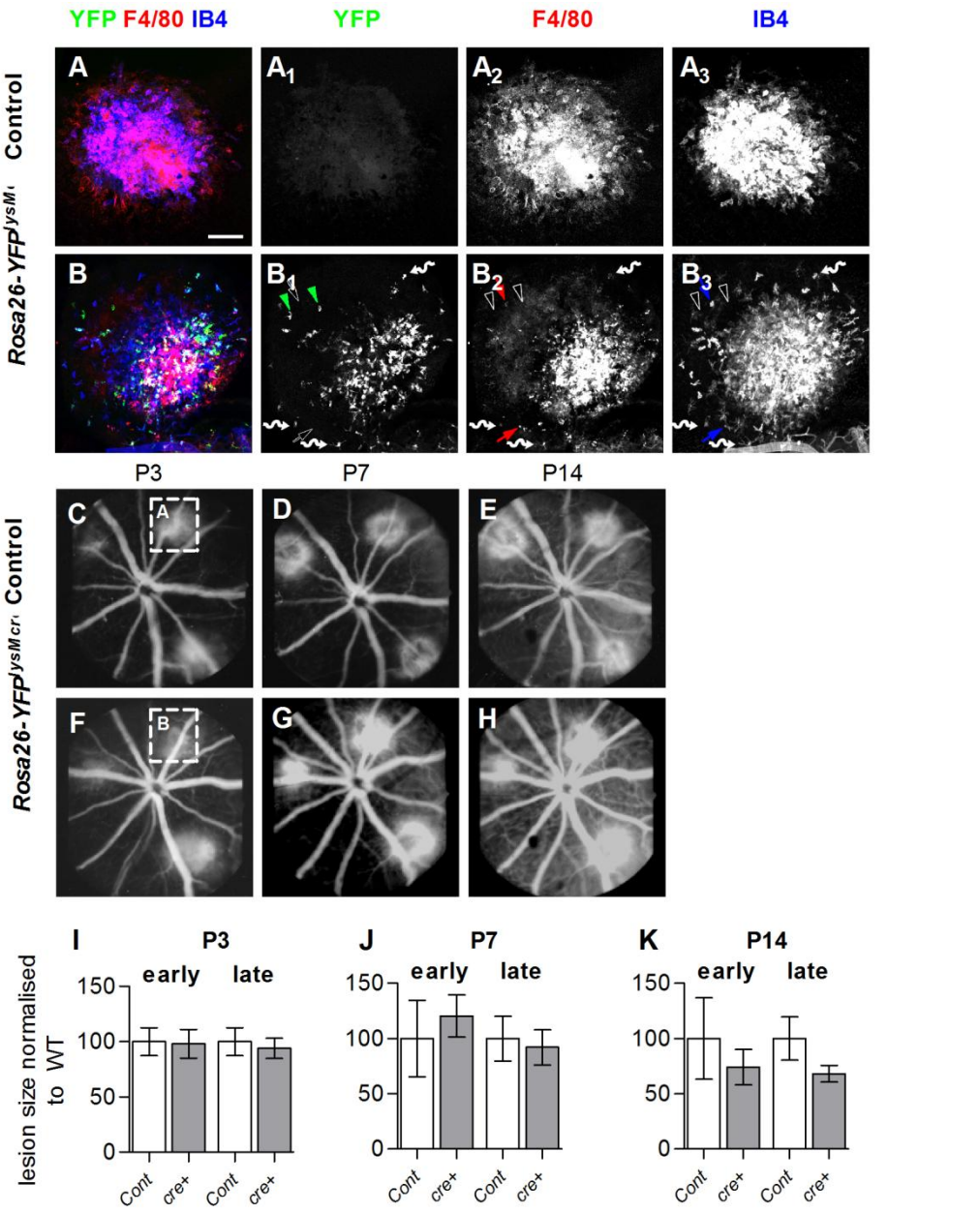

Figure 4.4 LysMcre expressing myeloid cells accumulate around laser-induced choroidal neovascularisation. Representative laser-induced CNV lesions on RPE/choroidal flatmounts stained for YFP, F4/80 and IB4 of a control **(A)** and a *Rosa26-YFP*^{lysMcre} mouse **(B)** 3 days after laser CNV induction. Wavy errors indicate cells that are positive for YFP, F4/80 and IB4, arrowheads show cells that are positive for YFP but negative for F4/80 and IB4 and arrows indicate cells that are negative for YFP but positive for F4/80 and IB4. Representative fluorescein angiograms **(C-H)** and relative quantification of CNV lesions in control and *Rosa26-YFP*^{lysMcre} littermates 3, 7 and 14 days after laser injury **(I-J)**. Scale bar: 10µm for A, B.

4.3.4 Conditional inactivation of *Hif1a* or *Vegf* in lysMcre myeloid cells reduces laser-induced CNV formation

To determine the role of Hif1a and Vegf in myeloid cells in the development of choroidal neovascularisation, *C57Bl6*^{lysMcre} mice were mated with *Vhl*$^{floxed/floxed}$ (Haase et al., 2001) *Hif1a*$^{floxed/floxed}$ (Ryan et al., 2000) or *Vegfa*-floxed mice (Gerber et al., 1999). 6-8 weeks old *Vhl*^{lysMcre}, *Hif1a*^{lysMcre}, *Vegf*^{lysMcre} and wildtype controls (range 5-9 animals per group) were assessed in the laser CNV model and fluorescein angiography was performed 3, 7 and 14 days after laser injury.

Vhl^{lysMcre} mice demonstrated a similar area of choroidal neovascularisation in the early phase of the angiography at 3 (112±27.4 vs. 100±31.3%, p=0.38), 7 (97.2±33.3% vs. 100±32.0%, p=0.97) and 14 days after laser CNV induction (90.9±22.5% vs. 100±31.0. p=0.94) compared with littermate controls indicating that conditional inactivation of *Vhl* in the myeloid cell lineage has no effect on the development of laser-induced choroidal neovascularisation. *Hif1a*^{lysMcre} mice revealed a similar area of choroidal neovascularisation in the early phase of the angiography at 3 days (94.2±10.0 vs. 100±31.3%, p=0.65), a reduced area of choroidal neovascularisation at 7 days (71.4±7.0% vs. 100±32.0%, p=0.34) and a significantly reduced area of choroidal neovascularisation at 14 days after laser injury (41.6±2.7% vs. 100±31.0. p=0.94, p=0.01). Similarly, *Vegf*^{lysMcre} mice demonstrated a normal area of choroidal neovascularisation in the early phase

of the angiography at 3 days after laser injury (114.9±20.4% vs. 100±31.3%, p=0.67), a reduced area of choroidal neovascularisation at 7 (75.6±5.6% vs. 100±32.0%, p=0.19) and a significantly reduced area of choroidal neovascularisation at 14 days after laser injury (35.3±9.6% vs. 100±31.0. p=0.009).

Taken together, these data indicate that both Hif1a activation and Vegf expression in myeloid cells contribute substantially to the development of choroidal neovascularisation. Conditional inactivation of *Hif1a* or *Vegf* in myeloid cells has no effect on the area of CNV at 3 days after laser but reduces the size of choroidal neovascularisation at 7 and 14 days after laser treatment.

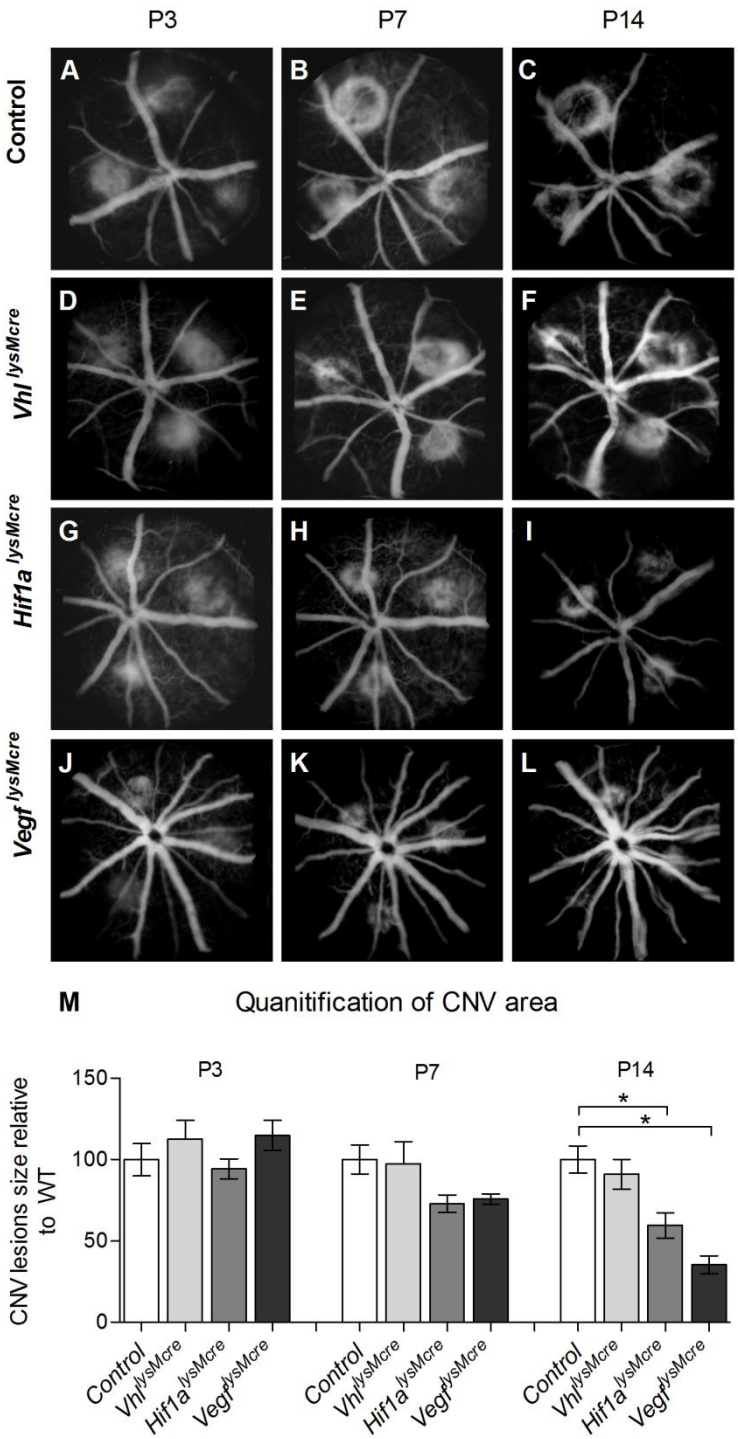

Figure 4.5 Conditional inactivation of *Hif1a* or *Vegf* in myeloid cells reduces CNV development. Representative fluorescein angiograms (early phase, 90sec) at 3, 7 and 14 days after laser injury in control **(A-C)**, *Vhl*^{lysMcre} **(D-F)**, *Hif1a*^{lysMcre} **(G-I)** and *Vegf*^{lysMcre} mice **(J-L).** Relative quantification of CNV lesion size at 3, 7 and 14 days after laser injury assessed on fluorescein angiograms **(M)**. Error bars indicate SEM. * = ANOVA p<0.05.

4.4 Discussion

Adaptive cellular responses to low levels of oxygen play a critical role in both physiological vascular development and in common neovascular blinding diseases. Myeloid cells are involved in normal retinal vascular development and implicated in the pathogenesis of hypoxia-induced retinal vascular disease. However, the role of the oxygen sensing Vhl/Hif1a pathway in myeloid cells in the development of pathological ocular neovascularisation has not previously been examined. In this chapter I investigated the function of Hif1a signalling and Vegf expression in myeloid cells in the development of retinal and choroidal neovascularisation using a tissue-specific conditional *knockout* approach and mouse models of retinal and laser-induced choroidal neovascularisation.

Myeloid cells accumulate at sites of retinal and choroidal neovascularisation

Results shown in this chapter demonstrate that *lysMcre* expressing myeloid cells accumulate at sites of retinal and choroidal neovascularisation in the OIR and CNV mouse model. This finding is in line with studies demonstrating that myeloid cells are a critical component in the formation of retinal and choroidal neovascularisation (Espinosa-Heidmann et al., 2003; Nishimura et al., 1990; Sakurai et al., 2003). The origin of myeloid cells that are recruited to the site of retinal and choroidal neovascularisation has been the subject of much inquiry. Results of this chapter demonstrate that the majority of *lysM* expressing myeloid cells that are recruited to the CNV lesion are positive for the macrophage and microglia markers F4/80 and IB4. Since these markers are expressed on both

resident microglia and infiltrating systemic macrophages it is impossible to deduce from this dataset if the myeloid cells surrounding the CNV lesion are recruited from the retina or the blood stream. Some of the *lysM* expressing recruited cells, however, were negative for both F4/80 and Ib4 suggesting that myeloid cells other than macrophages are recruited to CNV lesions such as circulating monocytes or neutrophils. This hypothesis is in line with recent findings demonstrating that the *lysM* promoter is active in neutrophils (Cramer et al., 2003) and that circulating neutrophils infiltrate sites of CNV as early as day 1 after laser injury (Zhou et al., 2005). Systemic depletion of macrophages and neutrophils by intravenous administration of clodronate liposomes has been shown to reduce the number of myeloid cells at sites of choroidal neovascularisation (Espinosa-Heidmann et al., 2003; Sakurai et al., 2003; Shi et al., 2011). Furthermore, mice deficient in the macrophage chemotactic protein (MCP)-1, which is secreted by RPE cells in the direction of choroidal vessels to attract circulating monocytes during inflammatory responses (Holtkamp et al., 1999), demonstrate a reduced CNV lesion size (Luhmann et al., 2009). These findings suggest that circulating myeloid cells accumulate and contribute to the development of choroidal neovascularisation. In addition, resident retinal microglia cells were suggested to migrate towards areas of laser injury in the outer retina and to contribute to the development of laser-induced choroidal neovascularisation (Combadiere et al., 2007).

In the OIR model, both microglia and circulating myeloid cells were shown to accumulate at sites of retinal neovascularisation. Depletion of these cells by

local or systemic administration of clodronate liposomes was shown to reduce the neovascular response in the OIR model indicating that both circulation-derived and resident myeloid cells contribute to the development of retinal neovascularisation (Ishida et al., 2003; Kataoka et al., 2011). These data are in line with the findings in this chapter indicating that both circulating and resident lysM positive myeloid cells are recruited to sites of retinal and laser-induced choroidal neovascularisation.

Hif1a activation and Vegf expression in myeloid cells contribute to the development of retinal and choroidal neovascularisation

Work in this chapter has shown that conditional inactivation of *Hif1a* or *Vegf* in myeloid cells reduces the development of pathological retinal and choroidal neovascularisation. This data is in line with the hypothesis that myeloid cells contribute to the development of retinal and choroidal neovascularisation by secreting proangiogenic factors. In the CNV mouse model, macrophage recruitment and Vegf expression has been shown to coincide and peak at 3 days after laser injury. Systemic depletion of circulating myeloid cells using clodronate liposomes reduces both myeloid recruitment and Vegf expression 3 days after laser injury indicating that circulating myeloid cells contribute to the secretion of proangiogenic factors including Vegf (Sakurai et al., 2003). Furthermore, resident retinal microglia cells expressing the CX3C chemokine receptor 1 (CX3CR1) – a chemokine involved in the adhesion and migration of

leukocytes - migrate towards laser-induced choroidal neovascularisation and contribute to CNV formation by expressing proangiogenic factors including Vegf (Combadiere et al., 2007). Likewise, in the OIR model, both resident and circulating myeloid cells have been shown to accumulate at sites of retinal neovascularisation (Ishida et al., 2003; Kataoka et al., 2011). The results of this chapter demonstrate that Vegf expression in myeloid cells contributes substantially to the development of retinal and choroidal neovascularisation in the OIR and CNV mouse model. This data is in line with recent findings demonstrating that intravitreous administration of $Vegf_{164}$ neutralizing aptamers reduces both myeloid cell adhesion at the neovascular front and the development of pathological neovascularisation (Ishida et al., 2003). Furthermore it has been shown that conditional inactivation of *Vegf* in myeloid cells leads to a reduction of pathological vessels in tumours suggesting that myeloid cell derived Vegf is a common culprit in the development of pathological angiogenesis (Stockmann et al., 2008).

Work presented in this chapter further indicates that *Vegf* expression in myeloid cells may be driven by Hif1a signalling in pathological angiogenesis. This suggestion is based on the finding that myeloid-cell-specific inactivation of both *Vegf* or *Hif1a* causes a similar reduction of retinal and choroidal neovascularisation in the OIR model and the laser CNV model.

In the OIR model, lysM expressing myeloid cells were found in the vasoobliterative area at P14 which is characterised by significant tissue hypoxia and activation of Hif1a in cells of the inner retina (Mowat et al., 2010). Hypoxia

has been shown to induce accumulation of Hif1a in primary human macrophages and mouse bone marrow–derived macrophages *in vitro* (Burke et al., 2002) and to increase the expression of Vegf120 and Vegf164 in circulating monocytes in a rat model of proliferative retinopathy (Ishida et al., 2003). The challenging hypoxic microenvironment in the vasoobliterative area may therefore induce Hif1a activation and *Vegf* expression in resident and infiltrating myeloid cells which contribute to the development of retinal neovascularisation.

In the CNV model, however, Hif1a activation in myeloid cells is more likely to occur in response to an inflammatory microenvironment than to tissue hypoxia as the oxygen saturation at the level of the RPE is very high (Linsenmeier and Braun, 1992; Yu and Cringle, 2006). Proinflammatory cytokines such as Ccl2 are released from the injured RPE in the laser-induced CNV model (Liu et al., 2011) and may induce Hif1a signalling and *Vegf* expression in myeloid cells (Hong et al., 2005). Intraocular injection of neutralizing antibodies against Ccl2 has been shown to reduce macrophage infiltration, Vegf levels and the development of choroidal neovascularisation by mechanisms which may involve Hif1a mediated *Vegf* expression (Itaya et al., 2007). Activation of Hif1a signalling in myeloid cells by inflammatory mechanisms may therefore be an important contributor to the expression of Vegf and aberrant angiogenesis in the laser-induced CNV model and in inflammatory retinal vascular disease such as AMD.

The finding that conditional inactivation of *Hif1a* results in a similar reduction of neovascularisation as conditional inactivation of *Vegf* in myeloid cells, suggests that Vegf is the principle downstream effector of Hif1a in myeloid cells in the

development of retinal and choroidal neovascularisation. However, it cannot be excluded that other Hif1a dependent factors in myeloid cells, such as Epo, contribute to the development of neovascularisation in the OIR and CNV mouse model. Furthermore, Hif1a activation in myeloid cells has been shown to be directly involved in regulating myeloid cell survival in hypoxic microenvironments (Walmsley et al., 2005) and to contribute to the recruitment of circulating myeloid cells to areas of inflammation (Cramer et al., 2003). Inactivation of *Hif1a* in myeloid cells may therefore reduce the recruitment and the survival of infiltrating proangiogenic myeloid cells in the OIR and CNV mouse model which may contribute to the observed reduction in retinal and choroidal neovascularisation.

Surprisingly, the results in this chapter demonstrate that conditional inactivation of *Vhl* in myeloid cells has no effect on the development of choroidal neovascularisation in the laser-induced CNV model. This result is unexpected as inactivation of *Vhl* in myeloid cells has been shown to activate Hif1a and increase oedema and macrophage infiltration in a model of cutaneous inflammation (Cramer et al., 2003). However, it may be possible that the Hif1a pathway in myeloid cells is already maximally activated in the OIR and CNV model and that an additional inactivation of *Vhl* has no effect on levels of Hif1a. Also, it might be possible that other Vhl dependent transcription factors, such as Hif2a, are increased in myeloid cells in $Vhl^{lysMcre}$ mice and counteract the proangiogenic effect of Hif1a in myeloid cells. Hif2a activation in myeloid cells has been shown to regulate macrophage function such as migration and cytokine expression in mouse models of acute and tumour inflammation (Imtiyaz

et al., 2010). Future studies will have to address the role of Hif2a in myeloid cells in the retina to further understand the role of oxygen sensing mechanisms in the development of retinal and choroidal neovascularisation.

The data presented in this chapter show that Hif1a signalling in myeloid cells contribute substantially to the development of retinal and choroidal neovascularisation in hypoxic and inflammatory microenvironments possibly by driving Vegf expression or by increasing the recruitment of other proangiogenic myeloid cells. Future studies will have to assess the expression levels of Vegf in myeloid cells and quantify the number of recruited myeloid cells in *Hif1a*^{lysMcre} mice in the OIR and CNV mouse model. This may help to answer the question whether the reduced neovascular response can be explained by a reduction in myeloid specific *Vegf* expression, by a lack of recruitment of proangiogenic myeloid cells or by both.

4.5. Conclusion

The work in this chapter has demonstrated that circulating and resident myeloid cells accumulate at sites of retinal and choroidal neovascularisation in the OIR and laser-induced CNV model and validated the use of *LysMCre* mice as an efficient tool to study the role of oxygen sensing mechanisms in myeloid cells in the development of retinal and choroidal neovascularisation.

Conditional inactivation of *Vegf* results in a significant reduction of retinal and choroidal neovascularisation demonstrating for the first time direct evidence that myeloid cell derived Vegf contributes to the development of retinal and choroidal neovascularisation. Conditional inactivation of *Hif1a* in myeloid cells leads to a significant reduction in retinal and choroidal neovascularisation, possibly through mechanisms involving a decrease in Hif1a mediated *Vegf* expression or myeloid cell recruitment. These findings demonstrate that Hif1a signalling and Vegf expression in myeloid cells contribute substantially to the development of retinal and choroidal neovascularisation and provide a rationale for developing antiangiogenic treatments that target myeloid cells in the eyes. In particular, myeloid cell specific inactivation of Hif1a may become an attractive target to effectively treat neovascular retinal eye disease.

5. Intraocular oxygen distribution and molecular mediators in proliferative diabetic retinopathy

5.1 Introduction

The normal function and survival of retinal cells is vulnerable to deficiencies in oxygen delivery. Insufficient perfusion of retinal or choroidal vessels leads to ischaemia and hypoxia that can cause retinal dysfunction and degeneration (Osborne et al., 2004). The importance of ischaemia-induced expression of retinal cytokines in the development of diabetic retinopathy is widely accepted. Ischaemia and hypoxia have been suggested to cause the release of proangiogenic factors, such as VEGF, which contribute to the development of neovascularisation in proliferative diabetic retinopathy (D'Amore, 1994). However, direct evidence of hypoxia in the human diabetic retina is weak and most of our understanding is based on oxygen measurements across the retina in diabetic animal models using polarographic electrodes (Alder et al., 1983; Linsenmeier and Braun, 1992). The direct measurement of oxygen tension within the human retina would present a significant risk of adverse effects and has not been reported. Measurement of oxygen tension in the vitreous, which is believed to reflect global oxygenation of the retina, has demonstrated lower levels of oxygen in the vitreous of diabetic individuals compared to non-diabetic individuals (Holekamp et al., 2006; Maeda et al., 1992). However, the oxygenation of the vitreous may be influenced by active metabolism of oxygen, for example by ascorbate (Shui et al., 2009) and does not help identify any

regional differences in retinal oxygenation. Experimental investigation in cats has demonstrated that measurement of preretinal oxygen tension closely reflects oxygenation of the inner retina (Alder and Cringle, 1985; Linsenmeier et al., 1981). To date preretinal oxygen measurements have been thoroughly mapped in cats and rabbits (Shui et al., 2006) but not yet in humans.

A causative association between retinal oxygen and the development of retinal neovascularisation was first suggested by Michaelson in 1954 (Michaelson et al., 1954) and further explored by Wise who speculated that a hypoxia-induced growth factor “factor X” was responsible for inducing retinal neovascularisation (Wise, 1956). Many candidate cytokines and growth factors have since been characterised, and VEGF has emerged as a particularly prominent mediator of intraocular angiogenesis (Aiello et al., 1994). The expression of VEGF is upregulated by HIF1a, which is activated in hypoxia (Forsythe et al., 1996). The concentrations of both VEGF and HIF1a are increased in the vitreous in proliferative diabetic retinopathy and appear to correlate with disease activity (Wang et al., 2009) suggesting that hypoxia and stabilisation of HIF1a are responsible for VEGF production and progression of retinopathy. However, there is accumulating evidence that the HIF system can be activated independently of hypoxia, for example in an inflammatory microenvironment (Sharp and Bernaudin, 2004) which is a common feature in the pathogenesis of proliferative diabetic retinopathy (Gardner et al., 2002). The association between ocular hypoxia, inflammation, HIF1a and VEGF expression in human proliferative diabetic retinopathy, however, has not been clarified yet.

5.1.1 Aims

The aim of this chapter was to analyse the distribution of oxygen across the vitreous and retina in proliferative diabetic retinopathy by measuring the preretinal oxygen tension in human subjects using an oxygen probe during surgery. Furthermore I aimed to investigate the extent to which hypoxia is associated with proliferative diabetic retinopathy by correlating intraocular oxygen tensions with the concentrations of HIF1a and vitreous cytokines.

5.2 Methods and results

5.2.1 *Ex vivo* assessment of sensor accuracy

To determine the reliability of the oxygen probe before and after gas sterilisation 6 different probes (figure 5.1A,B) were each tested in 6 sealed containers filled with a range of gas mixtures of known oxygen tensions (0-147.4 mmHg). A strong correlation between sensor readings and actual oxygen tensions was identified, both before (Pearson correlation 0.997, p=0.0001) and after gas sterilisation of the probes (Pearson correlation 0.996, p=0.0001, figure 5.1C,D). Furthermore, stable oxygen tension readings were recorded 20 seconds after transferring the probes from an oxygen rich to an oxygen poor environment (147 to 6.9 mmHg), and 30 seconds after transferring them within two low oxygen environments (6.9 to 0 mmHg, figure 5.1E,F). On the basis of these findings, the surgeon allowed the probe to settle for at least 30 seconds at each intraocular site in human subjects before recording the oxygen tension.

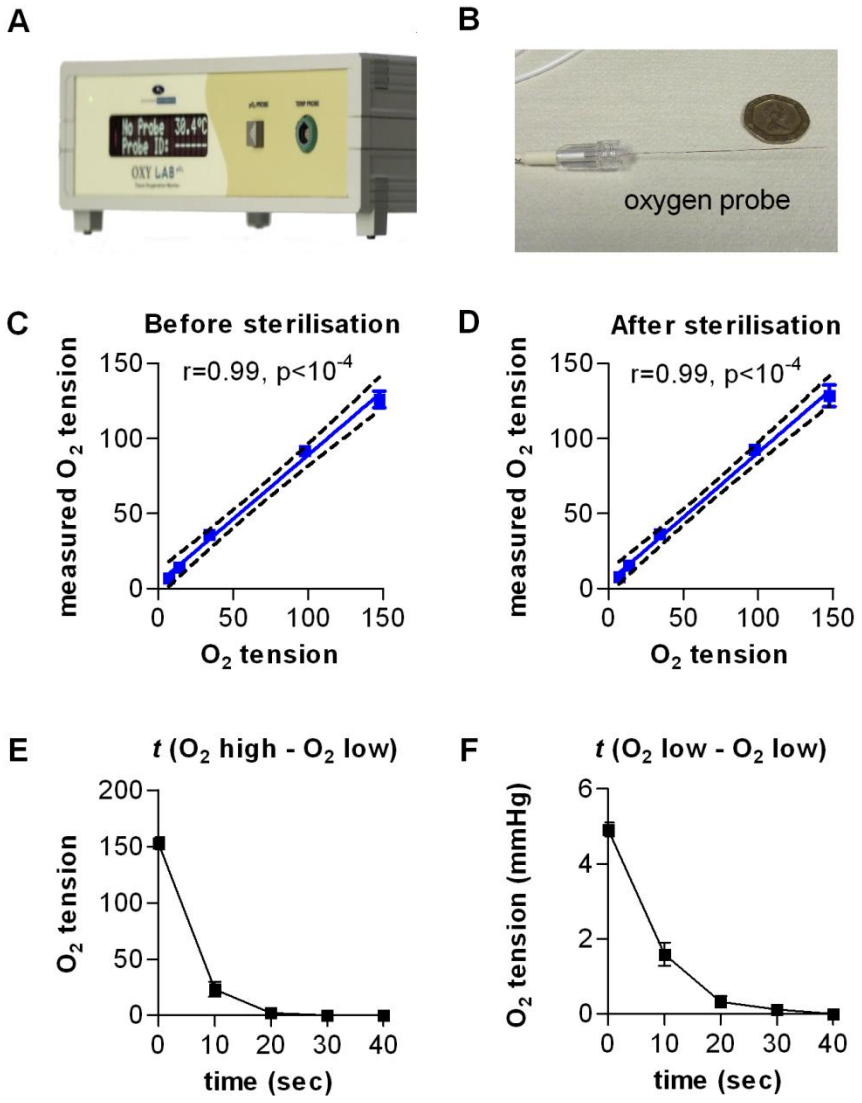

Figure 5.1 *Ex vivo* assessment of oxygen sensor accuracy.

A,B) Oxford Optronix Oxygen sensing monitor and probe. C,D) *Ex vivo* assessment of probe accuracy before and after gas sterilisation. The oxygen probe was tested in 6 different chamber containing different oxygen concentrations (0-150mmHg). r= Pearson correlation coefficient. E,F) Timecourse of probe readings when moving the probe from an oxygen rich to an oxygen poor environment (147 to 6.9 mmHg), or within two oxygen poor environments (6.9 to 0 mmHg).

5.2.2 Characteristics of subjects recruited

14 individuals with advanced proliferative diabetic retinopathy were included in this study. 6 of them had type-1 diabetes and 8 of them type-2 diabetes. All subjects presented with preretinal neovascularisation despite previous panretinal photocoagulation and had developed tractional retinal detachments involving the macula. None of the diabetic subjects had a vitreous haemorrhage at the time of surgery. 14 subjects without diabetes were included in this study as a control group. Ten of them were listed for intraocular surgery for idiopathic epiretinal membrane, and 4 of them for idiopathic full-thickness macular hole. The age of the subjects with diabetes ranged from 26 to 78 years (mean 52.2 ±13.6), and those in the control group from 58 to 78 years (mean 66.0 ±5.7).

Group	n	Age (mean, range)	Years since diagnosis	Gender (M/F)
PDR, diabetes type 1	6	42 (26-65)	24 (15-37)	5/1
PDR, diabetes type 2	8	58 (46-71)	20 (15-26)	8/0
Control	14	66 (58-78)	0.8 (0.6-2)	5/9

Table 5.1 Characteristics of study subjects

5.2.3 Measurement of intraocular oxygen tension

The *in vivo* measurements of intraocular oxygen tensions were kindly performed by Panagiotis Stavrakas (2 subjects), Zdenek Gregor (18 subjects) and James Bainbridge (8 subjects). Oxygen tensions were measured in the anterior vitreous (1), the mid-vitreous (2), at the retinal surface superior to the superotemporal arcade (3a), at the retinal surface one disc-macula diameter temporal to the macula (3b), at the retinal surface in the mid-periphery (4, superior equator), in between (5) and above areas of photocoagulation (6) and above areas of tractional retinal detachment (7, figure 5.2A-C). The measurement was completed within approximately 5 minutes in each subject. Except for an entry-site break in one subject, not directly associated with the use of the oxygen probe, there were no adverse events. To determine the test-retest variability *in vivo* and to identify any artefactual disturbance of intraocular oxygen tension caused by the measurement technique itself, the mid-vitreous oxygen tension measurement in 14 subjects was compared at the start and the completion of the process. Both measurements were found to be highly correlated (Pearson r=0.94, p=0.0001, figure 5.2D). Because the oxygen tensions measured at the retinal surface superior to the superotemporal arcade was very similar to that temporal to the macula in each group, the 2 values were averaged and used as an indicator for preretinal oxygen tension at the posterior pole.

The mean oxygen tension in the anterior vitreous of diabetic subjects was 47% reduced compared with control subjects (5.6 ±1.03 mmHg vs. 10.69 ±1.82

mmHg, p=0.023). The mean oxygen tension in the mid-vitreous of diabetic subjects was 46% lower than in control subjects (6.03 ±1.08 mmHg vs. 11.12 ±1.67 mmHg, p=0.017). The mean oxygen tension at the retinal surface of the posterior pole was 37% higher in diabetic subjects than in control subjects (15.42 ±2.55 vs. 9.78 ±0.64, p=0.039). Within the group of control subjects there was no significant difference in preretinal oxygen tension between the posterior pole and the mid-periphery (9.78 ±0.64 mmHg vs. 8.73 ±0.54 mmHg, p=0.39). In contrast, within the group of diabetic subjects the mean oxygen tension at the posterior pole was 47% higher than in the mid-periphery (15.42 ±2.55 vs. 8.22 ±1.34, p=0.024, figure 5.2E). No difference in oxygen tension above laser photocoagulated areas compared with non lasered areas was detected in the diabetic group (9.38 ±4.9 mmHg vs. 8.77 ±4.7 mmHg, p=0.86, figure 5.2G). The oxygen tension measured above areas of tractional retinal detachments was increased compared with attached retina in the mid-periphery of diabetic subjects (15.5 ±8.8 mmHg vs. 8.77 ±4.7 mmHg, p=0.07, figure 5.2H). This difference did not reach a significance level but showed a strong trend towards increased oxygen levels above areas of tractional retinal detachments compared with attached retina in the mid-periphery of diabetic subjects.

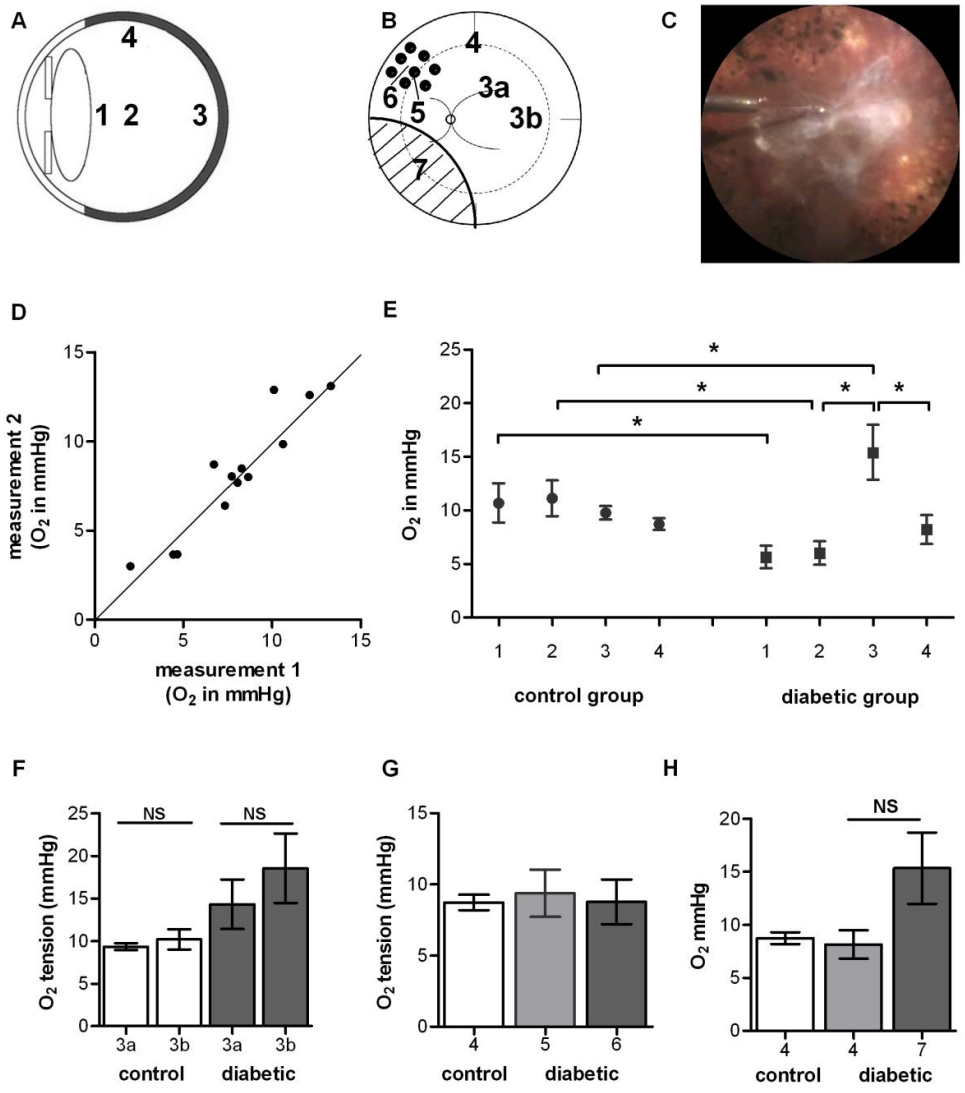

Figure 5.2 ***In vivo*** **oxygen measurements. (A,B)** Schematic cross section and map of the retina indicating the positions of O_2 measurements (1 anterior vitreous; 2 mid-vitreous; 3 retinal surface of the posterior pole (=(3a+3b)/2); 3a superior arcade; 3b temporal of macula; **4 retinal surface in the mid periphery;** 5 peripheral retina between laser coagulated areas; 6 peripheral retina above laser coagulated area; 7 tractional retinal detachment). (C) Intraoperative picture of the O_2 probe in position 3a. **D)** Mean oxygen tension (±SEM) in mmHg at different sites of the vitreous in control and diabetic subjects. **(E)** Correlation of intraoperative oxygen measurements in the mid-vitreous at the beginning and end of the recording. **(F)** Preretinal oxygen tension above the superior arcade (3a) and temporal of the macula (3b). **(G)** Preretinal oxygen tensions in the mid peripheral retina (4) above (5) and in between areas of photocoagulation (6) **(H).** Preretinal oxygen tensions in the mid peripheral retina (4) of control and diabetic subjects compared with areas with tractional retinal detachment (7). * = $p<0.05$. NS= no statistically significant difference.

5.2.4 HIF1a analysis

To determine whether the observed mid-vitreous hypoxia in PDR is associated with an increased activation of oxygen-sensing mechanisms, HIF1a protein levels were measured in the vitreous and plasma of diabetic and control subjects. HIF1a protein was on average about two fold higher in the diabetic vitreous compared with the control vitreous (7.9±12.3 vs. 3.4±7.0 pg/ml, p=0.06). Furthermore, HIF1a protein levels in the vitreous of both groups were increased compared with the corresponding plasma suggesting an endogenous expression and lower turn-over of Hif1a in the eye (figure 5.3A).

5.2.5 Protein and cytokine analysis

To investigate the role of cytokines in diabetic retinopathy, the concentration of 42 cytokines in the vitreous and plasma of diabetic and control subjects was measured using multiplex cytokine arrays. Apart from IL-4, IL-13, TGF-α and TNF-β all cytokines tested were detectable in vitreous and in plasma samples. The concentrations of PDGF-AA, PDGF-AB and RANTES could not be detected since their levels were greater than could be quantified with reference to the standard curve. Among the 35 measured cytokines detected, 10 cytokines were found to be significantly altered in the diabetic vitreous compared with the control group. Diabetic subjects revealed increased vitreous levels of Eotaxin, Flt-3 ligand, GRO (“growth related oncogen)”, IL-6, IL-7, IL-8, IP-10 (CCL22), MDC (“macrophage derived cytokine”) and VEGF compared to controls. With the exceptions of Eotaxin, MDC and GRO, these cytokines were present at higher concentrations in the vitreous than in the corresponding plasma. IL-9 was

the only cytokine found to be significantly reduced in the diabetic vitreous compared with the control vitreous. The other tested cytokines were present in similar concentrations in diabetes and control subjects, or at concentrations below the detection limit of the assay (table 3.2).

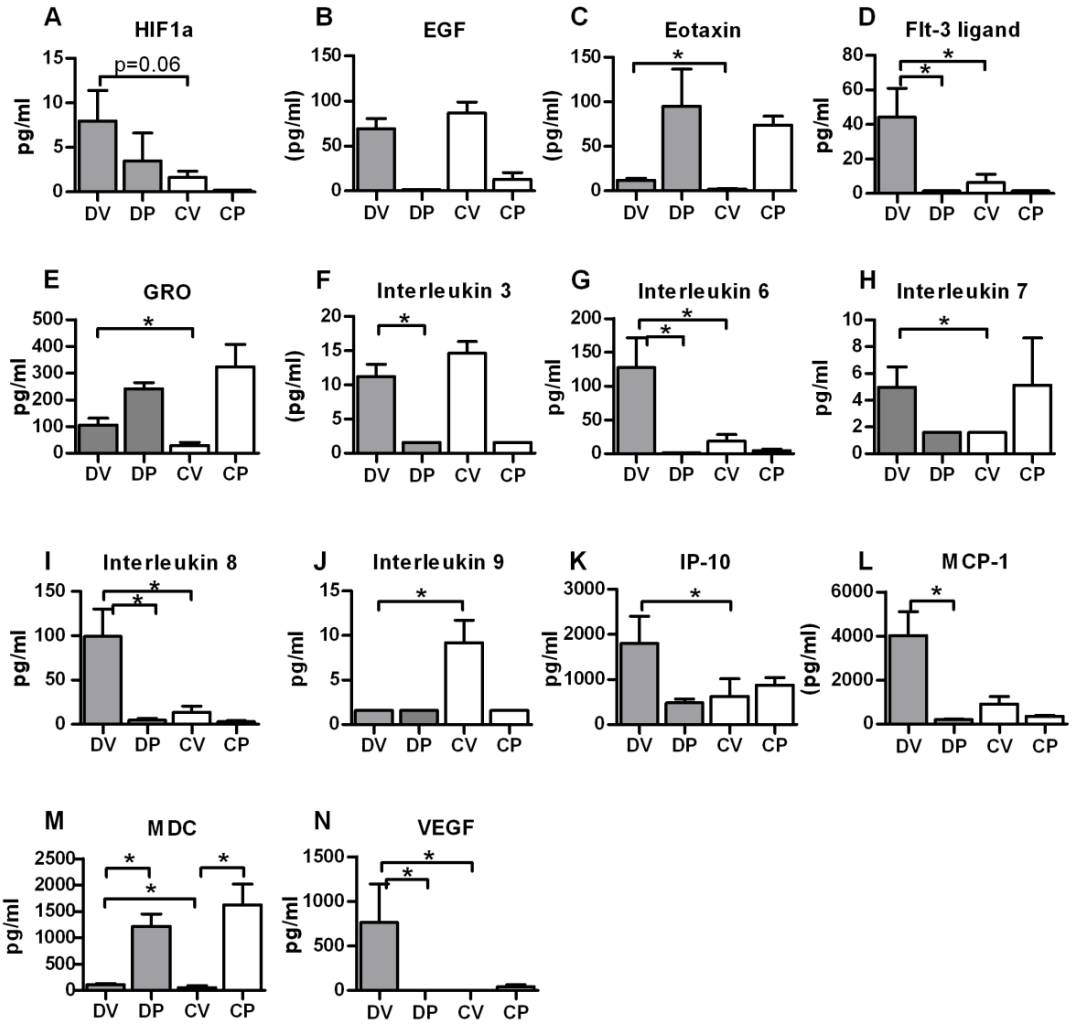

Figure 5.3 Molecular mediators in the vitreous and plasma of subjects with PDR and controls. (A-N) Mean concentration of HIF1a and cytokines (±SEM) in the vitreous and plasma of diabetic and control subjects. Analysis performed by Chris Cox (BioAnaLab Limited, Oxford, UK). DV = diabetic vitreous; DP = diabetic plasma; CV= control vitreous; CP = control plasma of *=statistically significant.

	Vitreous			**Plasma**	
	Diabetic group	Control group	p value	Diabetic group	Control croup
EGF	68.9 (1.6-125.6)	86.6 (1.6-134.0)	p = 0.2	ND	12.87 (1.6-39.0)
Eotaxin	12.2 (1.6-27.6)	2.2 (1.6-7.9)	p = 0.0001	95.2 (25.7-254)	73.8 (56.8-112.7)
FGF-2	ND	ND	NA	ND	8.45 (1.6-25.4)
Flt-3 Ligand	44.3 (1.6-220.6)	6.39 (1.6-68.6)	p = 0.002	ND	ND
Fractalkine	3.21 (1.6-22.5)	ND	NA	ND	25.7 (1.6-61.8)
G-CSF	5.4 (1.6-29.8)	10.1 (1.6-24.4)	p = 0.1	15.55 (10.8-24.0)	18.01 (10.57-24.0)
GM-CSF	7.2 (1.6-75.4)	3.0 (1.6-21.5)	NA	16.6 (1.6-51.7)	15.6 (1.6-21.6)
GRO	105.6 (1.6-380.8)	29.1 (1.6-132.3)	p = 0.001	241.2 (184.1-311)	323.2 (114.7-581)
IFN-α2	3.5 (1.6-26.4)	3.9 (1.6-13.6)	NA	ND	ND
IFN-γ	2.0 (1.6-7.6)	ND	NA	2.43 (1.6-5.77)	15.71 (1.6-60.44)
IL-1α	5.79 (1.6-36.81)	2.49 (1.6-14.1)	NA	ND	ND
IL-1β	ND	ND	NA	ND	5.07, (1.6-13.92)
IL-1Rα	ND	2.1 (1.6-9.6)	NA	6.08 (1.6-15.3)	3.02 (1.6-8.7)
IL-2	ND	ND	NA	ND	2.1 (1.6-6.3)
IL-3	11.2 (1.6-21.3)	14.6 (3.7-29.8)	p = 0.4	ND	ND
IL-5	ND	1.76 (1.6-3.77)	NA	ND	2.06 (1.6-3.9)
IL-6	127.6 (32.3-565.3)	18.50 (1.6-128.4)	p = 0.0004	ND	4.722 (1.6-12.3)
IL-7	4.9 (1.6-19.0)	ND	NA	ND	5.126 (1.6-19.2)
IL-8	99.1 (21.3-451.6)	11.2 (1.6-66.4)	p = 0.0001	4.28 (1.6-12.82)	3.104 (1.6-6.49)
IL-9	ND	9.195 (1.6-24.4)	p = 0.0036	ND	ND
IL-10	5.48 (1.6-47.8)	ND	NA	1.99 (1.6-3.55)	ND
IL12 (p40)	5.14 (1.6-47.6)	ND	NA	23.83 (1.6-82.5)	27.22 (1.6-79.07)
IL12 (p70)	ND	2.04 (1.6-5.1)	NA	ND	10.83 (1.6-30.59)
IL-15	3.73 (1.6-14.0)	ND	NA	ND	ND
IL-17	ND	1.84 (1.6-4.93)	NA	ND	33.62 (1.6-161.72)
IP-10	1801.0 (334.6-7102)	629.9 (100.2-5685)	p = 0.0004	629.9 (433-659)	881.15 (±358.5)
MCP-1	4021.0 (72.3-10000)	909.6 (1.6-4825.1)	p = 0.03	202.91 (129-321)	348.55 (252-551)
MCP-3	ND	ND	NA	ND	3.18 (1.6-9.54)
MDC	114.5 (50.0-229.3)	56.9 (1.6-445.1)	p = 0.004	1217 (588-1836)	1626 (771.9-3089)
MIP-1α	ND	ND	NA	3.6 (1.6-11.62)	18.5 (1.6-63.92)
MIP-1β	5.1 (1.6-31.9)	ND	NA	9.94 (1.6-18.16)	26.87 (6.25-46.83)
sCD40L	ND	ND	NA	290.64 (138-470	616.13 (184-2051)
sIL-2Rα	12.57 (1.6-144.2)	ND	NA	ND	ND
TNF-α	ND	1.79 (1.6-4.31)	NA	4.94 (1.6-9.14)	6.45 (1.6-11.56)
VEGF	762.59 (1.6-4899.7)	ND	p = 0.0008	ND	42.42 (1.6-113.6)

Table 5.2 Vitreous and plasma concentration of cytokines in diabetic and control subjects. Values are expressed as the mean (range) in pg/ml. ND = below the detection limit of 3.2 pg/ml. NA = not assessed, group differences were assessed for all cytokines that were found in more than 5 vitreous samples. In bold = significant difference after Bonferroni correction.

5.2.6 Correlation of intraocular oxygen tensions, transcription factor and vitreous cytokine concentrations

To explore the hypothesis that retinal oxygenation influences the molecular hypoxia sensing pathway and the profiles of cytokines present in the vitreous, intraocular oxygen levels were correlated to vitreous HIF1a and vitreous cytokine concentrations (figure 5.4). Mid-vitreous oxygen tension did not correlate with vitreous HIF1a levels (r=-0.17, p=0.56), VEGF (r=0.17, p=0.6) or any cytokine detected (figure 5.4A,B, table 5.3A). However, there was a significant positive correlation between HIF1a and Flt-3 ligand (r=0.7, p=0.02), G-CSF (r=0.71, p=0.01), IP-10 (r=0.67, p=0.02), MCP-1 (r=0.66, p=0.03) and VEGF (r=0.67, p=0.02) and a strong positive correlation between VEGF and MCP-1 (r=0.76, p=0.002) and between G-CSF and GRO (r=0.79, p=0.001, table 3.3). Furthermore, the vitreous concentration of HIF1a was found to correlate with the preretinal oxygen tension at the posterior pole (r=0.7, p=0.02). Similarly, a strong trend to statistical significance was observed between the vitreous concentration of VEGF and the preretinal oxygen tension at the posterior pole (r=0. 56, p=0.07, table 3.3).

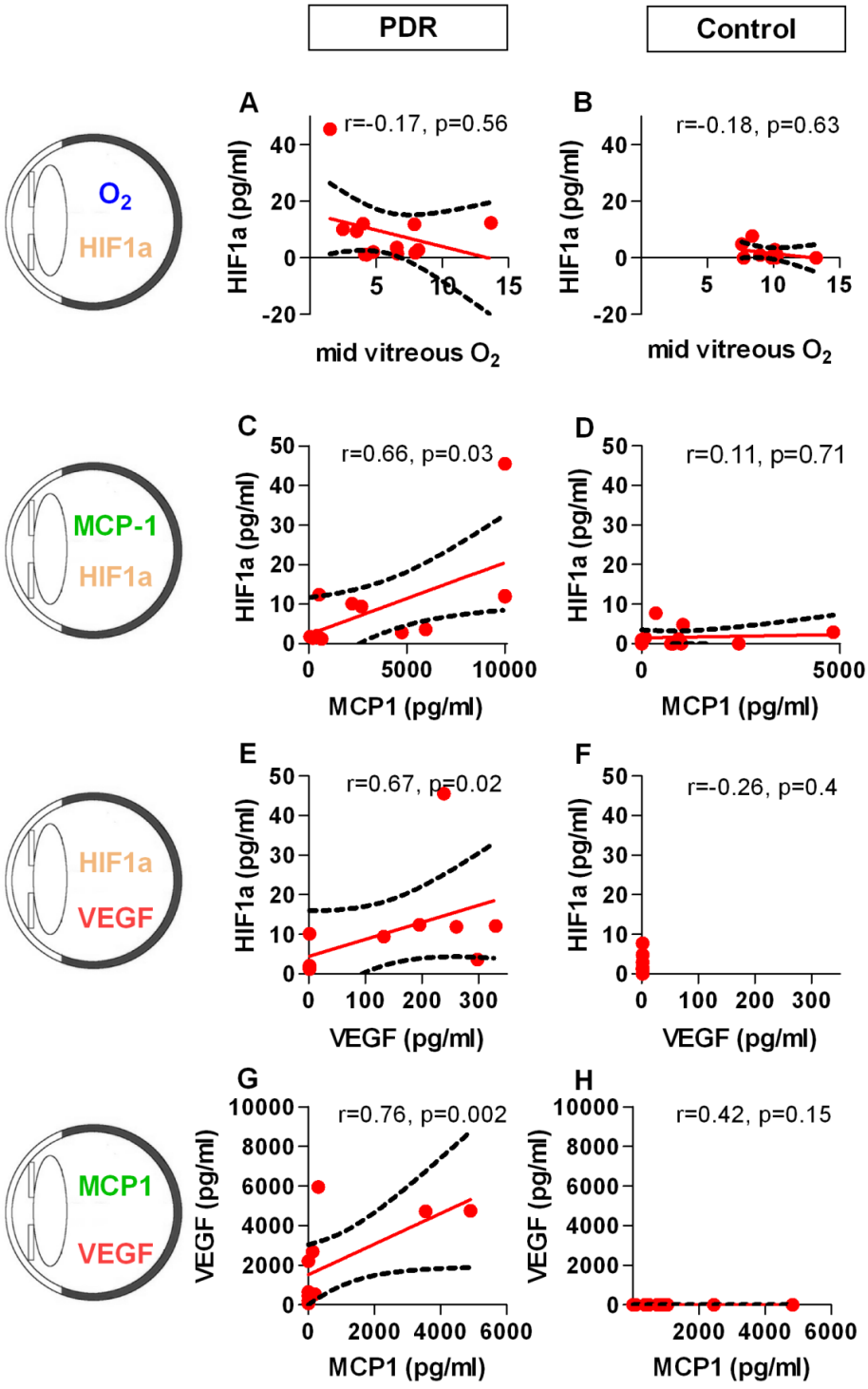

Figure 5.4 Correlation of intraocular oxygen and molecular mediators. Correlation of intraocular oxygen levels and vitreous HIF1a levels (row A), vitreous MCP-1 and HIF1a levels (row B), HIF1a and VEGF levels (row C) and VEGF levels and MCP-1 (row D) in subjects with PDR (column A) and controls (column B). Red line = linear regression. Dotted line = 95% CI, r = Spearman correlation factor. $P < 0.05$ = statistical significant correlation.

Analyses		Spearman r	p value
A) Correlation between O_2 measurements and cytokines/transcriptions factors			
mid-vitreous O_2	HIF1a	-0.17	p = 0.56
mid-vitreous O_2	VEGF	0.17	p = 0.6
preretinal O_2 posterior pole	HIF1a	0.7	p = 0.02
preretinal O_2 posterior pole	VEGF	0.56	p = 0.07
B) Correlation between vitreous Hif1a and cytokines			
HIF1a	Flt3 ligand	0.7	p = 0.02
HIF1a	G-CSF	0.71	p = 0.01
HIF1a	IP-10	0.67	p = 0.02
HIF1a	MCP-1	0.66	p = 0.03
HIF1a	VEGF	0.67	p = 0.02
C) Correlation between vitreous cytokines			
GRO	G-CSF	0.79	p = 0.001
VEGF	MCP-1	0.76	p = 0.002

Table 5.3 Correlation of oxygen, Hif1a and vitreous cytokines in proliferative diabetic retinopathy. Number of xy pairs = 13.

5.3 Discussion

The importance of ischaemia-induced expression of retinal cytokines in the development of diabetic retinopathy is widely accepted. Ischaemia and hypoxia have been suggested to cause the release of proangiogenic factors, such as VEGF, which contribute to the development of neovascularisation in proliferative diabetic retinopathy (D'Amore, 1994). However, direct evidence of retinal hypoxia is weak and there have been no direct measurements of retinal oxygen levels in humans. Previous studies on intraocular oxygen in human diabetic subjects have investigated oxygen tension in the mid-vitreous (Holekamp et al., 2005) or preretinal at sites of laser photocoagulation using a fiberoptic oxygen probe during surgery (Stefansson et al., 1992). Other groups have measured oxygen saturation in retinal vessels of diabetic subjects using a non-invasive imaging oximeter (Hammer et al., 2009) or assessed retinal tissue oxygenation by magnetic resonance imaging retinal oximetry (Trick et al., 2006). However, none of these studies has been able to demonstrate direct evidence of tissue hypoxia in the human diabetic retina. Secondly, none of these studies has investigated oxygen tensions at different preretinal sites to elucidate the presence of potential oxygen gradients along the diabetic retina. Finally, none of these studies has investigated the crucial link between oxygen tension, oxygen sensing transcription factors and molecular mediators in proliferative diabetic retinopathy.

In this chapter of my thesis, the feasibility of measuring preretinal oxygen tension in human subjects using an optical oxygen sensor during surgery was tested. The intraocular distribution and concentration of oxygen was determined in subjects with proliferative diabetic retinopathy and non-diabetic individuals. Furthermore, the link between oxygen tension, oxygen sensing transcription factor and molecular mediators in proliferative diabetic retinopathy was explored by correlating intraocular oxygen tensions with hypoxia-inducible transcription factors and the concentrations of 42 vitreous cytokines.

Using an optical oxygen sensor we were able to measure the oxygen tension at sites in the vitreous and at the retinal surface safely and reliably in human subjects undergoing vitreous surgery. Compared to polarographic oxygen probes (Maeda et al., 1992; Maeda and Tano, 1996; Stefansson et al., 1981) temperature-corrected fiberoptic oxygen probes possess the advantages that they do not consume oxygen and have greater sensitivity at low oxygen levels (Stefansson et al., 1989). A previous study on intraocular oxygen in human subjects assessed mid-vitreous and anterior vitreous oxygenation in non-diabetic and diabetic subjects using optical oxygen sensors during surgery but did not assess preretinal oxygenation because of the technical and surgical challenge (Holekamp et al., 2005). Another study did measure preretinal oxygenation safely and reliably in human diabetic subjects but focused on areas of photocoagulation in the peripheral retina and did not assess preretinal

oxygenation at other sites across the vitreous and retina (Stefansson et al., 1992).

Mid-vitreous O_2 tension is decreased in PDR

Using an optical oxygen sensor I found significantly lower oxygen levels in the anterior and mid-vitreous of diabetic subjects compared with control subjects which is in line with recently published data (Holekamp et al., 2006). Whereas Holekamp and coworkers demonstrated higher oxygen tension in the anterior vitreous than in the mid-vitreous (Holekamp et al., 2006), I identified no significant difference in oxygen tension between these sites. This may reflect differences in the exact location of oxygen measurement between the studies. Holekamp used a site near the equator of the crystalline lens whereas in the present study we measured 3mm posterior to the posterior pole of the crystalline lens; the lower oxygen tension measured at this site may reflect the greater distance from the vascularised tissue of the ciliary body.

Oxygen in the vitreous is derived from the retinal and iris vasculature via diffusion (Alder and Cringle, 1990; Shui et al., 2006). As the mid-vitreous site is equidistant to all regions of the retina, its oxygen tension represents the overall balance between retinal oxygen supply and consumption (Wangsa-Wirawan and Linsenmeier, 2003). The low vitreous oxygen tension in PDR may therefore be explained by an overall reduced oxygenation of the diabetic iris and retina. Areas of microinfarcts in the diabetic retina may not contribute to the oxygen

supply to the mid-vitreous and cause mid-vitreous hypoxia. Furthermore, vitreous cells are increased in the vitreous of diabetic subjects (Canton et al., 2004) which may contribute to mid-vitreous hypoxia by consuming oxygen. Finally, substances such as ascorbic acid are increased in the vitreous and act as an oxygen sink by metabolizing oxygen to water (Shui et al., 2009). Further studies will have to investigate if these oxygen sinks contribute to the detected low vitreous oxygen levels in PDR.

Preretinal oxygenation is increased at the posterior pole in PDR

Results of this chapter demonstrate that the diabetic retina is characterised by significant intraocular oxygen gradients that were not present in normal controls. The diabetic retina reveals significant differences in preretinal oxygen, with high oxygen tensions at the posterior pole and steep gradients towards the periphery. High oxygen tension measured at the posterior pole of the retina in proliferative diabetic retinopathy in this study suggests a rich supply of oxygen from the highly-perfused neovascular complexes that develop preferentially in this part of the eye (Shimizu et al., 1981). A negative oxygen gradient to the retinal periphery suggests that hyperoxia at the posterior pole may compensate to some extent for retinal hypoxia more peripherally. The gradient itself, however, is indicative that oxygen diffusion from the center to the periphery is either physically limited or that the peripheral retina acts as an oxygen sink that cannot be saturated. Removal of the vitreous body may facilitate redistribution of

oxygen from these neovascular complexes to areas of ischaemia by facilitating fluid flow and convection currents across the vitreous cavity (Barton et al., 2007). Despite hyperoxia at the posterior pole, the oxygen tension in the vitreous is lower than in non-diabetic controls, suggesting consumption of oxygen elsewhere in the eye.

Preretinal oxygenation in the mid periphery is normal in PDR

In contrast to the posterior pole, the preretinal oxygen tension in the mid periphery in PDR was similar to the one detected in non-diabetic subjects. This finding is in opposition to the hypothesis that the retinal periphery in diabetic retinopathy is hypoxic (Linsenmeier et al., 1998) and may be explained by the advanced state of the disease and increased oxygen supply to the posterior pole of the diabetic retina. Oxygen released from the neovascularisation at the posterior pole may diffuse along a steep gradient towards the mid-periphery and contribute to the normoxic mid-periphery. It is also possible that the retinal tissue in the diabetic mid periphery is partly infarcted and therefore consumes less oxygen. This may result in a relative normoxia in the mid peripheral retina even though the retinal oxygen supply is reduced. Finally, the normal oxygen tension in the diabetic mid peripheral retina may reflect the effect of panretinal photocoagulation on oxygen availability in these areas (Stefansson, 2006). Retinal photocoagulation has been reported to increase inner retinal oxygenation in human diabetics (Stefansson et al., 1992). It has been proposed

that the ablation of oxygen consuming cells in the outer retina by laser photocoagulation allows oxygen fluxes from the choroid to reach the inner retina and to account for an oxygen increase (Stefansson, 2006). The results presented in this chapter, however, do not demonstrate a difference in oxygen tension above areas of photocoagulation compared with non lasered areas in diabetic subjects which is in line with previous reports (Maeda et al., 1992). This may be explained by the fact that the subjects included in this and Maedas study were breathing normal air (21% oxygen) during surgery whereas the individuals included by Stefansson were exposed to inhalation of 30% oxygen. Therefore, autoregulatory retinal vasoconstriction, as observed by Wilson after retinal photocoagulation (Wilson et al., 1988), may have countered and masked the effect of the oxygen flux through the laser scar in our study. The surplus of oxygen used in Stefansson's study, however, may have helped to determine the difference in oxygen tension between laser treated and non-treated areas, as the compensatory effect of the retinal circulation was overpowered (Stefansson et al., 1992). To determine the effect of panretinal photocoagulation on vitreous oxygenation in advanced proliferative diabetic retinopathy, further studies will have to compare vitreous oxygen levels in subjects with non-proliferative diabetic retinopathy who have undergone panretinal photocoagulation with subjects who have not undergone panretinal photocoagulation.

Limitations of the oxygen measurements performed in this study include the design of the study which did not allow us to conduct the study in a masked

fashion and the standardisation of the sites where the oxygen probe was kept. However, the physicians involved in this study took great care to standardise the sites of oxygen measurements and an observer bias is highly unlikely. Another possible limitation of our study is the difference in mean age between the group of subjects with diabetes and the group of control subjects. However, recent evidence demonstrating that oxygen tension in the vitreous is not associated with age (Holekamp et al., 2006) validates the direct comparison of the two groups in this study.

Hif1a is increased in the vitreous of PDR

Having established the presence of vitreous hypoxia in the diabetic eye I aimed to determine the vitreous concentration of HIF1a which is known to be a critical link between tissue hypoxia and adaptive tissue responses. I found increased levels of HIF1a protein in the diabetic vitreous compared with the corresponding diabetic plasma and control vitreous. This finding is in line with recently published data and supports the idea that retinal production, not serum diffusion, is the main contributor to increased vitreous HIF1a in subjects with PDR (Wang et al., 2009). This hypothesis is supported by immunohistochemistry studies showing increased HIF1a and VEGF activity in surgically excised preretinal diabetic membranes compared with non-diabetic idiopathic epiretinal membranes (bu El-Asrar et al., 2007; Lim et al., 2010). HIF1a protein may be released from hypoxic inner retinal cells that undergo apoptosis and lose the

integrity of their cell membranes (Barber et al., 2011) or from hypoxic cells in the vitreous which are increased in PDR (Canton et al., 2004). Further studies will have to address these possibilities and assess the contribution of vitreous cells to vitreous cytokines and transcription factors.

Increased vitreous cytokines in PDR

As HIF1a is known to be a crucial link between tissue hypoxia and the expression and secretion of proangiogenic and inflammatory cytokines I determined vitreous cytokine levels using multiplex cytokine arrays and correlated their concentration to the corresponding HIF1a levels. Multiplex cytokine arrays provide a new and powerful method allowing the simultaneous measurement of multiple cytokines in one experiment (Banerjee et al., 2007; Maier et al., 2006; Maier et al., 2008; Yoshimura et al., 2009). As vitreous samples are limited in volume and therefore very precious, multiplex cytokine arrays provide an efficient tool to quantify multiple cytokines simultaneously in a small volume of vitreous. Among the 42 tested cytokines I found increased concentrations of Flt-3 ligand, IL-6, IL-7, IL-8, IP-10 and VEGF in the diabetic vitreous compared to the control vitreous and to the corresponding plasma, suggesting a local upregulation of these factors by cells in the retina and possibly by cells in the vitreous (El-Ghrably et al., 2001). Increased vitreous levels of VEGF (Murugeswari et al., 2008), IL-6 (Nakamura et al., 2003), IL-8 (Petrovic et al., 2007) and IP-10 (bu El-Asrar et al., 2006) have already been

described in PDR and associated with the proangiogenic and inflammatory state of the diabetic retina. For the first time, I found increased concentration of Flt-3 ligand and reduced concentration of IL-9 levels in PDR. Flt-3 ligand, expressed by immature hematopoietic cells, stimulates proliferation of stem cells, myeloid and lymphoid progenitor cells, dendritic cells and natural killer cells (Drexler and Quentmeier, 2004). Recent experiments in a mouse model of diabetes have shown that exogenous Flt3-ligand treatment is associated with a significant reduction in the development of diabetes and an increased production of myeloid and plasmacytoid dendritic cells suggesting a role of Flt3-ligand in inflammation and the pathogenesis of diabetes (Chilton et al., 2004). IL-9 is a T helper cell 2 (Th2) derived cytokine that stimulates cell proliferation and prevents apoptosis of Th2 cells. In contrast to the pro-inflammatory T helper cell 1 (Th1) subset of CD4 expressing T-lymphocytes, Th2 cells are known to have anti-inflammatory properties (Berger, 2000). Down-regulation of IL-9 in PDR might therefore be associated with decreased Th2 cells and a consequently Th1-weighted imbalance associated with chronic inflammatory processes in advanced diabetic retinopathy. Further work is required to define the specific roles of Flt-3 ligand and IL-9 in the pathogenesis of diabetic retinopathy and to evaluate their potential as therapeutic targets. Taken together, these results demonstrate that multiple cytokines are significantly altered in the vitreous of diabetic subjects compared with non-diabetic individuals. Both proangiogenic and pro-inflammatory cytokines are expressed and secreted locally in the

diabetic eye supporting the concept of a closely linked angiogenic and inflammatory element in proliferative diabetic retinopathy.

Vitreous Hif1a does not correlate with mid-vitreous O_2 levels but with inflammatory cytokines

To further explore the hypothesis that intraocular oxygen tension influences the expression of oxygen sensing molecules and effector proteins in PDR, I correlated intraocular oxygen levels with vitreous HIF1a and cytokine levels. If we accept that mid-vitreous oxygen tension indicates global retinal oxygenation we would anticipate that mid-vitreous hypoxia is associated with increased levels of HIF1a, proangiogenic factors and inflammatory cytokines in the presence of ischaemic retinopathy. I detected a positive correlation between HIF1a and VEGF in the diabetic vitreous which is in line with previously published data and supports the important role of HIF1a in the pathogenesis and progression of retinal neovascularisation (Wang et al., 2009). However, I did not detect a correlation between mid-vitreous hypoxia and vitreous HIF1a levels in advanced proliferative diabetic retinopathy. It is possible that the oxygen measurements and cytokine analysis of the core vitreous performed in this study fail to account sufficiently for the effect of local oxygen and cytokine gradients within the retina. Local hypoxia within the inner retina has been shown to result in an increase of HIF1a, HIF2a and VEGF protein levels in an animal model of ischaemia and hypoxia (Mowat et al., 2010). These molecular pathways may

also be active in hypoxic areas within the diabetic retina but may not be detectable by the measurements in the core vitreous performed in this study. Furthermore, a potential correlation between vitreous hypoxia and HIF1a levels may have been masked by the strong inflammatory component in PDR (Maier et al., 2008) which can activate HIF1a independent of hypoxia (Dehne and Brune, 2009). I found increased levels of numerous inflammatory cytokines and identified a strong correlation between MCP1 and HIF1a protein in the diabetic vitreous. This is consistent with previously published data demonstrating that inflammatory cytokines such as MCP-1 can induce HIF1alpha activity (Hong et al., 2005). The strong correlation between vitreous VEGF and MCP-1 levels in the diabetic vitreous further highlights the close relation between angiogenesis and inflammation in advanced proliferative diabetic retinopathy. MCP-1 can induce VEGF expression by stabilisation of HIF1a (Hong et al., 2005). On the other hand MCP-1 expression can be induced by VEGF which increases the MCP-1 promotor activity through binding to the activator protein-1 (AP-1) binding site of the MCP-1 promoter region (Marumo et al., 1999; Yamada et al., 2003). This data suggests a positive regulatory feedback loop between VEGF and MCP-1 expression which may escalate inflammatory responses and angiogenesis.

Furthermore, I identified a positive correlation between the preretinal oxygen tension at the posterior pole and vitreous levels of HIF1a and VEGF in PDR. Although the mid-vitreous HIF1a and VEGF levels reported in this study might

underestimate the concentration at the posterior pole (Shimada et al., 2009), the positive correlation found between HIF1a, VEGF levels and preretinal oxygenation is consistent with the hypothesis that HIF1a and VEGF induce the development of neovascular complexes in the posterior retina that are richly perfused and supply oxygen to the retina. Upregulation of VEGF may be the result of hypoxia-sensing mechanisms elsewhere that I was not able to detect in this study, or alternatively, oxygen-independent chronic inflammatory processes in advanced proliferative diabetic retinopathy.

Taken together these data suggest that HIF1a is activated by both hypoxia and inflammation in advanced PDR and thereby contributes to the proangiogenic cytokine profile and the formation of retinal neovascularisation. To investigate the hypothesis that local hypoxia is the initiating trigger for inflammation, angiogenesis and the progression of diabetic retinopathy using this approach further studies are needed that focus on subjects with less advanced retinopathy.

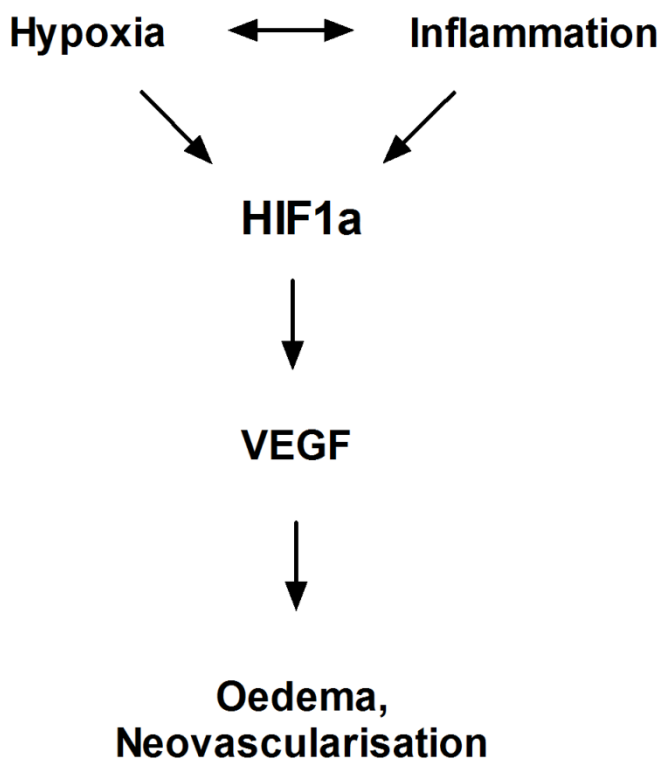

Figure 5.5 Proposed central role for HIF1a in advanced proliferative diabetic retinopathy.

5.4 Conclusion

In conclusion, I have identified significant intraocular oxygen gradients in human subjects with proliferative diabetic retinopathy with high oxygen tensions at the posterior pole and steep gradients towards the periphery and the mid-vitreous. I have found increased levels of HIF1a protein and downstream adaptive mediators such as VEGF in the vitreous of subjects with proliferative diabetic retinopathy. These findings are consistent with the hypothesis that HIF1a and VEGF induces the development of neovascular complexes in the posterior retina that are richly-perfused but nonetheless fail to redress hypoxia in the mid-vitreous. Upregulation of vitreous HIF1a and VEGF may be a consequence of retinal hypoxia at unidentified sites or of chronic inflammatory processes in advanced proliferative diabetic retinopathy.

6 General discussion

6.1 The role of oxygen sensing mechanisms in development

6.1.1 The roles of Vhl and Hifa's in development

Oxygen sensing mechanisms and the Vhl-Hif pathway are essential for normal development of different organ systems. Homozygous deletion of *Vhl* in mice leads to mid-gestational embryonic death secondary to failed placental vasculogenesis between embryonic day (E) 10.5 and 12.5 (Gnarra et al., 1997). Similarly, mouse embryos with homozygous deletion of *Hif1a* die during midgestation at E10.5 and are characterised by cardiac and vascular malformations (Kotch et al., 1999; Ryan et al., 1998). These findings demonstrate that both Hif1a activation and its stringent regulation by Vhl are essential for development of life. Systemic *Hif2a knockout* mice, in contrast, demonstrate various phenotypes, including embryonic lethality secondary to vascular defects (Peng et al., 2000), perinatal lethality due to decreased catecholamine production (Tian et al., 1998), postnatal lethality caused by progressive multiorgan failure (Scortegagna et al., 2003), or even normal viability into adulthood (Ding et al., 2005). The range of phenotypes of Hif2a deficient mice may depend on different genetic backgrounds and gene targeting strategies in different laboratories and suggests an important but - compared with Vhl and Hif1a - less critical role of Hif2a in murine development.

In order to elucidate the role of Vhl and Hifa's during development, cell specific *knockout* approaches using the Cre/loxP mediated recombination system have

been established. In line with the observation in this thesis, conditional inactivation of *Vhl* in developing tissues results in a severely abnormal growth and vascular development in different organ systems. Conditional inactivation of *Vhl* in developing thymocytes results in Hif1a mediated apoptosis of thymocytes and a significantly reduced size of the thymus in the adult (Biju et al., 2004). Similarly, conditional disruption of *Vhl* in chondrocytes during endochondral bone development leads to a Hif1a mediated reduction in proliferating chondrocytes and the development of severe dwarfism (Pfander et al., 2004). These findings are in line with results of this thesis showing that inactivation of *Vhl* in the RPE results in RPE apoptosis and secondarily in the development of microphthalmia. Conditional inactivation of *Vhl* in developing hepatocytes, however, does not result in growth defects of the liver (Rankin et al., 2005) suggesting that different tissues are differently susceptible to the effects of Hif activation during development. In addition to controlling organ growth and development, Vhl has also been shown to play a critical role for normal vascular development in different organ systems. Conditional inactivation of *Vhl* in hepatocytes (Rankin et al., 2005), thymocytes (Biju et al., 2004), epidermis (Boutin et al., 2008) or renal cells lead to an increase in angiogenesis and vascular density which is independent of Hif1a (Rankin et al., 2005). These findings suggest that other Vhl dependent molecules, such as Hif2a, regulate the angiogenic response in the *Vhl knockout* mice by driving the expression of proangiogenic genes including *Vegf* and *Epo*.

These data demonstrate that Vhl controls the growth and development of different organ systems, including the skeleton, the thymus and the eye, by depressing Hif1a activity and furthermore regulates vascular development by controlling other transcription factors, such as Hif2a. Also, these findings suggest that reduced systemic oxygenation, for example in placental insufficiency, may have major effects on the development and growth of organs through activation of HIF.

6.1.2 The roles of Vhl and Hifa's in development of the eye

Work in this thesis has shown that molecular oxygen-sensing mechanisms play a critical role in the development of the eye and its vasculature. Activation of Hif1a in the RPE and iris during development results in aniridia and microphthalmia whereas activation of other Vhl dependent molecules, e.g. Hif2a, causes an abnormal development of the retinal vasculature.

In the eye, the choroidal vasculature is the first vascular system to develop and provide adequate oxygen levels to the primordium of the eye (Saint-Geniez and D'Amore, 2004). As the retina matures and grows, the demand for oxygen and nutrition increases and the retina experiences a physiological period of reduced oxygen availability (Chan-Ling et al., 1995). Recent evidence from the developing murine retina indicates hypoxic areas and Hif1a activation throughout all retinal layers (Kurihara et al., 2010). This hypoxic period in the developing retina has been suggested to contribute to the regulation of developmental photoreceptor death (Maslim et al., 1997; Mervin and Stone, 2002) and to control normal retinal vascularisation in a Hif dependent manner

(Caprara et al., 2011; Chan-Ling et al., 1995). In contrast to the retina, there is no evidence of hypoxia or Hif activation in the RPE during development (Kurihara et al., 2010). This finding is in line with results presented in this thesis and may be explained by the close proximity of the RPE to the oxygen rich choroidal vessels which are characterised by a high blood flow and a surplus supply of oxygen (Wangsa-Wirawan and Linsenmeier, 2003). During retinal development, Hif1a levels in the inner retina decrease with age as the retina becomes vascularised and supplied with oxygen from the retinal vasculature (Kurihara et al., 2010; Ozaki et al., 1999). Furthermore, the increased oxygen saturation in the systemic circulation after birth (Rodesch et al., 1992) results in increased oxygen diffusion from the choroid to the retina which is accompanied by a considerable reduction of Hif1a protein levels in the deep retinal layers soon after birth (Kurihara et al., 2010). Even after the retina and its vasculature has been fully developed, Hif1a protein can be found to a low extend in the GCL indicating a role for Hif1a signalling in the adult retina (Grimm et al., 2005; Hughes et al., 2010), Hif2a in contrast, is predominantly found in endothelial cells of the hyaloid vessels and in retinal vessels of the superficial primary plexus during retinal development. In the adult murine retina, however, *Hif2a* is expressed by vascular endothelial cells as well as by cells within the GCL, INL, and retinal pigment epithelium (Ding et al., 2005). These observations demonstrate the responsiveinss of the retinal tissue to hypoxic events during development through mechanisms including the activation of Hifa proteins. Hif1a

and Hif2a appear to have specific spatio-temporal activation and expression patterns indicating distinct roles for both isoforms during retinal development.

Results in this thesis demonstrate that activation of Hif1a in the RPE and iris is detrimental during development and can cause cell death which is associated with development anomalies including microphthalmia and aniridia. Due to its close proximity to the oxygen rich choroidal vasculature, the RPE is unlikely to encounter hypoxia during development. Ocular hypoxia secondary to reduced systemic oxygenation, for example in placental insufficiency, however, could have major effects on oxygen levels at the level of the RPE and may be a previously unrecognised mechanism in the development of microphthalmia through mechanisms involving RPE specific activation of Hif1a. Future studies may test this hypothesis by exposing pregnant mice to reduced levels of oxygen in an oxygen incubator to determine if a decrease in systemic and RPE oxygenation results in Hif1a activation, RPE apoptosis and the development of microphthalmia in the offspring.

Results in this thesis further indicate that Vhl not only regulates Hif1a in the developing RPE but also controls the activity of other molecules and thereby normal retinal and choroidal vascularisation. The biological activity of Vhl is closely linked to the regulation of Hif1a and Hif2a and only a few other potential Vhl dependent molecules have been reported, most notably α-tubulin, fibronectin and the transcription factor Sp1 (Czyzyk-Krzeska and Meller, 2004). Recent work has demonstrated that Vhl dependent inactivation of Hif2a in the developing liver controls normal vascular development and prevents the

formation of cavernous liver haemangioma in the adult (Rankin et al., 2005). These findings suggest that Vhl dependent inactivation of Hif2a in the developing RPE may be essential for normal retinal and choroidal vascular development. To elucidate the role of Hif2a in the RPE for retinal and choroidal vascular development, future studies will have to assess the temporal and spatial expression of Hif2a in the neuroretina and RPE by immunohistochemistry and protein analysis at prenatal and postnatal timepoints. Furthermore, the characterisation of transgenic mice with conditional inactivation of *Hif2* in the RPE will help to understand the role of Hif2a in the RPE in ocular and vascular development. Finally, studies on transgenic mice with a conditional inactivation of both *Vhl* and *Hif2a* in the RPE may prove or disprove the hypothesis that the vascular phenotype in $Vhl^{trp1\text{-}creko}$ mice is mediated by activation of Hif2a in the RPE. In the possible event that these mice exhibit microphthalmia, analysis of transgenic mice with conditional inactivation of *Vhl*, *Hif1a* and *Hif2a* in the RPE will elucidate whether the vascular phenotype observed in $Vhl^{trp1\text{-}creko}$ mice is mediated by Hif2a or by other Vhl dependent factors.

6.2 The role of oxygen sensing mechanisms in neovascular eye disease

6.2.1 The role of Hif in the RPE in the development of AMD and choroidal neovascularisation

Hypoxia and activation of Hif's in the RPE have been suggested to play an important role in the development and progression of AMD and choroidal

neovascularisation (Stefansson et al., 2010). There is compelling evidence showing that patients with AMD can have decreased ocular blood flow and retinal haemodynamics (Ciulla et al., 2001; Friedman et al., 1995; Harris et al., 1999) and that a reduced choroidal perfusion is correlated with increased AMD severity (Grunwald et al., 1998; Grunwald et al., 2005). Measurements of blood flow, perfusion pressure and oxygen tension in the retina and at the optic nerve head have indicated that a decreased choroidal circulation results in tissue hypoxia in AMD patients (Grunwald et al., 2005; Metelitsina et al., 2008). This has led to the current hypothesis that hypoxia activates Hif signalling in the RPE in AMD which contributes to disease progression and the development of CNV. Indeed, recent studies have demonstrated that both HIF1A and HIF2A are activated in the endothelium, in macrophages and in the RPE in choroidal neovascular membranes in subjects with AMD (Inoue et al., 2007; Sheridan et al., 2009). Although the experiments presented in this thesis focus on the consequences of Hif signalling in the RPE during development, some basic mechanisms of Hif signalling in the RPE may be deduced for the adult situation.

Results in this thesis have shown that activation of Hif1a in the developing RPE induces RPE cell death and is followed by a secondary retinal degeneration in the adult. RPE cell loss and retinal degeneration are also central hallmarks in the pathogenesis of geographic atrophy (GA), the late stage form of atrophic AMD (Kinnunen et al., 2011). Recent work has demonstrated that individuals with GA exhibit increased apoptosis of photoreceptor and RPE cells compared with healthy controls (Dunaief et al., 2002). The question whether RPE cell loss

affects photoreceptor cell death or vice versa has been subject of much debate. The weight of opinions, however, supports the view that gradual failure of the RPE is the initial cause of GA and precedes retinal degeneration (Marshall, 1987; Sarks, 1976; Young, 1987).

The reason for RPE cell loss in GA has been suggested to depend on hypoxia and progressive oxidative insults by reactive oxygen species (ROS) (Jiang et al., 2008; Szaflik et al., 2009). ROS are increasingly produced in the mitochondria of the ageing RPE (Brennan and Kantorow, 2009) and upon hypoxia and can contribute to Hif1a stabilisation by preventing its degradation (Brunelle et al., 2005; Guzy et al., 2005; Kaelin, Jr., 2005). The findings that choroidal perfusion is reduced with age (Lutty et al., 1999) and that choriocapillaris vessels obliterate in the evolution of GA before retinal and RPE changes can be observed (Sarks, 1976), raise the possibility that hypoxia at the levels of the RPE increases both ROS and Hif1a in the early stages of GA which results in RPE cell loss and secondarily in retinal degeneration. This hypothesis is supported by the finding of this thesis that activation of Hif1a in the RPE results in cell apoptosis and secondarily in severe retinal degeneration. Activation of Hif1a in the RPE by hypoxia due to choroidal hypoperfusion may therefore be a so far unrecognised mechanism for RPE cell loss and disease progression in GA. Future immunohistochemical studies will have to determine whether Hif1a is stabilised in the RPE and associated with apoptosis in areas of choroidal vasoobliteration in early GA. These experiments may provide a rationale for developing treatment modalities to inhibit Hif1a stabilisation in the RPE in early

GA to prevent the sequel of RPE hypoxia, RPE cell death, retinal degeneration and loss of vision.

Results in this thesis have shown that activation of Hif's in the RPE is associated with an increase in the levels of angiogenic factors in the eye including Flt-1, Epo and Vegf. Whereas the increased expression of *Flt1* appears to be dependent on Hif1a activation, *Epo* and *Vegf* overexpression appear to be independent of Hif1a suggesting that other Vhl dependent molecules such as Hif2a may drive the expression of these angiogenic factors in the RPE. These data suggest that Hif1a and Hif2a control specific sets of target genes in the RPE and that Hif2a rather than Hif1a induces *Vegf* and *Epo* expression in the RPE. Furthermore, results in this thesis demonstrate that the increased expression of angiogenic factors in the RPE was associated with retinal vascular anomalies and the development of chorioretinal anastomosis which again developed independently of Hif1a in the RPE. These data suggest that Hif2a activation in the RPE contributes to the expression of Vegf and other angiogenic factors in the RPE and induces secondary vascular changes in the retina and choroid. This hypothesis is in line with experimental data demonstrating that stabilisation of Hif2a controls *Vegf* and *Epo* expression in the liver (Rankin et al., 2007) the brain (Chavez et al., 2006) and in the eye (Morita et al., 2003). If we accept that human RPE cells respond similar to Hif activation as developing murine RPE cells, it is plausible that activation of Hif2a signalling in the RPE by e.g. hypoxia or inflammation induces *Vegf* and *Epo* expression in the RPE and

may therefore be a so far unrecognised mechanism in the development of neovascular changes in AMD. This hypothesis is supported by recent studies showing a strong activation of Hif2a and Vegf in the RPE of patients with AMD (Sheridan et al., 2009). *In vitro* studies, in contrast, have indicated that HIF1A is the main HIF isoform induced in the RPE upon hypoxia and regulates VEGF expression (Forooghian et al., 2007; Zhang et al., 2007c). Furthermore, *siRNA* against *Hif1a* was shown to decrease the hypoxia-induced upregulation of *Vegf* in RPE cells (Zhang et al., 2007b). This discrepancy between the results presented in this thesis and the literature may be explained by the different systems in which the experiments were conducted (*in vitro* vs. *in vivo*) and/or by the different developmental stage of the RPE analysed (embryonic vs. adult).

Future studies will therefore have to determine the roles of Hif1a and Hif2a signalling in the adult RPE and to prove or disprove their potential contribution to RPE cell death and the development of choroidal neovascularisation. Hifa's activation in the adult RPE may be achieved by exposing the RPE to hypoxia or by inactivation of *Vhl* in the RPE. Future studies will have to investigate whether systemic exposure to low levels of oxygen, e.g. by keeping mice in a sealed chamber with reduced oxygen levels, may be sufficient to activate Hif1a in the RPE. However, this may prove to be difficult as the choroidal circulation carries an immense surplus of oxygen (Wangsa-Wirawan and Linsenmeier, 2003) which may be sufficient to degrade Hif1a despite of systemic hypoxia. Furthermore, it has to be kept in mind that systemic hypoxia induces adaptive responses in other organs, e.g. expression of *Epo* in the kidney to the

circulation, which may have an impact on the RPE and would present a significant confounding factor. A more localised activation of Hif1a in the RPE would therefore be desirable and may be achieved by inducing choroidal vasoocclusion in mice by laser photoactivation of an intravenously injected photosensitive dye (e.g. rose Bengal) (Kramer et al., 2009). This technique has been reported to result in a temporary occlusion of the central retinal artery when aiming the laser beam at the central retinal artery. Intravenous injection of a photosensitive dye in mice followed by lasering of the choroidal vasculature may therefore induce temporary choroidal occlusion resulting in tissue hypoxia and activation of Hif1a in the RPE. Induction of reproducible vasoocclusion and tissue hypoxia in this model, however, may be difficult to obtain as demonstrated in models of retinal vascular occlusion (Osborne et al., 2004). Future studies will have to investigate whether choroidal vascular occlusion is achievable and represents a reliable model to induce hypoxia and Hif activation in the RPE. Alternatively, Hif's may be activated in the adult RPE by using tissue specific *knockout* technology of *Vhl*. Inactivation of *Vhl* in the adult RPE may be achieved by subretinal delivery of a viral vector expressing cre-recombinase under the control of an RPE-specific promoter (e.g. the *trp-1* or the *Bestrophin* promotor (Iacovelli et al., 2011)) to animals carrying the floxed *Vhl* allele. Hif1a immunohistochemistry as applied in this work will help to identify RPE specificity and to determine how efficient the Lox-Cre recombination event was. The consequences of Hif1a and Hif2a activation in the adult RPE cells may be assessed by e.g. electroretinography, ultrastructural analysis of the RPE and

analysis of the retinal and choroidal vasculature. Should RPE apoptosis and/or spontaneous neovascularisation be evident, subretinal delivery of viral vector expressing *cre recombinase* under the control of an RPE-specific promoter to adult *Vhl;Hif1a*$^{flox/flox}$ and *Vhl;Hif2a*$^{flox/flox}$ mice will help to further delineate specific roles of Hif1a and Hif2a in the adult RPE. Alternatively, transgenic mice expressing cre recombinase under the control of an RPE specific and tamoxifen inducible promotor (e.g. the *iCreER* (Longbottom et al., 2009) or the *iCreBestrophin* mouse line (Le et al., 2008)) may be crossed to *Vhl*$^{flox/flox}$, *Vhl;Hif1a*$^{flox/flox}$ and *Vhl;Hif2a*$^{flox/flox}$ mice to study the role of Hif signalling in the adult RPE. These approaches may help to understand whether Hif activation in the adult RPE induces spontaneous angiogenesis originating from the retinal circulation as seen in transgenic mice overexpressing Vegf in the rod photoreceptor (Okamoto et al., 1997) or from the choroidal vasculature as seen in the developmental study of this thesis. Should spontaneous development of neovascularisation be absent, choroidal neovascularisation may be induced in these mice by using the CNV laser model. Finally, analysis of mice with a conditional *knockout* of different *Hif* isoforms in the RPE in the laser-induced CNV model will help to define the role of Hifs in the RPE in the development of choroidal neovascularisation. These experiments will help to find out if Hif's are an appropriate target for the development of therapy in choroidal neovascular disease.

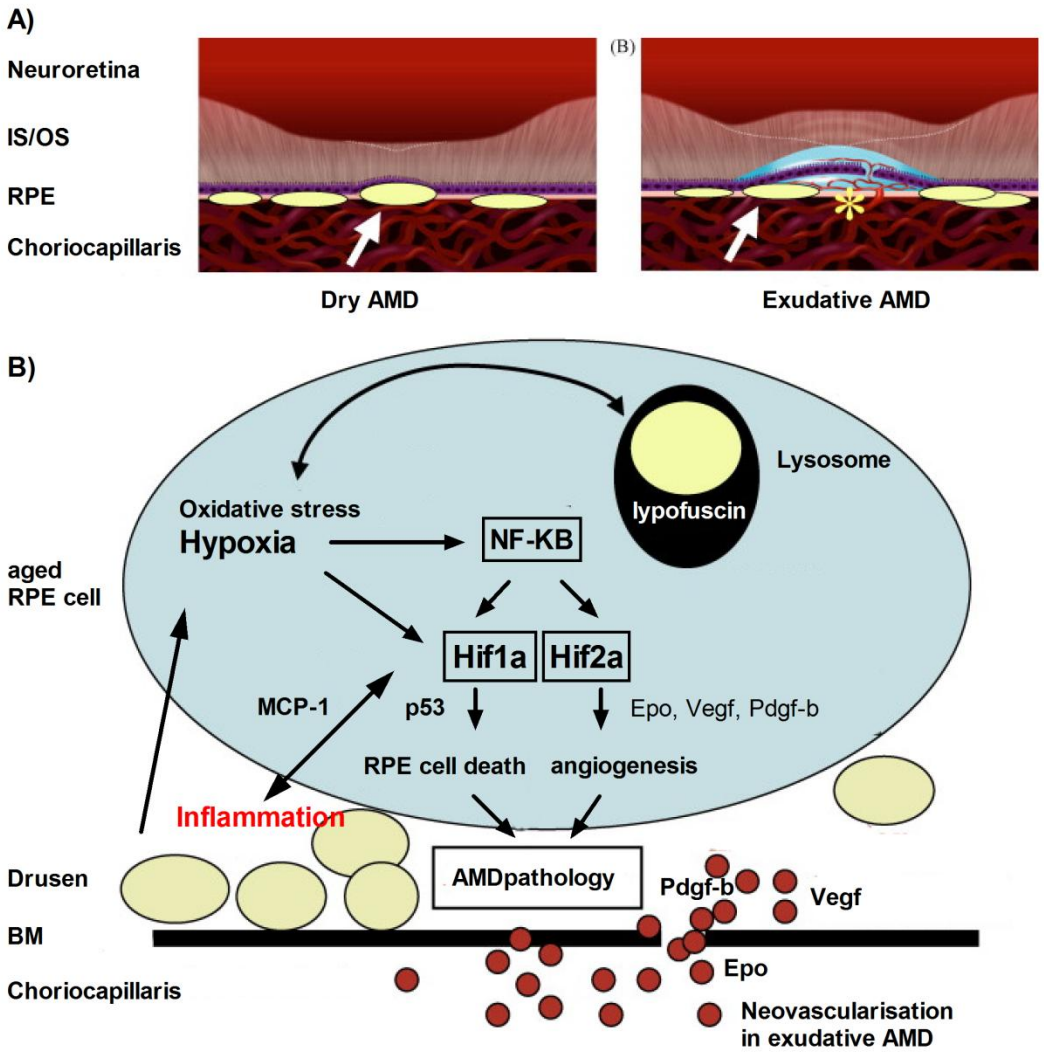

Figure 6.1 Proposed regulatory role of HIF1a and HIF2a in the pathogenesis of AMD. Schematic presentation of (A) dry AMD with drusen (arrow) and (B) exudative AMD with choroidal neovascularisation (asterisk). (C) Proposed regulatory role of Hif signalling in AMD pathology. Drusen formation between Bruch's membrane (BM) and RPE cells and choroidal hypoperfusion decreases oxygen delivery from choriocapillaris to the RPE and induce hypoxia. The aged RPE has a reduced capacity to respond to the continuous oxidative stress which leads to accumulation of lysosomal lipofuscin that is an antioxidant and increases oxidative stress damage in RPE cells. Both hypoxia and oxidative stress are major stimuli for NF-κB signalling which contributes to HIF activation and development of inflammation. In some cases chronic stress and hypoxia may induces Hif1a mediated cell apoptosis and rupture of BM which evokes choroidal neovascularisation. Adapted from (Arjamaa et al., 2009).

6.2.2 The role of Hif in myeloid cells in the development of retinal and choroidal neovascularisation

Bone marrow-derived myeloid cells, such as macrophages, neutrophils and dendritic cells have an important role in regulating the development and maintenance of blood vessels in development and disease. A common feature of many diseases, including tumour, inflammatory and ischaemic disease, is a decrease in oxygen levels in the affected tissue (Murdoch et al., 2008). Hypoxia develops within these tissues because of inadequate vascular perfusion due to vasoobliteration in ischaemic disease or due to disorganised and immature blood vessels in tumour disease. These areas of hypoxia attract circulating myeloid cells by releasing hypoxia-induced chemoattractants such as VEGF, MCP-1 and endothelins (Murdoch et al., 2008) and present a very challenging microenvironment characterised by hypoglycaemia, acidosis and hypoxia.

Experimental data provided in chapter 4 of this thesis demonstrate the importance of Hif1a activation and Vegf signalling in myeloid cells in the development of retinal and choroidal neovascularisation. Conditional inactivation of *Hif1a* in myeloid cells results in a substantial reduction of neovascularisation in the OIR and laser CNV mouse models indicating that Hif1a activation by hypoxia and/or inflammation in myeloid cells plays a pivotal role in inducing pathological angiogenesis.

The importance of HIF signalling in myeloid cells present in inflammatory and hypoxic microenvironments is widely established. The principle that myeloid cells respond to hypoxia was demonstrated by the initial finding from Knighton

and colleagues showing that macrophages exposed to hypoxia secrete angiogenic factors and are more effective in promoting angiogenesis *in vitro* (Knighton et al., 1983). These initial findings were supported by *in vivo* experiments showing that myeloid cells express higher levels of proangiogenic Hif target genes including Vegf in avascular and hypoxic areas of tumours (Harmey et al., 1998; Lewis et al., 2000). In addition to inducing angiogenesis, Hif1a signalling in myeloid cells has been shown to be critical for macrophage self-aggregation, invasion and motility as well as for killing of bacteria and ATP generation in areas of tissue hypoxia (Cramer et al., 2003). Activated microglia/macrophages have been found to be markedly increased in the retina in human diabetic retinopathy and in subretinal membranes in age-related macular degeneration (Skeie and Mullins, 2009; Zeng et al., 2008b) - two conditions that are characterised by tissue hypoxia and inflammation (Stefansson et al., 1992; Stefansson et al., 2010). Similarly, macrophages were found to accumulate in areas of hypoxia and acute inflammation in mouse models of retinal and choroidal neovascularisation and have been suggested to promote pathological angiogenesis by secreting Vegf (Sakurai et al., 2003). Recent work has shown, that deletion of the *hypoxia response element* (HRE) from the *Vegf* promoter in mice results in a significant reduction of Vegf levels and neovascularisation in both the OIR and the laser-induced CNV mouse model (Vinores et al., 2006). These data support the findings presented in this thesis and indicate that Hif1a signalling plays a significant role in the development of retinal and choroidal NV through mechanisms including

regulation of Vegf expression. However, it may also be possible that inactivation of *Hif1a* in myeloid cells reduces other Hif1a dependent proangiogenic cytokines, e.g. erythropoietin, and decreases the recruitment and survival of infiltrating proangiogenic myeloid cells (Cramer et al., 2003; Walmsley et al., 2005) which may contribute to the observed reduction in neovascularisation in the OIR and CNV model. Future studies will have to assess the number of recruited myeloid cells to retinal and choroidal NV and assess the expression levels of Vegf and Epo in $Hif1a^{lysMcre\text{-}YFP}$ myeloid cells to determine if a reduction of proangiogenic cytokines, an impaired recruitment or both contribute to the reduced neovascular response. These experiments will help to define the mechanism involved in the development of pathological neovascularisation and may provide a rationale for developing therapies that are capable of selectively inhibiting Hif1a or Vegf signalling in myeloid cell or alternatively their recruitment to pathological neovascularisation.

6.2.3 The role of hypoxia and Hif signalling in proliferative diabetic retinopathy in man

It is widely accepted that hypoxia plays a critical role in the development and progression of diabetic retinopathy (Stefansson, 2006). Work in this thesis has confirmed that oxygen tension in the mid vitreous of patients with PDR is significantly lower than that of non-diabetic patients (Holekamp et al., 2006; Stefansson, 2006). The oxygen availability in the vitreous will ultimately be the result of the net delivery and consumption of oxygen within the eye. The

observed mid vitreous hypoxia in PDR may therefore be explained by an overall reduction of oxygen availability in the diabetic retina which may be associated with a reduced oxygen diffusion from areas of retinal vasoobliteration to the mid vitreous. However, direct evidence of retinal tissue hypoxia in PDR in man is still lacking and measurements of oxygen tension in the vitreous overlying the retina in chapter 5 of this thesis suggest normal to increased retinal oxygen tension in PDR. This may be explained by the advanced stage of disease in which retinal neovascularisation increases oxygen levels at the posterior pole and areas of microinfarction and panretinal photocoagulation reduce oxygen consumption and thereby improve oxygen diffusion from the choroid to the inner retina in the peripheral retina. Studying the role of hypoxia in early diabetic retinopathy may therefore be the more informative disease stage to elucidate the role of hypoxia in the aetiology of this disease. This may be achieved by measuring the oxygen tension at the retinal surface of subjects with non-proliferative diabetic retinopathy who undergo retinal surgery for e.g. retinal detachment or macular oedema. A pre-operative assessment of areas of retinal vasoobliteration by fluorescein angiography may further help to identify areas of hypoperfusion which may consequently become the focus of oxygen measurements. A significant limitation of oxygen measurement using a probe during surgery is its invasive nature which almost excludes the possibility to study early changes in diabetic retinopathy for which surgery is not indicated. Assessing the retinal oxygen tension by non-invasive methods, e.g. by MRI (Trick and Berkowitz, 2005), may in the future provide an efficient tool to analyse retinal oxygenation

in early diabetic retinopathy and help to define the role of hypoxia in the development of diabetic retinopathy.

Although not yet proven, it is conceivable that tissue hypoxia due to capillary nonperfusion in early diabetic retinopathy plays a significant role in the development of diabetic retinopathy. Therefore, oxygen sensing mechanisms and adaptive response to hypoxia may have an important role in the development and progression of DR (Caprara and Grimm, 2011). However, additional information about the role of HIFs in the pathology of this disease, particularly in the development of the neovascular response, is needed.

Results in chapter 5 of this thesis have demonstrated that HIF1a and its downstream factor VEGF are significantly increased in the vitreous of diabetic subjects compared with non-diabetic subjects. These findings are in line with results of a recent study demonstrating that both VEGF and HIF1a are increased in the vitreous in PDR and appear to correlate with disease activity (Wang et al., 2009). Therefore it has been suggested that tissue hypoxia in DR induces HIF1a stabilisation in the inner retina which drives VEGF expression and progression of PDR (Stefansson, 2006). However, results in this thesis indicate that mechanisms other than hypoxia may contribute to HIF activation in PDR. It is widely established that inflammation and oxidative stress which are common features involved in the aetiology and progression of DR (Gardner et al., 2002) can induce HIFA stabilisation (Dehne and Brune, 2009; Yuan et al., 2008). It may therefore be possible that the described strong inflammatory microenvironment in PDR may contribute to HIF activation and the expression of

angiogenic and inflammatory cytokines in advanced PDR. Future studies will have to analyse HIF1a and its downstream factors in vitreous samples, or ideally in retinal biopsies of non-perfused areas, of subjects with non-proliferative diabetic retinopathy who undergo retinal surgery for e.g. retinal detachment or macular oedema. This may help to define the role of Hif signalling in early diabetic retinopathy and its contribution to the progression of the disease and may provide a rationale for developing treatment modalities targeting Hif1a.

Furthermore, the cell types that stabilise Hif1a protein in PDR remain to be identified. The finding that HIF1a protein levels are increased in the diabetic vitreous compared with the corresponding diabetic plasma supports the hypothesis that Hif1a is stabilised locally in retinal cells and is not derived from cells in the circulation. This is supported by immunohistochemical studies showing increased HIF1a and VEGF activity in surgically excised preretinal diabetic membranes compared with non-diabetic idiopathic epiretinal membranes (bu El-Asrar et al., 2007; Lim et al., 2010). Evidence from experimental models of diabetic retinopathy and ROP indicate that Mueller cells and astrocytes react to hypoxia by stabilisation of Hif1a and contribute to Vegf expression and disease progression (Ly et al., 2011; Mowat et al., 2010). The observed increase of HIF1a protein in the diabetic vitreous may therefore be explained by its release from hypoxic inner retinal cells that undergo apoptosis and lose integrity of their cell membranes (Barber et al., 2011). As Hif1a is normally degraded intracellularly by Vhl dependent proteasomal degradation, Hifa's derived from apoptotic inner retinal cells may accumulate in the diabetic

vitreous and be conserved. Additionally, cellular components are increased in the hypoxic diabetic vitreous (El-Ghrably et al., 2001; Esser et al., 1993) and may contribute to the observed increase of HIF1a protein in the vitreous. Recent studies have shown that lymphocytes, neutrophils and macrophages accumulate in areas of hypoxia and are attracted to the vitreous fluid in patients with PDR (Canton et al., 2004; Esser et al., 1993). These cells may not only contribute to mid vitreous hypoxia by consuming oxygen, but may also respond to mid vitreous hypoxia by stabilizing HIF1a and expressing VEGF which may contribute to the disease progression (El-Ghrably et al., 2001; Malecaze et al., 1994). This hypothesis is supported by experimental data presented in this thesis demonstrating the importance of Hif1a signalling in myeloid cell in retinal vascular disease in mice. Hif1a expressing myeloid cells were closely associated with preretinal neovascular tufts in the vitreous in the OIR mouse model. These cells may further invade sites of hypoxia in the mid vitreous and contribute to the cytokine milieu by Hif1a stabilisation. Future studies will have to elucidate the role of Hif signalling in vitreous macrophages in the development of retinal neovascularisation in PDR in more detail by determining their expression profile of Hif1a and Hif1a target genes, including *Vegf* and *Epo*. The identification of vitreous macrophages that induce pathological neovascularisation would open a wide new field of research and possibly lead to new targets for therapy. These pilot experiments may lead to further studies addressing potential therapeutical approaches that may include early surgical

vitrectomy or local molecular therapies modulating the phenotype of vitreous macrophages.

6.3 Outlook and therapeutic implications

6.3.1 Modifying adaptive responses to retinal hypoxia

Relieving retinal hypoxia has been suggested to be a potential treatment option to prevent the neovascular response and the associated complications in neovascular eye disease including PDR and vasoocclusive disease. Clinical management for patients with these conditions currently includes panretinal photocoagulation or in more severe cases vitrectomy. Both interventions can reduce the development of retinal neovascularisation by increasing the oxygen delivery to the hypoxic retina (Stefansson, 2006).

As these treatments are very invasive procedures and linked to potential adverse events, recent studies have suggested that molecular interference with the translation of hypoxia into molecular responses might become a promising treatment modality. As an alternative to improving retinal oxygen supply, the retina may be protected against the effects of local hypoxia by manipulating adaptive responses so as to inhibit harmful consequences and, potentially, to promote beneficial adaptive responses. Intraocular delivery of anti-VEGF antibodies can effectively control pathological neovascularisation and oedema. Clinical trials of VEGF inhibitors have demonstrated a significant benefit in age-

related macular degeneration (Martin et al., 2011) and considerable potential in diabetic retinopathy (Avery et al., 2006).

While these results demonstrate the enormous potential of local antiangiogenic therapy for retinal vascular disease there are considerable limitations. The short half-lives of Vegf antibodies in the eye necessitate multiple repeated intraocular injections that are not cost effective and cumulatively increase the risk of sight-threatening local adverse effects. Furthermore, anti VEGF therapy has been associated with systemic adverse effects including nonocular haemorrhage and stroke (Tolentino, 2011). While non-specific VEGF inhibitors target angiogenesis, they fail to address the underlying hypoxia and to consider appropriate endogenous compensatory responses including neuroprotective mechanisms and appropriate vascular remodelling. Future therapeutic strategies should therefore consider how to protect and promote appropriate retinal responses to hypoxia. An improved understanding of oxygen sensing and the HIF pathway may potentially help to identify new therapeutic modalities to promote neuroprotection and appropriate vascular remodelling, while preventing hypoxic/oxidative stress and pathological angiogenesis.

6.3.2 Manipulation of Hif signalling in retinal ischaemia

Due to its central role as a master-regulator of responses to hypoxia/ischaemia, HIF is a potentially relevant target for treating vascular disease in the eye. HIF signalling can be manipulated by RNA interference, by direct protein inhibition, or by modifying its degradation by PHD or VHL.

6.3.2.1 Activation of HIF signalling to improve neuroprotection

Activation of HIF signalling, for example by prolyl-hydroxlyase inhibition, offers a potential therapeutic option to improve ischaemic tolerance in retinal vascular disease by upregulating beneficial HIF dependent processes such as metabolic adaptation, neuroprotection and appropriate revascularisation (Sears et al., 2008). Systemic stabilisation of Hif by inhibition of prolyl-hydroxylases has been shown to protect against oxygen-induced retinopathy when applied in the early, non-proliferative phase of the OIR model (Sears et al., 2008). This finding is consistent with an observed protective effect of Epo supplementation on vascular and neuronal survival in the early phase of this model (Chen et al., 2009). Systemic stabilisation of HIF in the proliferative stage of the OIR model, however, exacerbates pathological neovascularisation (Sears et al., 2008). These findings indicate that activation of Hif signalling can have both beneficial and detrimental effects in neovascular eye disease depending on the stage of disease progression. Pharmaceutical activation of Hif may therefore only be suitable in early, non-proliferative retinal vascular disease, in order to improve ischaemic tolerance by upregulating beneficial HIF dependent processes such as metabolic adaptation and neuroprotection. This approach, however, has to be carefully evaluated as it may involve a significant risk of Hif1a mediated cell death as shown in this thesis.

6.3.2.2 Inhibition of HIF signalling to suppress neovascularisation

Based on its central role in regulating angiogenic factors such as VEGF, inactivation of HIF signalling has been proposed to be a promising treatment option to inhibit pathological angiogenesis in neovascular eye disease.

HIF inhibition may be achieved by RNA interference using small interfering RNA (*siRNA*) or small hairpin RNA (*shRNA*), by controlled activation of PHDs or by small molecule inhibitors that specifically target different HIF isoforms. *In vitro* studies have shown that HIFa RNA and protein expression can be effectively targeted using *siRNA* and *shRNA* (Mowat, 2009). Local inhibition of Hif by naked *siRNA in vivo,* however, has been shown to be difficult to achieve (Mowat, 2009) and may risk non-specific effects on extracellular receptors (Kleinman et al., 2008) and significant host immune effects (Alexopoulou et al., 2001). Viral or non-viral delivery of DNA constructs carrying HIF *siRNA* or *shRNA* to retinal cells may evade these problems and enable more efficient and prolonged delivery of interfering RNA. Furthermore, the use of cell specific promotors, such as the myeloid specific *lysM* promotor (Clausen et al., 1999), may be used to restrict *shRNA* and *siRNA* expression to the cells of interest. Furthermore, controlled activation of PHDs may be an efficient approach to reduce HIF levels. Viral or non-viral delivery of plasmids expressing different isoforms of PHD under a cell specific promotor may be used to reduce Hif activity in the cells of interest. As different isoforms of PHDs exhibit differential control over HIF1a and HIF2a (Appelhoff et al., 2004; Takeda et al., 2008), isoform specific activation of PHDs may allow to specifically induce degradation of HIF1a or HIF2a. Furthermore, small molecule inhibitors that specifically inhibit individual HIFa

isoforms are currently being investigated. Among these, YC-1, a small molecule inhibitor that specifically targets HIF1a, has been demonstrated to be a potent inhibitor and is currently undergoing clinical trials in cancer treatment (Yeo et al., 2003). Finally, antibody fragments known as intrabodies are sufficiently small to penetrate the cell membrane and the cytoplasmic space and have been shown to effectively inhibit HIF1a activity *in vitro* (Groot et al., 2008). Future studies may focus on the generation of intrabodies that are specific for HIF1a or HIF2a and assess their safety and efficacy in reducing HIF levels *in vivo*.

Systemic HIF inhibition – a viable treatment option?

Inhibition of Hif1a signalling by systemic administration of Digoxin has been shown to suppress the development of retinal and choroidal neovascularisation (Yoshida et al., 2010). Systemic administration of HIF inhibitors, however, provides a significant risk as HIF signalling pathways play a key role in multiple organs including the intestine, lung, heart, liver and the kidney (Stroka et al., 2001; Wiesener et al., 2003). In particular, in the context of human ROP, systemic inhibition of HIF during postnatal organ development may pose an even greater risk of side effects. Therefore, systemic HIF inactivation, particularly in new born infants, is unlikely to be a viable therapeutic option and should be avoided. To minimise the potential risk for systemic side effects of HIF inhibitors, future efforts should focus on intraocular administration of Hif inhibitors in proliferative neovascular eye disease.

Local inhibition of HIF in neovascular eye disease

Mounting evidence in the literature indicates that intraocular inhibition of Hif can reduce the development of retinal and choroidal neovascularisation. Intravitreal injection of anti-HIF1a *shRNA* has been shown to inhibit experimental CNV (Zhang et al., 2010). Similarly, local delivery of *siRNA* targeting Hif1a has been demonstrated to reduce Hif1a and Vegf protein levels by 90% and 65% respectively and suppress the neovascular response in the OIR mouse model (Xu et al., 2011). In line with these findings, intraocular injection of YC-1 has been reported to reduce pathological retinal neovascularisation in the retina of mice (DeNiro et al., 2010). Although these initial results are promising, great care needs to be taken to assess the feasibility, efficacy and safety of such therapy. Given the complexity of the HIF signalling system, in which multiple PHD and HIF isoforms regulate the transcription of numerous genes that intersect with multiple other signalling pathways, successful intervention is likely to depend on careful molecular targeting and on the timing of intervention. Whether targeting of PHDs can be sufficiently selective to avoid side effects, will require careful investigation. Target specificity may be improved by defining the cellular distribution of the PHD isoforms and their interaction with HIF isoforms in the retina, with a view to cell-specific targeting. Further animal studies will be needed to assess both safety and efficacy of HIF interference and to elucidate whether it may become a potential target for the treatment of proliferative retinopathies in man.

6.4 Conclusion

Insight into tissue oxygenation and oxygen sensing mechanisms in the retina will improve our understanding of the role and the consequences of hypoxia in retinal vascular diseases and is essential for the development of new treatments. Fluxes in oxygen tension represent perhaps the most important variable in physiology, and animal tissues have developed a number of adaptive mechanisms to cope both with low physiological oxygen levels and with hypoxic clinical conditions. This thesis has investigated the role of oxygen and oxygen sensing mechanism in health and disease. Among these mechanisms is the response mediated by the transcription factor HIF1a which has roles both in embryonic development and various retinal vascular disease pathologies. Even though the understanding of HIF1 oxygen sensing mechanisms has increased considerably in recent years, there are several areas where knowledge is lacking. For example, expression and activation mechanisms of HIF1, HIF2a, HIF3a and endogenous antagonists such as prolyl-hydroxylases in the different retinal cell types still need further study. Future investigations that aim to block HIF pathways might be of interest for treating retinal vascular disease, such as diabetic retinopathy or age-related macular degeneration in which an overwhelming, uncontrolled vascular response is associated with sight threatening vascular complications. The importance of HIF1a for neuroprotection, however, has to be carefully respected when considering HIF1a inhibition as an antiangiogenic therapy in the retina. Further understanding of the oxygen-sensing molecular mechanisms in the retina might

hopefully provide new tools to develop efficient treatments for various vascular retinopathies that are related to inflammation and hypoxia.

References

Reference List

Acampora,D., Mazan,S., Lallemand,Y., Avantaggiato,V., Maury,M., Simeone,A., and Brulet,P. (1995). Forebrain and midbrain regions are deleted in Otx2-/- mutants due to a defective anterior neuroectoderm specification during gastrulation. *Development* **121,** 3279-3290.

Adamis,A.P., Altaweel,M., Bressler,N.M., Cunningham,E.T., Jr., Davis,M.D., Goldbaum,M., Gonzales,C., Guyer,D.R., Barrett,K., and Patel,M. (2006). Changes in retinal neovascularization after pegaptanib (Macugen) therapy in diabetic individuals. *Ophthalmology* **113,** 23-28.

Agirbasli,M. (2005). Pivotal role of plasminogen-activator inhibitor 1 in vascular disease. *Int. J. Clin. Pract.* **59,** 102-106.

Ahmed,J., Braun,R.D., Dunn,R., Jr., and Linsenmeier,R.A. (1993). Oxygen distribution in the macaque retina. *Invest Ophthalmol Vis. Sci.* **34,** 516-521.

Aiello,L.P., Avery,R.L., Arrigg,P.G., Keyt,B.A., Jampel,H.D., Shah,S.T., Pasquale,L.R., Thieme,H., Iwamoto,M.A., Park,J.E. et al. (1994). Vascular endothelial growth factor in ocular fluid of patients with diabetic retinopathy and other retinal disorders. *N. Engl. J. Med.* **331,** 1480-1487.

Aizu,Y., Oyanagi,K., Hu,J., and Nakagawa,H. (2002). Degeneration of retinal neuronal processes and pigment epithelium in the early stage of the streptozotocin-diabetic rats. *Neuropathology.* **22,** 161-170.

Alder,V.A. and Cringle,S.J. (1985). The effect of the retinal circulation on vitreal oxygen tension. *Curr. Eye Res.* **4,** 121-129.

Alder,V.A. and Cringle,S.J. (1990). Vitreal and retinal oxygenation. *Graefes Arch. Clin. Exp. Ophthalmol* **228,** 151-157.

Alder,V.A., Cringle,S.J., and Constable,I.J. (1983). The retinal oxygen profile in cats. *Invest Ophthalmol Vis. Sci.* **24,** 30-36.

Alexopoulou,L., Holt,A.C., Medzhitov,R., and Flavell,R.A. (2001). Recognition of double-stranded RNA and activation of NF-kappaB by Toll-like receptor 3. *Nature* **413,** 732-738.

Ali,R.R. and Sowden,J.C. (2011). Regenerative medicine: DIY eye. *Nature* **472,** 42-43.

Alm,A. (1972). Effects of norepinephrine, angiotensin, dihydroergotamine, papaverine, isoproterenol, histamine, nicotinic acid, and xanthinol nicotinate on retinal oxygen tension in cats. *Acta Ophthalmol (Copenh)* **50,** 707-719.

Alm,A. and Bill,A. (1970). Blood flow and oxygen extraction in the cat uvea at normal and high intraocular pressures. *Acta Physiol Scand.* **80,** 19-28.

Alm,A. and Bill,A. (1972). The oxygen supply to the retina. II. Effects of high intraocular pressure and of increased arterial carbon dioxide tension on uveal and retinal blood flow in cats. A study with radioactively labelled microspheres including flow determinations in brain and some other tissues. *Acta Physiol Scand.* **84,** 306-319.

Ames,A., III (1992). Energy requirements of CNS cells as related to their function and to their vulnerability to ischemia: a commentary based on studies on retina. *Can. J. Physiol Pharmacol.* **70 Suppl,** S158-S164.

Ames,A., III, Li,Y.Y., Heher,E.C., and Kimble,C.R. (1992). Energy metabolism of rabbit retina as related to function: high cost of Na+ transport. *J. Neurosci.* **12,** 840-853.

An,W.G., Kanekal,M., Simon,M.C., Maltepe,E., Blagosklonny,M.V., and Neckers,L.M. (1998). Stabilization of wild-type p53 by hypoxia-inducible factor 1alpha. *Nature* **392,** 405-408.

Anand-Apte B and Hollyfield J K (2010). Developmental Anatomy of the Retinal and Choroidal Vasculature. *2010 Elsevier Ltd*.

ANDERSON,B., Jr. and SALTZMAN,H.A. (1964). RETINAL OXYGEN UTILIZATION MEASURED BY HYPERBARIC BLACKOUT. *Arch. Ophthalmol* **72,** 792-795.

Appelhoff,R.J., Tian,Y.M., Raval,R.R., Turley,H., Harris,A.L., Pugh,C.W., Ratcliffe,P.J., and Gleadle,J.M. (2004). Differential function of the prolyl hydroxylases PHD1, PHD2, and PHD3 in the regulation of hypoxia-inducible factor. *J. Biol. Chem.* **279,** 38458-38465.

Archer,D.B. and Gardiner,T.A. (1981a). Electron microscopic features of experimental choroidal neovascularization. *Am. J. Ophthalmol* **91,** 433-457.

Archer,D.B. and Gardiner,T.A. (1981b). Morphologic fluorescein angiographic, and light microscopic features of experimental choroidal neovascularization. *Am. J. Ophthalmol* **91,** 297-311.

Arden,G.B., Gunduz,M.K., Kurtenbach,A., Volker,M., Zrenner,E., Gunduz,S.B., Kamis,U., Ozturk,B.T., and Okudan,S. (2010). A preliminary trial to determine whether prevention of dark adaptation affects the course of early diabetic retinopathy. *Eye (Lond)* **24,** 1149-1155.

Arden,G.B., Wolf,J.E., and Tsang,Y. (1998). Does dark adaptation exacerbate diabetic retinopathy? Evidence and a linking hypothesis. *Vision Res.* **38,** 1723-1729.

Arjamaa,O., Nikinmaa,M., Salminen,A., and Kaarniranta,K. (2009). Regulatory role of HIF-1alpha in the pathogenesis of age-related macular degeneration (AMD). *Ageing Res. Rev.* **8,** 349-358.

Augustin,A.J., Keller,A., Koch,F., Jurklies,B., and Dick,B. (2001). [Effect of retinal coagulation status on oxidative metabolite and VEGF in 208 patients with proliferative diabetic retinopathy]. *Klin. Monbl. Augenheilkd.* **218,** 89-94.

Avery,R.L., Pearlman,J., Pieramici,D.J., Rabena,M.D., Castellarin,A.A., Nasir,M.A., Giust,M.J., Wendel,R., and Patel,A. (2006). Intravitreal bevacizumab (Avastin) in the treatment of proliferative diabetic retinopathy. *Ophthalmology* **113,** 1695-15.

Bacon,A.L. and Harris,A.L. (2004). Hypoxia-inducible factors and hypoxic cell death in tumour physiology. *Ann. Med.* **36,** 530-539.

Badr,G.A., Zhang,J.Z., Tang,J., Kern,T.S., and Ismail-Beigi,F. (1999). Glut1 and glut3 expression, but not capillary density, is increased by cobalt chloride in rat cerebrum and retina. *Brain Res. Mol. Brain Res.* **64,** 24-33.

Balaggan,K.S., Binley,K., Esapa,M., MacLaren,R.E., Iqball,S., Duran,Y., Pearson,R.A., Kan,O., Barker,S.E., Smith,A.J. et al. (2006). EIAV vector-mediated delivery of endostatin or angiostatin

inhibits angiogenesis and vascular hyperpermeability in experimental CNV. *Gene Ther.* **13,** 1153-1165.

Banerjee,S., Savant,V., Scott,R.A., Curnow,S.J., Wallace,G.R., and Murray,P.I. (2007). Multiplex bead analysis of vitreous humor of patients with vitreoretinal disorders. *Invest Ophthalmol. Vis. Sci.* **48,** 2203-2207.

Banin,E., Dorrell,M.I., Aguilar,E., Ritter,M.R., Aderman,C.M., Smith,A.C., Friedlander,J., and Friedlander,M. (2006). T2-TrpRS inhibits preretinal neovascularization and enhances physiological vascular regrowth in OIR as assessed by a new method of quantification. *Invest Ophthalmol Vis. Sci.* **47,** 2125-2134.

Barba,I., Garcia-Ramirez,M., Hernandez,C., Alonso,M.A., Masmiquel,L., Garcia-Dorado,D., and Simo,R. (2010). Metabolic fingerprints of proliferative diabetic retinopathy: an 1H-NMR-based metabonomic approach using vitreous humor. *Invest Ophthalmol Vis. Sci.* **51,** 4416-4421.

Barber,A.J., Gardner,T.W., and Abcouwer,S.F. (2011). The significance of vascular and neural apoptosis to the pathology of diabetic retinopathy. *Invest Ophthalmol Vis. Sci* **52,** 1156-1163.

Bardy,M. and Tsacopoulos,M. (1978). [Metabolic changes in the retina after experimental microembolism in the miniature pig (author's transl)]. *Klin. Monbl. Augenheilkd.* **172,** 451-460.

Barton,K.A., Shui,Y.B., Petrash,J.M., and Beebe,D.C. (2007). Comment on: the Stokes-Einstein equation and the physiological effects of vitreous surgery. *Acta Ophthalmol Scand.* **85,** 339-340.

Berger,A. (2000). Th1 and Th2 responses: what are they? *BMJ* **321,** 424.

Bergeron,M., Yu,A.Y., Solway,K.E., Semenza,G.L., and Sharp,F.R. (1999). Induction of hypoxia-inducible factor-1 (HIF-1) and its target genes following focal ischaemia in rat brain. *Eur. J. Neurosci.* **11,** 4159-4170.

Bharti,K., Nguyen,M.T., Skuntz,S., Bertuzzi,S., and Arnheiter,H. (2006). The other pigment cell: specification and development of the pigmented epithelium of the vertebrate eye. *Pigment Cell Res.* **19,** 380-394.

Biju,M.P., Neumann,A.K., Bensinger,S.J., Johnson,R.S., Turka,L.A., and Haase,V.H. (2004). Vhlh gene deletion induces Hif-1-mediated cell death in thymocytes. *Mol. Cell Biol.* **24,** 9038-9047.

Bill,A. and Sperber,G.O. (1990). Control of retinal and choroidal blood flow. *Eye (Lond)* **4 (Pt 2),** 319-325.

Bird,A.C. (1993). Choroidal neovascularisation in age-related macular disease. *Br. J. Ophthalmol* **77,** 614-615.

Blankenship,G.W. and Machemer,R. (1985). Long-term diabetic vitrectomy results. Report of 10 year follow-up. *Ophthalmology* **92,** 503-506.

Bosch,M.M., Merz,T.M., Barthelmes,D., Petrig,B.L., Truffer,F., Bloch,K.E., Turk,A., Maggiorini,M., Hess,T., Schoch,O.D. et al. (2009). New insights into ocular blood flow at very high altitudes. *J. Appl. Physiol* **106,** 454-460.

Boscia,F. (2010). Current approaches to the management of diabetic retinopathy and diabetic macular oedema. *Drugs* **70,** 2171-2200.

Boutin,A.T., Weidemann,A., Fu,Z., Mesropian,L., Gradin,K., Jamora,C., Wiesener,M., Eckardt,K.U., Koch,C.J., Ellies,L.G. et al. (2008). Epidermal sensing of oxygen is essential for systemic hypoxic response. *Cell* **133,** 223-234.

Bovolenta,P., Mallamaci,A., Briata,P., Corte,G., and Boncinelli,E. (1997). Implication of OTX2 in pigment epithelium determination and neural retina differentiation. *J. Neurosci.* **17,** 4243-4252.

Brahimi-Horn,M.C., Chiche,J., and Pouyssegur,J. (2007). Hypoxia signalling controls metabolic demand. *Curr. Opin. Cell Biol.* **19,** 223-229.

Braun,R.D. and Linsenmeier,R.A. (1995). Retinal oxygen tension and the electroretinogram during arterial occlusion in the cat. *Invest Ophthalmol Vis. Sci.* **36,** 523-541.

Brennan,L.A. and Kantorow,M. (2009). Mitochondrial function and redox control in the aging eye: role of MsrA and other repair systems in cataract and macular degenerations. *Exp. Eye Res.* **88,** 195-203.

Brinchmann-Hansen,O., Myhre,K., and Sandvik,L. (1989). Retinal vessel responses to exercise and hypoxia before and after high altitude acclimatisation. *Eye (Lond)* **3 (Pt 6),** 768-776.

Brown,D.M., Kaiser,P.K., Michels,M., Soubrane,G., Heier,J.S., Kim,R.Y., Sy,J.P., and Schneider,S. (2006). Ranibizumab versus verteporfin for neovascular age-related macular degeneration. *N Engl J Med.* **355,** 1432-1444.

Brown,D.M., Michels,M., Kaiser,P.K., Heier,J.S., Sy,J.P., and Ianchulev,T. (2009). Ranibizumab versus verteporfin photodynamic therapy for neovascular age-related macular degeneration: Two-year results of the ANCHOR study. *Ophthalmology.* **116,** 57-65.

Bruick,R.K. (2000). Expression of the gene encoding the proapoptotic Nip3 protein is induced by hypoxia. *Proc. Natl. Acad. Sci U. S. A* **97,** 9082-9087.

Bruick,R.K. and McKnight,S.L. (2001). A conserved family of prolyl-4-hydroxylases that modify HIF. *Science* **294,** 1337-1340.

Brunelle,J.K., Bell,E.L., Quesada,N.M., Vercauteren,K., Tiranti,V., Zeviani,M., Scarpulla,R.C., and Chandel,N.S. (2005). Oxygen sensing requires mitochondrial ROS but not oxidative phosphorylation. *Cell Metab* **1,** 409-414.

bu El-Asrar,A.M., Missotten,L., and Geboes,K. (2007). Expression of hypoxia-inducible factor-1alpha and the protein products of its target genes in diabetic fibrovascular epiretinal membranes. *Br. J. Ophthalmol.* **91,** 822-826.

bu El-Asrar,A.M., Struyf,S., Kangave,D., Geboes,K., and Van,D.J. (2006). Chemokines in proliferative diabetic retinopathy and proliferative vitreoretinopathy. *Eur. Cytokine Netw.* **17,** 155-165.

Bumsted,K.M. and Barnstable,C.J. (2000). Dorsal retinal pigment epithelium differentiates as neural retina in the microphthalmia (mi/mi) mouse. *Invest Ophthalmol Vis. Sci.* **41,** 903-908.

Burke,B., Tang,N., Corke,K.P., Tazzyman,D., Ameri,K., Wells,M., and Lewis,C.E. (2002). Expression of HIF-1alpha by human macrophages: implications for the use of macrophages in hypoxia-regulated cancer gene therapy. *J. Pathol.* **196,** 204-212.

Caicedo,A., Espinosa-Heidmann,D.G., Pina,Y., Hernandez,E.P., and Cousins,S.W. (2005). Blood-derived macrophages infiltrate the retina and activate Muller glial cells under experimental choroidal neovascularization. *Exp. Eye Res.* **81,** 38-47.

Canton,A., Martinez-Caceres,E.M., Hernandez,C., Espejo,C., Garcia-Arumi,J., and Simo,R. (2004). CD4-CD8 and CD28 expression in T cells infiltrating the vitreous fluid in patients with proliferative diabetic retinopathy: a flow cytometric analysis. *Arch. Ophthalmol* **122,** 743-749.

Caprara,C. and Grimm,C. (2011). From oxygen to erythropoietin: Relevance of hypoxia for retinal development, health and disease. *Prog. Retin. Eye Res.*

Caprara,C. and Grimm,C. (2012). From oxygen to erythropoietin: relevance of hypoxia for retinal development, health and disease. *Prog. Retin. Eye Res.* **31,** 89-119.

Caprara,C., Thiersch,M., Lange,C., Joly,S., Samardzija,M., and Grimm,C. (2011). HIF1A is essential for the development of the intermediate plexus of the retinal vasculature. *Invest Ophthalmol Vis. Sci.*

Carmeliet,P. (2000). Mechanisms of angiogenesis and arteriogenesis. *Nat. Med.* **6,** 389-395.

Carmeliet,P., Dor,Y., Herbert,J.M., Fukumura,D., Brusselmans,K., Dewerchin,M., Neeman,M., Bono,F., Abramovitch,R., Maxwell,P. et al. (1998). Role of HIF-1alpha in hypoxia-mediated apoptosis, cell proliferation and tumour angiogenesis. *Nature* **394,** 485-490.

Chan-Ling,T., Gock,B., and Stone,J. (1995). The effect of oxygen on vasoformative cell division. Evidence that 'physiological hypoxia' is the stimulus for normal retinal vasculogenesis. *Invest Ophthalmol. Vis. Sci.* **36,** 1201-1214.

Chan-Ling,T., McLeod,D.S., Hughes,S., Baxter,L., Chu,Y., Hasegawa,T., and Lutty,G.A. (2004). Astrocyte-endothelial cell relationships during human retinal vascular development. *Invest Ophthalmol Vis. Sci* **45,** 2020-2032.

Chang,T.S., Bressler,N.M., Fine,J.T., Dolan,C.M., Ward,J., and Klesert,T.R. (2007). Improved vision-related function after ranibizumab treatment of neovascular age-related macular degeneration: results of a randomized clinical trial. *Arch Ophthalmol.* **125,** 1460-1469.

Chang,Y.H., Chen,P.L., Tai,M.C., Chen,C.H., Lu,D.W., and Chen,J.T. (2006). Hyperbaric oxygen therapy ameliorates the blood-retinal barrier breakdown in diabetic retinopathy. *Clin. Experiment. Ophthalmol* **34,** 584-589.

Chavez,J.C., Baranova,O., Lin,J., and Pichiule,P. (2006). The transcriptional activator hypoxia inducible factor 2 (HIF-2/EPAS-1) regulates the oxygen-dependent expression of erythropoietin in cortical astrocytes. *J Neurosci.* **26,** 9471-9481.

Cheli,Y., Ohanna,M., Ballotti,R., and Bertolotto,C. (2010). Fifteen-year quest for microphthalmia-associated transcription factor target genes. *Pigment Cell Melanoma Res.* **23,** 27-40.

Chen,J., Connor,K.M., Aderman,C.M., Willett,K.L., Aspegren,O.P., and Smith,L.E. (2009). Suppression of retinal neovascularization by erythropoietin siRNA in a mouse model of proliferative retinopathy. *Invest Ophthalmol Vis. Sci.* **50,** 1329-1335.

Chen,J., Stahl,A., Hellstrom,A., and Smith,L.E. (2011). Current update on retinopathy of prematurity: screening and treatment. *Curr. Opin. Pediatr.* **23,** 173-178.

Chen,S.J., Cheng,C.Y., Lee,A.F., Lee,F.L., Chou,J.C., Hsu,W.M., and Liu,J.H. (2001). Pulsatile ocular blood flow in asymmetric exudative age related macular degeneration. *Br. J. Ophthalmol* **85,** 1411-1415.

Chiang,A. and Regillo,C.D. (2011). Preferred therapies for neovascular age-related macular degeneration. *Curr. Opin. Ophthalmol* **22,** 199-204.

Chilton,P.M., Rezzoug,F., Fugier-Vivier,I., Weeter,L.A., Xu,H., Huang,Y., Ray,M.B., and Ildstad,S.T. (2004). Flt3-ligand treatment prevents diabetes in NOD mice. *Diabetes* **53,** 1995-2002.

Chun,D.W., Heier,J.S., Topping,T.M., Duker,J.S., and Bankert,J.M. (2006). A pilot study of multiple intravitreal injections of ranibizumab in patients with center-involving clinically significant diabetic macular edema. *Ophthalmology* **113,** 1706-1712.

Chun,Y.S., Hyun,J.Y., Kwak,Y.G., Kim,I.S., Kim,C.H., Choi,E., Kim,M.S., and Park,J.W. (2003). Hypoxic activation of the atrial natriuretic peptide gene promoter through direct and indirect actions of hypoxia-inducible factor-1. *Biochem J.* **370,** 149-157.

Ciulla,T.A., Harris,A., and Martin,B.J. (2001). Ocular perfusion and age-related macular degeneration. *Acta Ophthalmol Scand.* **79,** 108-115.

Clausen,B.E., Burkhardt,C., Reith,W., Renkawitz,R., and Forster,I. (1999). Conditional gene targeting in macrophages and granulocytes using LysMcre mice. *Transgenic Res.* **8,** 265-277.

Cobleigh,M.A., Langmuir,V.K., Sledge,G.W., Miller,K.D., Haney,L., Novotny,W.F., Reimann,J.D., and Vassel,A. (2003). A phase I/II dose-escalation trial of bevacizumab in previously treated metastatic breast cancer. *Semin. Oncol.* **30,** 117-124.

Cohen,M.P., Hud,E., Shea,E., and Shearman,C.W. (2008). Vitreous fluid of db/db mice exhibits alterations in angiogenic and metabolic factors consistent with early diabetic retinopathy. *Ophthalmic Res.* **40,** 5-9.

Collins,T.J. (2007). ImageJ for microscopy. *Biotechniques* **43,** 25-30.

Combadiere,C., Feumi,C., Raoul,W., Keller,N., Rodero,M., Pezard,A., Lavalette,S., Houssier,M., Jonet,L., Picard,E. et al. (2007). CX3CR1-dependent subretinal microglia cell accumulation is associated with cardinal features of age-related macular degeneration. *J. Clin. Invest* **117,** 2920-2928.

Congdon,N.G., Friedman,D.S., and Lietman,T. (2003). Important causes of visual impairment in the world today. *JAMA* **290,** 2057-2060.

Cormack,T.G., Grant,B., Macdonald,M.J., Steel,J., and Campbell,I.W. (2001). Incidence of blindness due to diabetic eye disease in Fife 1990-9. *Br. J. Ophthalmol.* **85,** 354-356.

Cormier-Regard,S., Nguyen,S.V., and Claycomb,W.C. (1998). Adrenomedullin gene expression is developmentally regulated and induced by hypoxia in rat ventricular cardiac myocytes. *J. Biol. Chem.* **273,** 17787-17792.

Cramer,T., Yamanishi,Y., Clausen,B.E., Forster,I., Pawlinski,R., Mackman,N., Haase,V.H., Jaenisch,R., Corr,M., Nizet,V. et al. (2003). HIF-1alpha is essential for myeloid cell-mediated inflammation. *Cell* **112,** 645-657.

Crosson,L.A., Kroes,R.A., Moskal,J.R., and Linsenmeier,R.A. (2009). Gene expression patterns in hypoxic and post-hypoxic adult rat retina with special reference to the NMDA receptor and its interactome. *Mol. Vis.* **15,** 296-311.

Cunningham,E.T., Jr., Adamis,A.P., Altaweel,M., Aiello,L.P., Bressler,N.M., D'Amico,D.J., Goldbaum,M., Guyer,D.R., Katz,B., Patel,M. et al. (2005). A phase II randomized double-masked trial of pegaptanib, an anti-vascular endothelial growth factor aptamer, for diabetic macular edema. *Ophthalmology* **112,** 1747-1757.

Czyzyk-Krzeska,M.F. and Meller,J. (2004). von Hippel-Lindau tumor suppressor: not only HIF's executioner. *Trends Mol. Med.* **10,** 146-149.

D'Amore,P.A. (1994). Mechanisms of retinal and choroidal neovascularization. *Invest Ophthalmol. Vis. Sci.* **35,** 3974-3979.

Dalgard,C.L., Lu,H., Mohyeldin,A., and Verma,A. (2004). Endogenous 2-oxoacids differentially regulate expression of oxygen sensors. *Biochem J.* **380,** 419-424.

Daut,J., Maier-Rudolph,W., von,B.N., Mehrke,G., Gunther,K., and Goedel-Meinen,L. (1990). Hypoxic dilation of coronary arteries is mediated by ATP-sensitive potassium channels. *Science* **247,** 1341-1344.

de Gooyer,T.E., Stevenson,K.A., Humphries,P., Simpson,D.A., Gardiner,T.A., and Stitt,A.W. (2006). Retinopathy is reduced during experimental diabetes in a mouse model of outer retinal degeneration. *Invest Ophthalmol Vis. Sci.* **47,** 5561-5568.

de,V.C., Escobedo,J.A., Ueno,H., Houck,K., Ferrara,N., and Williams,L.T. (1992). The fms-like tyrosine kinase, a receptor for vascular endothelial growth factor. *Science* **255,** 989-991.

Dehne,N. and Brune,B. (2009). HIF-1 in the inflammatory microenvironment. *Exp. Cell Res.* **315,** 1791-1797.

DeNiro,M., Al-Halafi,A., Al-Mohanna,F.H., Alsmadi,O., and Al-Mohanna,F.A. (2010). Pleiotropic effects of YC-1 selectively inhibit pathological retinal neovascularization and promote physiological revascularization in a mouse model of oxygen-induced retinopathy. *Mol. Pharmacol.* **77,** 348-367.

Denko,N.C. (2008). Hypoxia, HIF1 and glucose metabolism in the solid tumour. *Nat. Rev. Cancer*.

Ding,K., Scortegagna,M., Seaman,R., Birch,D.G., and Garcia,J.A. (2005). Retinal disease in mice lacking hypoxia-inducible transcription factor-2alpha. *Invest Ophthalmol Vis. Sci* **46,** 1010-1016.

Ding,X., Patel,M., and Chan,C.C. (2009). Molecular pathology of age-related macular degeneration. *Prog. Retin. Eye Res.* **28,** 1-18.

Doberstein,C., Fineman,I., Hovda,D.A., Martin,N.A., Keenly,L., and Becker,D.P. (1994). Metabolic alterations accompany ionic disturbances and cellular swelling during a hypoxic insult to the retina: an in vitro study. *Acta Neurochir. Suppl (Wien.)* **60,** 41-44.

Dobi,E.T., Puliafito,C.A., and Destro,M. (1989). A new model of experimental choroidal neovascularization in the rat. *Arch. Ophthalmol* **107,** 264-269.

Donati,G., Kapetanios,A., Dubois-Dauphin,M., and Pournaras,C.J. (2008). Caspase-related apoptosis in chronic ischaemic microangiopathy following experimental vein occlusion in mini-pigs. *Acta Ophthalmol* **86,** 302-306.

Dorrell,M., Uusitalo-Jarvinen,H., Aguilar,E., and Friedlander,M. (2007). Ocular neovascularization: basic mechanisms and therapeutic advances. *Surv. Ophthalmol.* **52 Suppl 1:S3-19.,** S3-19.

Drasdo,N., Chiti,Z., Owens,D.R., and North,R.V. (2002). Effect of darkness on inner retinal hypoxia in diabetes. *Lancet* **359,** 2251-2253.

Drexler,H.G. and Quentmeier,H. (2004). FLT3: receptor and ligand. *Growth Factors* **22,** 71-73.

Dunaief,J.L., Dentchev,T., Ying,G.S., and Milam,A.H. (2002). The role of apoptosis in age-related macular degeneration. *Arch. Ophthalmol.* **120,** 1435-1442.

Ebert,B.L., Firth,J.D., and Ratcliffe,P.J. (1995). Hypoxia and mitochondrial inhibitors regulate expression of glucose transporter-1 via distinct Cis-acting sequences. *J. Biol. Chem.* **270,** 29083-29089.

Eckhart,A.D., Yang,N., Xin,X., and Faber,J.E. (1997). Characterization of the alpha1B-adrenergic receptor gene promoter region and hypoxia regulatory elements in vascular smooth muscle. *Proc. Natl. Acad. Sci U. S. A* **94,** 9487-9492.

El-Ghrably,I.A., Dua,H.S., Orr,G.M., Fischer,D., and Tighe,P.J. (2001). Intravitreal invading cells contribute to vitreal cytokine milieu in proliferative vitreoretinopathy. *Br. J. Ophthalmol* **85,** 461-470.

Espinosa-Heidmann,D.G., Suner,I.J., Hernandez,E.P., Monroy,D., Csaky,K.G., and Cousins,S.W. (2003). Macrophage depletion diminishes lesion size and severity in experimental choroidal neovascularization. *Invest Ophthalmol Vis. Sci* **44,** 3586-3592.

Esser,P., Heimann,K., and Wiedemann,P. (1993). Macrophages in proliferative vitreoretinopathy and proliferative diabetic retinopathy: differentiation of subpopulations. *Br. J. Ophthalmol.* **77,** 731-733.

Fandrey,J. (2004). Oxygen-dependent and tissue-specific regulation of erythropoietin gene expression. *Am. J. Physiol Regul. Integr. Comp Physiol* **286,** R977-R988.

Feeney,S.A., Simpson,D.A., Gardiner,T.A., Boyle,C., Jamison,P., and Stitt,A.W. (2003). Role of vascular endothelial growth factor and placental growth factors during retinal vascular development and hyaloid regression. *Invest Ophthalmol Vis. Sci.* **44,** 839-847.

Feldser,D., Agani,F., Iyer,N.V., Pak,B., Ferreira,G., and Semenza,G.L. (1999). Reciprocal positive regulation of hypoxia-inducible factor 1alpha and insulin-like growth factor 2. *Cancer Res.* **59,** 3915-3918.

Fine,S.L., Martin,D.F., and Kirkpatrick,P. (2005). Pegaptanib sodium. *Nat Rev Drug Discov.* **4,** 187-188.

Forooghian,F., Razavi,R., and Timms,L. (2007). Hypoxia-inducible factor expression in human RPE cells. *Br. J. Ophthalmol* **91,** 1406-1410.

Forsythe,J.A., Jiang,B.H., Iyer,N.V., Agani,F., Leung,S.W., Koos,R.D., and Semenza,G.L. (1996). Activation of vascular endothelial growth factor gene transcription by hypoxia-inducible factor 1. *Mol. Cell Biol.* **16,** 4604-4613.

Francois,J., De Laey,J.J., Cambie,E., Hanssens,M., and Victoria-Troncoso,V. (1975). Neovascularization after argon laser photocoagulation of macular lesions. *Am. J. Ophthalmol* **79,** 206-210.

Frayser,R., Gray,G., and Houston,C. (1974). Control of the retinal circulation at altitude. *J. Appl. Physiol* **93,** 302-304.

Friedman,E., Krupsky,S., Lane,A.M., Oak,S.S., Friedman,E.S., Egan,K., and Gragoudas,E.S. (1995). Ocular blood flow velocity in age-related macular degeneration. *Ophthalmology* **102,** 640-646.

Fruttiger,M. (2007). Development of the retinal vasculature. *Angiogenesis.* **10,** 77-88.

Fuchshofer,R., Yu,A.L., Teng,H.H., Strauss,R., Kampik,A., and Welge-Lussen,U. (2009). Hypoxia/reoxygenation induces CTGF and PAI-1 in cultured human retinal pigment epithelium cells. *Exp. Eye Res.* **88,** 889-899.

Fuhrmann,S. (2010). Eye morphogenesis and patterning of the optic vesicle. *Curr. Top. Dev. Biol.* **93,** 61-84.

Fukuda,R., Zhang,H., Kim,J.W., Shimoda,L., Dang,C.V., and Semenza,G.L. (2007). HIF-1 regulates cytochrome oxidase subunits to optimize efficiency of respiration in hypoxic cells. *Cell* **129,** 111-122.

Fulton,A.B., Hansen,R.M., Moskowitz,A., and Akula,J.D. (2009). The neurovascular retina in retinopathy of prematurity. *Prog. Retin. Eye Res.* **28,** 452-482.

Funatsu,H., Wilson,C.A., Berkowitz,B.A., and Sonkin,P.L. (1997). A comparative study of the effects of argon and diode laser photocoagulation on retinal oxygenation. *Graefes Arch. Clin. Exp. Ophthalmol* **235,** 168-175.

Garcia-Ramirez,M., Hernandez,C., and Simo,R. (2008). Expression of erythropoietin and its receptor in the human retina: a comparative study of diabetic and nondiabetic subjects. *Diabetes Care* **31,** 1189-1194.

Gardiner,T.A., Gibson,D.S., de Gooyer,T.E., de,l.C., V, McDonald,D.M., and Stitt,A.W. (2005). Inhibition of tumor necrosis factor-alpha improves physiological angiogenesis and reduces pathological neovascularization in ischemic retinopathy. *Am. J. Pathol.* **166,** 637-644.

Gardner,T.W., Antonetti,D.A., Barber,A.J., LaNoue,K.F., and Levison,S.W. (2002). Diabetic retinopathy: more than meets the eye. *Surv. Ophthalmol* **47 Suppl 2,** S253-S262.

Gerber,H.P., Condorelli,F., Park,J., and Ferrara,N. (1997). Differential transcriptional regulation of the two vascular endothelial growth factor receptor genes. Flt-1, but not Flk-1/KDR, is up-regulated by hypoxia. *J. Biol. Chem.* **272,** 23659-23667.

Gerber,H.P., Hillan,K.J., Ryan,A.M., Kowalski,J., Keller,G.A., Rangell,L., Wright,B.D., Radtke,F., Aguet,M., and Ferrara,N. (1999). VEGF is required for growth and survival in neonatal mice. *Development* **126,** 1149-1159.

Gilbert,C. (2008). Retinopathy of prematurity: a global perspective of the epidemics, population of babies at risk and implications for control. *Early Hum. Dev.* **84,** 77-82.

Gnarra,J.R., Ward,J.M., Porter,F.D., Wagner,J.R., Devor,D.E., Grinberg,A., Emmert-Buck,M.R., Westphal,H., Klausner,R.D., and Linehan,W.M. (1997). Defective placental vasculogenesis causes embryonic lethality in VHL-deficient mice. *Proc. Natl. Acad. Sci. U. S. A* **94,** 9102-9107.

Gonzales,C.R. (2005). Enhanced efficacy associated with early treatment of neovascular age-related macular degeneration with pegaptanib sodium: an exploratory analysis. *Retina.* **25,** 815-827.

Gottfredsdottir,M.S., Stefansson,E., Jonasson,F., and Gislason,I. (1993). Retinal vasoconstriction after laser treatment for diabetic macular edema. *Am. J. Ophthalmol* **115,** 64-67.

Grabmaier,K., Weijert MC,A.d., Verhaegh,G.W., Schalken,J.A., and Oosterwijk,E. (2004). Strict regulation of CAIX(G250/MN) by HIF-1alpha in clear cell renal cell carcinoma. *Oncogene* **23,** 5624-5631.

Graven,K.K., Yu,Q., Pan,D., Roncarati,J.S., and Farber,H.W. (1999). Identification of an oxygen responsive enhancer element in the glyceraldehyde-3-phosphate dehydrogenase gene. *Biochim. Biophys. Acta* **1447,** 208-218.

Grimm,C., Hermann,D.M., Bogdanova,A., Hotop,S., Kilic,U., Wenzel,A., Kilic,E., and Gassmann,M. (2005). Neuroprotection by hypoxic preconditioning: HIF-1 and erythropoietin protect from retinal degeneration. *Semin. Cell Dev. Biol.* **16,** 531-538.

Grimm,C., Wenzel,A., Groszer,M., Mayser,H., Seeliger,M., Samardzija,M., Bauer,C., Gassmann,M., and Reme,C.E. (2002). HIF-1-induced erythropoietin in the hypoxic retina protects against light-induced retinal degeneration. *Nat. Med.* **8,** 718-724.

Groer,M.W. and Shelton,M.M. (2009). Exercise is associated with elevated proinflammatory cytokines in human milk. *J. Obstet. Gynecol. Neonatal Nurs.* **38,** 35-41.

Groot,A.J., Gort,E.H., van der Wall,E., van Diest,P.J., and Vooijs,M. (2008). Conditional inactivation of HIF-1 using intrabodies. *Cell Oncol.* **30,** 397-409.

Grosfeld,A., Andre,J., Hauguel-De,M.S., Berra,E., Pouyssegur,J., and Guerre-Millo,M. (2002). Hypoxia-inducible factor 1 transactivates the human leptin gene promoter. *J. Biol. Chem.* **277,** 42953-42957.

Grunwald,J.E., Hariprasad,S.M., DuPont,J., Maguire,M.G., Fine,S.L., Brucker,A.J., Maguire,A.M., and Ho,A.C. (1998). Foveolar choroidal blood flow in age-related macular degeneration. *Invest Ophthalmol Vis. Sci.* **39,** 385-390.

Grunwald,J.E., Metelitsina,T.I., DuPont,J.C., Ying,G.S., and Maguire,M.G. (2005). Reduced foveolar choroidal blood flow in eyes with increasing AMD severity. *Invest Ophthalmol Vis. Sci.* **46,** 1033-1038.

Gunaratnam,L., Morley,M., Franovic,A., de,P.N., Mekhail,K., Parolin,D.A., Nakamura,E., Lorimer,I.A., and Lee,S. (2003). Hypoxia inducible factor activates the transforming growth factor-alpha/epidermal growth factor receptor growth stimulatory pathway in VHL(-/-) renal cell carcinoma cells. *J. Biol. Chem.* **278,** 44966-44974.

Guzy,R.D., Hoyos,B., Robin,E., Chen,H., Liu,L., Mansfield,K.D., Simon,M.C., Hammerling,U., and Schumacker,P.T. (2005). Mitochondrial complex III is required for hypoxia-induced ROS production and cellular oxygen sensing. *Cell Metab* **1,** 401-408.

Haase,V.H., Glickman,J.N., Socolovsky,M., and Jaenisch,R. (2001). Vascular tumors in livers with targeted inactivation of the von Hippel-Lindau tumor suppressor. *Proc. Natl. Acad. Sci. U. S. A* **98,** 1583-1588.

Hackenbeck,T., Huber,R., Schietke,R., Knaup,K.X., Monti,J., Wu,X., Klanke,B., Frey,B., Gaipl,U., Wullich,B. et al. (2011). The GTPase RAB20 is a HIF target with mitochondrial localization mediating apoptosis in hypoxia. *Biochim. Biophys. Acta* **1813,** 1-13.

Hagen,T., Taylor,C.T., Lam,F., and Moncada,S. (2003). Redistribution of intracellular oxygen in hypoxia by nitric oxide: effect on HIF1alpha. *Science* **302,** 1975-1978.

Halterman,M.W., Miller,C.C., and Federoff,H.J. (1999). Hypoxia-inducible factor-1alpha mediates hypoxia-induced delayed neuronal death that involves p53. *J. Neurosci.* **19,** 6818-6824.

Hammer,M., Vilser,W., Riemer,T., Mandecka,A., Schweitzer,D., Kuhn,U., Dawczynski,J., Liemt,F., and Strobel,J. (2009). Diabetic patients with retinopathy show increased retinal venous oxygen saturation. *Graefes Arch. Clin. Exp. Ophthalmol* **247,** 1025-1030.

Hammes,H.P., Lin,J., Bretzel,R.G., Brownlee,M., and Breier,G. (1998). Upregulation of the vascular endothelial growth factor/vascular endothelial growth factor receptor system in experimental background diabetic retinopathy of the rat. *Diabetes.* **47,** 401-406.

Hardarson,S.H. and Stefansson,E. (2010). Oxygen saturation in central retinal vein occlusion. *Am. J. Ophthalmol* **150,** 871-875.

Harmey,J.H., Dimitriadis,E., Kay,E., Redmond,H.P., and Bouchier-Hayes,D. (1998). Regulation of macrophage production of vascular endothelial growth factor (VEGF) by hypoxia and transforming growth factor beta-1. *Ann. Surg. Oncol.* **5,** 271-278.

Harris,A., Arend,O., Danis,R.P., Evans,D., Wolf,S., and Martin,B.J. (1996). Hyperoxia improves contrast sensitivity in early diabetic retinopathy. *Br. J. Ophthalmol* **80,** 209-213.

Harris,A., Chung,H.S., Ciulla,T.A., and Kagemann,L. (1999). Progress in measurement of ocular blood flow and relevance to our understanding of glaucoma and age-related macular degeneration. *Prog. Retin. Eye Res.* **18,** 669-687.

Harris,A., Ciulla,T.A., Chung,H.S., and Martin,B. (1998). Regulation of retinal and optic nerve blood flow. *Arch. Ophthalmol* **116,** 1491-1495.

Haugh,L.M., Linsenmeier,R.A., and Goldstick,T.K. (1990). Mathematical models of the spatial distribution of retinal oxygen tension and consumption, including changes upon illumination. *Ann. Biomed. Eng* **18,** 19-36.

Hayreh,S.S. (2005). Prevalent misconceptions about acute retinal vascular occlusive disorders. *Prog. Retin. Eye Res.* **24,** 493-519.

Hayreh,S.S. and Podhajsky,P. (1982). Ocular neovascularization with retinal vascular occlusion. II. Occurrence in central and branch retinal artery occlusion. *Arch. Ophthalmol* **100,** 1585-1596.

Hayreh,S.S., Rojas,P., Podhajsky,P., Montague,P., and Woolson,R.F. (1983). Ocular neovascularization with retinal vascular occlusion-III. Incidence of ocular neovascularization with retinal vein occlusion. *Ophthalmology* **90,** 488-506.

Hellstrom,A., Perruzzi,C., Ju,M., Engstrom,E., Hard,A.L., Liu,J.L., bertsson-Wikland,K., Carlsson,B., Niklasson,A., Sjodell,L. et al. (2001). Low IGF-I suppresses VEGF-survival signaling in retinal endothelial cells: direct correlation with clinical retinopathy of prematurity. *Proc. Natl. Acad. Sci U. S. A* **98,** 5804-5808.

Hever,A.M., Williamson,K.A., and van,H., V (2006). Developmental malformations of the eye: the role of PAX6, SOX2 and OTX2. *Clin. Genet.* **69,** 459-470.

Hickam,J. and Frayser,R. (1965). A photographic method for measuring the mean retinal circulation time using fluorescein. *Invest Ophthalmol* **4,** 876-884.

Hickam,J., Sieker,H., and Frayser,R. (1959). Studies of retinal circulation and A-V oxygen difference in man. *Trans. Am. Clin. Climatol. Assoc.* 34-44.

HICKAM,J.B. and FRAYSER,R. (1965). Aphotographic method for measuring the mean retinal circulation time using fluorescein. *Invest Ophthalmol* **4,** 876-884.

Higgins,D.F., Biju,M.P., Akai,Y., Wutz,A., Johnson,R.S., and Haase,V.H. (2004). Hypoxic induction of Ctgf is directly mediated by Hif-1. *Am. J. Physiol Renal Physiol* **287,** F1223-F1232.

Hill,R.E., Favor,J., Hogan,B.L., Ton,C.C., Saunders,G.F., Hanson,I.M., Prosser,J., Jordan,T., Hastie,N.D., and van,H., V (1991). Mouse small eye results from mutations in a paired-like homeobox-containing gene. *Nature* **354,** 522-525.

Hoch,R.V. and Soriano,P. (2003). Roles of PDGF in animal development. *Development* **130,** 4769-4784.

Hoerle,S., Poestgens,H., Schmidt,J., and Kroll,P. (2002). Effect of pars plana vitrectomy for proliferative diabetic vitreoretinopathy on preexisting diabetic maculopathy. *Graefes Arch. Clin. Exp. Ophthalmol* **240,** 197-201.

Holekamp,N.M., Shui,Y.B., and Beebe,D. (2006). Lower intraocular oxygen tension in diabetic patients: possible contribution to decreased incidence of nuclear sclerotic cataract. *Am. J. Ophthalmol* **141,** 1027-1032.

Holekamp,N.M., Shui,Y.B., and Beebe,D.C. (2005). Vitrectomy surgery increases oxygen exposure to the lens: a possible mechanism for nuclear cataract formation. *Am. J. Ophthalmol* **139,** 302-310.

Holmes,D.I. and Zachary,I. (2005). The vascular endothelial growth factor (VEGF) family: angiogenic factors in health and disease. *Genome Biol.* **6,** 209.

Holtkamp,G.M., De Vos,A.F., Peek,R., and Kijlsta,A. (1999). Analysis of the secretion pattern of monocyte chemotactic protein-1 (MCP-1) and transforming growth factor-beta 2 (TGF-beta2) by human retinal pigment epithelial cells. *Clin. Exp. Immunol.* **118,** 35-40.

Hong,K.H., Ryu,J., and Han,K.H. (2005). Monocyte chemoattractant protein-1-induced angiogenesis is mediated by vascular endothelial growth factor-A. *Blood* **105,** 1405-1407.

Hu,C.J., Wang,L.Y., Chodosh,L.A., Keith,B., and Simon,M.C. (2003). Differential roles of hypoxia-inducible factor 1alpha (HIF-1alpha) and HIF-2alpha in hypoxic gene regulation. *Mol. Cell Biol.* **23,** 9361-9374.

Hu,J., Discher,D.J., Bishopric,N.H., and Webster,K.A. (1998). Hypoxia regulates expression of the endothelin-1 gene through a proximal hypoxia-inducible factor-1 binding site on the antisense strand. *Biochem Biophys. Res. Commun.* **245,** 894-899.

Hu,L.H., Yang,J.H., Zhang,D.T., Zhang,S., Wang,L., Cai,P.C., Zheng,J.F., and Huang,J.S. (2007). The TKTL1 gene influences total transketolase activity and cell proliferation in human colon cancer LoVo cells. *Anticancer Drugs* **18,** 427-433.

Hughes,J.M., Groot,A.J., van der,G.P., Sersansie,R., Vooijs,M., van Diest,P.J., Van Noorden,C.J., Schlingemann,R.O., and Klaassen,I. (2010). Active HIF-1 in the normal human retina. *J. Histochem. Cytochem.* **58,** 247-254.

Hughes,S. and Chang-Ling,T. (2000). Roles of endothelial cell migration and apoptosis in vascular remodeling during development of the central nervous system. *Microcirculation.* **7,** 317-333.

Hurwitz,H., Fehrenbacher,L., Novotny,W., Cartwright,T., Hainsworth,J., Heim,W., Berlin,J., Baron,A., Griffing,S., Holmgren,E. et al. (2004). Bevacizumab plus irinotecan, fluorouracil, and leucovorin for metastatic colorectal cancer. *N Engl J Med.* **350,** 2335-2342.

Iacovelli,J., Zhao,C., Wolkow,N., Veldman,P., Gollomp,K., Ojha,P., Lukinova,N., King,A., Feiner,L., Esumi,N. et al. (2011). Generation of Cre transgenic mice with postnatal RPE-specific ocular expression. *Invest Ophthalmol. Vis. Sci.* **52,** 1378-1383.

ICROP (2005). The International Classification of Retinopathy of Prematurity revisited. *Arch. Ophthalmol* **123,** 991-999.

Imtiyaz,H.Z., Williams,E.P., Hickey,M.M., Patel,S.A., Durham,A.C., Yuan,L.J., Hammond,R., Gimotty,P.A., Keith,B., and Simon,M.C. (2010). Hypoxia-inducible factor 2alpha regulates macrophage function in mouse models of acute and tumor inflammation. *J. Clin. Invest* **120,** 2699-2714.

Inomata,Y., Hirata,A., Takahashi,E., Kawaji,T., Fukushima,M., and Tanihara,H. (2004). Elevated erythropoietin in vitreous with ischemic retinal diseases. *Neuroreport* **15,** 877-879.

Inoue,Y., Yanagi,Y., Matsuura,K., Takahashi,H., Tamaki,Y., and Araie,M. (2007). Expression of hypoxia-inducible factor 1alpha and 2alpha in choroidal neovascular membranes associated with age-related macular degeneration. *Br. J. Ophthalmol* **91,** 1720-1721.

Ishida,S., Yamashiro,K., Usui,T., Kaji,Y., Ogura,Y., Hida,T., Honda,Y., Oguchi,Y., and Adamis,A.P. (2003). Leukocytes mediate retinal vascular remodeling during development and vaso-obliteration in disease. *Nat. Med.* **9,** 781-788.

Itaya,M., Sakurai,E., Nozaki,M., Yamada,K., Yamasaki,S., Asai,K., and Ogura,Y. (2007). Upregulation of VEGF in murine retina via monocyte recruitment after retinal scatter laser photocoagulation. *Invest Ophthalmol Vis. Sci* **48,** 5677-5683.

Ito,M. and Yoshioka,M. (1999). Regression of the hyaloid vessels and pupillary membrane of the mouse. *Anat. Embryol. (Berl)* **200,** 403-411.

Ivan,M., Kondo,K., Yang,H., Kim,W., Valiando,J., Ohh,M., Salic,A., Asara,J.M., Lane,W.S., and Kaelin,W.G., Jr. (2001). HIFalpha targeted for VHL-mediated destruction by proline hydroxylation: implications for O2 sensing. *Science* **292,** 464-468.

Iwai,K., Yamanaka,K., Kamura,T., Minato,N., Conaway,R.C., Conaway,J.W., Klausner,R.D., and Pause,A. (1999). Identification of the von Hippel-lindau tumor-suppressor protein as part of an active E3 ubiquitin ligase complex. *Proc. Natl. Acad. Sci. U. S. A* **96,** 12436-12441.

Iyer,N.V., Kotch,L.E., Agani,F., Leung,S.W., Laughner,E., Wenger,R.H., Gassmann,M., Gearhart,J.D., Lawler,A.M., Yu,A.Y. et al. (1998). Cellular and developmental control of O2 homeostasis by hypoxia-inducible factor 1 alpha. *Genes Dev.* **12,** 149-162.

J J Kanski (1999). Clinical Ophthalmology. 4th edition. *Oxford: Butterworth-Heinemann*.

Jeong,J.W., Bae,M.K., Ahn,M.Y., Kim,S.H., Sohn,T.K., Bae,M.H., Yoo,M.A., Song,E.J., Lee,K.J., and Kim,K.W. (2002). Regulation and destabilization of HIF-1alpha by ARD1-mediated acetylation. *Cell* **111,** 709-720.

Jiang,Y., Liang,X., Li,X., Tao,Y., and Wang,K. (2008). Analysis of the clinical efficacy of intravitreal bevacizumab in the treatment of iris neovascularization caused by proliferative diabetic retinopathy. *Acta Ophthalmol.*

Jordan,T., Hanson,I., Zaletayev,D., Hodgson,S., Prosser,J., Seawright,A., Hastie,N., and van,H., V (1992). The human PAX6 gene is mutated in two patients with aniridia. *Nat. Genet.* **1,** 328-332.

Junk,A.K., Mammis,A., Savitz,S.I., Singh,M., Roth,S., Malhotra,S., Rosenbaum,P.S., Cerami,A., Brines,M., and Rosenbaum,D.M. (2002). Erythropoietin administration protects retinal neurons from acute ischemia-reperfusion injury. *Proc. Natl. Acad. Sci. U. S. A* **99,** 10659-10664.

Kador,P.F., Takahashi,Y., Wyman,M., and Ferris,F., III (1995). Diabeteslike proliferative retinal changes in galactose-fed dogs. *Arch Ophthalmol* **113,** 352-354.

Kaelin,W.G., Jr. (2005). ROS: really involved in oxygen sensing. *Cell Metab* **1,** 357-358.

Kaluz,S., Kaluzova,M., Chrastina,A., Olive,P.L., Pastorekova,S., Pastorek,J., Lerman,M.I., and Stanbridge,E.J. (2002). Lowered oxygen tension induces expression of the hypoxia marker MN/carbonic anhydrase IX in the absence of hypoxia-inducible factor 1 alpha stabilization: a role for phosphatidylinositol 3'-kinase. *Cancer Res.* **62,** 4469-4477.

Kataoka,K., Nishiguchi,K.M., Kaneko,H., van,R.N., Kachi,S., and Terasaki,H. (2011). The roles of vitreal macrophages and circulating leukocytes in retinal neovascularization. *Invest Ophthalmol Vis. Sci* **52,** 1431-1438.

Kaur,C., Sivakumar,V., and Foulds,W.S. (2006). Early response of neurons and glial cells to hypoxia in the retina. *Invest Ophthalmol Vis. Sci.* **47,** 1126-1141.

Kaur,C., Sivakumar,V., Foulds,W.S., Luu,C.D., and Ling,E.A. (2009). Cellular and vascular changes in the retina of neonatal rats after an acute exposure to hypoxia. *Invest Ophthalmol Vis. Sci* **50,** 5364-5374.

Kawagishi,T., Nishizawa,Y., Emoto,M., Konishi,T., Maekawa,K., Hagiwara,S., Okuno,Y., Inada,H., Isshiki,G., and Morii,H. (1995). Impaired retinal artery blood flow in IDDM patients before clinical manifestations of diabetic retinopathy. *Diabetes Care* **18,** 1544-1549.

Kelly,B.D., Hackett,S.F., Hirota,K., Oshima,Y., Cai,Z., Berg-Dixon,S., Rowan,A., Yan,Z., Campochiaro,P.A., and Semenza,G.L. (2003). Cell type-specific regulation of angiogenic growth factor gene expression and induction of angiogenesis in nonischemic tissue by a constitutively active form of hypoxia-inducible factor 1. *Circ. Res.* **93,** 1074-1081.

Kergoat,H., Marinier,J.A., and Lovasik,J.V. (2005). Effects of transient mild systemic hypoxia on the pulsatile choroidal blood flow in healthy young human adults. *Curr. Eye Res.* **30,** 465-470.

Kern,T.S. and Engerman,R.L. (1996). A mouse model of diabetic retinopathy. *Arch Ophthalmol.* **114,** 986-990.

Kibel,A., Iliopoulos,O., DeCaprio,J.A., and Kaelin,W.G., Jr. (1995). Binding of the von Hippel-Lindau tumor suppressor protein to Elongin B and C. *Science* **269,** 1444-1446.

Kietzmann,T., Roth,U., and Jungermann,K. (1999). Induction of the plasminogen activator inhibitor-1 gene expression by mild hypoxia via a hypoxia response element binding the hypoxia-inducible factor-1 in rat hepatocytes. *Blood* **94,** 4177-4185.

Kim,J.W., Tchernyshyov,I., Semenza,G.L., and Dang,C.V. (2006). HIF-1-mediated expression of pyruvate dehydrogenase kinase: a metabolic switch required for cellular adaptation to hypoxia. *Cell Metab* **3,** 177-185.

Kimble,E.A., Svoboda,R.A., and Ostroy,S.E. (1980). Oxygen consumption and ATP changes of the vertebrate photoreceptor. *Exp. Eye Res.* **31,** 271-288.

Kimura,H., Sakamoto,T., Hinton,D.R., Spee,C., Ogura,Y., Tabata,Y., Ikada,Y., and Ryan,S.J. (1995). A new model of subretinal neovascularization in the rabbit. *Invest Ophthalmol Vis. Sci.* **36,** 2110-2119.

Kinnunen,K., Petrovski,G., Moe,M.C., Berta,A., and Kaarniranta,K. (2011). Molecular mechanisms of retinal pigment epithelium damage and development of age-related macular degeneration. *Acta Ophthalmol*.

Kitamura,K., Kangawa,K., Kawamoto,M., Ichiki,Y., Nakamura,S., Matsuo,H., and Eto,T. (1993). Adrenomedullin: a novel hypotensive peptide isolated from human pheochromocytoma. *Biochem Biophys. Res. Commun.* **192,** 553-560.

Kleinman,M.E., Yamada,K., Takeda,A., Chandrasekaran,V., Nozaki,M., Baffi,J.Z., Albuquerque,R.J., Yamasaki,S., Itaya,M., Pan,Y. et al. (2008). Sequence- and target-independent angiogenesis suppression by siRNA via TLR3. *Nature* **452,** 591-597.

Kloss,C.U., Kreutzberg,G.W., and Raivich,G. (1997). Proliferation of ramified microglia on an astrocyte monolayer: characterization of stimulatory and inhibitory cytokines. *J. Neurosci. Res.* **49,** 248-254.

Knighton,D.R., Hunt,T.K., Scheuenstuhl,H., Halliday,B.J., Werb,Z., and Banda,M.J. (1983). Oxygen tension regulates the expression of angiogenesis factor by macrophages. *Science* **221,** 1283-1285.

Konno,S., Feke,G.T., Yoshida,A., Fujio,N., Goger,D.G., and Buzney,S.M. (1996). Retinal blood flow changes in type I diabetes. A long-term follow-up study. *Invest Ophthalmol Vis. Sci.* **37,** 1140-1148.

Kotch,L.E., Iyer,N.V., Laughner,E., and Semenza,G.L. (1999). Defective vascularization of HIF-1alpha-null embryos is not associated with VEGF deficiency but with mesenchymal cell death. *Dev. Biol.* **209,** 254-267.

Kramer,M., Dadon,S., Hasanreisoglu,M., Monselise,Y., Avraham,B.R., Feldman,A., Eldar,I., Weinberger,D., and Goldenberg-Cohen,N. (2009). Proinflammatory cytokines in a mouse model of central retinal artery occlusion. *Mol. Vis.* **15,** 885-894.

Kuiper,E.J., Van Nieuwenhoven,F.A., de,S., van Meurs,J.C., Tanck,M.W., Oliver,N., Klaassen,I., Van Noorden,C.J., Goldschmeding,R., and Schlingemann,R.O. (2008). The angio-fibrotic switch of VEGF and CTGF in proliferative diabetic retinopathy. *PLoS. ONE.* **3,** e2675.

Kurihara,T., Kubota,Y., Ozawa,Y., Takubo,K., Noda,K., Simon,M.C., Johnson,R.S., Suematsu,M., Tsubota,K., Ishida,S. et al. (2010). von Hippel-Lindau protein regulates transition from the fetal to the adult circulatory system in retina. *Development* **137,** 1563-1571.

Kurihara,T., Westenskow,P.D., Krohne,T.U., Aguilar,E., Johnson,R.S., and Friedlander,M. (2011). Astrocyte pVHL and HIF-alpha isoforms are required for embryonic-to-adult vascular transition in the eye. *J. Cell Biol.* **195,** 689-701.

Laatikainen,L. (1976). Vascular changes after central retinal vein occlusion. *Trans. Ophthalmol Soc. U. K.* **96,** 190-192.

Lahiri,S., Roy,A., Baby,S.M., Hoshi,T., Semenza,G.L., and Prabhakar,N.R. (2006). Oxygen sensing in the body. *Prog. Biophys. Mol. Biol.* **91,** 249-286.

Lai,C.M., Dunlop,S.A., May,L.A., Gorbatov,M., Brankov,M., Shen,W.Y., Binz,N., Lai,Y.K., Graham,C.E., Barry,C.J. et al. (2005). Generation of transgenic mice with mild and severe retinal neovascularisation. *Br. J. Ophthalmol* **89,** 911-916.

Lange,C., Caprara,C., Tanimoto,N., Beck,S., Huber,G., Samardzija,M., Seeliger,M., and Grimm,C. (2011). Retina-specific activation of a sustained hypoxia-like response leads to severe retinal degeneration and loss of vision. *Neurobiol. Dis.* **41,** 119-130.

Lange,C., Ehlken,C., Martin,G., Konzok,K., Moscoso Del,P.J., Hansen,L.L., and Agostini,H.T. (2007). Intravitreal injection of the heparin analog 5-amino-2-naphthalenesulfonate reduces retinal neovascularization in mice. *Exp. Eye Res.* **85,** 323-327.

Le,Y.Z., Zheng,W., Rao,P.C., Zheng,L., Anderson,R.E., Esumi,N., Zack,D.J., and Zhu,M. (2008). Inducible expression of cre recombinase in the retinal pigmented epithelium. *Invest Ophthalmol. Vis. Sci.* **49,** 1248-1253.

Lee,P.J., Jiang,B.H., Chin,B.Y., Iyer,N.V., Alam,J., Semenza,G.L., and Choi,A.M. (1997). Hypoxia-inducible factor-1 mediates transcriptional activation of the heme oxygenase-1 gene in response to hypoxia. *J. Biol. Chem.* **272,** 5375-5381.

Lee,S.C., Liu,W., Brosnan,C.F., and Dickson,D.W. (1994). GM-CSF promotes proliferation of human fetal and adult microglia in primary cultures. *Glia* **12,** 309-318.

Lei,B., Yao,G., Zhang,K., Hofeldt,K.J., and Chang,B. (2006). Study of rod- and cone-driven oscillatory potentials in mice. *Invest Ophthalmol Vis. Sci* **47,** 2732-2738.

Lewis,J.S., Landers,R.J., Underwood,J.C., Harris,A.L., and Lewis,C.E. (2000). Expression of vascular endothelial growth factor by macrophages is up-regulated in poorly vascularized areas of breast carcinomas. *J. Pathol.* **192,** 150-158.

Li,C., Xu,Y., Jiang,D., Hong,W., Guo,X., Wang,P., and Li,W. (2006). [The expression of HIF-1 in the early diabetic NOD mice]. *Yan. Ke. Xue. Bao.* **22,** 107-111.

Li,F., Chong,Z.Z., and Maiese,K. (2004). Erythropoietin on a tightrope: balancing neuronal and vascular protection between intrinsic and extrinsic pathways. *Neurosignals.* **13,** 265-289.

Liang,Y.G., Jorgensen,A.G., Kaestel,C.G., Wiencke,A.K., Lui,G.M., la Cour,M.H., Ropke,C.H., and Nissen,M.H. (2000). Bcl-2, Bax, and c-Fos expression correlates to RPE cell apoptosis induced by UV-light and daunorubicin. *Curr. Eye Res.* **20,** 25-34.

Lim,J.I., Spee,C., and Hinton,D.R. (2010). A comparison of hypoxia-inducible factor-alpha in surgically excised neovascular membranes of patients with diabetes compared with idiopathic epiretinal membranes in nondiabetic patients. *Retina* **30,** 1472-1478.

Lin,M., Chen,Y., Jin,J., Hu,Y., Zhou,K.K., Zhu,M., Le,Y.Z., Ge,J., Johnson,R.S., and Ma,J.X. (2011). Ischaemia-induced retinal neovascularisation and diabetic retinopathy in mice with conditional knockout of hypoxia-inducible factor-1 in retinal Muller cells. *Diabetologia*.

Linsenmeier,R.A. (1986). Effects of light and darkness on oxygen distribution and consumption in the cat retina. *J. Gen. Physiol* **88,** 521-542.

Linsenmeier,R.A. and Braun,R.D. (1992). Oxygen distribution and consumption in the cat retina during normoxia and hypoxemia. *J. Gen. Physiol* **99,** 177-197.

Linsenmeier,R.A., Braun,R.D., McRipley,M.A., Padnick,L.B., Ahmed,J., Hatchell,D.L., McLeod,D.S., and Lutty,G.A. (1998). Retinal hypoxia in long-term diabetic cats. *Invest Ophthalmol Vis. Sci.* **39,** 1647-1657.

Linsenmeier,R.A., Goldstick,T.K., Blum,R.S., and Enroth-Cugell,C. (1981). Estimation of retinal oxygen transients from measurements made in the vitreous humor. *Exp. Eye Res.* **32,** 369-379.

Liu,J., Jha,P., Lyzogubov,V.V., Tytarenko,R.G., Bora,N.S., and Bora,P.S. (2011). Relationship between complement membrane attack complex, chemokine (C-C motif) ligand 2 (CCL2) and vascular endothelial growth factor in mouse model of laser-induced choroidal neovascularization. *J. Biol. Chem.* **286,** 20991-21001.

Liu,X.L., Li,Y.J., Liu,Y.Z., and Ge,J. (2006). [Effects of human retinal glial cells under hypoxic conditions on circulating endothelial progenitor cells]. *Zhonghua Yan. Ke. Za Zhi.* **42,** 1089-1094.

Lofstedt,T., Fredlund,E., Holmquist-Mengelbier,L., Pietras,A., Ovenberger,M., Poellinger,L., and Pahlman,S. (2007). Hypoxia inducible factor-2alpha in cancer. *Cell Cycle* **6,** 919-926.

Longbottom,R., Fruttiger,M., Douglas,R.H., Martinez-Barbera,J.P., Greenwood,J., and Moss,S.E. (2009). Genetic ablation of retinal pigment epithelial cells reveals the adaptive response of the epithelium and impact on photoreceptors. *Proc. Natl. Acad. Sci. U. S. A* **106,** 18728-18733.

Loonstra,A., Vooijs,M., Beverloo,H.B., Allak,B.A., van,D.E., Kanaar,R., Berns,A., and Jonkers,J. (2001). Growth inhibition and DNA damage induced by Cre recombinase in mammalian cells. *Proc. Natl. Acad. Sci U. S. A* **98,** 9209-9214.

Lopez-Barneo,J., Ortega-Saenz,P., Molina,A., Franco-Obregon,A., Urena,J., and Castellano,A. (1997). Oxygen sensing by ion channels. *Kidney Int.* **51,** 454-461.

Lowe,J., Araujo,J., Yang,J., Reich,M., Oldendorp,A., Shiu,V., Quarmby,V., Lowman,H., Lien,S., Gaudreault,J. et al. (2007). Ranibizumab inhibits multiple forms of biologically active vascular endothelial growth factor in vitro and in vivo. *Exp. Eye Res.* **85,** 425-430.

Lu,H., Forbes,R.A., and Verma,A. (2002). Hypoxia-inducible factor 1 activation by aerobic glycolysis implicates the Warburg effect in carcinogenesis. *J. Biol. Chem.* **277,** 23111-23115.

Luhmann,U.F., Robbie,S., Munro,P.M., Barker,S.E., Duran,Y., Luong,V., Fitzke,F.W., Bainbridge,J.W., Ali,R.R., and MacLaren,R.E. (2009). The drusenlike phenotype in aging Ccl2-knockout mice is caused by an accelerated accumulation of swollen autofluorescent subretinal macrophages. *Invest Ophthalmol Vis. Sci.* **50,** 5934-5943.

Lutjen-Drecoll,E. (2006). Choroidal innervation in primate eyes. *Exp. Eye Res.* **82,** 357-361.

Lutty,G., Grunwald,J., Majji,A.B., Uyama,M., and Yoneya,S. (1999). Changes in choriocapillaris and retinal pigment epithelium in age-related macular degeneration. *Mol. Vis.* **5,** 35.

Ly,A., Yee,P., Vessey,K.A., Phipps,J.A., Jobling,A.I., and Fletcher,E.L. (2011). Early Inner Retinal Astrocyte Dysfunction during Diabetes and Development of Hypoxia, Retinal Stress, and Neuronal Functional Loss. *Invest Ophthalmol Vis. Sci* **52,** 9316-9326.

Maeda,N. and Tano,Y. (1996). Intraocular oxygen tension in eyes with proliferative diabetic retinopathy with and without vitreous. *Graefes Arch. Clin. Exp. Ophthalmol* **234 Suppl 1,** S66-S69.

Maeda,N., Tano,Y., Ikeda,T., Imai,T., Hamano,H., and Manabe,R. (1992). [Vitreous oxygen tension of proliferative diabetic retinopathy]. *Nippon Ganka Gakkai Zasshi* **96,** 511-515.

Maenhaut,N., Boussery,K., Delaey,C., and Van,d., V (2009). Adenosine enhances the relaxing influence of retinal tissue. *Exp. Eye Res.* **88,** 71-78.

Mahon,P.C., Hirota,K., and Semenza,G.L. (2001). FIH-1: a novel protein that interacts with HIF-1alpha and VHL to mediate repression of HIF-1 transcriptional activity. *Genes Dev.* **15,** 2675-2686.

Maier,R., Weger,M., Haller-Schober,E.M., El-Shabrawi,Y., Theisl,A., Barth,A., Aigner,R., and Haas,A. (2006). Application of multiplex cytometric bead array technology for the measurement of angiogenic factors in the vitreous. *Mol. Vis.* **12,** 1143-1147.

Maier,R., Weger,M., Haller-Schober,E.M., El-Shabrawi,Y., Wedrich,A., Theisl,A., Aigner,R., Barth,A., and Haas,A. (2008). Multiplex bead analysis of vitreous and serum concentrations of inflammatory and proangiogenic factors in diabetic patients. *Mol. Vis.* **14,** 637-643.

Makino,Y., Cao,R., Svensson,K., Bertilsson,G., Asman,M., Tanaka,H., Cao,Y., Berkenstam,A., and Poellinger,L. (2001). Inhibitory PAS domain protein is a negative regulator of hypoxia-inducible gene expression. *Nature* **414,** 550-554.

Malecaze,F., Clamens,S., Simorre-Pinatel,V., Mathis,A., Chollet,P., Favard,C., Bayard,F., and Plouet,J. (1994). Detection of vascular endothelial growth factor messenger RNA and vascular endothelial growth factor-like activity in proliferative diabetic retinopathy. *Arch. Ophthalmol.* **112,** 1476-1482.

Mantovani,A., Sozzani,S., Locati,M., Allavena,P., and Sica,A. (2002). Macrophage polarization: tumor-associated macrophages as a paradigm for polarized M2 mononuclear phagocytes. *Trends Immunol.* **23,** 549-555.

Marneros,A.G., Fan,J., Yokoyama,Y., Gerber,H.P., Ferrara,N., Crouch,R.K., and Olsen,B.R. (2005). Vascular endothelial growth factor expression in the retinal pigment epithelium is essential for choriocapillaris development and visual function. *Am. J. Pathol.* **167,** 1451-1459.

Marshall,J. (1987). The ageing retina: physiology or pathology. *Eye (Lond)* **1 (Pt 2),** 282-295.

Martin,D.F., Maguire,M.G., Ying,G.S., Grunwald,J.E., Fine,S.L., and Jaffe,G.J. (2011). Ranibizumab and bevacizumab for neovascular age-related macular degeneration. *N. Engl. J. Med.* **364,** 1897-1908.

Martinez-Morales,J.R., Signore,M., Acampora,D., Simeone,A., and Bovolenta,P. (2001). Otx genes are required for tissue specification in the developing eye. *Development* **128,** 2019-2030.

Marumo,T., Schini-Kerth,V.B., and Busse,R. (1999). Vascular endothelial growth factor activates nuclear factor-kappaB and induces monocyte chemoattractant protein-1 in bovine retinal endothelial cells. *Diabetes* **48,** 1131-1137.

Maslim,J., Valter,K., Egensperger,R., Hollander,H., and Stone,J. (1997). Tissue oxygen during a critical developmental period controls the death and survival of photoreceptors. *Invest Ophthalmol Vis. Sci* **38,** 1667-1677.

Mason,J.O., III, Yunker,J.J., Vail,R., and McGwin,G., Jr. (2008). INTRAVITREAL BEVACIZUMAB (AVASTIN) PREVENTION OF PANRETINAL PHOTOCOAGULATION-INDUCED COMPLICATIONS IN PATIENTS WITH SEVERE PROLIFERATIVE DIABETIC RETINOPATHY. *Retina*.

Matsunaga,N., Chikaraishi,Y., Izuta,H., Ogata,N., Shimazawa,M., Matsumura,M., and Hara,H. (2008). Role of soluble vascular endothelial growth factor receptor-1 in the vitreous in proliferative diabetic retinopathy. *Ophthalmology* **115,** 1916-1922.

Matsuo,I., Kuratani,S., Kimura,C., Takeda,N., and Aizawa,S. (1995). Mouse Otx2 functions in the formation and patterning of rostral head. *Genes Dev.* **9,** 2646-2658.

Maxwell,P.H., Wiesener,M.S., Chang,G.W., Clifford,S.C., Vaux,E.C., Cockman,M.E., Wykoff,C.C., Pugh,C.W., Maher,E.R., and Ratcliffe,P.J. (1999). The tumour suppressor protein VHL targets hypoxia-inducible factors for oxygen-dependent proteolysis. *Nature* **399,** 271-275.

Mazure,N.M., Chauvet,C., Bois-Joyeux,B., Bernard,M.A., Nacer-Cherif,H., and Danan,J.L. (2002). Repression of alpha-fetoprotein gene expression under hypoxic conditions in human hepatoma cells: characterization of a negative hypoxia response element that mediates opposite effects of hypoxia inducible factor-1 and c-Myc. *Cancer Res.* **62,** 1158-1165.

McGill,G.G., Horstmann,M., Widlund,H.R., Du,J., Motyckova,G., Nishimura,E.K., Lin,Y.L., Ramaswamy,S., Avery,W., Ding,H.F. et al. (2002). Bcl2 regulation by the melanocyte master regulator Mitf modulates lineage survival and melanoma cell viability. *Cell* **109,** 707-718.

McLeod,D.S., Grebe,R., Bhutto,I., Merges,C., Baba,T., and Lutty,G.A. (2009). Relationship between RPE and choriocapillaris in age-related macular degeneration. *Invest Ophthalmol Vis. Sci.* **50,** 4982-4991.

Medrano,C.J. and Fox,D.A. (1995). Oxygen consumption in the rat outer and inner retina: light- and pharmacologically-induced inhibition. *Exp. Eye Res.* **61,** 273-284.

Melillo,G., Musso,T., Sica,A., Taylor,L.S., Cox,G.W., and Varesio,L. (1995). A hypoxia-responsive element mediates a novel pathway of activation of the inducible nitric oxide synthase promoter. *J. Exp. Med.* **182,** 1683-1693.

Mervin,K. and Stone,J. (2002). Regulation by oxygen of photoreceptor death in the developing and adult C57BL/6J mouse. *Exp. Eye Res.* **75,** 715-722.

Metelitsina,T.I., Grunwald,J.E., DuPont,J.C., Ying,G.S., Brucker,A.J., and Dunaief,J.L. (2008). Foveolar choroidal circulation and choroidal neovascularization in age-related macular degeneration. *Invest Ophthalmol Vis. Sci.* **49,** 358-363.

Metzen,E., Zhou,J., Jelkmann,W., Fandrey,J., and Brune,B. (2003). Nitric oxide impairs normoxic degradation of HIF-1alpha by inhibition of prolyl hydroxylases. *Mol. Biol. Cell* **14,** 3470-3481.

Michaelson,I.C., HERZ,N., LEWKOWITZ,E., and KERTESZ,D. (1954). Effects of increased oxygen on the development of the retinal vessels; an experimental study. *Br. J. Ophthalmol* **38,** 577-587.

Michels,S., Rosenfeld,P.J., Puliafito,C.A., Marcus,E.N., and Venkatraman,A.S. (2005). Systemic bevacizumab (Avastin) therapy for neovascular age-related macular degeneration twelve-week results of an uncontrolled open-label clinical study. *Ophthalmology.* **112,** 1035-1047.

Millauer,B., Wizigmann-Voos,S., Schnurch,H., Martinez,R., Moller,N.P., Risau,W., and Ullrich,A. (1993). High affinity VEGF binding and developmental expression suggest Flk-1 as a major regulator of vasculogenesis and angiogenesis. *Cell* **72,** 835-846.

Miller,J.W., Adamis,A.P., Shima,D.T., D'Amore,P.A., Moulton,R.S., O'Reilly,M.S., Folkman,J., Dvorak,H.F., Brown,L.F., Berse,B. et al. (1994). Vascular endothelial growth factor/vascular permeability factor is temporally and spatially correlated with ocular angiogenesis in a primate model. *Am. J. Pathol.* **145,** 574-584.

Millhorn,D.E., Raymond,R., Conforti,L., Zhu,W., Beitner-Johnson,D., Filisko,T., Genter,M.B., Kobayashi,S., and Peng,M. (1997). Regulation of gene expression for tyrosine hydroxylase in oxygen sensitive cells by hypoxia. *Kidney Int.* **51,** 527-535.

Minchenko,O., Opentanova,I., and Caro,J. (2003). Hypoxic regulation of the 6-phosphofructo-2-kinase/fructose-2,6-bisphosphatase gene family (PFKFB-1-4) expression in vivo. *FEBS Lett.* **554,** 264-270.

Mintz-Hittner,H.A., Kennedy,K.A., and Chuang,A.Z. (2011). Efficacy of intravitreal bevacizumab for stage 3+ retinopathy of prematurity. *N. Engl. J. Med.* **364,** 603-615.

Mitchell,P., Smith,W., Attebo,K., and Wang,J.J. (1995). Prevalence of age-related maculopathy in Australia. The Blue Mountains Eye Study. *Ophthalmology* **102,** 1450-1460.

Moradian,S., Ahmadieh,H., Malihi,M., Soheilian,M., Dehghan,M.H., and Azarmina,M. (2008). Intravitreal bevacizumab in active progressive proliferative diabetic retinopathy. *Graefes Arch. Clin. Exp. Ophthalmol.* **246,** 1699-1705.

Mordes,J.P. and Rossini,A.A. (1981). Animal models of diabetes. *Am. J. Med.* **70,** 353-360.

Mori,M., Metzger,D., Garnier,J.M., Chambon,P., and Mark,M. (2002). Site-specific somatic mutagenesis in the retinal pigment epithelium. *Invest Ophthalmol Vis. Sci.* **43,** 1384-1388.

Morita,M., Ohneda,O., Yamashita,T., Takahashi,S., Suzuki,N., Nakajima,O., Kawauchi,S., Ema,M., Shibahara,S., Udono,T. et al. (2003). HLF/HIF-2alpha is a key factor in retinopathy of prematurity in association with erythropoietin. *EMBO J* **22,** 1134-1146.

Mowat,F.M. Hypoxia-induced retinal disease: pathogenic mechanisms and therapeutic strategies. 5-9-2009. University College of London.
Ref Type: Thesis/Dissertation

Mowat,F.M., Luhmann,U.F., Smith,A.J., Lange,C., Duran,Y., Harten,S., Shukla,D., Maxwell,P.H., Ali,R.R., and Bainbridge,J.W. (2010). HIF-1alpha and HIF-2alpha are differentially activated in distinct cell populations in retinal ischaemia. *PLoS. ONE.* **5,** e11103.

Mukhopadhyay,C.K., Mazumder,B., and Fox,P.L. (2000). Role of hypoxia-inducible factor-1 in transcriptional activation of ceruloplasmin by iron deficiency. *J. Biol. Chem.* **275,** 21048-21054.

Murdoch,C., Muthana,M., Coffelt,S.B., and Lewis,C.E. (2008). The role of myeloid cells in the promotion of tumour angiogenesis. *Nat. Rev. Cancer* **8,** 618-631.

Murugeswari,P., Shukla,D., Rajendran,A., Kim,R., Namperumalsamy,P., and Muthukkaruppan,V. (2008). Proinflammatory cytokines and angiogenic and anti-angiogenic factors in vitreous of patients with proliferative diabetic retinopathy and eales' disease. *Retina* **28,** 817-824.

Nakamura,N., Hasegawa,G., Obayashi,H., Yamazaki,M., Ogata,M., Nakano,K., Yoshikawa,T., Watanabe,A., Kinoshita,S., Fujinami,A. et al. (2003). Increased concentration of pentosidine, an advanced glycation end product, and interleukin-6 in the vitreous of patients with proliferative diabetic retinopathy. *Diabetes Res. Clin. Pract.* **61,** 93-101.

Ng,E.W. and Adamis,A.P. (2006). Anti-VEGF aptamer (pegaptanib) therapy for ocular vascular diseases. *Ann. N Y. Acad. Sci.* **1082,** 151-171.

Ng,E.Y., Connolly,B.P., McNamara,J.A., Regillo,C.D., Vander,J.F., and Tasman,W. (2002). A comparison of laser photocoagulation with cryotherapy for threshold retinopathy of prematurity at 10 years: part 1. Visual function and structural outcome. *Ophthalmology* **109,** 928-934.

Ng,Y.S., Rohan,R., Sunday,M.E., Demello,D.E., and D'Amore,P.A. (2001). Differential expression of VEGF isoforms in mouse during development and in the adult. *Dev. Dyn.* **220,** 112-121.

Nguyen,Q.D., Shah,S.M., Van,A.E., Sung,J.U., Vitale,S., and Campochiaro,P.A. (2004). Supplemental oxygen improves diabetic macular edema: a pilot study. *Invest Ophthalmol Vis. Sci.* **45,** 617-624.

Nikitenko,L.L., Smith,D.M., Bicknell,R., and Rees,M.C. (2003). Transcriptional regulation of the CRLR gene in human microvascular endothelial cells by hypoxia. *FASEB J.* **17,** 1499-1501.

Nishijima,K. (2007). Vascular endothelial growth factor-A is a survival factor for retinal neurons and a critical neuroprotectant during the adaptive response to ischemic injury. *Am. J. Pathol.* **171,** 53-67.

Nishimura,T., Goodnight,R., Prendergast,R.A., and Ryan,S.J. (1990). Activated macrophages in experimental subretinal neovascularization. *Ophthalmologica* **200,** 39-44.

Nizet,V. and Johnson,R.S. (2009). Interdependence of hypoxic and innate immune responses. *Nat. Rev. Immunol.* **9,** 609-617.

Noma,H., Funatsu,H., Mimura,T., Eguchi,S., Shimada,K., and Hori,S. (2011). Vitreous levels of pigment epithelium-derived factor and vascular endothelial growth factor in macular edema with central retinal vein occlusion. *Curr. Eye Res.* **36,** 256-263.

Noonan,D.M., De Lerma,B.A., Vannini,N., Mortara,L., and Albini,A. (2008). Inflammation, inflammatory cells and angiogenesis: decisions and indecisions. *Cancer Metastasis Rev.* **27,** 31-40.

O'Rourke,J.F., Pugh,C.W., Bartlett,S.M., and Ratcliffe,P.J. (1996). Identification of hypoxically inducible mRNAs in HeLa cells using differential-display PCR. Role of hypoxia-inducible factor-1. *Eur. J. Biochem* **241,** 403-410.

Ohya,Y. and Sperelakis,N. (1989). Fast Na+ and slow Ca2+ channels in single uterine muscle cells from pregnant rats. *Am. J. Physiol* **257,** C408-C412.

Okamoto,N., Tobe,T., Hackett,S.F., Ozaki,H., Vinores,M.A., LaRochelle,W., Zack,D.J., and Campochiaro,P.A. (1997). Transgenic mice with increased expression of vascular endothelial growth factor in the retina: a new model of intraretinal and subretinal neovascularization. *Am. J. Pathol.* **151,** 281-291.

Okashiro,T., Tokuno,H., Fukumitsu,T., Hayashi,H., and Tomita,T. (1992). Effects of intracellular ATP on calcium current in freshly dispersed single cells of guinea-pig portal vein. *Exp. Physiol* **77,** 719-731.

Olson,N. and van,d., V (2011). Interactions between nitric oxide and hypoxia-inducible factor signaling pathways in inflammatory disease. *Nitric. Oxide.*

Osborne,N.N., Casson,R.J., Wood,J.P., Chidlow,G., Graham,M., and Melena,J. (2004). Retinal ischemia: mechanisms of damage and potential therapeutic strategies. *Prog. Retin. Eye Res.* **23,** 91-147.

Oshima,Y., Oshima,S., Nambu,H., Kachi,S., Hackett,S.F., Melia,M., Kaleko,M., Connelly,S., Esumi,N., Zack,D.J. et al. (2004). Increased expression of VEGF in retinal pigmented epithelial cells is not sufficient to cause choroidal neovascularization. *J. Cell Physiol* **201,** 393-400.

Ozaki,H., Yu,A.Y., Della,N., Ozaki,K., Luna,J.D., Yamada,H., Hackett,S.F., Okamoto,N., Zack,D.J., Semenza,G.L. et al. (1999). Hypoxia inducible factor-1alpha is increased in ischemic retina: temporal and spatial correlation with VEGF expression. *Invest Ophthalmol. Vis. Sci.* **40,** 182-189.

Palmer,E.A. (1996). The continuing threat of retinopathy of prematurity. *Am. J. Ophthalmol* **122,** 420-423.

Palmer,L.A., Semenza,G.L., Stoler,M.H., and Johns,R.A. (1998). Hypoxia induces type II NOS gene expression in pulmonary artery endothelial cells via HIF-1. *Am. J. Physiol* **274,** L212-L219.

Papandreou,I., Cairns,R.A., Fontana,L., Lim,A.L., and Denko,N.C. (2006). HIF-1 mediates adaptation to hypoxia by actively downregulating mitochondrial oxygen consumption. *Cell Metab* **3,** 187-197.

Papst,N., Demant,E., and Niemeyer,G. (1982). Changes in pO2 induce retinal autoregulation in vitro. *Graefes Arch. Clin. Exp. Ophthalmol* **219,** 6-10.

Parnaik,R., Raff,M.C., and Scholes,J. (2000). Differences between the clearance of apoptotic cells by professional and non-professional phagocytes. *Curr. Biol.* **10,** 857-860.

Patterson,A.J. and Zhang,L. (2010). Hypoxia and fetal heart development. *Curr. Mol. Med.* **10,** 653-666.

Patz,A. (1968). The role of oxygen in retrolental fibroplasia. *Trans. Am. Ophthalmol Soc.* **66,** 940-985.

Pause,A., Lee,S., Worrell,R.A., Chen,D.Y., Burgess,W.H., Linehan,W.M., and Klausner,R.D. (1997). The von Hippel-Lindau tumor-suppressor gene product forms a stable complex with human CUL-2, a member of the Cdc53 family of proteins. *Proc. Natl. Acad. Sci. U. S. A* **94,** 2156-2161.

Peng,J., Zhang,L., Drysdale,L., and Fong,G.H. (2000). The transcription factor EPAS-1/hypoxia-inducible factor 2alpha plays an important role in vascular remodeling. *Proc. Natl. Acad. Sci U. S. A* **97,** 8386-8391.

Penn,J.S., Henry,M.M., and Tolman,B.L. (1994). Exposure to alternating hypoxia and hyperoxia causes severe proliferative retinopathy in the newborn rat. *Pediatr Res.* **36,** 724-731.

Perbal,B. (2004). CCN proteins: multifunctional signalling regulators. *Lancet* **363,** 62-64.

Petrovic,M.G., Korosec,P., Kosnik,M., and Hawlina,M. (2007). Vitreous levels of interleukin-8 in patients with proliferative diabetic retinopathy. *Am. J. Ophthalmol.* **143,** 175-176.

Peyssonnaux,C., Datta,V., Cramer,T., Doedens,A., Theodorakis,E.A., Gallo,R.L., Hurtado-Ziola,N., Nizet,V., and Johnson,R.S. (2005). HIF-1alpha expression regulates the bactericidal capacity of phagocytes. *J. Clin. Invest* **115,** 1806-1815.

Pfander,D., Kobayashi,T., Knight,M.C., Zelzer,E., Chan,D.A., Olsen,B.R., Giaccia,A.J., Johnson,R.S., Haase,V.H., and Schipani,E. (2004). Deletion of Vhlh in chondrocytes reduces cell proliferation and increases matrix deposition during growth plate development. *Development* **131,** 2497-2508.

Pfister,F., Feng,Y., vom,H.F., Hoffmann,S., Molema,G., Hillebrands,J.L., Shani,M., Deutsch,U., and Hammes,H.P. (2008). Pericyte migration: a novel mechanism of pericyte loss in experimental diabetic retinopathy. *Diabetes* **57,** 2495-2502.

Pournaras,C.J., Ilic,J., Gilodi,N., Tsacopoulos,M., and Leuenberger,M.P. (1985). [Experimental venous thrombosis: preretinal PO2 before and after photocoagulation]. *Klin. Monbl. Augenheilkd.* **186,** 500-501.

Pournaras,C.J., Miller,J.W., Gragoudas,E.S., Husain,D., Munoz,J.L., Tolentino,M.J., Kuroki,M., and Adamis,A.P. (1997). Systemic hyperoxia decreases vascular endothelial growth factor gene expression in ischemic primate retina. *Arch. Ophthalmol* **115,** 1553-1558.

Pournaras,C.J., Riva,C.E., Tsacopoulos,M., and Strommer,K. (1989). Diffusion of O2 in the retina of anesthetized miniature pigs in normoxia and hyperoxia. *Exp. Eye Res.* **49,** 347-360.

Pournaras,C.J., Rungger-Brandle,E., Riva,C.E., Hardarson,S.H., and Stefansson,E. (2008). Regulation of retinal blood flow in health and disease. *Prog. Retin. Eye Res.* **27,** 284-330.

Pournaras,C.J., Tsacopoulos,M., Strommer,K., Gilodi,N., and Leuenberger,P.M. (1990a). Experimental retinal branch vein occlusion in miniature pigs induces local tissue hypoxia and vasoproliferative microangiopathy. *Ophthalmology* **97,** 1321-1328.

Pournaras,C.J., Tsacopoulos,M., Strommer,K., Gilodi,N., and Leuenberger,P.M. (1990b). Scatter photocoagulation restores tissue hypoxia in experimental vasoproliferative microangiopathy in miniature pigs. *Ophthalmology* **97,** 1329-1333.

Provis,J.M. (2001). Development of the primate retinal vasculature. *Prog. Retin. Eye Res.* **20,** 799-821.

Rankin,E.B., Biju,M.P., Liu,Q., Unger,T.L., Rha,J., Johnson,R.S., Simon,M.C., Keith,B., and Haase,V.H. (2007). Hypoxia-inducible factor-2 (HIF-2) regulates hepatic erythropoietin in vivo. *J Clin Invest.* **117,** 1068-1077.

Rankin,E.B., Higgins,D.F., Walisser,J.A., Johnson,R.S., Bradfield,C.A., and Haase,V.H. (2005). Inactivation of the arylhydrocarbon receptor nuclear translocator (Arnt) suppresses von Hippel-Lindau disease-associated vascular tumors in mice. *Mol. Cell Biol.* **25,** 3163-3172.

Ransohoff,R.M. and Cardona,A.E. (2010). The myeloid cells of the central nervous system parenchyma. *Nature* **468,** 253-262.

Ratner,M. (2004). Genentech discloses safety concerns over Avastin. *Nat Biotechnol.* **22,** 1198.

Raval,R.R., Lau,K.W., Tran,M.G., Sowter,H.M., Mandriota,S.J., Li,J.L., Pugh,C.W., Maxwell,P.H., Harris,A.L., and Ratcliffe,P.J. (2005). Contrasting properties of hypoxia-inducible

factor 1 (HIF-1) and HIF-2 in von Hippel-Lindau-associated renal cell carcinoma. *Mol. Cell Biol.* **25,** 5675-5686.

Raymond,S.M. and Jackson,I.J. (1995). The retinal pigmented epithelium is required for development and maintenance of the mouse neural retina. *Curr. Biol.* **5,** 1286-1295.

Regillo,C.D., Brown,D.M., Abraham,P., Yue,H., Ianchulev,T., Schneider,S., and Shams,N. (2008). Randomized, double-masked, sham-controlled trial of ranibizumab for neovascular age-related macular degeneration: PIER Study year 1. *Am J Ophthalmol.* **145,** 239-248.

Rehak,M. and Wiedemann,P. (2010). Retinal vein thrombosis: pathogenesis and management. *J. Thromb. Haemost.* **8,** 1886-1894.

Rekalov,V., Juranek,I., Malekova,L., and Bauer,V. (1997). Hypoxia-induced inhibition of calcium channels in guinea-pig taenia caeci smooth muscle cells. *J. Physiol* **505 (Pt 1),** 107-119.

Remtulla,S. and Hallett,P.E. (1985). A schematic eye for the mouse, and comparisons with the rat. *Vision Res.* **25,** 21-31.

Ren,H., Liu,N.Y., Song,X.F., Ma,Y.S., and Zhai,X.Y. (2011). A novel specific application of pyruvate protects the mouse retina against white light damage: differential stabilization of HIF-1{alpha} and HIF-2{alpha}. *Invest Ophthalmol Vis. Sci.*

Rennie,D. and Morrissey,J. (1975). Retinal changes in Himalayan climbers. *Arch. Ophthalmol* **93,** 395-400.

Ribatti,D., Nico,B., Spinazzi,R., Vacca,A., and Nussdorfer,G.G. (2005). The role of adrenomedullin in angiogenesis. *Peptides* **26,** 1670-1675.

Riva,C.E., Pournaras,C.J., and Tsacopoulos,M. (1986). Regulation of local oxygen tension and blood flow in the inner retina during hyperoxia. *J. Appl. Physiol* **61,** 592-598.

Rodesch,F., Simon,P., Donner,C., and Jauniaux,E. (1992). Oxygen measurements in endometrial and trophoblastic tissues during early pregnancy. *Obstet. Gynecol.* **80,** 283-285.

Rodriguez,G.M., Borregero Leon,J.M., Gonzalez,R.E., Vina Rodriguez,J.J., Serrano,G.M., and Santolaria,F.F. (2010). [Vascular risk factors and retinal occlusive disease]. *Med. Clin. (Barc.)* **134,** 95-100.

Roider,J., Michaud,N.A., Flotte,T.J., and Birngruber,R. (1992). Response of the retinal pigment epithelium to selective photocoagulation. *Arch. Ophthalmol* **110,** 1786-1792.

Rolfs,A., Kvietikova,I., Gassmann,M., and Wenger,R.H. (1997). Oxygen-regulated transferrin expression is mediated by hypoxia-inducible factor-1. *J. Biol. Chem.* **272,** 20055-20062.

Ronkainen,V.P., Ronkainen,J.J., Hanninen,S.L., Leskinen,H., Ruas,J.L., Pereira,T., Poellinger,L., Vuolteenaho,O., and Tavi,P. (2007). Hypoxia inducible factor regulates the cardiac expression and secretion of apelin. *FASEB J.* **21,** 1821-1830.

Rosenfeld,P.J., Schwartz,S.D., Blumenkranz,M.S., Miller,J.W., Haller,J.A., Reimann,J.D., Greene,W.L., and Shams,N. (2005). Maximum tolerated dose of a humanized anti-vascular endothelial growth factor antibody fragment for treating neovascular age-related macular degeneration. *Ophthalmology.* **112,** 1048-1053.

Roy,S., Sato,T., Paryani,G., and Kao,R. (2003). Downregulation of fibronectin overexpression reduces basement membrane thickening and vascular lesions in retinas of galactose-fed rats. *Diabetes.* **52,** 1229-1234.

Ryan,H.E., Lo,J., and Johnson,R.S. (1998). HIF-1 alpha is required for solid tumor formation and embryonic vascularization. *EMBO J.* **17,** 3005-3015.

Ryan,H.E., Poloni,M., McNulty,W., Elson,D., Gassmann,M., Arbeit,J.M., and Johnson,R.S. (2000). Hypoxia-inducible factor-1alpha is a positive factor in solid tumor growth. *Cancer Res.* **60,** 4010-4015.

Ryan,S.J. (1979). The development of an experimental model of subretinal neovascularization in disciform macular degeneration. *Trans. Am. Ophthalmol Soc.* **77,** 707-745.

Saadi,S., Wrenshall,L.E., and Platt,J.L. (2002). Regional manifestations and control of the immune system. *FASEB J.* **16,** 849-856.

Saint-Geniez,M. and D'Amore,P.A. (2004). Development and pathology of the hyaloid, choroidal and retinal vasculature. *Int. J. Dev. Biol.* **48,** 1045-1058.

Saint-Geniez,M., Maharaj,A.S., Walshe,T.E., Tucker,B.A., Sekiyama,E., Kurihara,T., Darland,D.C., Young,M.J., and D'Amore,P.A. (2008). Endogenous VEGF is required for visual function: evidence for a survival role on muller cells and photoreceptors. *PLoS. ONE.* **3,** e3554.

Sakaguchi,D.S., Janick,L.M., and Reh,T.A. (1997). Basic fibroblast growth factor (FGF-2) induced transdifferentiation of retinal pigment epithelium: generation of retinal neurons and glia. *Dev. Dyn.* **209,** 387-398.

Sakanaka,M., Wen,T.C., Matsuda,S., Masuda,S., Morishita,E., Nagao,M., and Sasaki,R. (1998). In vivo evidence that erythropoietin protects neurons from ischemic damage. *Proc. Natl. Acad. Sci. U. S. A* **95,** 4635-4640.

Sakurai,E., Anand,A., Ambati,B.K., van,R.N., and Ambati,J. (2003). Macrophage depletion inhibits experimental choroidal neovascularization. *Invest Ophthalmol Vis. Sci.* **44,** 3578-3585.

Sanchez-Elsner,T., Botella,L.M., Velasco,B., Langa,C., and Bernabeu,C. (2002). Endoglin expression is regulated by transcriptional cooperation between the hypoxia and transforming growth factor-beta pathways. *J. Biol. Chem.* **277,** 43799-43808.

Sarks,S.H. (1976). Ageing and degeneration in the macular region: a clinico-pathological study. *Br. J. Ophthalmol.* **60,** 324-341.

Sato,T., Kusaka,S., Shimojo,H., and Fujikado,T. (2009). Vitreous levels of erythropoietin and vascular endothelial growth factor in eyes with retinopathy of prematurity. *Ophthalmology* **116,** 1599-1603.

Schachat,A.P., Oyakawa,R.T., Michels,R.G., and Rice,T.A. (1983). Complications of vitreous surgery for diabetic retinopathy. II. Postoperative complications. *Ophthalmology* **90,** 522-530.

Schaffer,L., Scheid,A., Spielmann,P., Breymann,C., Zimmermann,R., Meuli,M., Gassmann,M., Marti,H.H., and Wenger,R.H. (2003). Oxygen-regulated expression of TGF-beta 3, a growth factor involved in trophoblast differentiation. *Placenta* **24,** 941-950.

Scholtz,C.L. and Chan,K.K. (1987). Complicated colobomatous microphthalmia in the microphthalmic (mi/mi) mouse. *Development* **99,** 501-508.

Scortegagna,M., Ding,K., Oktay,Y., Gaur,A., Thurmond,F., Yan,L.J., Marck,B.T., Matsumoto,A.M., Shelton,J.M., Richardson,J.A. et al. (2003). Multiple organ pathology, metabolic abnormalities and impaired homeostasis of reactive oxygen species in Epas1-/- mice. *Nat. Genet.* **35,** 331-340.

Sears,J.E., Hoppe,G., Ebrahem,Q., and nand-Apte,B. (2008). Prolyl hydroxylase inhibition during hyperoxia prevents oxygen-induced retinopathy. *Proc. Natl. Acad. Sci. U. S. A* **105,** 19898-19903.

Semenza,G.L., Roth,P.H., Fang,H.M., and Wang,G.L. (1994). Transcriptional regulation of genes encoding glycolytic enzymes by hypoxia-inducible factor 1. *J. Biol. Chem.* **269,** 23757-23763.

Sharp,F.R. and Bernaudin,M. (2004). HIF1 and oxygen sensing in the brain. *Nat. Rev. Neurosci.* **5,** 437-448.

Sheridan,C.M., Pate,S., Hiscott,P., Wong,D., Pattwell,D.M., and Kent,D. (2009). Expression of hypoxia-inducible factor-1alpha and -2alpha in human choroidal neovascular membranes. *Graefes Arch. Clin. Exp. Ophthalmol* **247,** 1361-1367.

Shi,Y.Y., Wang,Y.S., Zhang,Z.X., Cai,Y., Zhou,J., Hou,H.Y., and van,R.N. (2011). Monocyte/macrophages promote vasculogenesis in choroidal neovascularization in mice by stimulating SDF-1 expression in RPE cells. *Graefes Arch. Clin. Exp. Ophthalmol* **249,** 1667-1679.

Shimada,H., Akaza,E., Yuzawa,M., and Kawashima,M. (2009). Concentration gradient of vascular endothelial growth factor in the vitreous of eyes with diabetic macular edema. *Invest Ophthalmol Vis. Sci.* **50,** 2953-2955.

Shimizu K and Kazuyoshi U (1978). Structure of ocular vessels. *New York: Igaku-Shoin*.

Shimizu,K., Kobayashi,Y., and Muraoka,K. (1981). Midperipheral fundus involvement in diabetic retinopathy. *Ophthalmology* **88,** 601-612.

Shinohara,M., Masuyama,T., Shoda,T., Takahashi,T., Katsuda,Y., Komeda,K., Kuroki,M., Kakehashi,A., and Kanazawa,Y. (2000). A new spontaneously diabetic non-obese Torii rat strain with severe ocular complications. *Int. J Exp. Diabetes Res.* **1,** 89-100.

Shui,Y.B., Fu,J.J., Garcia,C., Dattilo,L.K., Rajagopal,R., McMillan,S., Mak,G., Holekamp,N.M., Lewis,A., and Beebe,D.C. (2006). Oxygen distribution in the rabbit eye and oxygen consumption by the lens. *Invest Ophthalmol Vis. Sci.* **47,** 1571-1580.

Shui,Y.B., Holekamp,N.M., Kramer,B.C., Crowley,J.R., Wilkins,M.A., Chu,F., Malone,P.E., Mangers,S.J., Hou,J.H., Siegfried,C.J. et al. (2009). The gel state of the vitreous and ascorbate-dependent oxygen consumption: relationship to the etiology of nuclear cataracts. *Arch. Ophthalmol* **127,** 475-482.

Simo,R. and Hernandez,C. (2008). Intravitreous anti-VEGF for diabetic retinopathy: hopes and fears for a new therapeutic strategy. *Diabetologia* **51,** 1574-1580.

Simon,M.C. and Keith,B. (2008). The role of oxygen availability in embryonic development and stem cell function. *Nat. Rev. Mol. Cell Biol.* **9,** 285-296.

Singerman,L.J., Masonson,H., Patel,M., Adamis,A.P., Buggage,R., Cunningham,E., Goldbaum,M., Katz,B., and Guyer,D. (2008). Pegaptanib sodium for neovascular age-related macular degeneration: third-year safety results of the VEGF Inhibition Study in Ocular Neovascularisation (VISION) trial. *Br. J. Ophthalmol.* **92,** 1606-1611.

Sivakumar,V., Foulds,W.S., Luu,C.D., Ling,E.A., and Kaur,C. (2011). Retinal ganglion cell death is induced by microglia derived pro-inflammatory cytokines in the hypoxic neonatal retina. *J. Pathol.* **224,** 245-260.

Sivakumar,V., Zhang,Y., Ling,E.A., Foulds,W.S., and Kaur,C. (2008). Insulin-like growth factors, angiopoietin-2, and pigment epithelium-derived growth factor in the hypoxic retina. *J. Neurosci. Res.* **86,** 702-711.

Skeie,J.M. and Mullins,R.F. (2009). Macrophages in neovascular age-related macular degeneration: friends or foes? *Eye (Lond)* **23,** 747-755.

Smith,L.E., Wesolowski,E., McLellan,A., Kostyk,S.K., D'Amato,R., Sullivan,R., and D'Amore,P.A. (1994). Oxygen-induced retinopathy in the mouse. *Invest. Ophthalmol. Vis. Sci.* **35,** 101-111.

Stahl,A., Agostini,H., Jandeck,C., and Lagreze,W. (2011). [Pharmacological treatment for retinopathy of prematurity]. *Ophthalmologe* **108,** 777-785.

Stahl,A., Buchwald,A., Martin,G., Junker,B., Chen,J., Hansen,L.L., Agostini,H.T., Smith,L.E., and Feltgen,N. (2010). Vitreal levels of erythropoietin are increased in patients with retinal vein occlusion and correlate with vitreal VEGF and the extent of macular edema. *Retina* **30,** 1524-1529.

Staller,P., Sulitkova,J., Lisztwan,J., Moch,H., Oakeley,E.J., and Krek,W. (2003). Chemokine receptor CXCR4 downregulated by von Hippel-Lindau tumour suppressor pVHL. *Nature* **425,** 307-311.

Standen,N.B., Quayle,J.M., Davies,N.W., Brayden,J.E., Huang,Y., and Nelson,M.T. (1989). Hyperpolarizing vasodilators activate ATP-sensitive K+ channels in arterial smooth muscle. *Science* **245,** 177-180.

Stefansson,E. (2006). Ocular oxygenation and the treatment of diabetic retinopathy. *Surv. Ophthalmol.* **51,** 364-380.

Stefansson,E. (2009). Physiology of vitreous surgery. *Graefes Arch. Clin. Exp. Ophthalmol* **247,** 147-163.

Stefansson,E., Geirsdottir,A., and Sigurdsson,H. (2010). Metabolic physiology in age related macular degeneration. *Prog. Retin. Eye Res.*

Stefansson,E., Hatchell,D.L., Fisher,B.L., Sutherland,F.S., and Machemer,R. (1986). Panretinal photocoagulation and retinal oxygenation in normal and diabetic cats. *Am. J. Ophthalmol* **101,** 657-664.

Stefansson,E., Landers,M.B., III, and Wolbarsht,M.L. (1981). Increased retinal oxygen supply following pan-retinal photocoagulation and vitrectomy and lensectomy. *Trans. Am. Ophthalmol Soc.* **79,** 307-334.

Stefansson,E., Machemer,R., de Juan E Jr, McCuen,B.W., and Peterson,J. (1992). Retinal oxygenation and laser treatment in patients with diabetic retinopathy. *Am. J. Ophthalmol* **113,** 36-38.

Stefansson,E., Peterson,J.I., and Wang,Y.H. (1989). Intraocular oxygen tension measured with a fiber-optic sensor in normal and diabetic dogs. *Am. J. Physiol* **256,** H1127-H1133.

Stefater,J.A., III, Lewkowich,I., Rao,S., Mariggi,G., Carpenter,A.C., Burr,A.R., Fan,J., Ajima,R., Molkentin,J.D., Williams,B.O. et al. (2011). Regulation of angiogenesis by a non-canonical Wnt-Flt1 pathway in myeloid cells. *Nature* **474,** 511-515.

Stevens,B., Allen,N.J., Vazquez,L.E., Howell,G.R., Christopherson,K.S., Nouri,N., Micheva,K.D., Mehalow,A.K., Huberman,A.D., Stafford,B. et al. (2007). The classical complement cascade mediates CNS synapse elimination. *Cell* **131,** 1164-1178.

Stockmann,C., Doedens,A., Weidemann,A., Zhang,N., Takeda,N., Greenberg,J.I., Cheresh,D.A., and Johnson,R.S. (2008). Deletion of vascular endothelial growth factor in myeloid cells accelerates tumorigenesis. *Nature* **456,** 814-818.

Stone,J., Itin,A., Alon,T., Pe'er,J., Gnessin,H., Chan-Ling,T., and Keshet,E. (1995). Development of retinal vasculature is mediated by hypoxia-induced vascular endothelial growth factor (VEGF) expression by neuroglia. *J. Neurosci.* **15,** 4738-4747.

Streit,W.J. (2001). Microglia and macrophages in the developing CNS. *Neurotoxicology* **22,** 619-624.

Stroka,D.M., Burkhardt,T., Desbaillets,I., Wenger,R.H., Neil,D.A., Bauer,C., Gassmann,M., and Candinas,D. (2001). HIF-1 is expressed in normoxic tissue and displays an organ-specific regulation under systemic hypoxia. *FASEB J.* **15,** 2445-2453.

Szaflik,J.P., Janik-Papis,K., Synowiec,E., Ksiazek,D., Zaras,M., Wozniak,K., Szaflik,J., and Blasiak,J. (2009). DNA damage and repair in age-related macular degeneration. *Mutat. Res.* **669,** 169-176.

Tacchini,L., Bianchi,L., Bernelli-Zazzera,A., and Cairo,G. (1999). Transferrin receptor induction by hypoxia. HIF-1-mediated transcriptional activation and cell-specific post-transcriptional regulation. *J. Biol. Chem.* **274,** 24142-24146.

Tachi,N. and Ogino,N. (1996). Vitrectomy for diffuse macular edema in cases of diabetic retinopathy. *Am. J. Ophthalmol* **122,** 258-260.

Takahashi,Y., Takahashi,S., Shiga,Y., Yoshimi,T., and Miura,T. (2000). Hypoxic induction of prolyl 4-hydroxylase alpha (I) in cultured cells. *J. Biol. Chem.* **275,** 14139-14146.

Takeda,K., Aguila,H.L., Parikh,N.S., Li,X., Lamothe,K., Duan,L.J., Takeda,H., Lee,F.S., and Fong,G.H. (2008). Regulation of adult erythropoiesis by prolyl hydroxylase domain proteins. *Blood* **111,** 3229-3235.

Tamura,M. (2001). Neovascularization in experimental retinal venous obstruction in rabbits. *Jpn. J Ophthalmol.* **45,** 144-150.

Tazuke,S.I., Mazure,N.M., Sugawara,J., Carland,G., Faessen,G.H., Suen,L.F., Irwin,J.C., Powell,D.R., Giaccia,A.J., and Giudice,L.C. (1998). Hypoxia stimulates insulin-like growth factor binding protein 1 (IGFBP-1) gene expression in HepG2 cells: a possible model for IGFBP-1 expression in fetal hypoxia. *Proc. Natl. Acad. Sci U. S. A* **95,** 10188-10193.

Terry,T.L. (1944). Retrolental Fibroplasia in the Premature Infant: V. Further Studies on Fibroplastic Overgrowth of the Persistent Tunica Vasculosa Lentis. *Trans. Am. Ophthalmol Soc.* **42,** 383-396.

Thew,M. (2009). Rapid resolution of severe retinal neovascularisation in proliferative diabetic retinopathy following adjunctive intravitreal bevacizumab (Avastin). *Clin. Exp. Optom.* **92,** 34-37.

Thiersch,M., Raffelsberger,W., Frigg,R., Samardzija,M., Wenzel,A., Poch,O., and Grimm,C. (2008). Analysis of the retinal gene expression profile after hypoxic preconditioning identifies candidate genes for neuroprotection. *BMC. Genomics* **9,** 73.

Thompson,C.R., Gerstman,B.S., Jacques,S.L., and Rogers,M.E. (1996). Melanin granule model for laser-induced thermal damage in the retina. *Bull. Math. Biol.* **58,** 513-553.

Tian,H., Hammer,R.E., Matsumoto,A.M., Russell,D.W., and McKnight,S.L. (1998). The hypoxia-responsive transcription factor EPAS1 is essential for catecholamine homeostasis and protection against heart failure during embryonic development. *Genes Dev.* **12,** 3320-3324.

Tian,H., McKnight,S.L., and Russell,D.W. (1997). Endothelial PAS domain protein 1 (EPAS1), a transcription factor selectively expressed in endothelial cells. *Genes Dev.* **11,** 72-82.

Tielsch,J.M., Javitt,J.C., Coleman,A., Katz,J., and Sommer,A. (1995). The prevalence of blindness and visual impairment among nursing home residents in Baltimore. *N. Engl. J. Med.* **332,** 1205-1209.

Tolentino,M. (2011). Systemic and ocular safety of intravitreal anti-VEGF therapies for ocular neovascular disease. *Surv. Ophthalmol* **56,** 95-113.

Treins,C., Giorgetti-Peraldi,S., Murdaca,J., Semenza,G.L., and Van,O.E. (2002). Insulin stimulates hypoxia-inducible factor 1 through a phosphatidylinositol 3-kinase/target of rapamycin-dependent signaling pathway. *J. Biol. Chem.* **277,** 27975-27981.

Trick,G.L. and Berkowitz,B.A. (2005). Retinal oxygenation response and retinopathy. *Prog. Retin. Eye Res.* **24,** 259-274.

Trick,G.L., Edwards,P., Desai,U., and Berkowitz,B.A. (2006). Early supernormal retinal oxygenation response in patients with diabetes. *Invest Ophthalmol Vis. Sci* **47,** 1612-1619.

Trollmann,R. and Gassmann,M. (2009). The role of hypoxia-inducible transcription factors in the hypoxic neonatal brain. *Brain Dev.* **31,** 503-509.

Udono,T., Takahashi,K., Nakayama,M., Murakami,O., Durlu,Y.K., Tamai,M., and Shibahara,S. (2000). Adrenomedullin in cultured human retinal pigment epithelial cells. *Invest Ophthalmol Vis. Sci.* **41,** 1962-1970.

Ullah,M.S., Davies,A.J., and Halestrap,A.P. (2006). The plasma membrane lactate transporter MCT4, but not MCT1, is up-regulated by hypoxia through a HIF-1alpha-dependent mechanism. *J. Biol. Chem.* **281,** 9030-9037.

van Meurs,J.C., Bolt,B.J., Mertens,D.A., Peperkamp,E., and De,W.P. (1996). Rubeosis of the iris in proliferative vitreoretinopathy. *Retina* **16,** 292-295.

Vinores,S.A., Xiao,W.H., Aslam,S., Shen,J., Oshima,Y., Nambu,H., Liu,H., Carmeliet,P., and Campochiaro,P.A. (2006). Implication of the hypoxia response element of the Vegf promoter in mouse models of retinal and choroidal neovascularization, but not retinal vascular development. *J. Cell Physiol* **206,** 749-758.

vis-Silberman,N., Kalich,T., Oron-Karni,V., Marquardt,T., Kroeber,M., Tamm,E.R., and shery-Padan,R. (2005). Genetic dissection of Pax6 dosage requirements in the developing mouse eye. *Hum. Mol. Genet.* **14,** 2265-2276.

Wagner,K.D., Wagner,N., Wellmann,S., Schley,G., Bondke,A., Theres,H., and Scholz,H. (2003). Oxygen-regulated expression of the Wilms' tumor suppressor Wt1 involves hypoxia-inducible factor-1 (HIF-1). *FASEB J.* **17,** 1364-1366.

Walmsley,S.R., Print,C., Farahi,N., Peyssonnaux,C., Johnson,R.S., Cramer,T., Sobolewski,A., Condliffe,A.M., Cowburn,A.S., Johnson,N. et al. (2005). Hypoxia-induced neutrophil survival is mediated by HIF-1alpha-dependent NF-kappaB activity. *J. Exp. Med.* **201,** 105-115.

Wang,D., Wang,L.H., Zhao,Y., Lu,Y.P., and Zhu,L. (2010). Hypoxia regulates the ferrous iron uptake and reactive oxygen species level via divalent metal transporter 1 (DMT1) Exon1B by hypoxia-inducible factor-1. *IUBMB. Life* **62,** 629-636.

Wang,G.L. and Semenza,G.L. (1993). General involvement of hypoxia-inducible factor 1 in transcriptional response to hypoxia. *Proc. Natl. Acad. Sci. U. S. A* **90,** 4304-4308.

Wang,G.L. and Semenza,G.L. (1996). Molecular basis of hypoxia-induced erythropoietin expression. *Curr. Opin. Hematol.* **3,** 156-162.

Wang,V., Davis,D.A., Haque,M., Huang,L.E., and Yarchoan,R. (2005). Differential gene up-regulation by hypoxia-inducible factor-1alpha and hypoxia-inducible factor-2alpha in HEK293T cells. *Cancer Res.* **65,** 3299-3306.

Wang,X., Wang,G., and Wang,Y. (2009). Intravitreous vascular endothelial growth factor and hypoxia-inducible factor 1a in patients with proliferative diabetic retinopathy. *Am. J. Ophthalmol* **148,** 883-889.

Wangsa-Wirawan,N.D. and Linsenmeier,R.A. (2003). Retinal oxygen: fundamental and clinical aspects. *Arch. Ophthalmol.* **121,** 547-557.

Watson, Paxinos, and Puelles (2012). The Mouse Nervous System. *Elsevier Inc.* **First Edition**.

Weir,E.K., Lopez-Barneo,J., Buckler,K.J., and Archer,S.L. (2005). Acute oxygen-sensing mechanisms. *N. Engl. J. Med.* **353,** 2042-2055.

West,E.L., Pearson,R.A., Tschernutter,M., Sowden,J.C., MacLaren,R.E., and Ali,R.R. (2008). Pharmacological disruption of the outer limiting membrane leads to increased retinal integration of transplanted photoreceptor precursors. *Exp. Eye Res.* **86,** 601-611.

Wiesener,M.S., Jurgensen,J.S., Rosenberger,C., Scholze,C.K., Horstrup,J.H., Warnecke,C., Mandriota,S., Bechmann,I., Frei,U.A., Pugh,C.W. et al. (2003). Widespread hypoxia-inducible expression of HIF-2alpha in distinct cell populations of different organs. *FASEB J.* **17,** 271-273.

Williamson,T.H., Grewal,J., Gupta,B., Mokete,B., Lim,M., and Fry,C.H. (2009). Measurement of PO2 during vitrectomy for central retinal vein occlusion, a pilot study. *Graefes Arch. Clin. Exp. Ophthalmol* **247,** 1019-1023.

Wilson,C.A., Stefansson,E., Klombers,L., Hubbard,L.D., Kaufman,S.C., and Ferris,F.L., III (1988). Optic disk neovascularization and retinal vessel diameter in diabetic retinopathy. *Am. J. Ophthalmol* **106,** 131-134.

Wise,G. (1956). Retinal neovascularization. *Trans. Am. Ophthalmol Soc.* **54,** 729-826.

WISE,G.N. (1956). Retinal neovascularization. *Trans. Am. Ophthalmol. Soc.* **54,** 729-826.

Wright,W.S., McElhatten,R.M., Messina,J.E., and Harris,N.R. (2010). Hypoxia and the expression of HIF-1alpha and HIF-2alpha in the retina of streptozotocin-injected mice and rats. *Exp. Eye Res.* **90,** 405-412.

Xu,H., Chen,M., Mayer,E.J., Forrester,J.V., and Dick,A.D. (2007a). Turnover of resident retinal microglia in the normal adult mouse. *Glia* **55,** 1189-1198.

Xu,H., Dawson,R., Forrester,J.V., and Liversidge,J. (2007b). Identification of novel dendritic cell populations in normal mouse retina. *Invest Ophthalmol Vis. Sci* **48,** 1701-1710.

Xu,H.Z., Liu,S.Z., Xiong,S.Q., and Xia,X.B. (2011). [HIF-1alpha siRNA reduces retinal neovascularization in a mouse model of retinopathy of prematurity]. *Zhongguo Dang. Dai Er. Ke. Za Zhi.* **13,** 680-683.

Yamada,H., Yamada,E., Higuchi,A., and Matsumura,M. (2005). Retinal neovascularisation without ischaemia in the spontaneously diabetic Torii rat. *Diabetologia.* **48,** 1663-1668.

Yamada,M., Kim,S., Egashira,K., Takeya,M., Ikeda,T., Mimura,O., and Iwao,H. (2003). Molecular mechanism and role of endothelial monocyte chemoattractant protein-1 induction by vascular endothelial growth factor. *Arterioscler. Thromb. Vasc. Biol.* **23,** 1996-2001.

Yancopoulos,G.D., Davis,S., Gale,N.W., Rudge,J.S., Wiegand,S.J., and Holash,J. (2000). Vascular-specific growth factors and blood vessel formation. *Nature* **407,** 242-248.

Yang,J.C., Haworth,L., Sherry,R.M., Hwu,P., Schwartzentruber,D.J., Topalian,S.L., Steinberg,S.M., Chen,H.X., and Rosenberg,S.A. (2003). A randomized trial of bevacizumab, an anti-vascular endothelial growth factor antibody, for metastatic renal cancer. *N Engl J Med.* **349,** 427-434.

Yeo,E.J., Chun,Y.S., Cho,Y.S., Kim,J., Lee,J.C., Kim,M.S., and Park,J.W. (2003). YC-1: a potential anticancer drug targeting hypoxia-inducible factor 1. *J. Natl. Cancer Inst.* **95,** 516-525.

Yoneya,S., Saito,T., Nishiyama,Y., Deguchi,T., Takasu,M., Gil,T., and Horn,E. (2002). Retinal oxygen saturation levels in patients with central retinal vein occlusion. *Ophthalmology* **109,** 1521-1526.

Yoshida,T., Zhang,H., Iwase,T., Shen,J., Semenza,G.L., and Campochiaro,P.A. (2010). Digoxin inhibits retinal ischemia-induced HIF-1alpha expression and ocular neovascularization. *FASEB J.* **24,** 1759-1767.

Yoshimura,T., Sonoda,K.H., Sugahara,M., Mochizuki,Y., Enaida,H., Oshima,Y., Ueno,A., Hata,Y., Yoshida,H., and Ishibashi,T. (2009). Comprehensive analysis of inflammatory immune mediators in vitreoretinal diseases. *PLoS. One.* **4,** e8158.

Young,R.W. (1987). Pathophysiology of age-related macular degeneration. *Surv. Ophthalmol.* **31,** 291-306.

Yu,D.Y. and Cringle,S.J. (2001a). Oxygen distribution and consumption within the retina in vascularised and avascular retinas and in animal models of retinal disease. *Prog. Retin. Eye Res.* **20,** 175-208.

Yu,D.Y. and Cringle,S.J. (2001b). Oxygen distribution and consumption within the retina in vascularised and avascular retinas and in animal models of retinal disease. *Prog. Retin. Eye Res.* **20,** 175-208.

Yu,D.Y. and Cringle,S.J. (2006). Oxygen distribution in the mouse retina. *Invest Ophthalmol Vis. Sci* **47,** 1109-1112.

Yu,D.Y., Cringle,S.J., Alder,V.A., and Su,E.N. (1994). Intraretinal oxygen distribution in rats as a function of systemic blood pressure. *Am. J. Physiol* **267,** H2498-H2507.

Yu,D.Y., Townsend,R., Cringle,S.J., Chauhan,B.C., and Morgan,W.H. (2005). Improved interpretation of flow maps obtained by scanning laser Doppler flowmetry using a rat model of retinal artery occlusion. *Invest Ophthalmol Vis. Sci.* **46,** 166-174.

Yuan,G., Nanduri,J., Khan,S., Semenza,G.L., and Prabhakar,N.R. (2008). Induction of HIF-1alpha expression by intermittent hypoxia: involvement of NADPH oxidase, Ca2+ signaling, prolyl hydroxylases, and mTOR. *J. Cell Physiol* **217,** 674-685.

Zeng,H.Y., Green,W.R., and Tso,M.O. (2008a). Microglial activation in human diabetic retinopathy. *Arch. Ophthalmol.* **126,** 227-232.

Zeng,H.Y., Green,W.R., and Tso,M.O. (2008b). Microglial activation in human diabetic retinopathy. *Arch. Ophthalmol* **126,** 227-232.

Zhang,C., Wang,Y.S., Wu,H., Zhang,Z.X., Cai,Y., Hou,H.Y., Zhao,W., Yang,X.M., and Ma,J.X. (2010). Inhibitory efficacy of hypoxia-inducible factor 1alpha short hairpin RNA plasmid DNA-loaded poly (D, L-lactide-co-glycolide) nanoparticles on choroidal neovascularization in a laser-induced rat model. *Gene Ther.* **17,** 338-351.

Zhang,H., Gao,P., Fukuda,R., Kumar,G., Krishnamachary,B., Zeller,K.I., Dang,C.V., and Semenza,G.L. (2007a). HIF-1 inhibits mitochondrial biogenesis and cellular respiration in VHL-deficient renal cell carcinoma by repression of C-MYC activity. *Cancer Cell* **11,** 407-420.

Zhang,P., Wang,Y., Hui,Y., Hu,D., Wang,H., Zhou,J., and Du,H. (2007b). Inhibition of VEGF expression by targeting HIF-1 alpha with small interference RNA in human RPE cells. *Ophthalmologica* **221,** 411-417.

Zhang,P., Wang,Y., Hui,Y., Hu,D., Wang,H., Zhou,J., and Du,H. (2007c). Inhibition of VEGF expression by targeting HIF-1 alpha with small interference RNA in human RPE cells. *Ophthalmologica* **221,** 411-417.

Zhang,Y., Fortune,B., Atchaneeyasakul,L.O., McFarland,T., Mose,K., Wallace,P., Main,J., Wilson,D., Appukuttan,B., and Stout,J.T. (2008). Natural history and histology in a rat model of laser-induced photothrombotic retinal vein occlusion. *Curr. Eye Res.* **33,** 365-376.

Zhong,Y.S., Liu,X.H., Cheng,Y., and Min,Y.J. (2008). Erythropoietin with retrobulbar administration protects retinal ganglion cells from acute elevated intraocular pressure in rats. *J. Ocul. Pharmacol. Ther.* **24,** 453-459.

Zhou,J., Pham,L., Zhang,N., He,S., Gamulescu,M.A., Spee,C., Ryan,S.J., and Hinton,D.R. (2005). Neutrophils promote experimental choroidal neovascularization. *Mol. Vis.* **11,** 414-424.

Zhu,Y., Zhang,L., and Gidday,J.M. (2008). Deferroxamine preconditioning promotes long-lasting retinal ischemic tolerance. *J. Ocul. Pharmacol. Ther.* **24,** 527-535.

Appendix

1) Gene names, NCBI accession numbers and mRNA coding sequences.

Gene name	Accession no.	Coding sequence
Hif1a	NM_010431.1	258-2768
HIF1a	NM_001530.2	285-2765
Hif2a	NM_010137.3	382-3006
HIF2a	NM_001430.3	489-3101
mβ-actin	NM_007393.3	80-1207
hβ-actin	NM_001101.2	85-1212

2) PCR primers and conditions:

***a) trp cre* genotyping**

primers (5'-3')

Cre forward AGG TGT AGA GAA GGC ACT TAG C

Cre reverse CTA ATC GCC ATC TTC CAG CAG G

PCR reaction:

30 cycles of:

30s 94˚C

30s 60˚C

1min 72˚C

Product of 411bp in *cre* positive animals.

***b) lysM cre* genotyping**

primers (5'-3')

Cre forward AGG TGT AGA GAA GGC ACT TAG C

Cre reverse CTA ATC GCC ATC TTC CAG CAG G

PCR reaction:

30 cycles of:

30s 94˚C

30s 60˚C

1min 72˚C

Product of 411bp in *cre* positive animals.

c) Vhl genotyping

$VHL^{flox/flox}$ genotyping primers to distinguish floxed/wild-type alleles.

Flox 1 AGAGCGGCTTCACTTGTTTTTCAT

Flox 3 CCCAGTTCCCGGTCAGGTTC

PCR reaction:

35 cycles of:

30s 94˚C

5s 56˚C

30s 72˚C

Product of 457bp wild-type, 637bp floxed.

d) Hif1a genotyping

Hif1a$^{flox/flox}$ genotyping primers to distinguish floxed/wild-type alleles.

HF :15’ tgatgtgggtgctggtgtc 3’

HR3: 5’ ttgtgttggggcagtactg 3’

Amplification program: 53 degrees C x35

PCR reaction:

35 cycles of:

30s 94˚C

45s 53˚C

60s 72˚C

72C 10 mins

4C ad infinitum

Product of 200 bp for wild-type and 250bp for floxed genes

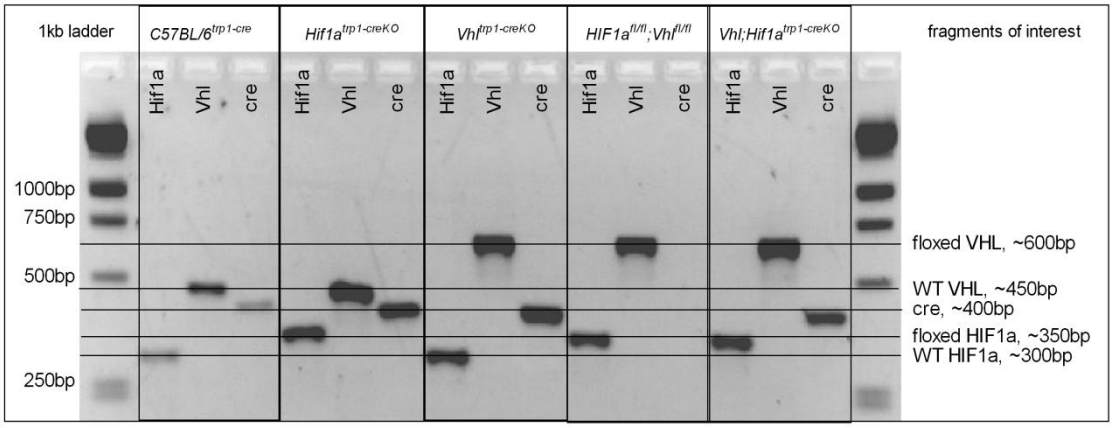

Figure Appendix 1. Genotyping PCR for *Hif1a*, *Vhl* and *cre recombinase* in *C57B6-trpcre, Hif1a$^{trp1\text{-}cre}$, Vhl$^{trp1\text{-}creKO}$, Vhl$^{fl/fl}$;Hif1a$^{fl/fl}$ and Vhl;Hif1a$^{trp1\text{-}creKO}$* mice

<u>*R*eal-time PCR</u>:

Murine Pax6 forward: 5'-CAGTTCTCAGAGCCCCGTAT-3'

Murine Pax6 reverse: 5'-CCACCAAGCTGATTCACTCC-3'.

Murine *Mitf* forward: 5'-TGAGTGCCCAGGTATGAACA-3'.

Murine *Mitf* reverse: 5'-GGATCCATCAAGCCCAAAA-3'.

Murine *Otx2* forward: 5'-GGTATGGACTTGCTGCATCC-3'.

Murine *Otx2* reverse: 5'-CGAGCTGTGCCCTAGTAAATG-3'.

Murine *Epo* forward: 5'-TCTGCGACAGTCGAGTTCTG-3'.

Murine *Epo* reverse: 5'-CTTCTGCACAACCCATCGT-3'.

Murine *Flt-1* forward: 5'-CCTCTGCATTTGGCATTAAGA-3'.

Murine *Flt-1* reverse: 5'-AGAGCTTTGTACTCACTGGCTGT-3'.

Murine *Pdgfa* forward: 5'-GGCTGGCTCGAAGTCAGAT-3'.

Murine *Pdgfa* reverse: 5'-TGTCTCCAAGGCATCCTCA-3'.

Murine *Pdgfb* forward: 5'-CGGCCTGTGACTAGAAGTCC-3'.

Murine *Pdgfb* reverse: 5'- GAGCTTGAGGCGTCTTGG-3'.

Murine *β-actin* forward: 5'-AAGGCCAACCGTGAAAAGAT-3'.

Murine *β-actin* reverse: 5'-GTGGTACGACCAGAGGCATAC-3'.

Murine *Vegf* forward: 5'-GACTTGTGTTGGGAGGAGGA-3'.

Murine *Vegf* reverse: 5'-TCTGGAAGTGAGCCAATGTG-3'.

Real-time PCR cycle:

50˚C 2 minutes, 95˚C 10 minutes

then 40 cycles of:

94˚C 30 seconds

60˚C 1 minute.

Publications